ISSN 1854-6250

APEM journal

Advances in Production Engineering & Management

Volume 19 | Number 4 | December 2024

University of Maribor

Published by CPE
apem-journal.org

Advances in Production Engineering & Management

Identification Statement

APEM journal

ISSN 1854-6250 | Abbreviated key title: **Adv produc engineer manag** | Start year: 2006
ISSN 1855-6531 (on-line)

Published quarterly by **Chair of Production Engineering (CPE)**, **University of Maribor**
Smetanova ulica 17, SI – 2000 Maribor, Slovenia, European Union (EU)

Phone: 00386 2 2207522, Fax: 00386 2 2207990
Language of text: English

University of Maribor

APEM homepage: apem-journal.org
University homepage: www.um.si

APEM Editorial

OPEN ACCESS

Subsidizer: The journal is subsidized by Slovenian Research and Innovation Agency

Published by CPE, University of Maribor.

Advances in Production Engineering & Management is indexed and abstracted in the **WEB OF SCIENCE** (maintained by **Clarivate**): **Science Citation Index Expanded**, **Journal Citation Reports** – Science Edition, **Current Contents** – Engineering, Computing and Technology • **Scopus** (maintained by **Elsevier**) • **Inspec** • **EBSCO**: Academic Search Alumni Edition, Academic Search Complete, Academic Search Elite, Academic Search Premier, Engineering Source, Sales & Marketing Source, TOC Premier • **ProQuest**: CSA Engineering Research Database – Cambridge Scientific Abstracts, Materials Business File, Materials Research Database, Mechanical & Transportation Engineering Abstracts, ProQuest SciTech Collection • **TEMA** (**DOMA**) • The journal is listed in **Ulrich's** Periodicals Directory and **Cabell's** Directory

University of Maribor
Chair of Production Engineering (CPE)

Advances in Production Engineering & Management

Volume 19 | Number 4 | December 2024 | pp 411–542

Contents

Journal homepage: apem-journal.org

ISSN 1854-6250 (print)
ISSN 1855-6531 (on-line)

Published by CPE, University of Maribor.

Scope and topics

Advances in Production Engineering & Management (*APEM journal*) is an interdisciplinary refereed international academic journal published quarterly by the *Chair of Production Engineering* at the *University of Maribor*. The main goal of the *APEM journal* is to present original, high quality, theoretical and application-oriented research developments in all areas of production engineering and production management to a broad audience of academics and practitioners. In order to bridge the gap between theory and practice, applications based on advanced theory and case studies are particularly welcome. For theoretical papers, their originality and research contributions are the main factors in the evaluation process. General approaches, formalisms, algorithms or techniques should be illustrated with significant applications that demonstrate their applicability to real-world problems. Although the *APEM journal* main goal is to publish original research papers, review articles and professional papers are occasionally published.

Fields of interest include, but are not limited to:

Additive Manufacturing Processes
Advanced Production Technologies
Artificial Intelligence in Production
Assembly Systems
Automation
Big Data in Production
Block Chain in Manufacturing
Computer-Integrated Manufacturing
Cutting and Forming Processes
Decision Support Systems
Deep Learning in Manufacturing
Discrete Systems and Methodology
e-Manufacturing
Evolutionary Computation in Production
Fuzzy Systems
Human Factor Engineering, Ergonomics
Industrial Engineering
Industrial Processes
Industrial Robotics
Intelligent Manufacturing Systems
Joining Processes
Knowledge Management
Logistics in Production
Machine Learning in Production
Machine-to-Machine Economy
Machine Tools
Machining Systems
Manufacturing Systems
Materials Science, Multidisciplinary
Mechanical Engineering
Mechatronics
Metrology in Production
Modelling and Simulation
Numerical Techniques
Operations Research
Operations Planning, Scheduling and Control
Optimisation Techniques
Project Management
Quality Management
Risk and Uncertainty
Self-Organizing Systems
Smart Manufacturing
Statistical Methods
Supply Chain Management
Virtual Reality in Production

APEM journal
Advances in Production Engineering & Management
Volume 19 | Number 4 | December 2024 | pp 415–434
https://doi.org/10.14743/apem2024.4.516
ISSN 1854-6250
Journal home: apem-journal.org
Original scientific paper

A bi-objective Genetic Algorithm for flexible flow shop scheduling: A real-world application in the electrical industry

Escobar, D.[a], **Chivata, B.**[a], **Nino, K.**[b,*]

[a]School of Exact Sciences and Engineering, Sergio Arboleda University, Bogotá, Colombia
[b]Industrial Engineering Program, Universidad Militar Nueva Granada, Bogotá, Colombia

ABSTRACT

The electrical sector forces manufacturing companies of electrical solutions to continually innovate and implement new processes for greater efficiency. The growing demand for electrical energy, as well as the need to adapt to hybrid operations that combine multi-project operation models with continuous production models, requires efficient workflow management. Accordingly, this article proposes a Genetic Algorithm (GA) approach for solving the scheduling problem in a Flexible Hybrid Flow Shop (FHFS) environment considering a transfer batch approach to minimize makespan and total tardiness. The approach is inspired by a real-world application in the electrical industry and also accounts for unrelated parallel machines, precedence, release times, and due dates for jobs at each production center as key constraints. Three real-data scenarios were generated and evaluated. In the first scenario, a 7 % improvement in makespan was observed compared to real execution times. In Scenario 2, the makespan improved significantly by 33 %, and only 17.4 % of jobs were delayed, compared to 96 % in the real data. Likewise, GA showed a lightly better performance over Tabu Search (TS) in 3.01 % for makespan while the delayed jobs found by GA were 25 % below those obtained by TS. These results highlight the potential of the proposed method to improve overall production efficiency, not only in the electrical sector but also in similar industries.

ARTICLE INFO

Keywords:
Production scheduling;
Flexible flow shop;
Genetic algorithm;
Makespan;
Tardiness;
Transfer batch;
Electrical sector

**Corresponding author:*
karen.nino@unimilitar.edu.co
(Nino, K.)

Article history:
Received 7 October 2024
Revised 21 December 2024
Accepted 23 December 2024

1. Introduction

In the rapidly evolving electrical sector, manufacturing companies face continuous challenges to innovate and implement new processes aimed at enhancing efficiency. The growing demand for electrical energy, driven by the increasing interconnectivity of devices through the Internet of Things (IoT) and emerging technologies, necessitates a shift toward hybrid operational models that blend multi-project frameworks with continuous production systems. This trend underscores the urgent need for effective workflow management and highlights the complexities of production processes. As the sector increasingly adopts electronic equipment and the infrastructure required for its operation, planning, scheduling, and production control have become critical to ensuring competitiveness and success. Companies are tasked with not only meeting rising production demands but also adapting to the customization requirements of their customers in an ever-changing market. This dynamic environment compels firms in the electrical sector to consistently align their operations with the rapid pace of technological advancements and evolving customer expectations.

Consequently, the production processes within these companies must navigate the dual challenge of enhancing efficiency while accommodating the growing demand for tailored solutions. This delightful balance is essential for maintaining relevance and achieving long-term sustainability in a sector characterized by constant change. Accordingly, the literature during the last decades has been describing a great amount of research focused on solving these kinds of problems from both real applications and theory points of view. Thus, this work made a review on this literature focus the search mainly on scheduling problems considering flexible production systems, one of the most used metaheuristics known as Genetic Algorithm and application on several industries, especially in electrical sector.

Initially, the flexible production systems, also known as Hybrid Systems (HS) or Flexible Hybrid Flow Shop Systems (FHFS), are defined as the scheduling of n jobs across m processing stages that consider a specific objective function, as determined by the production sequence of the job according to Xu *et al*. [1]. The scheduling problem in FHFS is known for its high combinatorial complexity. The allocation of resources to perform different operations in the production process results in a combinatorial complexity problem that must be optimized. In other words, the number of possible sequences and production route combinations can grow exponentially with the number of jobs and workstations; therefore, scheduling problems in an FHFS system are considered NP-Hard according to Gupta *et al*. [2]. Similarly, the objective functions considered are mainly the minimizing of total production time (makespan) [1, 4, 6-12, 14-17], followed by total tardiness [3, 5, 8, 12-13], productivity [1, 4-5, 7, 14, 16-17], among others.

The inherent flexibility of a flexible hybrid system implies the system must dynamically adapt to changes in demand, machine failures, or new work orders [1, 3, 5-7, 9-12, 16]. Optimization under these changing conditions requires algorithms that can handle uncertainty and variability, which is inherently complex and difficult to solve in polynomial time [1-17]. Most problems in an FHFS do not have a single objective [5, 8-9, 11-12, 15]. Generally, there are multiple objectives in conflict, such as minimizing production time, maximizing machine utilization, and minimizing costs, meaning that optimizing multiple objectives is even more complex. For example, Hasani *et al*. [15] proposed solving a bi-objective scheduling problem in a flexible Flow Shop with unrelated parallel machines, minimizing makespan and total production cost; authors introduced an approximate solution method based on a Non-dominated Sorting Genetic Algorithm (NSGA-II). Also, Jeen and Rajkumar [4] implemented a modified genetic algorithm in a Flow Shop production environment to minimize the makespan.

In addition, considering the approaches addressed to solve the FHFS scheduling problem, the Genetic Algorithm, which is nature-inspired, is one of the most used metaheuristics for this problem. For instance, Espitia and Mendoza [11] developed a scheduling methodology based on the use of a genetic algorithm as a solution method to minimize makespan and tardy jobs. Similarly, Salazar and Sarzuri [3] Considered a FSF environment with anticipatory sequence-dependent setup times, applying a genetic algorithm to minimize total tardiness by using dispatching rules for the initial population of EDD (Earliest Due Date). They also considered an IP neighbourhood search to enhance the performance of the proposed genetic algorithm. Likewise, Xu *et al*. [1] presents a case study where they develop a mathematical model aimed at minimizing the maximum completion time for a mixed flow shop scheduling problem, using a genetic algorithm to solve the problem. Najarro *et al*. [6] analysed the effect of including various constraints that negatively impact scheduling in a real Flow Shop environment, introducing an efficient genetic algorithm combined with a variable neighbourhood search, minimizing makespan. Han. and Lee [17] explored HFS pro-duction management based on an improved Genetic Algorithm (GA), proposing several assumptions for the multi-objective optimization problem of HFS production management. They introduced new constraints to the problem, such as multi-period control and job transport time, achieving efficiency in the experiments. As well, López *et al*. [16] selected a textile company as their case study and, through the coding of a simple genetic algorithm, developed a production scheduling methodology for Flexible Hybrid Flow Shop configurations, successfully reducing makespan.

Table 1 Classification of articles by production types

Method	Articles	Heuristic and Metaheuristic methods									Objective Function				Approach			Approach	
		AG	LS	TS	EA	ICA	NEH	NQ-L	NSGAII	SPEA 2	MOGA	Cmax	Tj	Energy	Tt	Cost	SP	ST	Stages	Hybrid	Lots
Flow Shop	[1] Xu, W. *et al.* (2022)	0										x					x			x	
	[3] Salazar, E. and Sarzuri R. (2015)	0											x							x	
	[4] Jeen, R and Rajkumar R. (2017)	0										x				x	x				
	[5] Kazemi, H. *et al.* (2017)					0							x				x		x	x	
	[6] Najarro, R. *et al.* (2017)	0	0									x								x	
	[7] Bedhief, A.O and Dridi. N. (2019)						0					x					x		x	x	
	[8] Tian, X. K. *et al.* (2019)	0										x	x								x
	[9] Shijin, W. *et al.* (2019)			0								x		x					x	x	
	[10] Waraporn, F. *et al.* (2020)			0								x								x	
	[11] Espitia, J.A. and Mendoza, G.L. (2021)	0									0	x			x					x	
	[12] Chen, D. and Zhao, X.R. (2021)	0										x	x			x		x		x	
	[13] Ištoković, D. *et al.* (2021)	0											x								x
	[14] Ren, J.F. *et al.* (2021)							0				x					x				x
	[15] Hasani, A. *et al.* (2022)	0			0				0	0		x				x			x		
	[16] López, J.C. *et al.* (2014)	0										x							x	x	
	[17] Han, J.H. and Lee, J.Y. (2023)	0										x					x	x	x		

AG: Genetic Algorithm; LS: Local Search; TS: Tabu Search; EA: Evolutionary Algorithm; ICA: Imperialist Competitive Algorithm; NEH: Nawaz, Enscore, Ham
NSGAII: Non-dominated Sorting Genetic Algorithm; NQ-L: Reinforcement Learning Method; SPEA2: Strength Pareto Evolutionary Algorithm
MOGA: Multi-Objective Genetic Algorithm SP: Scheduling Problem; ST: Setup Time; Cmax: Makespan; Tj: Total Tardiness; Tt: Tardy Jobs

In summary, Table 1 shows the consolidation of the main research reviewed, highlighting the different objectives, approaches, and research methodologies for solving production planning problems. Thus, one of the relevant findings is the predominant interest in makespan ($C_{\max}$) and tardiness (T_j) minimization. Thus, this paper describes a Genetic Algorithm (GA) approach for solving the scheduling problem in a Flexible Hybrid Flow Shop (FHFS) environment, inspired by a real-world application in the electrical industry, the results show an important improvement on the current performance of production system resulting in a valuable tool in decision making for company.

The remaining content of this work is as follows. Section 1 provides a clear introduction to the problem being addressed, along with a literature review focused on the main topics, particularly in electrical industry applications and scheduling solution approaches. Section 2 presents the characterization of the production process for the real case. Sections 3 and 4 detail the problem definition and the proposed solution method, respectively. Section 5 explains the real instance of the production process in the case study as well as presents the results and analysis of the evaluated scenarios. Finally, Section 6 addresses the conclusions and potential ways for future research.

2. Description of production process

The electrical company specializes in the design and manufacturing of customized solutions under an Engineering to Order (ETO) production scheme. Its operation is divided into two key phases: the project-based model and the production-based model. The first phase encompasses all related from sales to the availability of materials, managing each project individually. This stage includes subprocesses such as sales, project management, engineering, procurement, logistics, and storage, where opportunities are identified, contractual aspects are managed, technical designs are developed, and necessary materials are ensured. The second phase, focused on productive execution through a Flexible Flow Shop approach, primarily concentrates on production processes, where raw materials are transformed, and the final product is assembled. This model allows manufacturing to be adapted to the specifications of each project, addressing several challenges in a structured manner. Mainly, the scheduling approach of this research is focusing only on the stages of the process that are directly related to product manufacturing. Thus, the set of production and project jobs merged from project-based model phase. Table 2 describes, for the project-based model, only the electrical and mechanical engineering stages, while the production-based model includes the production centres, and the stages required for the transformation of raw materials and assembly.

Table 2 Grouping of production and project tasks

Phase	Production center	Cod	Description
Project-based model	Electrical engineering	RITM	Information review
		ECU	Equalization meeting with the client – Tecnichal clarifications
		L090	List of electrical materials with delivery time greater than 90 days
		EPA	Development of basic engineering for client approval
		APRB	Approval of basic engineering by the client
		PED	Detailed electrical engineering by the client
		APRD	Approval of detailed engineering by the client
	Mechanical engineering	LME	List of mechanical materials for structures
		LMV	List of various mechanical materials and cooper vbars
Production-based model	Manufacturing	PCN	CNC programing
		FMC	Cutting and punching of steel metal
		FMD	Bending of sheet metal
		SOL	Welding
		TPI	Treatment and painting
		FBC	Manufacturing of cooper bars
	Assembly	EME	Mechanical assembly
		EEL	Electrical assembly
		EBC	Assembly of cooper busbars
		PRU	Testing

2.1 Production centre capacity

The capacity of the production centres is defined in terms of the amount of work each can perform within a specific time; it is measured in effective working hours for the context of this research. Each centre's capacity is determined by the number of personnel and/or the effective

availability of the machines it comprises. The total capacity of the centre is obtained by adding up these individual capacities, expressed in terms of available working hours. Table 3 provides a detailed breakdown of the production centres (CP1, CP2, and CP3), which includes the production stages, the duration of each stage of 9 hours, the work shifts, and the required human resources, equipment, or machines. CP1 includes the electrical and mechanical engineering stages, each requiring six human resources. Meanwhile, CP2 focuses on manufacturing processes such as CNC programming, cutting, bending, welding, treatment, and copper bar fabrication, with personnel needs varying between one and four human resources, in addition to the use of machines. Finally, CP3 is dedicated to assembly, where the stages require between two and eight human resources. The distribution of work capacity among the various production centres illustrates the complexity and specialization of each stage in the production process. As manufacturing progresses, it is essential to consider both resource availability and process efficiency, as these factors will impact on the total production capacity and, ultimately, the timely delivery of the final products.

According to capacity determined in each production centre (CP1, CP2 and CP3), as well as the work centres into them, the production times were established and shown in Table 4; this table provides a comprehensive overview of the processing time required (in days) for various products across different production centres and stages of the process, organized into families and specific items. The columns "Family" and "Item" indicate the type of product being manufactured, where each "Family" represents a broader category, such as Medium Voltage (MT), which includes products designed for electrical solutions in installations ranging from 1 to 57.7 kV, and Low Voltage (BT), which encompasses solutions for electrical installations below 1 kV. Each "Item" specifies a product within that category, such as the Motor Control Centre (CCM) or the Auxiliary Services Panel (TSA). In addition, the table highlights the time required for each process—engineering, manufacturing, and assembly—across the production centres (CP1, CP2, and CP3). For example, the "Power Distribution Centre" (CDP) requires approximately 3.94 days for electrical engineering (CP1), 0.76 days for bending (CP2), and 4.68 days for testing (CP3). This detailed breakdown is essential for understanding production timelines and efficiently managing resource allocation.

Table 3 Production centre capacity

Production center	Stage	Description	Duration (hrs)	Work shifts	Human resources	Description
CP1	A	Electrical engineering	9	1	6	HR + CE
	B	Mechanical enginering	9	1	6	HR + CE
CP2	C	CNC programming	9	1	1	HR + CE
	D	Cutting and punching	9	1	2	HR + M
	E	Bending	9	1	2	HR + M
	F	Welding	9	1	4	HR + M
	G	Treatment and painting	9	1	2	HR + M
	H	Cooper busbar fabrication	9	1	2	HR + M
CP3	I	Mechanical assembly	9	1	4	HR + CE
	J	Electrical assembly	9	1	8	HR + CE
	K	Cooper busbar assembly	9	1	2	HR + CE
	L	Quality control and electrical testing	9	1	4	HR + CE

HR: Human resources; CE: Computer equipment; M: Machines

The result of data shown in Table 4, is the production system is settled as the diagram described in Fig. 1. At the top of the diagram, the general production centres are identified: CP1 (Engineering), CP2 (Manufacturing), and CP3 (Assembly). In the next level, the stages of the process are located, while the subsequent level details, the available resources, whether human or machine. The arrows represent the different routes the product can take through the various production centres and stages for its manufacturing. Thus, the production process is considered

as a flexible flow shop model. Each box shows the number of machines and the consecutive id to identify it into the model. For example, the CP1 production centre has in total six (6) machines which are the first machines from the total list of resources which has in total 43 machines.

Table 4 Time required (days)

Description of products				Time required by process (days)											
				CP1 – Enginnering		CP2 – Manufacturing						CP3 – Assembly			
				1	2	3	4	5	6	7	8	9	10	11	12
Family	Item	Description	Type of solution	Electrical engineering	Mechanical engineering	PCN-CNC programing	FMC-Cutting and punching	FMD-Bending	SOL-Welding	TPI-Treatment and painting	FBC-Cu busbar fabrication	EME-Mechanical assembly	EEL-Electrical assembly	EBC-Cu busbar assembly	PRU-Testing
BT	1	Power distribution center	CDP	**3.94**	2.40	0.39	0.42	**0.76**	0.67	0.39	0.64	1.70	2.98	0.94	**4.68**
	2	Motor control center	CCM	4.92	3.20	0.39	0.31	0.66	0.40	0.57	0.81	1.93	4.25	1.02	5.78
	3	Auxiliary services panel	TSA	2.95	2.40	0.19	0.38	0.50	0.41	0.38	0.39	1.23	1.91	0.21	2.76
	4	Low voltage variable frecuency drives	VVB	3.94	2.54	0.19	0.44	0.86	0.97	0.42	0.56	1.75	4.46	0.79	4.82
	5	Low voltage soft starters	ASB	3.94	2.40	0.19	0.42	0.77	0.89	0.45	0.44	1.28	3.93	0.68	4.04
	6	Low voltage distribution panel	TDB	2.95	2.91	0.19	0.38	0.50	0.41	0.38	0.39	1.23	1.91	0.21	2.76
	7	Control and protection panel	TCP	6.89	2.40	0.19	0.38	0.58	0.42	0.30	0.11	0.89	6.38	0.19	6.80
MT	8	Medium voltage secondary switchgear 24 kV	CMS2	2.95	2.40	0.39	0.28	0.50	0.22	0.13	0.15	0.78	1.91	0.31	2.27
	9	Medium voltage secondary switchgear 36 kV	CMS3	3.94	3.20	0.39	0.28	0.79	0.29	0.13	0.16	1.35	2.34	0.34	2.59
	10	Medium voltage primary switchgear 17.5 kV	CMP1	4.92	3.20	0.39	0.51	0.88	0.67	0.39	0.64	2.07	5.38	0.94	4.68
	11	Medium voltage primary switchgear 36 kV	CMP3	4.92	3.20	0.39	0.58	0.92	0.78	0.56	0.68	2.14	5.38	1.20	4.68
	12	Primary medium voltage GIS switchgear	CMPG	4.92	4.00	0.39	0.58	0.93	1.29	0.86	0.34	2.53	5.54	0.71	4.68
	13	Medium voltage variable frecuency drives	VVMT	5.90	4.00	0.39	0.42	0.76	0.67	0.39	0.64	1.70	3.83	0.85	4.68
	14	Medium voltage soft starters	ASMT	5.90	4.00	0.39	0.36	0.65	0.57	0.33	0.55	1.45	3.32	0.72	4.68

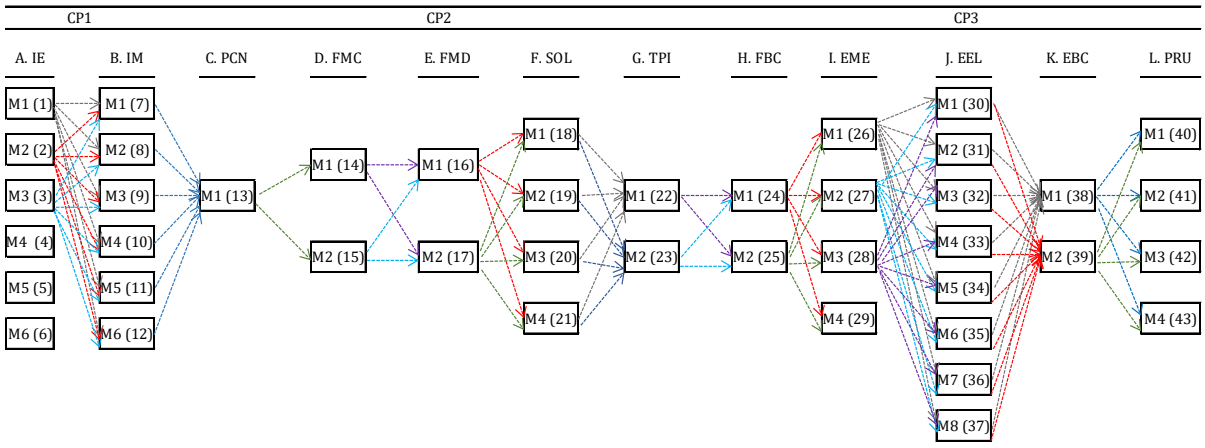

Fig. 1 Flow diagram of the production process

3. Construction of the HFS scheduling model

This study addresses the scheduling and permutation of tasks in a project planning environment within a Flexible Hybrid Flow Shop (HFS) production system. This system includes three production centres with unrelated parallel machines, dedicated to the fabrication, transformation, and testing of semi-finished and finished products for industrial electrical equipment projects. Key variables such as processing times, release times, and due dates are directly influenced by the production centre assigned. The objective functions considered are makespan and total tardiness, as main constraints are related to transfers lots, unrelated parallel machines, setup times. Accordingly, to Graham *et al*. [21], notation, the problem addressed is:

$$HFFS_m \,/\, R_m, r_j, S_{jk}, batch(b) \,/\, C_{max}, \sum T_j$$

The Hybrid Flow Shop (HFS) manufacturing environment presents complex scheduling challenges, involving the coordination of multiple jobs across various processing stages [1]. This problem is classified as strongly NP-Hard, meaning exact methods become infeasible for large instances, as confirmed by prior studies like those of Gupta *et al*. [2]. To address this complexity, metaheuristic algorithms, specifically Genetic Algorithms (GA), from mathematical model, is performed to provide approximate solutions.

In this study, a GA algorithm is adapted to optimize the scheduling process by minimizing makespan, total tardiness, and the number of delayed jobs in the HFS system; it means it is necessary to determine the optimal assignment of jobs j to machines k, within a sequence of production centres l, in such makespan (C_{max}) and total tardiness ($\sum T_j$) are minimized.

In addition, the developed algorithm does not consider dynamic inputs, which means that production orders arriving continuously or in real-time during the execution of the plan are not included; so, all production orders are predefined, and their characteristics are known at the beginning of the process due to this information is given by Planning and Production control Department of the company. Thus, the proposed Hybrid Flow Shop (HFS) production model is developed considering the following assumptions:

- Each machine can process only one job at a time.
- Each job is processed by only one machine at any given time.
- Jobs follow a fixed sequence of production centres (e.g. CP1, CP2, and CP3).
- Once started, a job is processed to completion without interruptions.
- The number of jobs and their processing times are deterministic.
- Setup times are considered negligible to simplify the model.
- Jobs can only be processed if the corresponding production centre is available.
- Transportation times between machines depend on the predefined sequence.
- Jobs can be assigned to any available machine within their respective set.
- Maintenance schedules are predefined and occur outside production times.
- Materials and inputs required are guaranteed to be continuously available throughout the scheduling process.

To establish a mathematical model for the HFS scheduling problem for electrical companies, the following notation is defined:

j	Set of jobs to be processed on the machines $\{1,2,\dots,n\}$ where n is the total number of jobs, ($j \in J$, for every job)
l	Set of production centres $\{1,2,\dots,L\}$ where L is the total number of production centres, ($l \in L$, for every production centre)
N_i	Set of operations per job $\{1,2,\dots,n_i\}$, where n_i is number of operations for job j, ($j \in N_i$, for every operation)
K	Set of machines $\{1,2,\dots,k\}$, where k is the total number of machines, ($k \in K$, for every machine)
TP_{ikl}	Processing time of job j assigned to machine k in production center l
CP_l	Time capacity in production centres
d_j	Due date of job j

P_{jkl} Duration of job j on machine k in production center l
ω_j Weighting factor
r_j Release time of job j
X_{jkl} Binary variable equal to 1 if job j is processed by machine k in production center l, and 0 otherwise X_{jkl} for X_{jkl} = 0, 1 j = 1, 2..., n, k = 1, 2..., n, l = 1, 2..., n
C_{jkl} Completion time of job j on machine k in production center l
T_{jkl} Star time of job j on machine k in production center l
T_j Job j tardiness
T_{kl} Start time of machine k in production center l
β_k Total number of jobs assigned to machine k
T_{nj} Start time of operation n of job j
$C_{\max}$ Makespan, the maximum completion time of all processes in the last production centre

The bi-objective function, denoted as Z, seeks to minimize both the weighted total production time $Z_{makespan}$ and the weighted total tardiness $Z_{tardiness}$. Thus, a unique objective function is defined using a weight ω_j which works as ponderator obtaining as a result the following equations.

$$Min\ Z = \omega_j \cdot Makespan + (1 - \omega_j) \cdot Tardiness \qquad 0 \leq w \leq 1 \tag{1}$$

where:

$$Z_{makespan} = max_j(max_l(C_{jkl}) \tag{2}$$

$$Z_{tardiness} = \sum_{j=1}^{n} T_j \tag{3}$$

In this way, the objective function is obtained as follows:

$$Z = (\omega_1 \cdot z_{makespan}) + (\omega_2 \cdot z_{tardiness}) \tag{4}$$

Subject to:

$$\sum_{j,k}^{N} X_{Jkl} \cdot TP_{jkl} \leq CP_l \quad \forall\ l \in L \tag{5}$$

$$\sum_{k}^{k} X_{jkl} = 1,\ \forall\ j, l \tag{6}$$

$$\sum_{j=1}^{n} X_{jkl} \leq 1,\ \forall\ k, l \tag{7}$$

$$\sum_{j}^{n} X_{jkl} = \beta_k \quad \forall\ k, l \tag{8}$$

$$C_{jkl} = T_{jkl} + P_{jkl} \tag{9}$$

$$T_j = \max(0, C_{jkl} - d_j) \tag{10}$$

$$T_{nj} \geq T_{kl} + P_{jkl} \cdot (1 - X_{jkl}) \quad \forall\ j, k, l \tag{11}$$

$$C_{jl} \leq d_j \quad \forall\ j,\ l \tag{12}$$

$$P_{jkl} \geq 0, \quad \forall\ j, k, l \tag{13}$$

$$\beta_k \geq 0, \quad \forall\ k \tag{14}$$

$$T_{jkl} > 0, \quad \forall\ j \tag{15}$$

$$C_{jl} \geq 0, \quad \forall\ j, l \tag{16}$$

The set of constraints (Eqs. 1 to 16) describes mathematical model. Eqs. 1 to 4 refer to objective function. Likewise, constraint Eq. 5 corresponds to the capacity constraint associated with the processing times of the jobs; constraint Eq. 6 ensures that each job (j) is assigned to exactly one machine (k) in the production centre (l); constraint Eq. 7 limits the number of jobs assigned to a specific machine (k) and production centre, ensuring that no more than one job is assigned in each case. Meanwhile, constraint Eq. 8 ensures that the total number of jobs (j) assigned and

not assigned to each machine and production centre is balanced; constraint Eq. 9 calculates the completion time of the jobs; constraint Eq. 10 guarantees that jobs are completed within their deadlines and penalizes any delays; constraint Eq. 11 ensures that an operation cannot begin until the machine to which it has been assigned is available and until its predecessor has been completed. Constraint Eq. 12 guarantees that job (j) is not completed after its due date. Finally, constraints Eqs. 13 to 16 correspond to non-negativity constraints, ensuring that the initial and final times are greater than 0.

It is worth to mention that, not only this approach could be focusing on electrical sector manufacturing production process, but also it could be easily applicable to production environments with similar structures, particularly those that operate with production centres and stages, processing products in a defined sequence using parallel machines. It is especially suitable for systems where production times at each stage are known in advance, enabling planning and process optimization. This latter is possible because of the algorithm is constructed modularly and sequentially in stages, allowing for modifications to the network structure of the proposed production model. Thanks to this design, machines can be added or removed at each stage, and the processing times of products can be dynamically adjusted at every stage.

4. Genetic algorithm for scheduling in a flexible hybrid flow shop (FHFS)

Based on the mechanisms of artificial selection, the Genetic Algorithm (GA) combines the concept of fittest survival among solutions with a structured random exchange of information, and the creation of offspring [18]. The Genetic Algorithm repeats the processes of evaluation, selection, crossover, and mutation after initialization until the stopping condition is reached. The GA is inherently parallel and exhibits implicit parallelism [19], which means that it does not evaluate and improve a single solution but rather analyses and modifies a set of solutions simultaneously. Fig. 2 describes the flowchart of the GA addressed in this study.

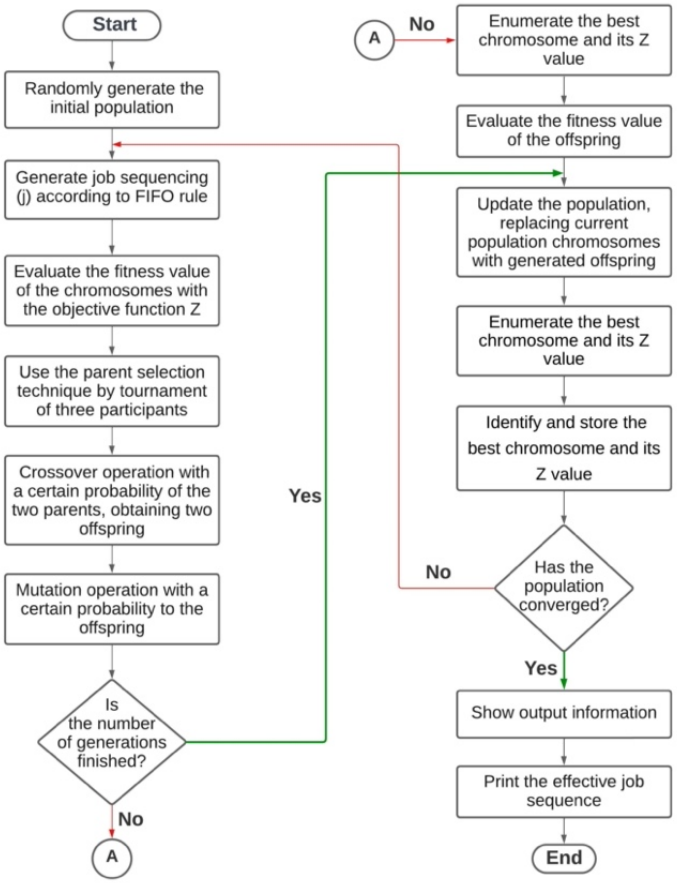

Fig. 2 GA approach flowchart (Adapted from Jeen and Rajkumar [4])

4.1 Parameters

The encoding of each solution alternative for the Flexible Sequential Hybrid Flow (FSHF) problem is represented by a vector of size n, where each position k of the vector indicates the job that will be performed in the k^{th} place [6]. The population (set of solutions) is created from a specific number of chromosomes, which each one represents the sequence that jobs will be scheduled. To ensure the validity of the chromosome, no job should be repeated, ensuring that all of them are completed and the total completion time and total tardiness of all jobs can be calculated. Fig. 3 shows the composition of the vector for a chromosome for 8 jobs.

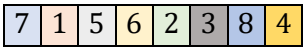

Fig. 3 Vector – representation of job order

Regarding the initial population, according to the study by López *et al*. [16], a binary matrix of size $i\ x\ k$ was used to represent jobs and machines, where each row is a chromosome. In the study by Najarro *et al*. [6], the initial population is generated randomly, and its size varies depending on the number of jobs (n) and machines (m), where $Pob_{ini} = n * m$. The initial population is created by repeating the chromosome generation process as many times as the population size is set. The genetic algorithm in this study involves several key steps to optimize task scheduling by minimizing makespan and weighted tardiness, as is shown in Fig. 4. The fitness function evaluates everyone in the population, assigning a value that reflects the quality of the task sequence in meeting the scheduling objectives [3]. A lower fitness value indicates a superior solution. About selection is performed using the tournament selection method, which balances exploration and exploitation [19]. In this study, individuals compete in tournaments, with the best-performing ones proceeding to genetic operations. A tournament size of three is used, allowing for quicker algorithm convergence compared to methods like roulette wheel selection.

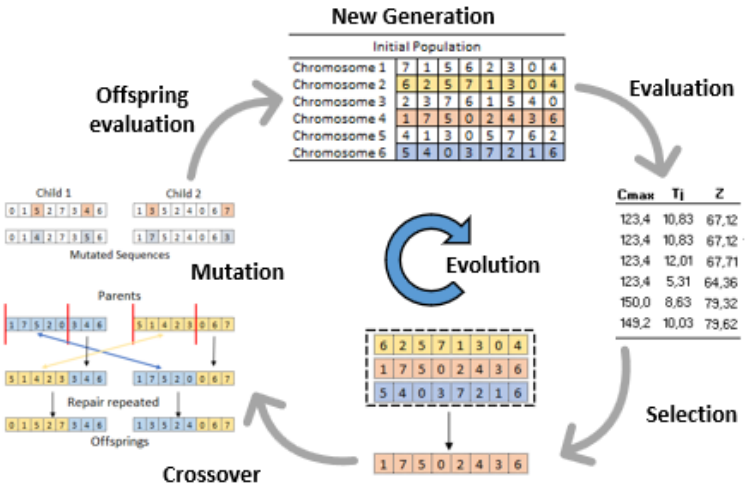

Fig. 4 Process cycle in genetic algorithm

Likewise, the Double Point Crossover (DPX) operator is applied to combine genetic material from two parent solutions, with repair mechanisms preventing duplicate jobs in the offspring [20]. After crossover, the offspring's fitness is evaluated, and the best individuals are selected for the next generation. Regarding, mutation is performed using a two-point mutation technique, where two positions in the offspring's sequence are randomly selected, and the segment between them is re-versed. This probabilistic process generates new solutions, which are evaluated for fitness, with the best-performing solutions advancing to the next generation [20]. In addition, the replacement process ensures the evolution of the population by selecting individuals from the current generation to create the next, based on their fitness. Finally, the algorithm employs stopping criteria that prevent infinite runs, including a maximum number of generations and stopping after several generations without improvement.

5. Results and discussion

This section explains how the instances were created with real data from electrical sector. In addition, three scenarios were created and performed, and the obtained results of each are discussed. Likewise, the GA algorithm is compared to TS (Tabu Search) method to evaluate its performance and results obtained are also argued. Finally, Computational time behaviour of all tests was analysed to evaluate the functioning of the model.

5.1 Real instance of the production process

Previously, in the planning process at the company, a dedicated department handles production planning and control, conducted daily with the support of an expert professional using Excel. The planning process varies depending on project complexity, often leading to delays in both planning and production. The production area receives a schedule, which includes project details, task numbers, product references, and start and delivery dates. Based on this information, production management is expected to allocate resources effectively to meet delivery deadlines, heavily relying on staff experience. Fig. 5 shows the behaviour of deliveries in the evaluated period. The red line illustrates the planned deliveries, and the black line identifies the actual behaviour of the same.

An analysis of a six-month period for 27 tasks revealed a 96 % non-compliance rate, with 25 tasks delivered late. The planned makespan was 370 days, but the actual execution took 538 days, a 31 % increase, resulting in a weighted tardiness of 102.96 days.

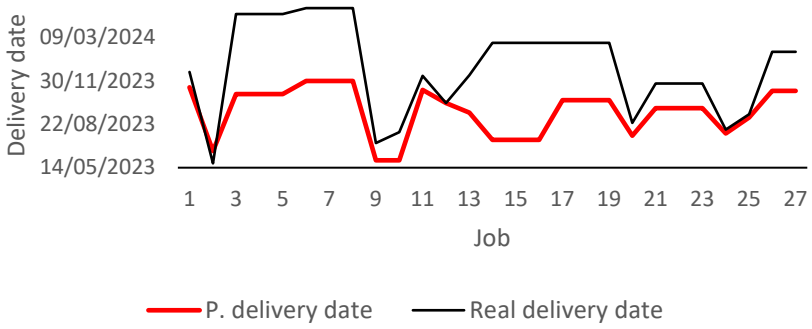

Fig. 5 Actual delivery performance – 6-month period

5.2 Test instances

Based on the results obtained during the data analysis, changes are proposed to focus on the number of jobs to be processed. This involves adjusting quantities to create more efficient transfer batches that provide effective solutions in the transformation and execution processes within each production centre based on the research made by Kazemi *et al*. [5].

A set of three simulations was managed considering the number of jobs to be performed and the number of available machines, referred to as scenarios 1, 2, and 3. Additionally, the Genetic Algorithm (GA) parameters were adjusted for each scenario to achieve more efficient results closer to the optimal. The scenarios included three production centres with a total of 43 machines; the only difference between them lies in the number of jobs: scenarios 1, 2, and 3 have 27, 46, and 87 jobs, respectively. These jobs are divided into transfer batches, which are scheduled independently. To illustrate the distribution of these transfer batches, Table 5 shows how the distribution of jobs is planned.

The Gantt charts show the job distribution, and the convergence graphs confirm that the algorithm reached solutions close to the optimum. To ensure job precedence in each scenario, the difference between due dates and completion times is compared for each task. The results of the best sequencing in Production Centre 1 (CP1) determine the start times for each job in Production Centre 2 (CP2), and in turn, the results from CP2 establish the release times for Production Centre 3 (CP3). Once the simulation for CP3 is complete, the results are used to evaluate the performance of each scenario and transfer batch.

Table 5 Transfer batch – Scenarios 1, 2 and 3

Job	Project	Product	T. batch size
1	Proj. # 1	CMP1	27

Job	Project	Product	T. batch size
1	Proj. # 1	CMP1	5
2		CMP1	5
3		CMP1	5
4		CMP1	6
5		CMP1	6

Job	Project	Product	T. batch size
1	Proj. # 1	CMP1	3
2		CMP1	3
3		CMP1	3
4		CMP1	3
5		CMP1	3
6		CMP1	3
7		CMP1	3
8		CMP1	3
9		CMP1	3

5.3 Results of Scenario 1

Fig. 6 presents the results obtained for this scenario. Gantt charts are divided into three production centres, each showing the behaviour of jobs in terms of sequencing, indicating the completion time of each task and the makespan for each centre, highlighting the best sequencing solutions. The analysis reveals that in Production Centre 1 (CP1), Task 27 is the last to finish, with a makespan of 243.1 days. In Production Centre 2 (CP2), Task 26 is the last to finish, with a makespan of 262.9 days. Finally, in Production Centre 3 (CP3), Task 1 is the last to complete the process on the last machine, with a total time of 502 days.

Fig. 7 shows the convergence behaviour of the algorithm in each phase of the production process. Thus, in the first 10 generations, the convergence is slow; after that, the best fitness value decreases until it reaches optimal convergence around 40 generations. Likewise, Fig. 8 describes the difference between the delivery dates of the real execution and those obtained with the GA algorithm. On average, it is seen that the GA finds earlier delivery dates for jobs, which results in better tardiness performance. These results suggest a slight improvement in reducing delayed tasks across the different production centres, which may be related to the large number of jobs assigned to each project. However, there are still high delay values that require further analysis to optimize task planning and sequencing. Fig. 6 also details the behaviour of the genetic algorithm in this first scenario. Upon analysing the results, a 26.3 % increase is observed compared to the planned makespan of 370 days, while there is a 6.7 % reduction when compared to the actual makespan of 538 days.

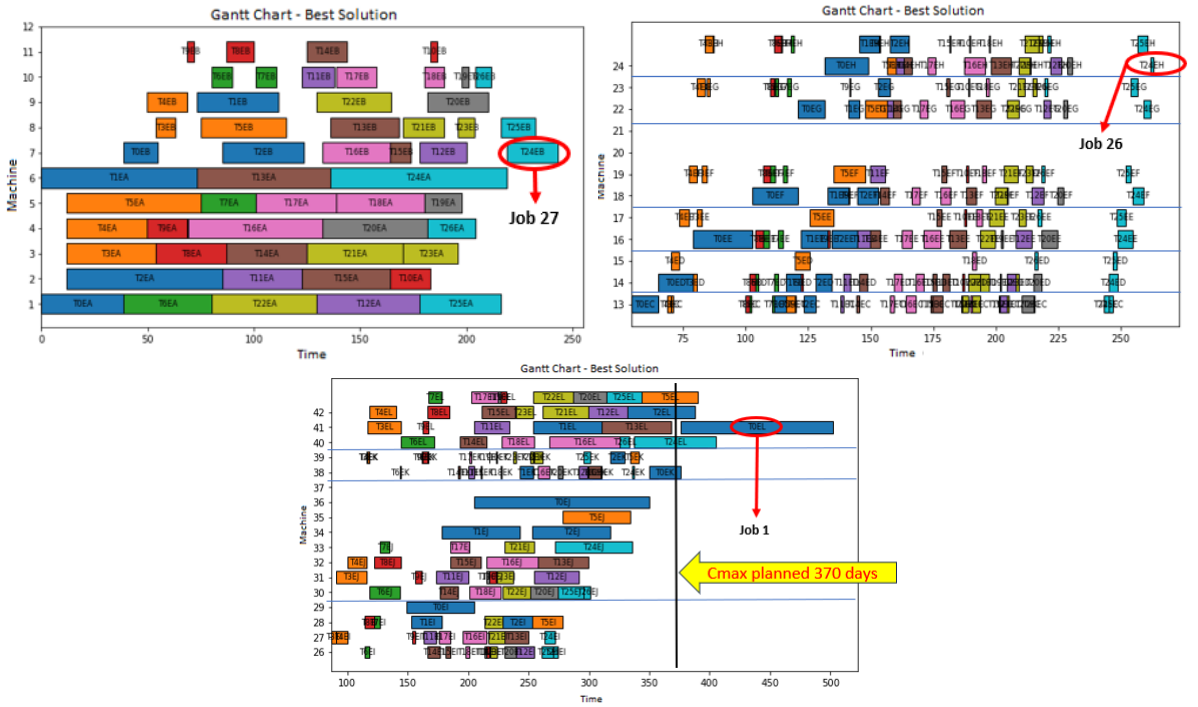

Fig. 6 Gantt chart – Transfer batch 1 – PC 1, PC 2, PC 3 – 27 jobs

In conclusion, although the genetic algorithm has proven to be more effective than the real instance, it has not yet reached the efficiency needed to surpass the company's planned objectives. These findings emphasize the importance of continuing to investigate and adjust the algorithm's parameters to improve its performance in future production scenarios. Here is where transfer batch approach gets importance into the model.

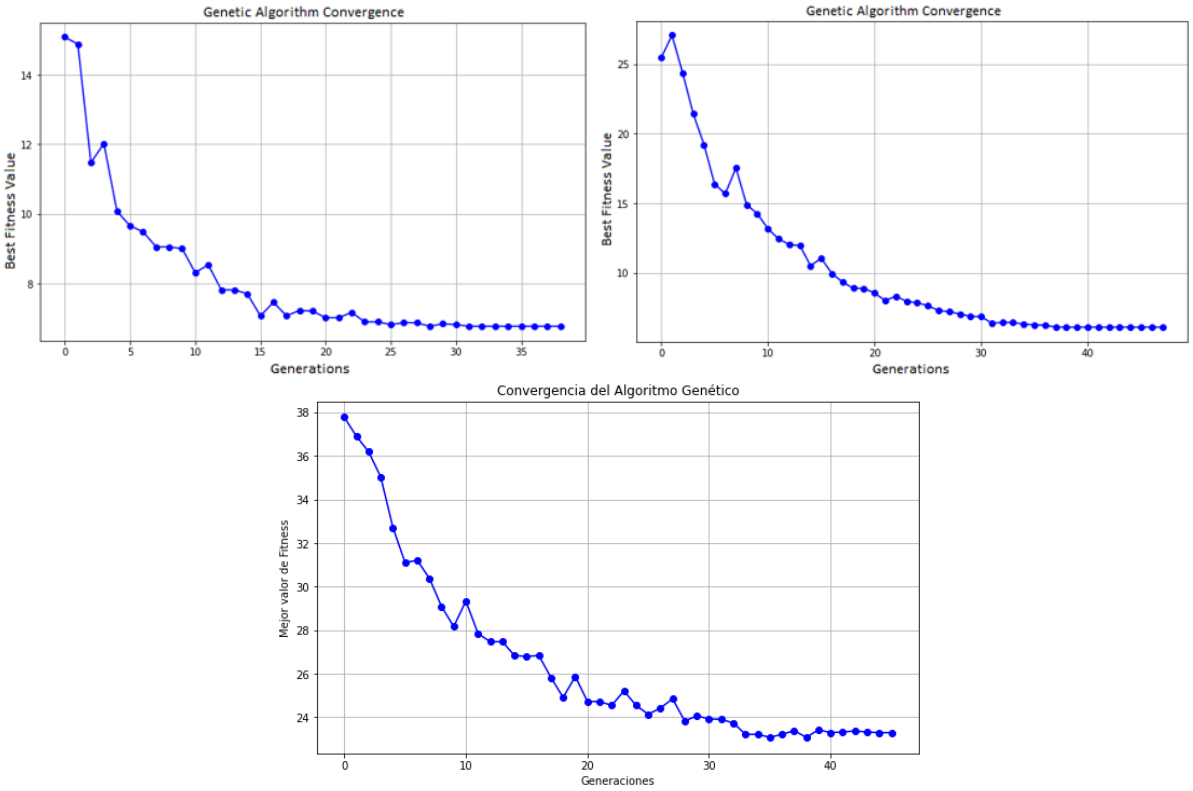

Fig. 7 Convergence graph – Transfer batch 1 – PC 1, PC 2, PC 3 – 27 jobs

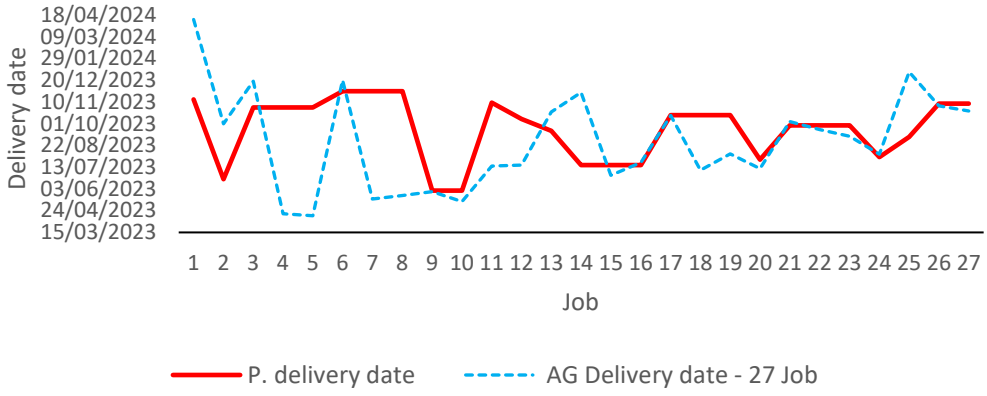

Fig. 8 Real delivery performance vs GA – 27 jobs

5.4 Results of Scenario 2

In this scenario, 46 jobs were evaluated with the aim of improving production through batch transfers. Project 26, initially composed of 27 jobs, was divided into smaller batches. As a result, makespan was reduced by 2.4 % compared to the previous scenario. At the same time, delayed jobs decreased, and only 17.4 % of the jobs missed their deadlines. Among the results obtained, it was observed that in CP1 and CP2, job 32 had the greatest delay, with 99.1 and 104.2 days, respectively. In CP3, the job with the greatest delay was job 23, with 91.5 days, processed on machine 40 and at stage L.

Figs. 9, 10 and 11 show the sequencing behavior found by the G.A in this scenario. The results show that the use of transfer batches and genetic operators in this scenario achieved significant improvements in delivery times. The makespan was reduced to 361.29 days, compared to the actual makespan of 538 days, and the number of delayed jobs decreased from 46 to 8. Additionally, the weighted tardiness was reduced to 6.27 days. These results highlight the effectiveness of the genetic algorithm in achieving the planned completion time of 370 days, improving the efficiency of the production system in this second scenario.

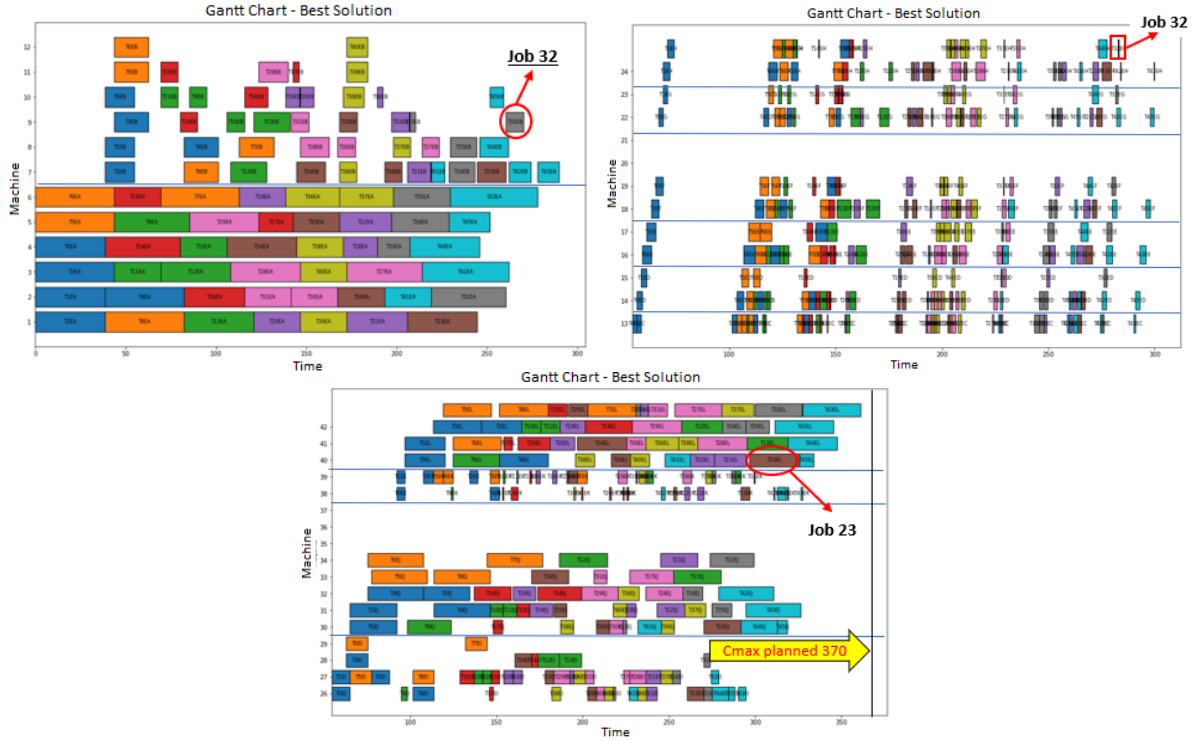

Fig. 9 Gantt chart – Transfer batch 2 – PC 1, PC 2, PC 3 – 46 jobs

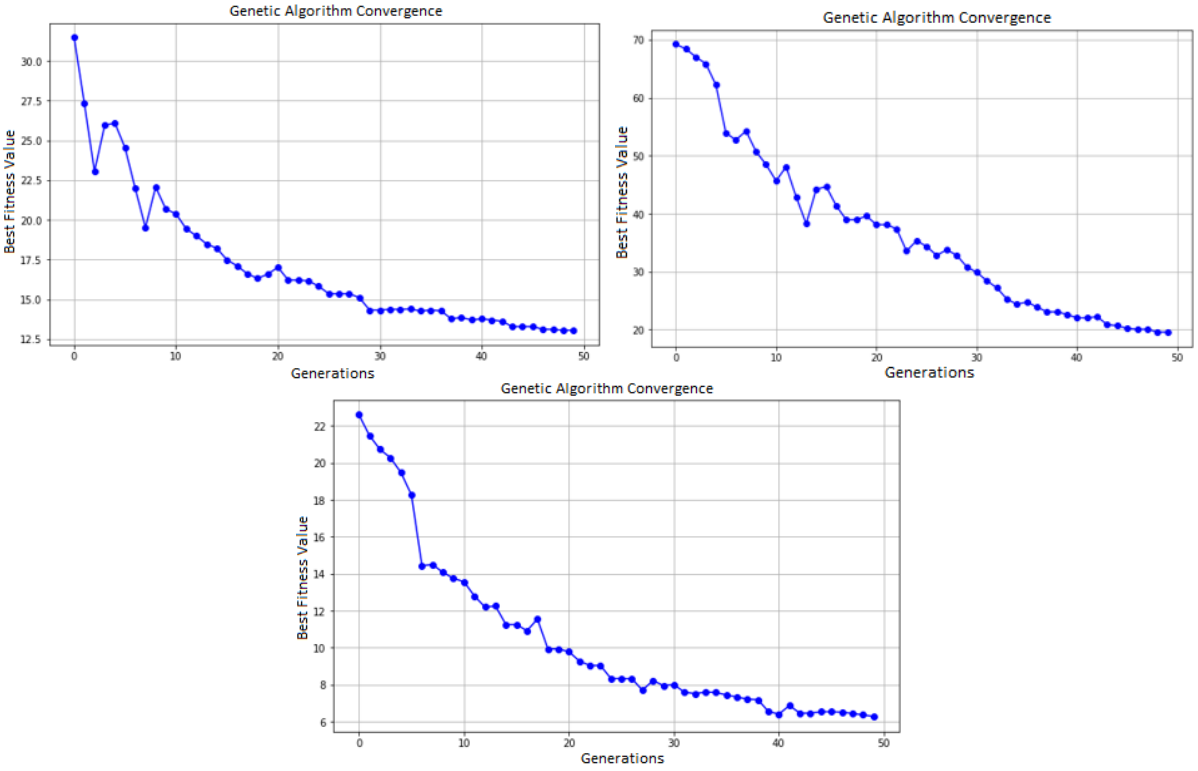

Fig. 10 Convergence graph – Transfer batch 2 – PC 1, PC 2, PC 3 – 46 jobs

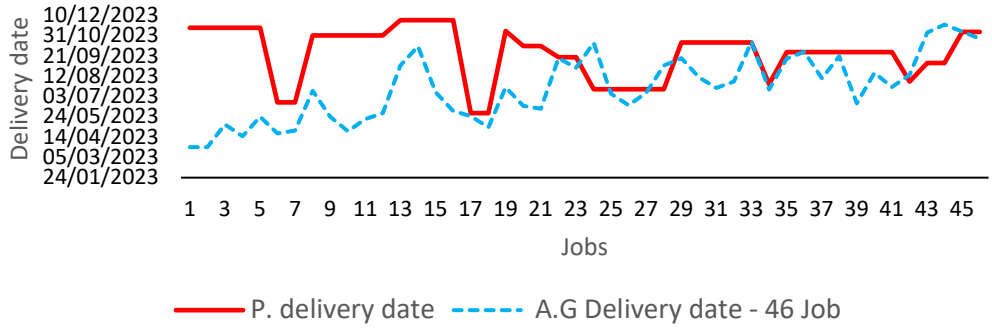

Fig. 11 Real delivery performance vs GA – 46 jobs

5.5 Results of Scenario 3

This scenario involved 87 jobs and revealed a compact distribution of tasks due to uniform processing times, which led to efficient sequencing. However, the larger number of machines required more computational resources, and the high number of delays (peaks) indicated that this approach was less effective for higher work volumes.

Figs. 12, 13, and 14 present the distribution and sequencing of the solution found by the genetic algorithm. They illustrate how the use of the largest number of available machines has been optimized at each stage of the process, and they also allow the convergence process to be identified. The results indicate that this scenario presents significantly high delay values. Although the number of delayed jobs was reduced by 52 % compared to the initial 87 jobs, this percentage is not substantial enough to be considered effective for implementation in the production plant. When compared to other scenarios, the obtained makespan of 443 days represents a 19.7 % increase over the planned makespan of 370 days. However, compared to the actual makespan of 538 days, there is a 17.7 % reduction, and relative to scenario 1 (502 days), there is an 11.8 % decrease. Finally, when analysing the difference with scenario 2 (361.29 days), there is an 18.4 % increase.

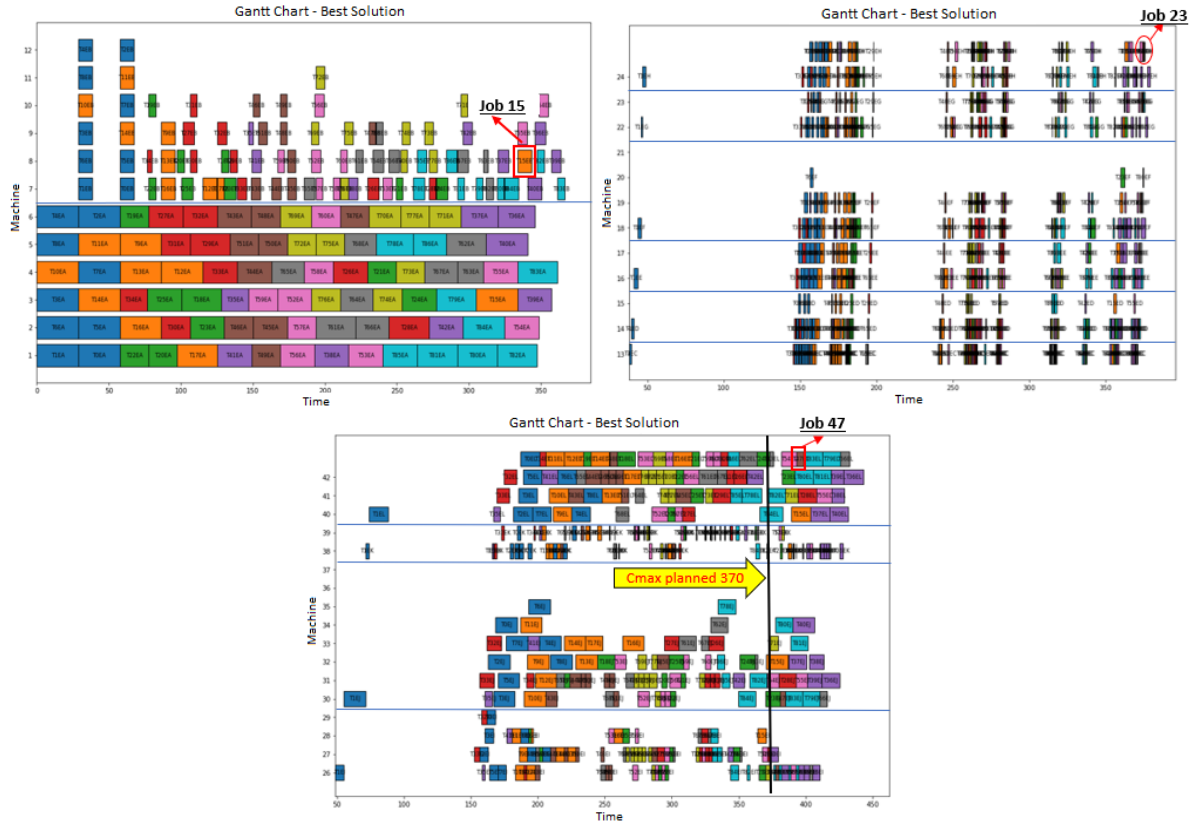

Fig. 12 Gantt chart – Transfer batch 3 – PC 1, PC 2, PC 3 – 87 jobs

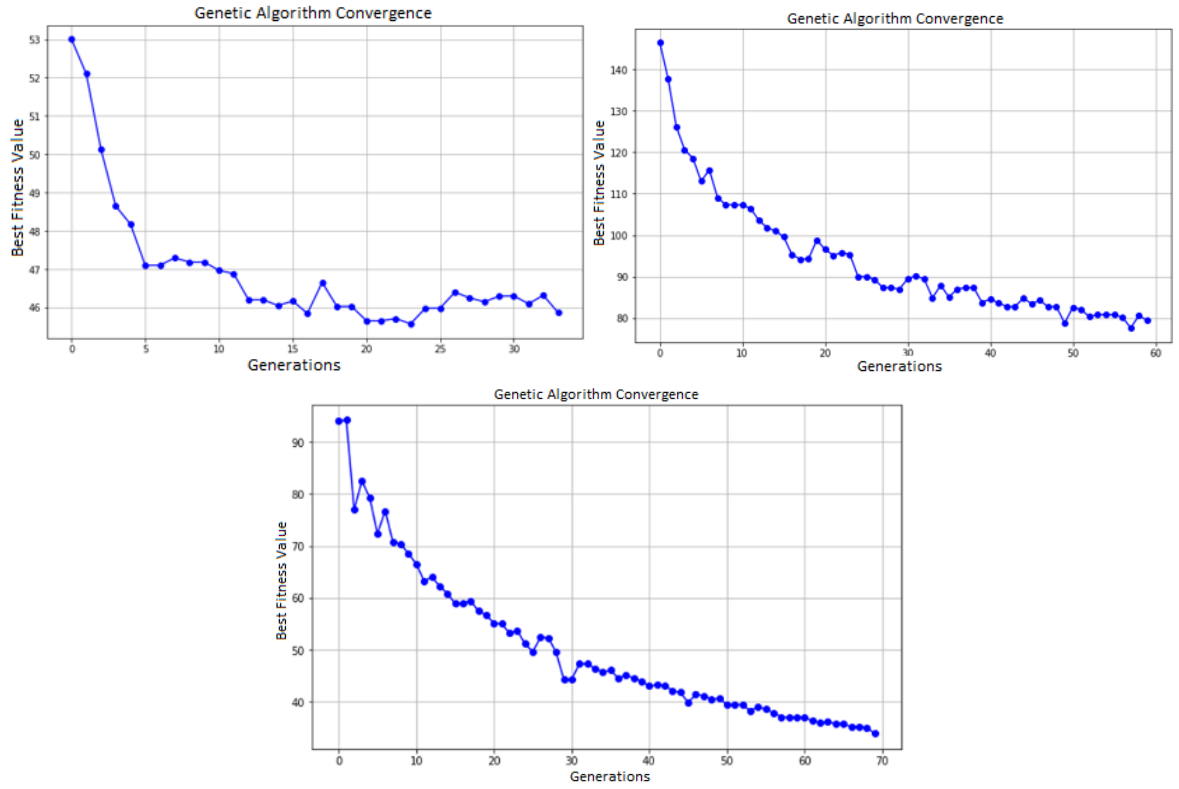

Fig. 13 Convergence graph – Transfer batch 3 – PC 1, PC 2, PC 3 – 87 jobs

This third scenario demonstrates that, although the transfer batch approach has potential, its effectiveness significantly decreases with a substantial increase in the number of jobs. The high delay values suggest that further adjustments in planning and the configuration of the genetic algorithm are necessary to efficiently handle larger workloads.

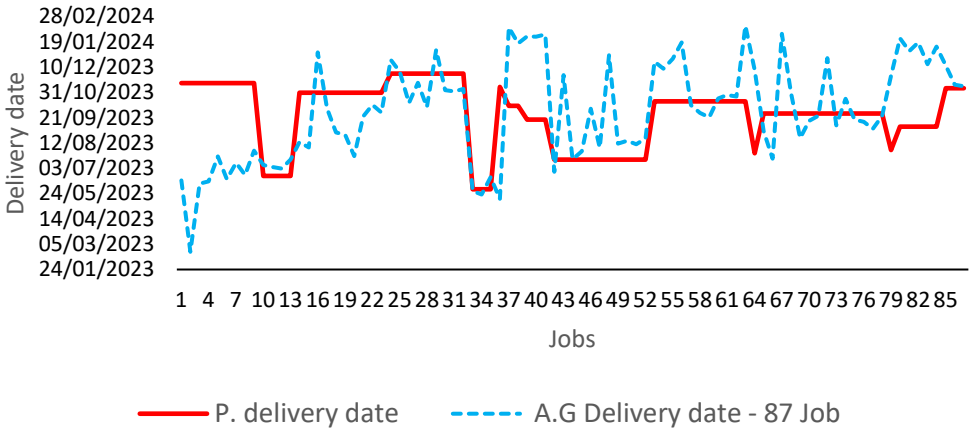

Fig. 14 Real delivery performance vs GA – 87 jobs

5.6 Genetic Algorithm vs. Tabu Search for HFS

The Genetic Algorithm approach was compared with another well-studied method known as Tabu Search (TS). TS is a metaheuristic based on local search, whose primary objective is to escape local optima and efficiently explore the solution space through adaptive memory, known as the tabu list [10].

By applying Tabu Search to the case study and comparing it with GA, Scenario 2, previously described, was evaluated. This scenario had previously demonstrated the best performance using the Genetic Algorithm in terms of execution time (makespan) and total tardiness. Fig. 15

shows the sequencing of jobs in the production centers in a Gantt chart. After analysing the data obtained through TS, slight differences were identified at each stage of Scenario 2. For example, in Production Centre 1 (CP1), the execution time (makespan) was reduced by 8.57 %, while total tardiness and the number of delayed jobs increased by 20.71 % and 9.09 %, respectively, compared to GA.

Likewise, a reduction was observed compared to GA in the completion time (makespan), total tardiness, and the number of delayed jobs by 6.4 %, 47 %, and 44.44 %, respectively. For Production Centre 3 (CP3), the data is particularly significant, as it evaluates how closely the planned in Production Centre 2 (CP2), completion time of 370 days is achieved. In this centre, an increase of 3.01 % in the makespan was observed when employing the TS method. Additionally, 12 delayed jobs were recorded compared to the 8 delayed jobs obtained using GA.

Table 6 provides a summary of the results obtained through both methods, highlighting the differences in their performance and showcasing the behaviour of TS as an effective alternative for solving the problem under study.

Table 6 Results of scenario 2, AG and TS

Metrics	Scenario 2					
	CP1		CP2		CP3	
	AG	TS	AG	TS	AG	TS
Makespan	**290,09**	**267,2**	**300**	**282,9**	**361,29**	**372,5**
Weighted Tardiness	13,04	15,74	19,56	9,19	6,27	5,13
Number of Delays	24	0	27	12	8	12

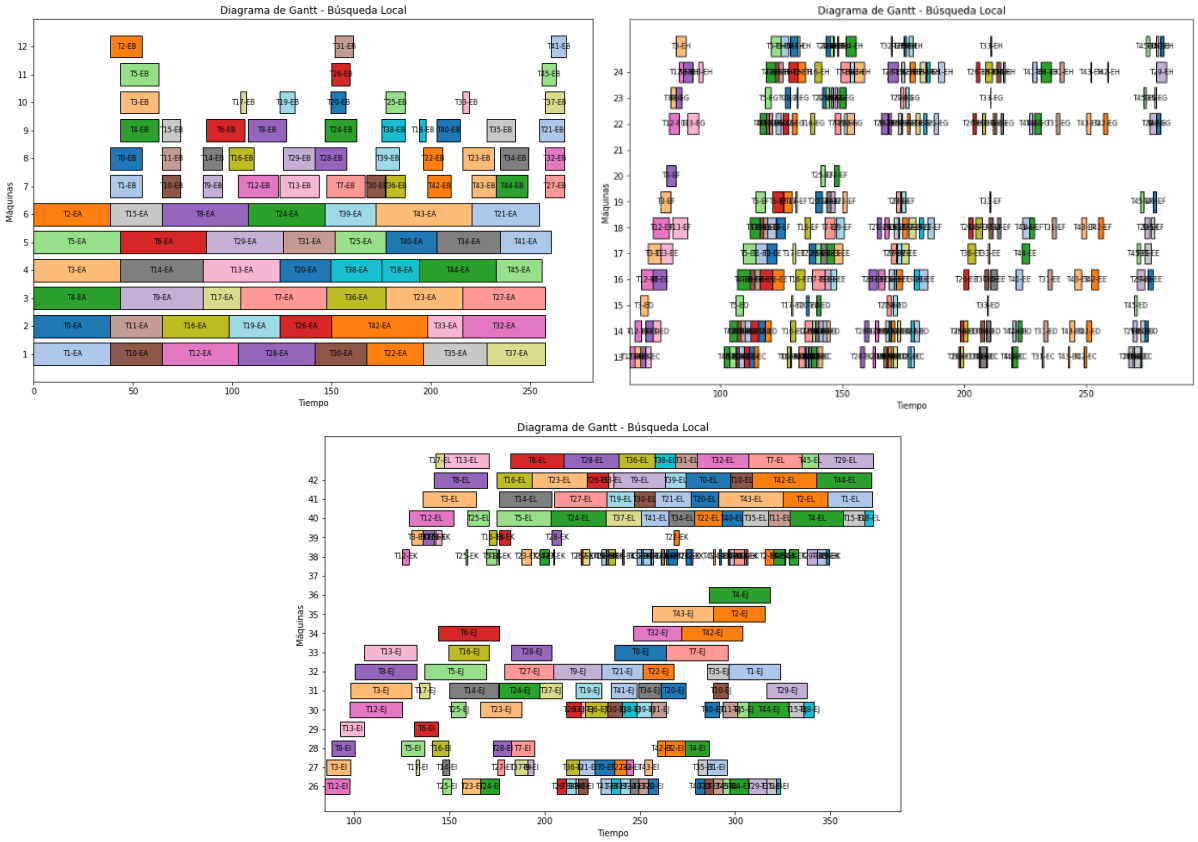

Fig. 15 Gantt chart – Transfer batch 2 – PC 1, PC 2, PC 3 – 46 jobs – TS

A comparative analysis of the two methods reveals very similar behaviour. As shown in Fig. 16, jobs tend to meet the planned delivery dates. However, in both methods, there are jobs that exceed the planned times. It is determined that the GA meets the planned makespan constraint

of 370 days and results with a lower number of delays. Nevertheless, the results obtained with Tabu Search (TS) demonstrate it can be considered like an alternative approach for achieving positive outcomes in FHFS production environments.

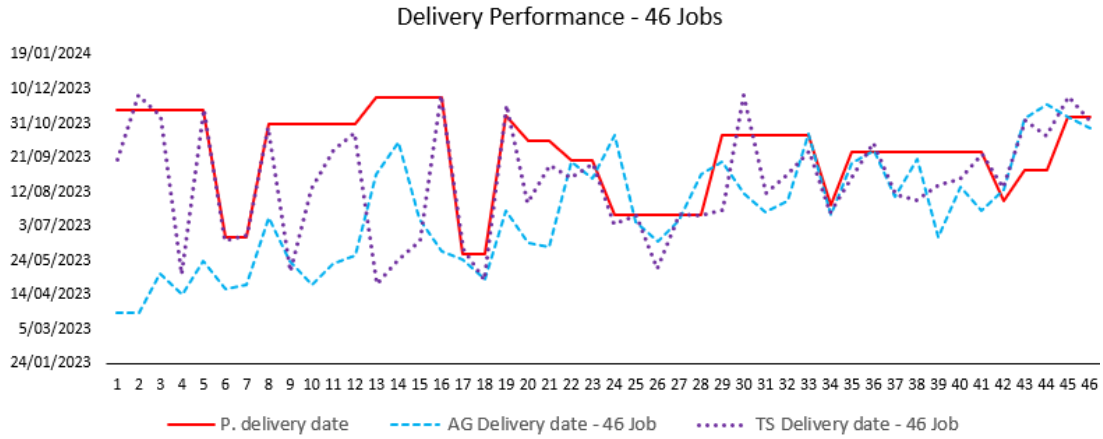

Fig. 16 TS vs GA performance – 46 jobs

5.7 Evaluation of robustness under disruptive production environments

In the context of production planning in real-world environments, it is common to face significant disruptions that hinder the achievement of objectives within the planned time horizon. These disruptions include machine failures or shutdowns and the introduction of new orders with tight delivery schedules.

To evaluate the performance and robustness of the Genetic Algorithm (GA) under these conditions, modifications to the algorithm were introduced, and two test instances were generated using the transfer batch from Scenario 2. In the first instance (AG-1), machines were randomly selected across different production centres, simulating their inactivity. In the second instance (AG-2), eight new jobs with various products, delivery times, and release times were added. The corresponding simulations were conducted, consolidating the results in Table 7, which allowed for analysing the impact of these disruptions on the algorithm's performance.

The results obtained show that disturbances in the evaluated scenarios have a significant impact on makespan and total tardiness, especially in more complex environments such as Production Centre 3 (CP3). It is observed that, in general, both indicators tend to increase in the disturbed scenarios (AG-1 and AG-2) compared to the baseline scenario (AG).

Table 7 Results of scenario 2, different environments

	CP 1			CP 2			CP 3		
	AG	AG - 1	AG - 2	AG	AG - 1	AG - 2	AG	AG - 1	AG - 2
Makespan	**290.1**	**339.9**	**325.0**	**300.0**	**350.8**	**345.2**	**361.3**	**421.0**	**436.5**
Total Tardiness	13.04	32.98	16.34	19.56	40.62	33.92	6.27	25.46	44.75
Number Delays	24	27	24	27	33	26	8	18	20

5.8 Computational time

Based on the data in Table 8, a growing trend in CPU time is observed as the number of jobs increases. In Scenario 1, with 27 jobs, CPU time ranges between 22 and 72 minutes, being the lowest compared to the other scenarios. In Scenario 2, with 46 jobs, CPU time progressively increases from 62 to 142 units as the stages advance. Finally, in Scenario 3, with 87 jobs, the highest CPU times are recorded, rising from 76 to 304 minutes.

Likewise, there is a correlation between CPU time and makespan; as the makespan increases, CPU time also tends to grow. This is clear in Scenario 3, Stage 3, where the makespan reaches 443.0, and CPU time registers its highest value (304 minutes). In conclusion, the number of jobs and the computational load required in later stages significantly increase CPU time. This sug-

gests that the Genetic Algorithm (GA) solution demands greater computational time as the size and complexity of the problem increase.

Table 8 Performance metrics and CPU time in FHFS

Solution	Flexible Flow Shop Scheduling							
	Scenario	Stage	Makespan	F.O (Z)	T. Tardiness	Jobs	N° Delays	CPU Time
Actual (empirical)	*	*	**538**	*	**1.933**	27	25	**5040**
AG	1	1	243	124.93	6.8	27	13	22
		2	263	134.5	6.1	27	12	43
		3	**502**	262.5	23.1	27	10	**72**
	2	1	290	151.6	13.0	46	24	62
		2	300	159.8	19.6	46	27	97
		3	**361**	183.8	6.3	46	8	**142**
	3	1	366	206	45.6	87	50	76
		2	379	228.2	88.8	87	78	186
		3	**443**	254.8	34.1	87	45	**304**

6. Conclusion

The results of this research demonstrate that the proposed model for production scheduling, sequencing, and control achieves significant reductions in both makespan and tardiness. In Scenario 2, a makespan of 361.29 days was achieved, representing a 32.85 % improvement compared to the 538 days of the current model. Similarly, tardiness was reduced from 96 % to 17.4 %, significantly enhancing customer satisfaction and operational efficiency.

In addition, the comparative analysis between the GA and TS (Tabu Search) methods reveals similar behaviours in job scheduling. Regarding the planned completion time of 370 days, the GA achieved a 2.41 % reduction, while the TS showed a 0.54 % increase. Furthermore, 8 delays were observed with the GA compared to 12 with the TS. Based on these results, the GA method is identified as the most suitable tool for addressing scenarios like the one presented in the case study.

Also, it was observed that CPU time is directly influenced by the number of jobs, the size of the makespan, and the number of machines at each stage. This suggests that, as the size and complexity of the problem increase, the solution based on the Genetic Algorithm requires more computational time.

A key advantage of the model is the substantial reduction in scheduling time when using the Genetic Algorithm (GA) compared to manual methods using transfer batches. Results showed this approach improves resource allocation, ensures more efficient deliveries, and has proven to be robust, adapting to various production scenarios. Additionally, it offers flexibility to meet the specific needs of other production systems, allowing customization based on the characteristics of the environment, such as product types, machine capacities, and operational constraints. This makes it applicable to various production models, including hybrid flow shops, assembly lines, cellular manufacturing systems, and batch production configurations.

Finally, as an opportunity for future research, the development of algorithms that allow dynamic inputs for real-time decision-making is proposed. The incorporation of variables such as maintenance, inventory, and logistics could significantly expand the applicability of the model to different industrial sectors.

References

[1] Xu, W., Sun, H.Y., Awaga, A.L., Yan, Y., Cui, J.Y. (2022). Optimization approaches for solving production scheduling problem: A brief overview and a case study for hybrid flow shop using genetic algorithms, *Advances in Production Engineering & Management,* Vol. 17, No. 1. 45-56, doi: 10.14743/apem2022.1.420.

[2] Gupta, J.N.D., Krüger, K., Lauff, V., Werner, F., Sotskov, Y.N. (2002). Heuristic for hybrid flow shops with controllable processing times and asignable due dates, *Computers & Operations Research,* Vol. 29, No. 10, 1417-1439, doi: 10.1016/S0305-0548(01)00040-5.

[3] Hornig, E.S., Guarachi, R.A.S. (2015). Improved genetic algorithm for total tardiness minimization in a flexible flowshop with sequence-dependent setup times, *Ingeniare. Revista chilena de ingeniería,* Vol. 23, No. 1, 118-127, doi: 10.4067/S0718-33052015000100014.
[4] Jeen, R.R.B., Rajkumar, R. (2017). An effective genetic algorithm for flow shop scheduling problems to minimize makespan, *Mechanika,* Vol. 23, No. 4, 594-603, doi: 10.5755/j01.mech.23.4.15053.
[5] Kazemi, H., Mahdavi Mazdeh, M., Rostami, M. (2017). The two-stage assembly flow-shop scheduling problem with batching and delivery, *Engineering Applications of Artificial Intelligence,* Vol. 63, No. 1, 98-107, doi: 10.1016/j.engappai.2017.05.004.
[6] Najarro, R., López, R., Racines, R.E., Puris, A. (2017). An hybrid genetic algorithm to optimization of flow shop scheduling problems under real environments constraints, *Enfoque UTE,* Vol. 8, No. 5. 14-25, doi: 10.29019/ enfoqueute.v8n5.176.
[7] Ouled bedhief, A., Dridi, N. (2019). Minimizing makespan in a three-stage hybrid flow shop with dedicated machines, *International Journal of Industrial Engineering Computations,* Vol. 10, 161-176, doi: 10.5267/j.ijiec.2018.10.001.
[8] Tian, X.K., Ma, B.C., Zhang, J.W., Zhao, R.Y., Wang, J. (2019). Research on multi-objective optimization and simulation to HFSSP hybrid flow-shop scheduling problem for energy saving, *IOP Conference Series: Materials Science and Engineering,* Vol. 504, Article No. 012108, doi: 10.1088/1757-899X/504/1/012108.
[9] Wang, S., Wang, X., Chu, F., Yu, J. (2019). An energy-efficient two-stage hybrid flow shop scheduling problem in a glass production, *International Journal of Production Research,* Vol. 58, No. 8, 2283-2314, doi: 10.1080/00207543.2019.1624857.
[10] Fangrit, W, Yap, H.J., Hamza, M.F., Chang, S.-W., Yap, K.S., Wong, S.Y. (2020). An efficiency improvement of flexible flow shop scheduling in automotive part company, *Intelligent Decision Technologies,* Vol. 14, No. 4, 493-506, doi: 10.3233/IDT-200006.
[11] Espitia Méndez, J.A., Mendoza Rojas, G.L. (2021). Methodology based on genetic algorithm for a textil industry company production scheduling, *Ingeniería Investigación y Tecnología,* Vol. 22, No. 4, 1-16, doi: 10.22201/fi.25940732e.2021.22.4.032.
[12] Chen, D., Zhao, X.R. (2021). Production management of hybrid flow shop based on genetic algorithm, *International Journal of Simulation Modelling,* Vol. 20, No. 3, 571-582, doi: 10.2507/IJSIMM20-3-CO12.
[13] Istokovic, D., Perinic, M., Boric, A. (2021). Determining the minimum waiting times in a hybrid flow shop using simulation-optimization approach, *Tehnički Vjesnik – Technical Gazette,* Vol. 28, No. 2, 568-575, doi: 10.17559/TV-20210216132702.
[14] Ren, J.F., Ye, C.M., Li, Y. (2021). A new solution to distributed permutation flow shop scheduling problem based on NASH Q-Learning, *Advances in Production Engineering & Management,* Vol. 16, No. 3, 269-284, doi: 10.14743/apem2021.3.399.
[15] Hasani, A., Hosseini, S.M.H., Sana, S.S. (2022). Scheduling in a flexible flow shop with unrelated parallel machines and machine-dependent process stages: Trade-off between Makespan and production costs, *Sustainability Analytics and Modeling,* Vol. 2, Article No. 100010, doi: 10.1016/j.samod.2022.100010.
[16] López, J.C., Giraldo, J.A., Arango, J.A. (2015). Reduction of the makespan in scheduling the production of a hybrid-flexible flow shop (HFS), *Información Tecnológica,* Vol. 26, No. 3, 157-172, doi: 10.4067/S0718-07642015000300019.
[17] Han, J.H., Lee, J.Y. (2023). Genetic algorithm-based approach for makespan minimization in a flow shop with queue time limits and skipping jobs, *Advances in Production Engineering & Management,* Vol. 18, No. 2. 152-162, doi: 10.14743/apem2023.2.463.
[18] Jones Martínez, S., Castillo Corrales, A., Arce Obando, J., Álvarez González, M., Rivera Leaver, D. (2023). Multi-objective partially flexible job-shop scheduling problem, based on a genetic natural selection algorithm, *Revista de Iniciación Científica,* Vol. 9, No. 1. 81-89, doi: 10.33412/rev-ric.v9.1.3561.
[19] Gutiérrez Reina, D., Tapia Córdoba, A., Rodríguez del Nozal, A. (2020). *Algoritmos Genéticos con Python: Un enfoque práctico para resolver problemas de ingeniería,* Marcombo, Madrid, España.
[20] Xu, E.B., Yang, M.S., Li, Y., Gao, X.Q., Wang, Z.Y., Ren, L.J. (2021). A multi-objective selective maintenance optimization method for series-parallel systems using NSGA-III and NSGA-II evolutionary algorithms, *Advances in Production Engineering & Management,* Vol. 16, No. 3, 372-384, doi: 10.14743/apem2021.3.407.
[21] Graham, R.L., Lawler, E.L., Lenstra, J.K., Kan, A.H.G.R. (1979). Optimization and approximation in deterministic sequencing and scheduling: A survey, *Annals of Discrite Mathematics,* Vol. 5, 287-326, doi: 10.1016/S0167-5060(08)70356-X.

APEM journal

Advances in Production Engineering & Management
Volume 19 | Number 4 | December 2024 | pp 435–442
https://doi.org/10.14743/apem2024.4.517

ISSN 1854-6250
Journal home: apem-journal.org
Original scientific paper

Reducing scrap in long rolled round steel bars using Genetic Programming after ultrasonic testing

Kovacic, M.[a,b,c,*], **Zupanc, A.**[a], **Zuperl, U.**[d], **Brezocnik, M.**[d]

[a]ŠTORE STEEL, d.o.o., Research and Development, Štore, Slovenia
[b]University of Ljubljana, Faculty of Mechanical Engineering, Laboratory for Fluid Dynamics and Thermodynamics, Ljubljana, Slovenia
[c]College of Industrial Engineering, Celje, Slovenia
[d]University of Maribor, Faculty of mechanical engineering, Maribor, Slovenia

ABSTRACT

At Štore Steel Ltd., continuously cast billets (180 mm × 180 mm) are reheated and rolled after cooling to room temperature. Hot-rolled bars are controlled as they cool to room temperature in specially designed cooling chambers, minimizing residual stresses and the development of pre-existing surface and internal defects. The bar ends can be additionally covered with insulating material. The cooled, rolled bars undergo examination using automated control lines to detect surface and internal defects, which primarily originate from the casting process. Internal defects are identified using ultrasonic testing. Between January 2022 and June 2023, 1550.0 tons of 61SiCr7 rolled bars, with diameters ranging from 53 mm to 72 mm and lengths from 7010 mm to 7955 mm, were examined using ultrasonic testing. The scrap was 109.6 tons (7.07 %). After collecting data on chemical composition (C, Si, Mn, Cr, Mo, Ni content), the casting process (casting temperature, cooling water pressure and flow in the first, second, and third zones of secondary cooling, as well as the temperature difference between input and output mould cooling water), and rolled bar geometry (diameter, length), scrap modelling after ultrasonic testing was carried using genetic programming. The genetic programming model suggested reducing the length of the rolled bar. Due to length multiplication, it was possible to reduce the rolled bar length from the initial lengths of 7010-7955 mm to the current lengths of 4558-6720 mm in June 2023. Based on this adjustment, a new production of rolled bars was established. By August 2024, 1251.9 tons of 61SiCr7 rolled bars were produced with the mentioned length adjustments. These rolled bars were subsequently examined using ultrasonic testing. The scrap was reduced by nearly 14 times, amounting to only 8.1 tons (0.64 %).

ARTICLE INFO

Keywords:
Steel industry;
Rolling;
Long bars;
Ultrasonic testing;
Scrap;
Defects;
Modelling;
Genetic programming

**Corresponding author:*
miha.kovacic@store-steel.si
(Kovacic, M.)

Article history:
Received 2 September 2024
Revised 5 December 2024
Accepted 9 December 2024

1. Introduction

In the steel industry, the solidified steel is usually cooled to room temperature, additionally heated and hot deformed. Warm deformation is usually conducted during rolling. Rolled material is often further processed, either through heat treatment or mechanical methods. Consequently, the quality of the cast semi-finished product directly impacts the quality of the rolled and subsequently processed material. Thermo-mechanically induced defects, which may arise during or after plastic deformation and originate from the solidification process, can be minimized or eliminated either by addressing their root causes (e.g., melt preparation, casting parameters) [1-3] or reducing the

consequences of the post-processed material (e.g., reduction of residual stresses, heat treatment, appropriate deformation during deformation) [4-7].

A review of the literature reveals that research on the deformation of cast semi-products with surface and internal defects, as well as their post-processing, has been ongoing for several decades [6-8]. However, investigating the behaviour of surface and internal defects in cast semi-finished products during and after deformation, particularly in industrial environments, continues to be a significant priority.

The authors in [7] analysed the influence of the orientation of surface and internal defects of continuously cast steel ingots on occurrence of defects on rolled material. Smooth flat rolls were used for the deformation process. They found that with an optimal orientation angle of the internal defects, their complete elimination is achievable.

Similarly, in [9], the authors analysed the influences of previously deformed continuously cast billets of chromium steel grades on the structure and properties of seamless pipe produced with radial-shear rolling in Pervoural'sk New Pipe Plant JSC. Their analysis of the cast macrostructure and the seamless pipe microstructure revealed that grain refinement depends on the preliminary deformation and the resulting changes in the cast macrostructure, which can be further adjusted through heat treatment. Accordingly, the required properties of seamless pipe can be achieved.

The authors in [8] describe the optimization of groove geometry, which influences the occurrence of ductility cracks during hot rolling of the remaining brittle dendritic macrostructure from the solidification process. Based on finite element simulations, the changes of the groove geometry have been made to reduce strains and stresses that promote crack openings. As a result, ductility cracks were no longer occurred.

A similar approach was used in [10], where the 3D finite element method was used to analyze the effect of stresses occurring during the three-roll planetary rolling process on existing internal voids and newly formed internal cracks. Furthermore, experimental rolling of bismuth-containing austenitic stainless steel bars was performed. The study found that the most important parameters were rolling elongation and temperature. Rolling elongation is primarily influenced by discontinuous contact between the rolls.

The article [11] investigates cross-wedge rolling of Inconel 718 for aero-engine blades to reduce internal defects. The grain size, heating temperature and rolling speed were monitored. The study found that defects nucleate at the interface between carbide particles and the matrix, subsequently propagating along chain carbides or grain boundaries. Based on sulphur addition, the grain size was reduced, the heating temperature was selected to range from 950 °C to 1020 °C, and the rolling speed was increased. The individual influences of gathered parameters were also calculated and the optimal values selected.

The authors of the study [12] attempted to analyse the occurrence of lamination during forming of seamless tube or pipe. Lamination is essentially a subsurface or surface defect that affects the inner or outer diameter of tube. Lamination can cause additional crack propagation. These types of defects are not easily detected through nondestructive testing. The recrystallization temperature, soaking time, furnace temperature, process parameters and mechanical properties were monitored to predict the surface quality of the final product. Analytical models were used. It was found that process parameters have a significant impact during production of seamless tube.

The influence of process parameters on the occurrence of asymmetrical camber defects during hot rough rolling of plate shapes was studied in [13]. The serial production data from the Xichang Steel was analysed. An Interpretable Prediction Model and Shapley additive explanation models were used to predict the occurrence of asymmetrical camber defects for two steel grades (Q335B and ST12). The theoretical analyses were consistent with the obtained models. The authors also prepared a detailed process optimization plan.

In [14], an attempt to reduce surface cracks during hot charging of high-strength, low-alloy steel thick plates is presented. Hot charging is the processes in which hot cast products (e.g., billets, slabs) are directly transported (without cooling down and reheating) from the steel plant to the rolling mill. Laboratory reports indicated that the presence of austenite in the microstructure significantly increased the size of recrystallized austenite grains, contributing to grain size non-uniformity. Based on the data on microstructure, charging temperature, and recrystallized

austenite content, it was determined that the root cause of surface cracks was the presence of recrystallized austenite. As a result, the hot charging process was optimized. Based on the effort applied, the surface cracks were reduced from 7.38 % to 0.12 %.

The paper [15] presents the evolution of surface cracks that were already present on the cast semi-finished product during the rolling of heavy plates made of carbon-manganese steel. Cut samples of both the cast semi-finished product and the heavy plates were used for microstructural analysis. Additionally, electron microscopy was employed. All analyzed defects exhibited decarburization, indicating that they were present on the cast semi-finished product prior to rolling. To reduce the propagation of existing defects and prevent the occurrence of additional defects, a change in processing parameters was proposed.

This article presents an attempt to reduce the formation of internal defects or the development of defects originating from the casting process using genetic programming. The article begins with an overview of the production and rolling of 61SiCr7 rolled bars, ranging from a diameter of 53 mm to 72 mm and a length of 7010 mm to 7955 mm. After collecting data on chemical composition, casting process, and rolled bar geometry, the article describes in detail the modelling of scrap after ultrasonic testing using genetic programming. Following the modelling results, efficient practical implementations are presented, and future work is suggested in the conclusion.

2. Materials and methods

2.1 Materials and experimental setup

Production at Štore Steel plant starts with the scrap melting in an electric arc furnace, tapping, ladle treatment (i.e. secondary metallurgy) and continuous casting of billets (180 mm × 180 mm). The billets can be additionally heat-treated or control cooled under hoods. The cast billets are then reheated and rolled in the rolling plant using three rolling stands. The first two stands are duo reversible stands (800 mm and 650 mm diameter rolls), and the final continuous rolling line (460 mm diameter rolls) consists of 6 horizontal and 4 vertical stands. The cooling bed is equipped with the hoods that are adjusted according to the steel grades and the geometry of the rolled bars. The bars can be stacked individually or in pairs in cooling bed. After leaving the cooling bed, the rolled bars are cut according to the customer requirements and automatically bonded in the bundle. The bundles are transported by overhead cranes to additional cooling chambers. When the bars enter the cooling chamber, the temperature of the material is at least 500 °C. The bar ends are additionally covered with insulation material. After at least 24 hours of cooling in the chambers, the bars can be straightened, examined for internal soundness and surface quality, cut, sawed, chamfered, drilled, and peeled.

Rolled round bars can be examined (internal and surface control) using an automatic control line. Internal defects are detected using the Karl Deutsch ECHOGRAPH Ultrasonic Flaw Detector. The root causes of internal defects are typically shrinkage porosity, centre porosity, and segregations, which are linked to the solidification process – in our case, the continuous casting process. The introduction of additional stresses (e.g., bar end cutting, straightening, cooling, heating) and the presence of residual stresses increase the likelihood of internal cracking in the rolled bars. Fig. 1 shows rolled round bars with insulating material (cloths) in a cooling chamber. The ends of the three longer bars in Fig. 1 are not covered with insulating material, increasing the risk of thermally induced cracking during cooling in the chamber.

61SiCr7 is commonly used for heavy-duty springs (e.g., flat, round, and helical), as well as stabilizers and torsion bars. Between January 2022 and June 2023, 1550 tons of 61SiCr7 rolled bars, with diameters ranging from 53 mm to 72 mm and lengths from 7010 mm to 7955 mm, were inspected using an automatic control line and the Karl Deutsch ECHOGRAPH Ultrasonic Flaw Detector. A total of 152 instances were recorded, where the inspected quantity of an individual product varied from 0.8 tons to 37 tons. The scrap rate varied from 0 % to 100 %. The total scrap amount was 109.6 tons, accounting for 7.07 % of the total. To reduce the occurrence of internal defects of 61SiCr7 steel, several parameters were gathered:

- Chemical composition: Content of carbon (C), silicon (Si), manganese (Mn), chromium (Cr), molybdenum (Mo) and nickel (Ni) (%).
- Casting parameters:
  - The average temperature of the melt in tundish (TEMP) (°C).
  - The average difference between input and output mould cooling water temperature (DELTAT) (°C).
  - The average cooling water pressure (bar) and flow (l/min) in the first (directly below the mould) (Z1P, Z1Q), second (Z2P, Z2Q) and third zone (Z3P, Z3Q) of secondary cooling.
- Rolled bar diameter (DIA).
- Rolled bar length (LONG).
- Scrap ratio after ultrasonic testing using Karl Deutsch ECHOGRAPH Ultrasonic Flaw Detector (i.e. ratio between scrap and examined material quantity).

Based on gathered data, a correlation between influential parameters and the scrap ratio using genetic programming was established.

Fig. 1 The rolled round bars with insulation material (cloths) in the cooling chamber

2.2 Used methods

The scrap ratio after ultrasonic testing with Karl Deutsch ECHOGRAPH Ultrasonic Flaw Detector was predicted using genetic programming, a method belonging to the field of evolutionary computation.

Evolutionary computation is inspired by natural evolutionary processes such as selection, crossover, and mutation. Two of the most well-known methods in evolutionary computing are genetic algorithms and genetic programming. Genetic algorithms focus on finding optimal solutions by simulating evolutionary processes, where solutions evolve over generations. Genetic programming is an extension of this, where computer programs (i.e., predictive models for description of the studied system) themselves are generated and evolved to solve specific tasks. These methods are highly versatile and can be applied across various fields, including optimization, machine learning, prediction, engineering, and data analysis, as they allow for the discovery of solutions to complex problems without the need for predefined solutions [19-22].

In genetic programming, the computer programs (e.g., predictive models) consist of genes that can be selected functions (e.g., essential arithmetical functions), selected input variables, and random constants. For more details on genetic programming, please refer primarily to sources [16-18]. Based on selected genes, random mathematical expressions are built at the beginning of the simulated evolution. For this research, basic arithmetic operations (i.e., addition, subtraction, multiplication, and division) were utilized as functions. Selected input variables (parameters)

included factors such as carbon content (*C*), the average difference between the input and output mould cooling water temperatures (*DELTAT*), rolled bar diameter (*DIA*), etc. A comprehensive list of variables is provided in Subsection 2.1 (since they are now considered as variables, they are presented in italics). Predictive models are constantly being modified with genetic operations during several generations. In the research, we used crossover and mutation operations to modify organisms. The reproduction operation was incorporated as a standard mechanism to enhance the probability of higher-fitness organisms progressing to subsequent generations. After the completion predictive models' modification, a new generation is obtained. All predictive models are evaluated using the fitness function. In this study, the average of absolute differences between the actual and predicted scrap ratio was chosen as the fitness function. The process is repeated until the termination criterion is fulfilled. For this research, the termination criterion was defined as reaching the maximum prescribed number of generations.

3. Results and discussion

We developed a general-purpose genetic programming system to model predictive models [23-26]. This self-developed system was designed to handle a wide range of tasks, enabling the effective evolution of models tailored to specific prediction needs. After performing 100 runs of the genetic programming system, we analysed the results and obtained the best predictive model for predicting the scrap ratio after ultrasonic testing. The resulting model is as follows.

$$\frac{DIA}{DIA-\frac{\left(Mo+\frac{LONG}{-Cr+\frac{DELTAT}{Ni}}+2\,Si+Z2P+Z3P+\frac{Cr\,Z3P}{DIA\,(DELTAT+Z2Q)}\right)\left(Mo-\frac{Z1P\left(DIA-\frac{Z3P\left(-DELTAT+Mo+\frac{DELTAT}{Ni}+Si+Z3P\right)}{DELTAT}\right)}{C\left(TEMP+\frac{LONG}{\frac{DELTAT}{Ni}-Z2Q}\right)}\right)}{LONG\,Mo}} \quad (1)$$

The average of absolute differences between the actual and predicted scrap rate is 5.96 %. Additionally, it is necessary to note that the genetically developed model does not contain the following parameters: *Z1Q* (average cooling water flow in the first zone of secondary cooling), *Z3Q* (average cooling water flow in the first zone of secondary cooling) and *Mn* (manganese content). Similarly, while checking the developed models from other runs obtained using genetic programming, it can be concluded that the *LONG* (rolled bar length) is one of the top 5 (out of 16) parameters which were not excluded from the developed models. The number of excluded parameters is presented in Fig. 2.

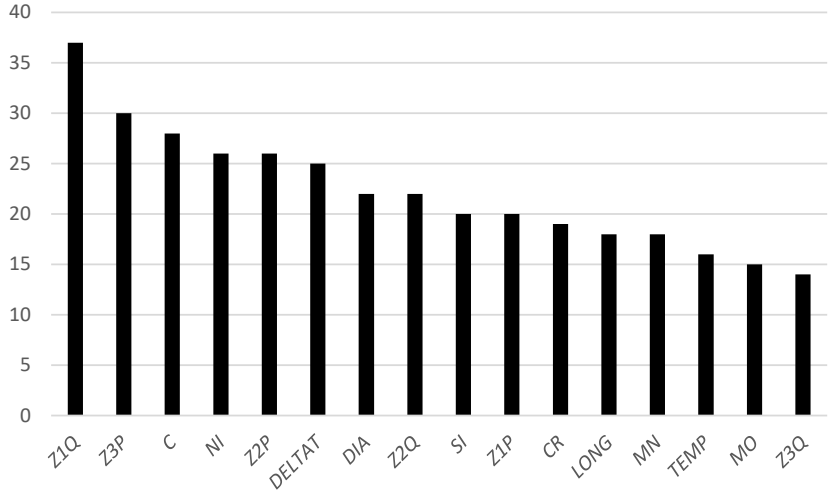

Fig. 2 The number of excluded parameters from 100 genetically developed models

Additionally, the influences of individual parameters can be calculated using a genetic programming model. When changing the values within the actual interval of individual parameters, the values of the other parameters remained the same. The results of the genetic programming model are shown in Fig. 3. The length of the rolled bars (parameter *LONG*) appears to be the most influential factor, with scrap rates ranging from 93.81 % to 100.05 %.

Based on the technical delivery conditions, required chemical composition, rolled bar diameter, post-rolling treatment in cooling chambers, the number of parameters extracted from 100 genetically developed models, and the calculated effects of individual parameters using genetic programming, the only viable option was to change the length of the rolled bars. It should be emphasized that length multiplications were possible.

For informational purposes, in this phase of the research, we envisioned shorter rolled bar lengths from 4558-6720 mm (until now, we have been producing bars with lengths of 7010-7955 mm) to be used with the obtained genetic programming model. Other parameters gathered from January 2022 to June 2023 remained the same. The genetically developed model predicted that the scrap rate would be 0.00 % (currently 7.07 %) if shorter bars were used.

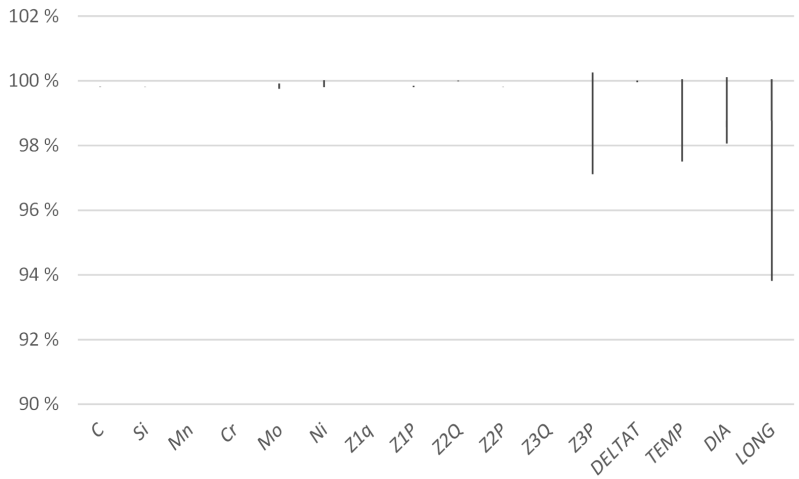

Fig. 3 The calculated influences of individual parameters using genetic programming model

Validation of modelling results

Based on the modelling results and the length multiplications, the rolled bar lengths were reduced from the initial range of 7010-7955 mm to 4558-6720 mm for all orders starting from June 2023. By August 2024, a total of 1251.9 tons of 61SiCr7 rolled bars with adjusted lengths had been examined using ultrasonic testing. As a result, scrap was reduced by nearly 14 times, amounting to only 8.1 tons (0.64 %). This result clearly demonstrates that with relatively simple measures, we can reduce the carbon footprint in the steel processing industry and thus contribute to environmental sustainability.

4. Conclusion

This paper examines the use of genetic programming to reduce internal defects in 61SiCr7 steel bars originating from the casting process. The billets are reheated, rolled, and cooled in a controlled cooling bed, followed by further treatment in cooling chambers. After cooling, the bars are inspected, straightened, and cut.

Internal defects, such as porosity and segregations, are detected using the Karl Deutsch ECHOGRAPH Ultrasonic Flaw Detector. A total of 1550 tons of 61SiCr7 bars were examined, with a scrap rate ranging from 0 % to 100 %, resulting in 109.6 tons of scrap (7.07 %).

Data on chemical composition, casting conditions, and bar geometry were used to develop a genetic programming model to predict the scrap rate. The model achieved an average error of 5.96 %, and the most influential parameter was the bar length (*LONG*). Shortening the rolled bars from 7010-7955 mm to 4558-6720 mm resulted in a predicted reduction in scrap to 0.00 %.

Since June 2023, all orders have been produced using shorter bar lengths, as suggested by the research, leading to a significant reduction in scrap by nearly 14 times. By August 2024, a total of 1251.9 tons of bars had been examined, and only 8.1 tons (0.64 %) of scrap were produced, demonstrating the effectiveness of the length adjustments in minimizing waste. This approach also significantly improves the carbon footprint, contributing to a greener and more sustainable production process.

Future plans include optimizing the cooling processes in continuous casting to improve internal quality and exploring the potential for shortening bars for other steel grades and shapes.

References

[1] Kovacic, M., Zuperl, U., Gusel, L., Brezocnik, M. (2023). Reduction of surface defects by optimization of casting speed using genetic programming: An industrial case study, *Advances in Production Engineering & Management*, Vol. 18, No. 4, 501-511, doi: 10.14743/apem2023.4.488.

[2] Kovačič, M., Župerl, U. (2023). Continuous caster final electromagnetic stirrers position optimization using genetic programming, *Materials and Manufacturing Processes*, Vol. 38, No. 16, 2009-2017, doi: 10.1080/10426914.2023.2219317.

[3] Kovacic, M., Zuperl, U., Brezocnik, M. (2022). Optimization of the rhomboidity of continuously cast billets using linear regression and genetic programming: A real industrial study, *Advances in Production Engineering & Management*, Vol. 17, No. 4, 469-478, doi: 10.14743/apem2022.4.449.

[4] Kovačič, M., Zupanc, A., Vertnik, R., Župerl, U. (2024). Optimization of billet cooling after continuous casting using genetic programming – Industrial study, *Metals*, Vol. 14, No. 7, Article No. 819, doi: 10.3390/met14070819.

[5] Kirpichnikov, M.S., Sinitsyn, E.O., Borovinskikh, M.P. (2011). Heat treatment technology for roll billets of steel 150KhNM for improving their quality and operating life, *Metallurgist*, Vol. 54, No. 11-12, 791-793, doi: 10.1007/s11015-011-9375-9.

[6] Lukin, S.V., Levashev, K.Y. (2019). Improvement of heat-treatment conditions for square-cross-section steel billets downstream of a continuous-section billet casting machine, *Metallurgist*, Vol. 63, No. 3, 249-256, doi: 10.1007/s11015-019-00818-7.

[7] Smirnov, E.N., Sklyar, V.A., Smirnov, O.E., Belevitin, V.A., Pivovarov, R.E. (2018). Behavior of structural defects of already-deformed continuous-cast bar on rolling, *Steel in Translation*, Vol. 48, 289-295, doi: 10.3103/S0967091218050091.

[8] Coppola, T., Vici, F.D., Gotti, A., Langellotto, L., Notargiacomo, S. (2014). Plastic deformation and metallurgical evolution modelling for defects reduction and quality optimization, *Procedia Engineering*, Vol. 81, 1240-1245, doi: 10.1016/j.proeng.2014.10.104.

[9] Galkin, S.P., Aleschenko, A.S., Romantsev, B.A., Gamin, Y.V., Iskhakov, R.V. (2021). Effect of preliminary deformation of continuously cast billets by radial-shear rolling on the structure and properties of hot-rolled chromium-containing steel pipes, *Metallurgist*, Vol. 65, No. 1, 185-195, doi: 10.1007/s11015-021-01147-4.

[10] Li, L., Li, J., Ye, B. (2022). Internal damage mechanism and deformation process window of a free-cutting stainless steel bar rolled by three-roll planetary mill, *Journal of Materials Engineering and Performance*, Vol. 31, 1187-1194, doi: 10.1007/s11665-021-06234-w.

[11] Liu, J., Shi, M., Cheng, M., Chen, S., Zhang, S., Vladimir, P. (2024). Susceptibility of internal defects to process parameters and control mechanism of defects in cross wedge rolling of Inconel 718 alloy, *Journal of Manufacturing Processes*, Vol. 125, 337-353, doi: 10.1016/j.jmapro.2024.07.045.

[12] Bag, S., Maity, P. (2023). A case study: Micro analysis on lamination defect of seamless tube, *Materials Today: Proceedings*, Vol. 82, 91-95, doi: 10.1016/j.matpr.2022.11.482.

[13] Tong, P., Zhang, Z., Liu, Q., Liu, X., Luo, X., Ran, H., Lan, T. (2024). Interpretable prediction model for decoupling hot rough rolling camber-process parameters, *Expert Systems with Applications*, Vol. 256, Article No. 124872, doi: 10.1016/j.eswa.2024.124872.

[14] Shen, W., Cheng, G., Zhang, C., Pan, S. (2024). Effect of charging temperature of continuous casting slab on the surface cracks of HSLA steel thick plate, *Engineering Failure Analysis*, Vol. 165, Article No. 108737, doi: 10.1016/j.engfailanal.2024.108737.

[15] Bahrami, A., Kiani Khouzani, M., Mokhtari, S.A., Zareh, S., Yazdan Mehr, M. (2019). Root cause analysis of surface cracks in heavy steel plates during the hot rolling process, *Metals,* Vol. 9, No. 7, Article No. 801, doi: 10.3390/met9070801.

[16] Koza, J.R. (1990). *Genetic programming: A paradigm for genetically breeding populations of computer programs to solve problems,* Stanford University, Department of Computer Science, Stanford, USA.

[17] Koza, J.R. (1994). *Genetic programming II: Automatic discovery of reusable programs,* MIT Press Cambridge, USA.

[18] Koza, J.R., Bennett, F.H., Andre, D., Keane, M.A. (1999). Genetic programming III: Darwinian invention and problem solving [Book Review], *IEEE Transactions on Evolutionary Computation,* Vol. 3, No. 3, 251-253, doi: 10.1109/TEVC.1999.788530.

[19] Ji, Y., Liu, S., Zhou, M., Zhao, Z., Guo, X., Qi, L. (2022). A machine learning and genetic algorithm-based method for predicting width deviation of hot-rolled strip in steel production systems, *Information Sciences*, Vol. 589, 360-375, doi: 10.1016/j.ins.2021.12.063.

[20] Poursina, M., Dehkordi, N.T., Fattahi, A., Mirmohammadi, H. (2012). Application of genetic algorithms to optimization of rolling schedules based on damage mechanics, *Simulation Modelling Practice and Theory*, Vol. 22, 61-73, doi: 10.1016/j.simpat.2011.11.005.
[21] Van, A.-L., Nguyen, T. (2023). Multi-response optimization of burnishing variables for minimizing environmental impacts, *Tehnički Vjesnik – Technical Gazette,* Vol. 30, No. 1, 169-177, doi: 10.17559/TV-20220709090615.
[22] Luo, T., Sun, J., Zhang, G., Li, Z., Li, C. (2023). Analysis of influencing factors of green building energy consumption based on genetic algorithm, *Tehnički Vjesnik – Technical Gazette,* Vol. 30, No. 5, 1486-1495, doi: 10.17559/TV-20230601000689.
[23] Kovačič, M., Župerl, U. (2020). Genetic programming in the steelmaking industry, *Genetic Programming and Evolvable Machines,* Vol. 21, No. 1-2, 99-128, doi: 10.1007/s10710-020-09382-5.
[24] Kovačič, M., Salihu, S., Gantar, G., Župerl, U. (2021). Modeling and optimization of steel machinability with genetic programming: Industrial study, *Metals*, Vol. 11, No. 3, Article No. 426, doi: 10.3390/met11030426.
[25] Kovačič, M., Župerl, U. (2022). Modeling of tensile test results for low alloy steels by linear regression and genetic programming taking into account the non-metallic inclusions, *Metals*, Vol. 12, No. 8, Article No. 1343, doi: 10.3390/met12081343.
[26] Kovačič, M., Lešer, B., Brezocnik, M. (2021). Modelling and optimization of sulfur addition during 70MnVS4 steelmaking: An industrial case study, *Advances in Production Engineering & Management*, Vol. 16, No. 2, 253-261, doi: 10.14743/apem2021.2.398.

APEM journal
Advances in Production Engineering & Management
Volume 19 | Number 4 | December 2024 | pp 443–459
https://doi.org/10.14743/apem2024.4.518
ISSN 1854-6250
Journal home: apem-journal.org
Original scientific paper

Optimizing electric vehicle charging strategies using multi-layer perception-based spatio-temporal prediction of charging station load

Wang, Y.N.[a], **Zhang, Z.J.**[a], **Ping, A.**[a,*], **Wang, R.J.**[a], **Gong, D.Q.**[a]

[a]School of Economics and Management, Beijing Jiaotong University, Beijing, P.R. China

ABSTRACT

The production and sales of electric vehicles have been increasing in line with the gradual adaptation of consumers to electric vehicles, driven by various government policies and subsidies over the past decade. As a result, the deployment of charging facilities, which are essential for supporting electric vehicles, has also been extensive. However, despite the rapid development in scale, charging facilities face challenges such as low utilization during off-peak hours and excessive congestion during peak hours, leading to resource wastage and a diminished user charging experience. To address these issues, this study proposes a spatio-temporal prediction model for charging station load. The model introduces a global spatial enhancement module to simultaneously learn short-range and long-range spatial dependencies in the data, resulting in improved prediction accuracy. The aim of this research is to provide practical guidance in terms of conserving charging resources and enhancing user charging experience based on spatio-temporal prediction effectiveness.

ARTICLE INFO

Keywords:
Electric vehicles;
Spatio-temporal prediction;
Charging station load;
Multi-layer perception (MLP)

**Corresponding author:*
23111184@bjtu.edu.cn
(Ping, A.)

Article history:
Received 6 August 2024
Revised 5 December 2024
Accepted 12 December 2024

1. Introduction

With the increasing awareness of environmental protection and the increasing preciousness of fossil energy, Electric Vehicle (EV) has gradually become a key to address the issues of environmental pollution and energy shortage due to its clean and low-carbon features [1]. Hence, it is evident that the electric vehicle industry has garnered substantial attention and support worldwide. Numerous governments have implemented a range of policy measures to facilitate the development of electric vehicles. The Chinese government, in particular, has demonstrated a high level of commitment to the electric vehicle industry. In recent years, the National Development and Reform Commission, the Ministry of Finance, the Ministry of Industry and Information Technology, and other relevant departments have jointly issued the Notice on Financial Subsidies for the Promotion and Application of New Energy Vehicles (Caijian [2020] No. 86) [2]. With incentives such as financial subsidies, tax incentives and quotas for vehicle purchase targets, the production and sales of electric vehicles have continued to rise in the domestic market. According to the China Association of Automobile Manufacturers (CAAM), the production and sales of new energy vehicles in 2022 were completed at 7,058,000 and 6,887,000 units, respectively, representing year-

on-year growth of 96.9 % and 93.4 %. In the development plan for the future, the Energy Saving and New Energy Technology Roadmap of the China Society of Automotive Engineering expects that by 2025, China's new energy vehicle production and sales will reach 8 million units. In the next five years, the market size of new energy vehicles will grow even more rapidly and is expected to reach 15 million units by 2030 [3]. In addition, the promotion of electric vehicles is a key initiative to promote the development of green transformation in the global power and transportation sectors, and to achieve the strategic goals of carbon peaking and carbon neutrality (dual-carbon), and the Paris Agreement has set a target of 100 million electric vehicles in the world by 2030. This indicates that the number of electric vehicles worldwide has exploded in recent years and will continue to grow in the coming years.

Therefore, electric vehicle charging infrastructure, which is the energy supply for electric vehicles, will develop rapidly under the trend of growth in the number of electric vehicles. To meet the increasingly diverse charging demands of electric vehicle drivers, governments and enterprises at all stages have invested in the construction of charging piles, charging stations and other facilities. However, some issues need to be resolved while the number and scale of charging facilities are expanding. First, 'no pile for vehicles, no vehicle for piles' means that the layout and distribution of electric vehicle charging facilities are not reasonable enough, and the situation has gradually revealed itself. In some regions, the supply of charging piles at charging stations is well below the demand of electric vehicles, and the symptom of charging difficulty has appeared [4]. Simultaneously, in other regions, charging stations are overbuilt with a large number of charging piles lying idle, which is a severe waste of resources. This situation reflects the mismatch between the construction of charging facilities and EV ownership. Moreover, the generally low utilization rate of charging infrastructure is accompanied by the phenomenon of peak congestion. Due to the uneven distribution of charging facilities and the volatility of EV users' charging demand, there are obvious peaks and troughs in the utilization of many charging facilities. Underutilization not only wastes resources, but also reduces the experience of EV users during peak congestion, which in turn affects the acceptance of EVs in the EV consumption market. This study finds that the centrepiece of the above issues is the result of the uneven spatial and temporal spread of EV charging station loads that is specifically evident [5].

A possible solution is to analyse the spatial and temporal distribution patterns of loads at EV charging stations and use them as a basis for predicting the spatial and temporal distribution of loads [6]. The main contributions of this study are summarized as follows:

- We built the model structure with higher prediction performance for loaded spatio-temporal data.
- In the spatio-temporal prediction model, we innovatively built a global spatial enhancement module, which enables the model to learn global spatial information directly. Compared with the traditional convolutional learning method that gradually improves the sensory field by stacking, the global spatial reinforcement module improves the model's learning effect on the spatial-dependent features of charging station loading over long distances.
- In terms of prediction model accuracy, the model we built is better than the baseline model in comparison tests, as quantified by two evaluation metrics, with 10.2 % and 7.3 % improvement, respectively.

2. Literature review

2.1 Charging selection behaviour

The charging choice behaviour of electric vehicle users is quite different from the traditional refuelling behaviour of fuel vehicle users. Therefore, the study of EV users' charging choice behaviour has begun to receive extensive attention from both the academic and technical communities. Li *et al.* revealed that range uncertainty has a significant impact on users' charging behaviour [7]. When the range uncertainty is high, users will have a greater tendency to charge their EVs when the remaining power is high, in order to reduce the contingencies caused by insufficient power.

Therefore, its subsequent study proposed an ordered probability distribution model and suggested that the availability of charging facilities, distance and charging time are important influences on users' charging behaviour [8]. Meanwhile, Yang *et al.* studied charging behaviour selection optimization by using a bi-level optimization model and found that EV drivers are influenced by a variety of factors in charging and route selection, including charging facility availability, distance, charging time, and charging price, etc. [9]. Latinopoulos and Sivakumar found that there is also a close relationship between charging location, driving distance, and range anxiety. The above studies reveal that the charging choice behaviour of EV users is influenced by a variety of factors including availability of charging facilities, distance, charging time, price, remaining charge [10], and battery range.

2.2 Charging station load capacity and influencing factor

The load of charging station comes from the selection and interaction behaviour of users with charging station, so the charging selection behaviour of users influences the distribution and change rule of charging station load. Al-Kandari and Soliman in 2003 proposed a load prediction model that integrates the consideration of multi-source information and the adjustment of users' decision-making, and the study considered the influence of users' behavioural patterns and decision-making strategies on the prediction effect [11]. Sani's team also conducted a study on the robust integration of electric vehicle charging loads in smart grid capacity expansion planning [12], to improve the robustness and reliability of grid operation. The study focuses on the impact of user behaviour on the planning and integration process, where user behaviour includes uncertainty in charging demand, user's charging time period selection, and fluctuation in charging behaviour.

The EV charging station load in this study is defined as the number of charging piles working at a charging station at a given point in time is equal to the number of EVs undergoing charging operations. If the number of EVs in a charging station is close to or equal to the maximum charging load limit of the current charging station, queuing and congestion occurs at that charging station, i.e., the charging station is overloaded. If the number of EVs being charged is significantly less than the maximum charging position limit of the current charging station, this represents a more relaxed idle state of the current charging station. Therefore, the influencing factors affecting the charging station load and its spatio-temporal distribution is a relatively complex dynamic problem [13].

First, regarding the charging price factor, two scholars proposed a data-driven approach based on using conditional random field modelling in order to perform a spatio-temporal price elasticity analysis of public charging demand for EVs [14]. Meanwhile, Wang *et al.* proposed an integer hybrid planning model in which a vehicle-to-grid (V2G) model is implemented by analysing spatio-temporal electricity prices and grid load profiles, which integrates electric vehicles into the grid for energy delivery and exchange through battery swapping, thus acting as a peak-shaving and valley-filling agent for electricity [15]. Second, geographic factors: The location of charging stations and the characteristics of the surrounding environment are also an important factor affecting the spatial and temporal distribution of charging station loads. Both factors can affect the utilization rate and charging capacity of charging stations. Bian found that the planning of EV fast charging stations should be based on point-of-interest segmentation, functional zones, and multiple spatio-temporal features [16]. Points of interest (POIs) help identify potential charging needs, functional zones enhance services and functions for charging stations, and multiple spatio-temporal features further optimize the planning and layout of charging stations. Zhang *et al.* proposed an EV charging demand prediction method considering the fine division of functional zones based on the characteristics of the functional zones of the city, which are divided into different functional zones, such as residential, commercial, and industrial zones [17].

The time factor is a key influence on charging station loads, with effects from factors such as morning and evening peak hours, weekends, holidays, and seasons impacting the spatial and temporal distribution of charging station loads. Bayram and Galloway focused on pricing strategies and distributed control for fast EV charging stations operating in cold climates [18]. Research has shown that cold weather can affect battery performance, leading to reduced charging efficiency, increased charging time, and influencing user charging behaviour decisions to some extent. Louie

modelled the time series of EV charging station loads. By analysing the data of EV charging station loads, it was found by Louis that the loads exhibit distinct time series characteristics, including random fluctuations, multiple periodicities, and long-term trends [19]. Additionally, Bampos *et al.* developed a predictive model for the electric vehicle load curve (EVLC) [20]. Seasonal variations in the predicted performance are explored, deepening the importance of the impact of seasonal characteristics on research in this field.

Spatial factors also play a role in influencing charging station loads. This is because the loads between adjacent charging stations may affect each other, depending on factors such as their distance, number, capacity, type, usage patterns, and demand. In areas with high charging station density, stations may compete with each other, leading to uneven loads. Conversely, in more dispersed layouts, users may consider additional factors when selecting a station, reducing mutual impact. Huang and Kockelman developed a network equilibrium model and considered the elasticity of demand for EV charging and congestion at charging stations [21]. It was found that the location selection of charging stations should consider the spatial and temporal distribution of EV charging demand, the congestion of charging stations, and the interaction between charging stations. In particular, an excessive number of charging stations on a regional scale can lead to intense competition between charging stations and network congestion, thus reducing the efficiency of the entire charging network.

The travel demand and charging demand of EV users can also be affected by special circumstances such as holiday periods and participation in large events. Unterluggauer proposed a short-term load prediction model for EV charging stations using a multivariate multi-step short-term memory approach [22]. The effect of holidays was used as one of the input variables of the model in the study, this is because the researcher found that holidays may have a significant effect on the load of EV charging stations. For example, during holidays, people's travel patterns and charging needs may be very different from normal working days, which may lead to results such as higher load fluctuations at charging stations.

3. Research methodology

3.1 Multi-source data

In this study, the data types of multi-source dataset are used to cover the business data of EV users' charging behaviours at charging stations in Shanghai, the equipment information data of EV charging stations, the POI basic information data, the weather data, holidays, and other environmental data. Table 1 shows a brief introduction of the data names and contents.

The total amount of data on charging behaviour at charging stations for the period of August 30, 2020 to February 28, 2021 for the specific data involved in this study is approximately 117.6 million. The total number of data items is 64 columns. The number of data pieces totals 1,095,889. By processing the business data and equipment data of charging stations, based on the latitude and longitude location of the charging stations, we get the specific allocation of the relevant charging stations shown in Fig. 1.

Table 1 Detailed introduction of data source and data content

Data name	Data content	Data source
Operational data	Operational data generated by users during charging	Shanghai charging station online platform
Charging station facility data	Charging station facility information and geographic location	Shanghai charging station online platform
Road network data	Shanghai's road location and road property	OpenStreetMap open-source dataset
Points of interest data	POI name, type and geographic location	Gaode Map API
Weather data	Temperature, precipitation, wind, etc. of the day	National meteorological data sharing platform
Holiday data	The dates of national legal holidays	State council website announcement

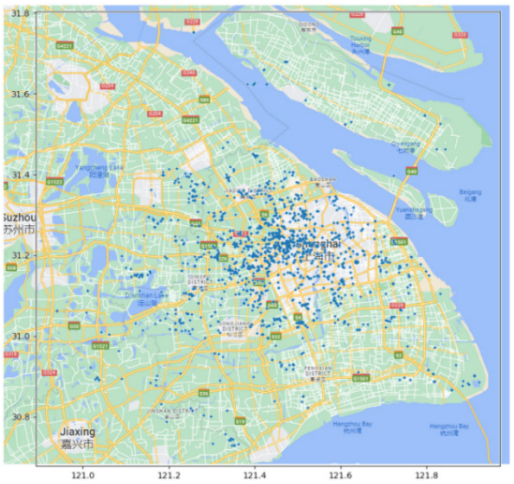

Fig. 1 Distribution diagram of charging station

Fig. 2 Visualization of Shanghai road network data classification

Meanwhile, by using the Shanghai road network data from the OpenStreetMap open source road information database, we simplified the road types in the data structure of the open source database for the convenience of the study. First, according to the *TYPE-Road Type* attribute, *highway* and *urban expressway* are grouped into *A* and *B* road types, which represent the roads that need to be connected to the road network *A*, which represents the type of road that requires the user to drive faster across the spatial distance per unit of time. Second, *urban main roads* and *urban secondary roads* are grouped together as *B* roads, which represent a road type that requires users to cross a moderate distance per unit of time while driving. Finally, *urban branch roads* and *rural roads* are categorized as *C* roads, which represent a type of road that crosses a slower distance per unit of time when the user is driving. The road network visualization of the above three road types is shown in Fig. 2.

3.2 Time distribution characteristics

The patterns of change in charging station loadings in the time dimension include short-term patterns of change, multiple periodicities, long-term trends, and the effects of special events.

Fig. 3 shows the short time variation of the load of the charging station. The results indicate that the load at a specific time of day is influenced by the load values from the preceding neighbouring hours. Analysing the daily load trend reveals a consistent pattern, characterized by gentle upward and downward fluctuations.

Figs. 4 and 5 show the multiple periodicities characterising the variation of the charging station load values. Multiple periodicity refers to the presence of several cycles with different lengths in the load values. The charging station loads at a specific time are influenced by loads spanning

multiple previous cycles. The periodic effects observed include the same hour of previous days as well as the same hour of the corresponding days from previous weeks, which affect the charging station load at the target time. This pattern is derived from the results of the autocorrelation function method.

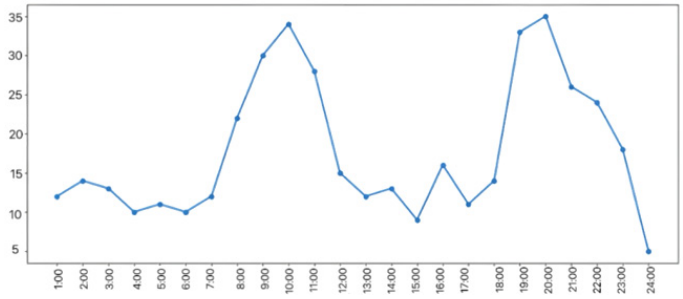

Fig. 3 Diagram of daily charging load variation at a charging station in Shanghai

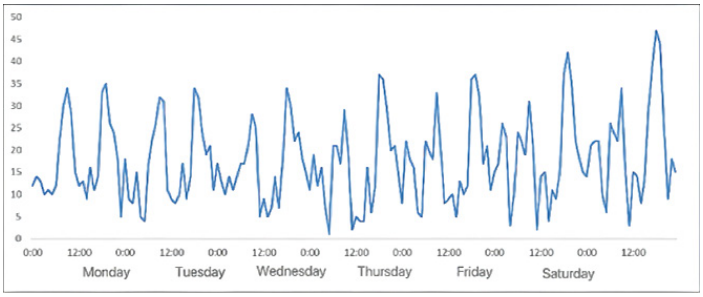

Fig. 4 Change in load capacity of charging station within one week

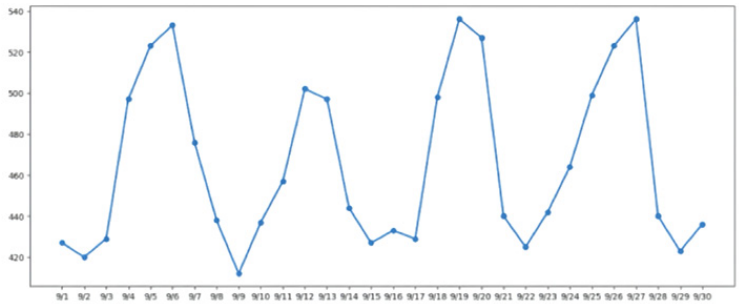

Fig. 5 Loading capacity of charging station varies continuously for multiple weeks

As shown in Fig. 6, this represents a long-term trend in the values of charging station loads. By changing through time, the charging station loads will have an overall trend of increasing in fluctuation. This regularity is reflected according to the results of the exponential smoothing method.

The pattern of change in the value of the charging station load is affected by some special effects, including legal holidays (Fig. 7) and special weather such as rainy and snowy days. This feature is analysed by multiple linear regression method.

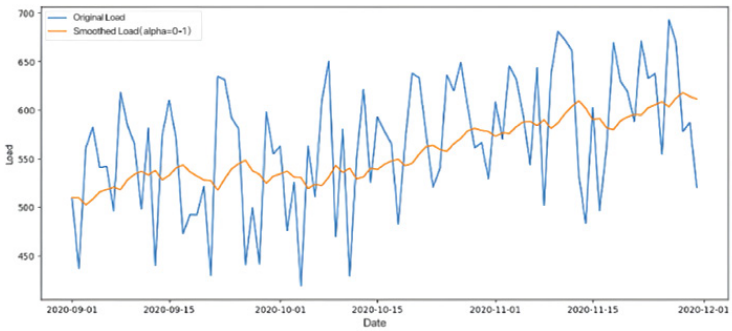

Fig. 6 Smoothing result of charging station load index

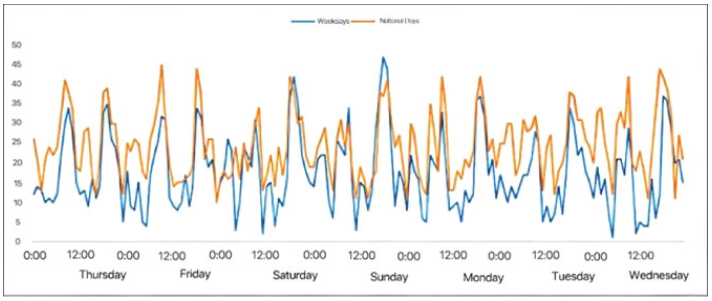

Fig. 7 Trend of load changes during the National Day holiday(seven-day time period)

Despite holidays, weather should also be considered as a factor that affects the time series trend of charging station loads. This is because special weather, such as rain, fog, and snow, can affect the travel decisions and charging decisions of electric vehicle users. Similar to the method of observing the effect of legal holiday factors on the time series of charging station loads, the study compares the trends of the hourly granularity of loads within an average single day under four types of weather, namely, rainy day, snowy day, foggy day, and normal. It is found that the charging station loads in rainy, snowy, and foggy days are overall smaller than the charging station loads under normal days in all hours. This study attempts to find a linear function such that the dependent variable can be explained by a weighted combination of the independent variables.

In this case, Y is the dependent variable, X_1 to X_k are independent variables, β_0 is the intercept, β_1 to β_k are the regression coefficients, and ε is the error term.

$$Y = \beta_0 + \beta_1 X_1 + \beta_2 X_2 + \cdots + \beta_k X_k + \varepsilon \quad (1)$$

The study in this paper uses four dummy variables to represent weather conditions (holiday, rain, snow, and fog). Each dummy variable is a binary indicator variable that takes the value of 0 or 1. Such variables can help in understanding the effect of different weather conditions on loadings. Thereafter, least squares regression was used and statistical information such as estimates of regression coefficients, t-statistics, and p-values were obtained. This information helps to understand the relationship between the independent and dependent variables. For example, the regression coefficient indicates the amount of change expected in the dependent variable when the independent variable is increased by one unit. The p-value helps to determine whether the relationship is significant or not. In the data of this paper, it was found that holidays have a significant positive effect on loadings at the $p < 0.01$ level, while rainy and snowy days have a negative effect on loadings at the $p < 0.05$ level, and foggy days have a non-significant effect on loadings, as detailed in the analyses shown in Table 2.

Table 2 Multiple linear regression results with special time effects

Special time	Coefficient	t value	p value
Legal holidays	14.25	7.476	0.004**
Rainy days	-3.49	-1.828	0.039*
Snowy days	-6.52	-3.417	0.045*
Foggy days	-4.50	-2.361	0.077

3.3 Spatial distribution characteristics

This study defines charging stations with straight line distance between charging stations within 3 km and road form distance within 5 km as relatively close charging stations. Others are defined as relatively distant charging stations. There are three patterns of influence of charging station loads in the spatial dimension. Firstly, a charging station with saturated charging load will transmit the excess charging demand in the area to the close charging station. This means that when a charging station reaches saturation charging load, it will transfer a portion of the load to neighbouring charging stations, causing the loads of the neighbouring charging stations to rise This phenomenon is particularly common during peak periods. As well, there is competition between neighbouring charging stations that have not yet saturated their loads. Because they need to share limited resources, if the load of a charging station that has not yet saturated increases, it will affect

the load of neighbouring charging stations, as shown in Fig. 8. Secondly, high-load charging stations near points of special interest, such as commercial centres, tend to cluster. This is because charging stations located near commercial centres attract more electric vehicles (EVs), leading to an increase in charging demand at multiple stations in the surrounding area.

In this study, the effect of point-of-interest factors on EV mobility patterns and charging load distribution is considered. Charging stations within 2 km from the point of interest are defined as charging stations around the point of interest. Using multiple linear regression and least squares method, the study quantitatively assesses the degree of influence and the confidence level of different types of points of interest on charging station loads. The details are shown in Table 3, where the coefficients represent the degree and direction of the influence of the point of interest feature on the load of the surrounding charging stations, and the *p*-value represents the confidence level of whether an influence exists. $p < 0.05$ means that there is a confidence in the influence of the corresponding point of interest feature, and $p < 0.01$ represents a higher level of confidence.

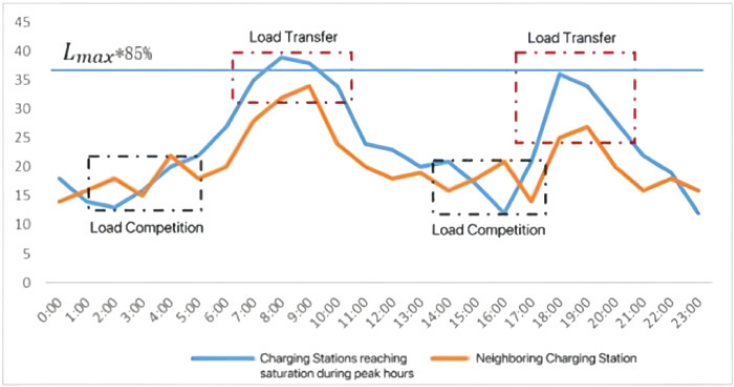

Fig. 8 Influence of saturated charging stations on adjacent charging stations

Table 3 Multiple linear regression results of the influence of interest points

POI	Regression coefficient	*p* value
Transportation facilities	6.35	0.022*
Commercial zone	4.37	0.032*
Official zone	2.72	0.047*
Residential zone	-8.64	0.009**
Recreation	2.48	0.015*

The results of the multiple linear regression with point of interest as a variable show that transportation facilities, such as train stations, bus stations, and subway stations, lead to an increase in the load of nearby charging stations. Commercial areas lead to a smaller increase in the load of nearby charging stations. Office areas likewise increase the load on nearby charging stations to some extent, especially during peak commuting hours. Residential areas may have relatively low loads on nearby charging stations, and recreational areas, such as movie theatres, parks, and restaurants, can lead to an increase in loads on nearby charging stations, especially during legal holidays. As a third pattern, there is also a relationship between charging stations that are farther apart where loads affect each other, mainly due to user behaviour. This is because user charging needs migrate to more distant areas with their individual driving behaviour. Therefore, the spatial dependency of long distances should also be considered.

3.4 Models construction

The objective of this paper is to predict the spatial distribution of charging loads at the target time X_{t+1} based on the historical data $\{ X_t \mid t = 0,1,\cdots,n-1 \}$ of the spatial and temporal distribution of electric vehicle electric loads within a single city. Each time period is a matrix containing the load values of all EV charging stations for the current time period. The relative position of each charging station is also reflected in the number of rows and columns of each value in the matrix.

On top of the historical data on the spatial and temporal distribution of loads, the influence of multiple sources of factors is also considered and their information is introduced into the prediction model, including relevant road network characteristics, point-of-interest characteristics, legal holidays, and weather characteristics.

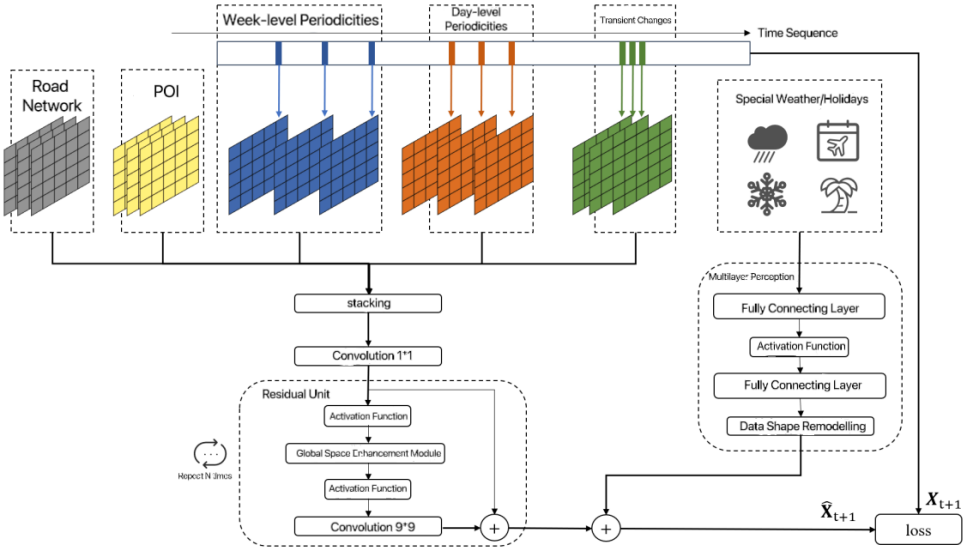

Fig. 9 Model framework

Fig. 9 shows the model architecture developed in this paper. The architecture consists of 4 parts, which are historical feature inputs, residual structure, global spatial enhancement module, and multi-layer perceptron with the introduction of time vectors. In a single round of model training, weekly-level periodicity, daily-level periodicity, short-term variations, road network information, and point-of-interest data from the historical dataset must be stacked together. A convolution operation is then performed to reduce the number of channels in the feature map through channel fusion, while keeping the feature map size unchanged. This operation aims to reduce the network's parameters and computational complexity while maintaining its performance. The result of the convolution operation is fed into the residual neural network, which undergoes an activation function, a global spatial reinforcement module, a second activation function, and this convolution operation to produce a final output of the matrix with the number of channels as one. At the same time, information about rainy days, snowy days, legal holidays, and other special times is input into the multi-layer perceptron in the form of vectors. The perceptron outputs a matrix with the same structure as the residual structure output matrix. These matrices are fused to produce the predicted value. The predicted value is then evaluated using a loss function to calculate the loss value for the current round of training. This loss value quantifies the degree of fit between the predicted value and the true value. Finally, the backpropagation method is used to calculate the gradient of the loss value, enabling the weights and biases of the network to be updated accordingly.

The historical characteristics of the inputs in the model include time-varying and stationary characteristics. The temporal variation characteristics change with the forecast target time change, and it includes weekly periodic information, daily periodic information and short time variation information, the support for introducing this information comes from the temporal characterization in Section 3.2 of this paper, and their model equations are as follows:

$$X_i^w = \left[X_{i-l_w}, X_{i-(l_w-1)}, \cdots, X_{i-w}\right] \tag{2}$$

$$X_i^d = \left[X_{i-l_d}, X_{i-(l_d-1)}, \cdots, X_{i-d}\right] \tag{3}$$

$$X_i^h = \left[X_{i-l_h}, X_{i-(l_h-1)}, \cdots, X_{i-1}\right] \tag{4}$$

It is assumed that the length of the selected time period is 1 hour (a = 24 hours). The week-level periodicity information X_i^w represents the information about the spatial distribution of the

charging station loadings on the same day and at the same hour in the same week w weeks prior to the target time i that needs to be predicted. For example, if the target time to be predicted is 17:00 on March 15, 2021 (Monday), the information of X_i^w is the spatial distribution matrix of charging station loads at 17:00 on March 8, March 1, and so on for the previous w Mondays. The day-level periodicity information X_i^d represents the information on the spatial distribution of the charging station loadings at the same hour on the d previous day i to the target time to be forecasted. For example, if the target time to be predicted is 17:00 on March 15, 2021, the information of X_i^d is the spatial distribution matrix of charging station loadings at 17:00 on March 14 at 17:00, March 13 at 17:00, and so on for the previous d days. The short time variation information X_i^h represents the spatial distribution information of the charging station loadings for the h hours before the target time i to be predicted. For example, if the target time to be predicted is March 15, 2021 at 17:00, the information of X_i^h is the spatial distribution matrix of charging station loadings for the h hours before March 15 at 16:00, March 15 at 15:00, etc.

Fixed features, on the other hand, do not change with the predicted target time. It includes point of interest and road network information. The support for introducing this information comes from the spatial characterization in 3.3. The equations are as follows:

$$X^{road} = [X_{A1}, X_{A2}, X_{B1}, X_{B2}, X_{C1}, X_{C2}] \tag{5}$$

$$X^{POI} = [X_{Trans}, X_{Busi}, X_{Admin}, X_{Residen}, X_{Enter}] \tag{6}$$

X_{road}consists of 6 layers of matrix stacking. Each layer represents the spatial distribution information of different types of roads. The corner symbols in the Eq. 5 are explained as follows.

$A1$ Unidirectional road of fast road type
$A2$ Bidirectional road of fast road type
$B1$ Unidirectional road of medium-speed road type
$B2$ Bidirectional road of medium-speed road type
$C1$ Unidirectional road of slow road type
$C2$ Bidirectional road of slow road type

X^{POI} consists of a stack of 5 layers of matrices, with each layer representing the spatial distribution information of different types of points of interest. The corner symbols in the equation are explained as follows.

$Trans$ Transportation facilities
$Busi$ Commercial area
$Admin$ Official area
$Residen$ Residential area
$Enter$ Recreational area

The rationale for introducing this information is that points of interest can have varying degrees of impact on the charging station loadings in their neighbourhoods. The charging station load prediction model built in this paper will stack the data mentioned above and feed it together into a convolutional layer. It is hoped that the model will establish connections between different times in this way as a way of extracting time-dependent information from the data.

A residual neural network is a framework for deep convolutional neural networks. The core idea of residual neural networks is to introduce residual connections into the model. These residual connections make it easier for the network to learn by skipping certain layers and passing information directly. Specifically, assuming that the input to a certain layer is X. It is desired that the model learns a mapping of $F(X)$. In the residual module, the mapping is actually learned as $F(X) - X$,which is the residual mapping. After that the input X needs to be added with the residual mapping to get the final output$F(X) = F(X) - X + X$. This process can be represented by the following equation:

$$output = F(X) + X \tag{7}$$

Compared to traditional convolutional neural networks, this jump connection makes it easier for gradients to circulate during back-propagation, thus alleviating the problems of gradient vanishing and gradient explosion, and allowing the network to be trained deeper as well as more easily. In the study of this paper, the residual unit that performs a single loop can be expressed as:

$$y = F(x, \{W\}) + x \tag{8}$$

where x represents input, y is output, $F(x, \{W\})$ is a function with a set of weights $\{W\}$. It represents a series of convolutional layers and activation functions. The result of the computation $F(x, \{W\})$ is added to the input x to get the output y. In a practical implementation, two or more convolutional layers may be included in $F(x, \{W\})$, as shown below:

$$F(x, \{W1, W2\}) = W2 * ReLU(W1 * x) \tag{9}$$

Here, $W1$ and $W2$ are the weights of the convolutional layers. $ReLU$ is the nonlinear activation function chosen for this model. Substituting this equation into the residual unit equation gives the final:

$$y = W2 * ReLU(W1 * x) + x \tag{10}$$

As shown in Fig. 10, the global spatial enhancement module we have created can extract the spatial dependency relationships at long distances within the network structure. The global spatial enhancement module first separates a portion of the channels from the regular convolution. These channels undergo global average pooling to reduce the number of parameters before entering the fully connected layer. The fully connected layer is designed to capture the long-range spatial dependency patterns between each pair of charging stations. Its output is added to the synchronous convolution output to provide the global spatial dependency parameters learned from the convolution output. This approach ensures that the global spatial enhancement module can output data of the same shape as the output of the regular convolution operation and can be used as input for the residual unit in the next loop.

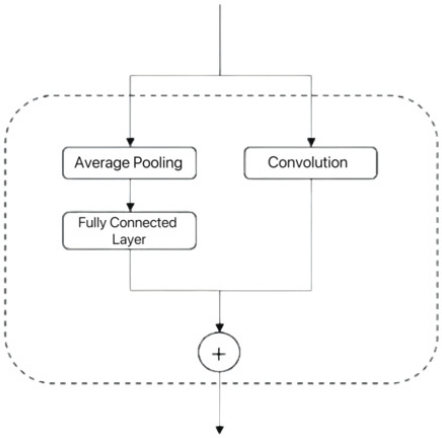

Fig. 10 Global space enhancement module

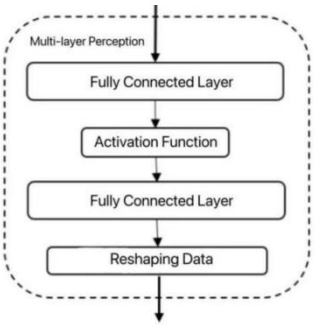

Fig. 11 Multi-layer percepton

In this model, the medium for learning special fixed-time features such as rainy or snowy weather and statutory holidays is a time vector introduced into the entire model through a multi-layer perceptron.

The time vector in the model is a vector of length $\alpha + 7 + 12 + 1 + 2$, where each component takes on the value of 0 or 1. The vector encodes the month to which the predicted target time belongs, the day of the week, the time interval within a day, whether it is a statutory holiday, and whether there is rainy or snowy weather on that day. Among them, the part of the time vector with a length of α encodes all time intervals within a day. If 1 hour is chosen as the time interval, then $\alpha = 24$. The part with a fixed length of 7 encodes the 7 days of the week. The part with a fixed length of 12 encodes the 12 months of the year. The part with a length of 1 indicates whether it is a statutory holiday. The part with a length of 2 indicates two types of weather found in the data that have a significant impact on the spatial-temporal distribution of the load.

The data format of the time vector is not a grid-like data graph that is passed between the structures of the model, so convolutional neural networks cannot be directly used to extract information from it. Therefore, a multi-layer perceptron is used here to learn the vector data and transform it into the same data shape as the output of other parts of the model.

A multi-layer perceptron is a type of feed-forward neural network where each layer is fully connected, enabling it to learn complex relationships between input features. In this model, the structure of the multi-layer perceptron is shown in Fig. 11. The time vector inputted is first dimensionally increased in the first fully connected layer, then goes through an activation function to enhance the model's non-linear expressive power. It then goes through additional fully connected layers to reach the desired data dimension $H \times W$, which is the matrix shape used for extracting the spatial distribution features of the charging stations in this study. Finally, after reshaping the data shape, it matches the output of the residual unit, and the two are added together to generate the prediction data.

4. Result and discussion

4.1 Modelling effectiveness evaluation

The evaluation metrics used in this study include Root Mean Square Error *(RMSE)* and the previously mentioned *MAE*. *RMSE* and *MAE* directly assess the error between predicted values and true values, facilitating an objective observation of the magnitude of deviations. Here, $X_i$represents the true value, and $\hat{X}_i$ represents the predicted value. The specific equation for RMSE is as follows:

$$RMSE = \sqrt{\frac{1}{T}\sum_{i=1}^{T} \|X_i - \hat{X}_i\|_2^2} \tag{11}$$

Consistent with the loss function, X_i and $\hat{X}_i$ represent the actual data and predicted data for the i^{th}time interval, respectively. T is the total number of samples in the test data.

After four-stages ablation experiments, as shown in Table 4, the smaller the value of the evaluation metric, the smaller the deviation between the predicted values and the actual values, indicating a better model performance. It can be observed from the evaluation metric data that gradually introducing the global spatial enhancement module, road network and point-of-interest information, legal holidays, and special weather information into the model leads to a gradual improvement in the overall model effectiveness. This demonstrates that incrementally adding new components to the model during its construction can optimize the accuracy of the model predictions.

Table 4 Results of ablation experiment

Modelling stage	RMSE	MAE
Base model	5.87	3.54
Base model + global space enhancement module	5.49	3.41
Base model + global spatial enhancement module + road network & points of interest	5.34	3.32
Full model	5.27	3.28

Table 5 presents the performance of the model constructed in this study compared to other baseline models in terms of evaluation metrics. It also compares the performance of models with different parameters. The parameter selection for the number of time periods within a day is set to 24 hours, representing the division of a day into 24 time periods, each lasting 1 hour. The parameter selection of 48 hours represents dividing a day into 48 time periods, each lasting 30 minutes. The best performance in terms of evaluation metrics is highlighted in bold in the table.

In the evaluation results, it was observed that the performance of various models with a time period length of 30 minutes was better than the performance with a time period length of 1 hour. Additionally, the model proposed in this paper outperformed the best-performing baseline model, which was a Residual Neural Network model, in two evaluation metrics. When compared to the Residual Neural Network model, the proposed model achieved a 10.2 % decrease in *RMSE* and a 7.3 % decrease in *MAE*. This indicates that the proposed model exhibits good performance in predicting the spatial-temporal distribution of electric vehicle charging station loads.

Table 5 Baseline model comparison results

Model	1 hour		30 minutes	
	RMSE	*MAE*	*RMSE*	*MAE*
Historical Average Model	10.17	6.59	9.24	6.02
Auto-regressive Integrated Moving Average Model (ARIMA)	9.88	6.51	8.19	5.69
Recurrent Neural Network (RNN)	9.12	5.86	6.97	4.28
Long Short-Term Memory Network (LSTM)	8.79	5.83	6.81	4.13
Convolutional Long Short-Term Memory Network (ConvLSTM)	7.32	4.22	6.02	3.85
Graph Convolutional Neural Network (GCN)	7.87	4.28	6.23	3.99
Residual Neural Network (ResNet)	7.05	4.02	5.87	3.54
The model proposed in this paper	6.35	3.71	5.27	3.28

4.2 Predictive results analysis

In this section, to demonstrate the predictive effectiveness of the model in real-world applications, the predictive results of the model are visualized. In the specific process, two charging stations are randomly selected from the dataset, and the actual load variations from Monday to Friday within a single week are extracted. The real data variations are then compared with the predicted data variations. The comparisons are illustrated in Figs. 12 and 13.

From the comparison between the predicted values and the actual values, it can be seen that the spatiotemporal load forecasting model in this paper can accurately predict the trends and magnitudes of load variations for each charging station. While the model successfully predicts the general trends of load increase and decrease for the majority of cases, there are discrepancies in predicting the specific numerical values of load peaks and valleys, especially in complex and variable real-world scenarios. Overall, the predictive performance of the model is in line with expectations.

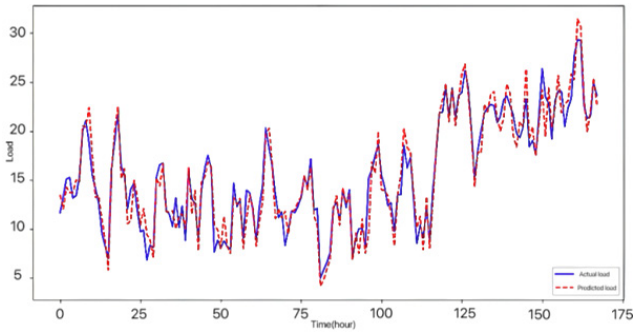

Fig. 12 Comparison between predicted and actual load values of a charging station A

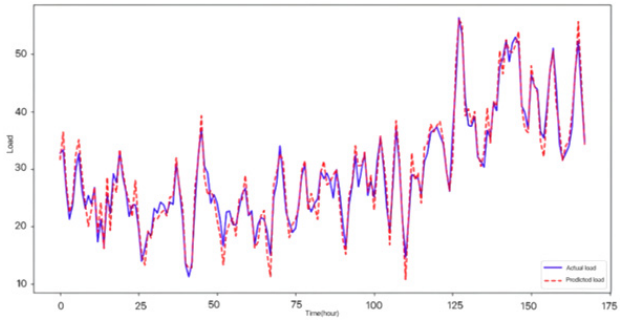

Fig. 13 Comparison between the predicted and actual load values of a charging station B

4.3 Parameter impact analysis

In the global spatial enhancement module, to capture long-distance spatial dependencies, some channels of the convolutional neural network are allocated to the fully connected layer. The role of the fully connected layer is to learn global spatial information. Fig. 14 illustrates the impact of the number of channels allocated to the fully connected layer on the model's predictive performance while keeping the total number of channels constant at 128. The graph shows that as the number of channels allocated to the fully connected layer increases from 0 to 1, the model immediately benefits, indicating that learning long-distance spatial dependencies in the dataset is meaningful for prediction. The model performs better with 24 separate channels, but performance decreases with more separate channels. This suggests that both short-distance spatial dependencies and long-distance spatial dependencies are significant and cannot be ignored.

The impact of the total number of channels in the convolutional neural network on the prediction results is shown in Fig. 15. The evaluation covers a range of total channels from 16 to 128. The results indicate that as the number of channels increases, the computational cost also increases, and the model's predictive performance benefits from the increase in the number of channels. However, the rate of improvement decreases gradually with the increase in the number of channels. An increase in the total number of channels leads to diminishing returns in the model's predictive performance. Therefore, we clearly defined the predictive goals for the spatiotemporal distribution of electric vehicle charging station loads and proposed a multi-feature fusion prediction model based on residual neural networks. This model learns the short-term variations, multi-periodicity, long-term trends, and special time influences of electric vehicle charging station loads in the time dimension. In the spatial dimension, it integrates road network information, charging station location information, and various points of interest locations, enabling the model to learn the spatial distribution patterns of electric vehicle charging station loads. Additionally, spatial dependencies are categorized into short-distance and long-distance categories, and a global spatial enhancement module is designed to help the model focus on long-distance spatial dependencies while retaining some channels for learning short-distance spatial dependencies.

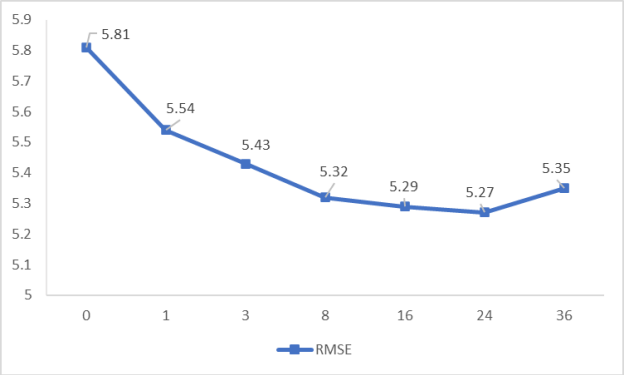

Fig. 14 The effect of the number of channels in the full connection layer on the results

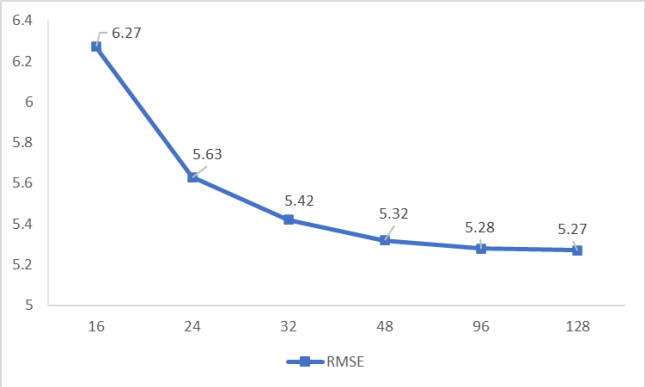

Fig. 15 Influence of amount of all channels

In the training process, the loss function *MSE* and relevant parameters in the model are defined. During the model evaluation phase, *RMSE* and *MAE* are used as evaluation metrics, and ablation experiments and comparative experiments are conducted. Ablation experiments involve gradually adding key components to observe the prediction errors, showing that the introduction of each component significantly enhances the model's predictive performance. In comparative experiments, the proposed model's superior performance in predicting the spatio-temporal distribution of electric vehicle charging station loads is demonstrated by comparing *RMSE* and *MAE* metrics, with reductions of 10.2 % and 7.3 %, respectively, compared to existing baseline models in the field.

4.4 User demand analysis

To avoid queuing at congested charging stations, users currently rely on real-time information provided by charging station operation platforms and map-based navigation applications to determine which charging stations still have available spaces. However, the rapid fluctuations in the load and availability of charging stations make the information on the saturation status of charging stations outdated by the time users arrive at the station or during their journey. This lag in information may lead to discrepancies between users' expectations and the actual situation when making charging station selection decisions based on outdated information, such as arriving at a station only to find it fully occupied, necessitating a waiting queue. User decisions on charging station selection heavily rely on the saturation status information of charging stations, but the uncertainty stemming from the time lag in this information has become a major pain point in the chain of electric vehicle charging behaviour for users.

Currently, the pain point primarily lies in the fact that electric vehicle users need to plan their charging station selections along the route in advance before embarking on long-distance drives. However, since the arrival times at each charging station along the long-distance route vary, the pre-queried saturation status information of charging stations also varies in terms of time lag based on the different arrival times. Due to the varying time lag of the real-time saturation status information that users rely on, planning a rational strategy for selecting multiple charging stations before a long-distance journey becomes challenging. This strategy requires accurate prediction of the saturation status information at multiple charging stations in the future, serving as deterministic information to support decision-making.

4.5 Charging station selection strategy support

The electric vehicle charging station load spatial-temporal prediction model established in this paper can output predicted values of load levels at multiple charging stations across various time intervals and locations in the future. By combining the predicted load data with the actual saturation levels of the charging stations, it is possible to determine which stations will experience queue congestion or excessive idleness at specific times in the future. In a specific process, defining the saturation load level of a particular electric vehicle charging station as L_{max} and the predicted load level at a future time as L_i, queue congestion coefficient as α, and idleness coefficient as β, where $\alpha > \beta$. Based on the comparison between the load levels L_{max} and L_i of a charging station

at a specific time in the future, the load saturation status of any charging station at any time and location in the future can be defined. The load saturation status can be categorized into the following three states:

Queue Congestion State (C): $L_i \geq \alpha * L_{max}$
Excessive Idle State (L): $L_i \leq \beta * L_{max}$
Normal Load State (N): $\beta * L_{max} < L_i < \alpha * L_{max}$

Based on the three divisions of load saturation states, the distribution of load saturation states for various charging stations at multiple future time points can be obtained. The schematic diagram of the load saturation states of each charging station in Shanghai at a single time point is shown in Fig. 16.

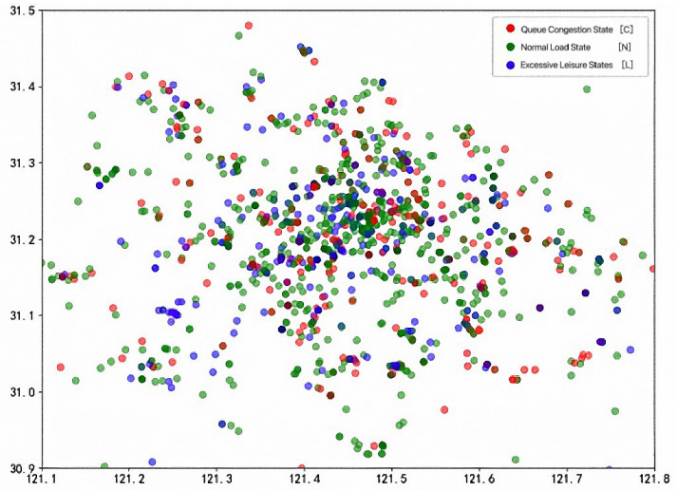

Fig. 16 Influence of amount of all channels

5. Conclusion and outlook

On this paper, the load capacity prediction model helps users to predict the load saturation state of charging stations at different locations within a certain range at different times. To help users identify charging stations where queuing is expected to occur at the target time for circumvention, it also helps users to identify charging stations with a large number of idle charging posts at the target time to minimize the risk of congestion. This provides users with relatively more accurate real-time predictive information for both one-time temporary charging station selection decisions and long-term charging plan development. However, the prediction model in this study mainly focuses on spatial and temporal distribution characteristics, and in the future, we can consider integrating more dimensions of information such as user behaviour and driving behaviour to improve the model's generalization ability and practicality.

Acknowledgments

This work was supported by the [National Natural Science Foundation of China] under Grant [62276020], [Beijing Natural Science Foundation] under Grant [9222025]. We appreciate their support very much.

References

[1] Chen, L.D., Zhang, Y., Figueiredo, A. (2019). A review of electric vehicle charging and discharging load forecasting research, *Automation of Electric Power Systems,* Vol. 43, No. 10, 177-197, doi: 10.7500/AEPS20180814001.
[2] Production and sales of major new energy vehicle enterprises in December 2020, *Automobile and Accessories* (2021), No. 2, 19.
[3] Liu, H., Yan, J., Ge, S.Y., Han, J. (2020). Dynamic response of electric vehicle and fast charging station considering the influence of multi-vehicle interaction, *Proceedings of the CSEE,* Vol. 40, No. 20, 6455-6468, doi: 10.13334/j.0258-8013.pcsee.191612.

[4] Liu, J.-Y., Liu, S.-F., Gong, D.-Q. (2021). Electric vehicle charging station layout based on particle swarm simulation, *International Journal of Simulation Modelling*, Vol. 20, No. 4, 754-765, doi: 10.2507/IJSIMM20-4-CO17.
[5] Ren, Q.L., Liu, H., Xiong, W. (2015). Introduction to the development of electric vehicle, *Power Supply Technologies and Application*, Vol. 18, No. 5, 10-16.
[6] Wang, Y., Shi, J., Wang, R., Liu, Z., Wang, L. (2018). Siting and sizing of fast charging stations in highway network with budget constraint, *Applied Energy*, Vol. 228, No. 17, 1255-1271, doi: 10.1016/j.apenergy.2018.07.025.
[7] Li, H., Yu, L., Chen, Y., Tu, H., Zhang, J. (2023). Uncertainty of available range in explaining the charging choice behavior of BEV users, *Transportation Research Part A: Policy and Practice*, Vol. 170, Article No. 103624, doi: 10.1016/j.tra.2023.103624.
[8] Daina, N., Polak, J.W., Sivakumar, A. (2015). Patent and latent predictors of electric vehicle charging behavior, *Transportation Research Record*, Vol. 2502, No.1, 116-123, doi: 10.3141/2502-14.
[9] Yang, Y., Yao, E., Yang, Z., Zhang, R. (2016). Modeling the charging and route choice behavior of BEV drivers, *Transportation Research Part C: Emerging Technologies*, Vol. 65, 190-204, doi: 10.1016/j.trc.2015.09.008.
[10] Latinopoulos, C., Sivakumar, A., Polak, J.W. (2017). Response of electric vehicle drivers to dynamic pricing of parking and charging services: Risky choice in early reservations, *Transportation Research Part C: Emerging Technologies*, Vol. 80, 175-189, doi: 10.1016/j.trc.2017.04.008.
[11] Al-Kandari, A.M., Soliman, S.A., El-Hawary, M.E. (2003). Fuzzy systems application to electric short-term load forecasting: Part II - Computational results, In: *Proceedings of Large Engineering Systems Conference on Power Engineering,* Montreal, Canada,131-137, doi: 10.1109/LESCPE.2003.1204692.
[12] Aliakbari Sani, S., Bahn, O., Delage, E., Tchuendom, R.F. (2022). Robust integration of electric vehicles charging load in smart grid's capacity expansion planning, *Dynamic Games and Applications*, Vol. 12, No. 3, 1010-1041, doi: 10.1007/s13235-022-00454-y.
[13] Huang, N., He, Q., Qi, J., Hu, Q., Wang, R., Cai, G., Yang, D. (2022). Multinodes interval electric vehicle day-ahead charging load forecasting based on joint adversarial generation, *International Journal of Electrical Power & Energy Systems*, Vol. 143, Article No. 108404, doi: 10.1016/j.ijepes.2022.108404.
[14] Liu, K., Liu, Y. (2023). Stochastic user equilibrium based spatial-temporal distribution prediction of electric vehicle charging load, *Applied Energy*, Vol. 339, Article No. 120943, doi: 10.1016/j.apenergy.2023.120943.
[15] Wang, D.L., Ding, A., Chen, G.L., Zhang, L. (2023). A combined genetic algorithm and A* search algorithm for the electric vehicle routing problem with time windows, *Advances in Production Engineering & Management*, Vol. 18, No. 4, 403-416, doi: 10.14743/apem2023.4.481.
[16] Bian, H., Zhou, C., Guo, Z., Wang, X., He, Y., Peng, S. (2022). Planning of electric vehicle fast-charging station based on POI interest point division, functional area, and multiple temporal and spatial characteristics, *Energy Reports*, Vol. 8, Supplement 15, 831-840, doi: 10.1016/j.egyr.2022.10.161.
[17] Zhang, K., Tian, Y., Shi, S., Su, Y., Xu, L., Zhang, M. (2021). Electric vehicle charging demand forecasting based on city grid attribute classification, In: *Proceedings of 2021 11th International Conference on Power and Energy Systems (ICPES),* Shanghai, China, 592-597, doi: 10.1109/ICPES53652.2021.9683949.
[18] Bayram, I.S., Galloway, S. (2022). Pricing-based distributed control of fast EV charging stations operating under cold weather, *IEEE Transactions on Transportation Electrification*, Vol. 8, No. 2, 2618-2628, doi: 10.1109/TTE.2021.3135788.
[19] Louie, H.M. (2017). Time-series modeling of aggregated electric vehicle charging station load, *Electric Power Components and Systems*, Vol. 45, No. 14, 1498-1511, doi: 10.1080/15325008.2017.1336583.
[20] Bampos, Z.N., Laitsos, V.M., Afentoulis, K.D., Vagropoulos, S.I., Biskas, P.N. (2024). Electric vehicles load forecasting for day-ahead market participation using machine and deep learning methods, *Applied Energy*, Vol. 360, Article No. 122801, doi: 10.1016/j.apenergy.2024.122801.
[21] Huang, Y., Kockelman, K.M. (2020). Electric vehicle charging station locations: Elastic demand, station congestion, and network equilibrium, *Transportation Research Part D: Transport and Environment*, Vol. 78, Article No. 102179, doi: 10.1016/j.trd.2019.11.008.
[22] Unterluggauer, T., Rauma, K., Järventausta, P., Rehtanz, C. (2021). Short-term load forecasting at electric vehicle charging sites using a multivariate multi-step long short-term memory: A case study from Finland, *IET Electrical Systems in Transportation*, Vol. 11, No. 4, 405-419, doi: 10.1049/els2.12028.

APEM journal

Advances in Production Engineering & Management
Volume 19 | Number 4 | December 2024 | pp 460–488
https://doi.org/10.14743/apem2024.4.519

ISSN 1854-6250
Journal home: apem-journal.org
Original scientific paper

Sustainable design of products: Balancing quality, life cycle impact, and social responsibility

Siwiec, D.[a], **Gawlik, R.**[b,c,*], **Pacana, A.**[d]

[a]Faculty of Mechanical Engineering and Aeronautics, Rzeszow University of Technology, Rzeszow, Poland
[b]College of Public Economy and Administration, Krakow University of Economics, Krakow, Poland
[c]NWU Business School, North-West University, Potchefstroom, South Africa
[d]Faculty of Mechanical Engineering and Aeronautics, Rzeszow University of Technology, Rzeszow, Poland

ABSTRACT

The shift towards sustainable mobility has increased the demand for energy-efficient and environmentally friendly vehicles, such as Hybrid Electric Vehicles (HEVs). However, designing HEVs that simultaneously meet high product quality, minimize environmental impact, and adhere to social responsibility standards remains a complex challenge. This study presents a decision-making model aimed at integrating these key sustainability criteria into the design and improvement of HEVs. The model combines three indices: the Aggregated Quality Index (AQI), Environmental Impact Index (EII) based on Life Cycle Assessment (LCA), and Social Responsibility Index (SRI), to assess and compare different HEV prototypes. By processing customer expectations, environmental impacts, and social responsibility considerations, the model predicts the optimal prototype that balances quality, environmental sustainability, and social standards. The findings demonstrate that applying this model can significantly enhance decision-making in sustainable vehicle development and support the creation of HEVs that better align with global sustainability goals. This approach has practical implications for automotive manufacturers aiming to innovate responsibly in the green mobility sector.

ARTICLEINFO

Keywords:
Hybrid Electric Vehicle (HEV);
Eco-innovation;
Product quality;
Sustainable development;
Life Cycle Assessment (LCA);
Multiple Criteria Decision-Making (MCDM);
Mechanical engineering;
Public management

**Corresponding author:*
remigiusz.gawlik@uek.krakow.pl
(Gawlik, R.)

Article history:
Received 27 October 2024
Revised 18 December 2024
Accepted 19 December 2024

1. Introduction

The diversity of considerations in product design reflects efforts towards achieving sustainable development. Actions in this area should simultaneously address quality, environmental impact, and social responsibility [1, 2]. This approach aligns with modern solutions that prioritize designing products satisfying customer needs, social acceptance, and environmental friendliness throughout their life cycle [3]. Integrating these considerations during product design sets milestones but also presents challenges due to the multitude and diversity of necessary decision-making criteria [4]. This process requires involving various decision-makers to establish comprehensive priorities across different application areas [5, 6].

However, research on sustainable product development often lacks equivalent and comprehensive analysis of these considerations, typically focusing on one or two aspects [1], as noted by

authors in [7]. For instance, Life Cycle Assessment (LCA) methods continue to neglect product design and development (PDD) [8]. Considering all aspects collectively is challenging due to the interdisciplinary nature and scarcity of studies that address all sustainable development criteria – economic growth, social well-being, and environmental protection – simultaneously [9, 10].

Despite the development of several methods and tools supporting sustainable product design, there is still a lack of unified consensus, including clear frameworks, methods, and standards for supporting prospective design for sustainable product development that integrates quality, environmental, and social responsibility aspects. Critically discussed conceptual design processes providing analysis of current products and alternative product solutions (prototypes) in a multidimensional evaluation process considering sustainable development criteria (quality, environmental, and social responsibility) are notably absent, and therefore were identified as our research gap.

The main research question of this research is: "How to support the process of improving current products based on possible design prototypes in a multidimensional approach that integrates product quality (customer satisfaction), environmental impact of the product life cycle, and social responsibility compliance?" We assumed that it can be answered by developing a model that provides three separate indexes: i) quality, ii) environment, and iii) social responsibility, subsequently aggregated into a coherent decision-making indicator, used to rank the product design and improvement for their compatibility with sustainable development criteria.

This research aims to develop a decision-making model to anticipate the direction of improving current products based on prototypes (production alternatives) methodically verified in a multidimensional approach encompassing key aspects of sustainable development: quality, life cycle environmental impact, and social responsibility compliance.

The model is primarily dedicated to managerial decision-making in product design and production management, aiming to support private individuals, companies, and public entities in sustainable product development decisions, focusing on achieving socially responsible production engineering that also ensures high-quality offered products and environmental friendliness.

2. Literature review

A literature review was conducted on product design and improvement concerning sustainable development aspects: quality, environmental impact throughout the life cycle, and social responsibility. Due to the limited popularity of simultaneously combining these aspects, the review was conducted in three stages, analysing works that address: i) customer satisfaction with product quality while reducing negative environmental impact throughout the entire life cycle; ii) customer satisfaction with product quality considering social responsibility; iii) product LCA considering social responsibility.

All analysed works came from the Web of Science (WoS) international database. The literature review was conducted in March 2024 within a specified timeframe. Works were categorized based on title, abstract, and keywords. The identified works included: i) LCA, product design, and customer (10 out of 28 works); ii) socially responsible design, product (7 out of 82 works); iii) LCA, product design, quality, and social responsibility (0 works). Initially, a preliminary selection was based on publication abstracts, resulting in a lower number of works analysed compared to those identified.

In total, 17 relevant works were identified, including 12 scientific articles and 5 conference papers. The selected works were further analysed for their distribution, as depicted in Fig. 1. Next, the keywords included in the selected papers were analysed using the WordArt software "Word Cloud" tool. The word cloud visually presents the frequency of individual keywords, with larger font sizes indicating higher frequency of occurrence (Fig. 1).

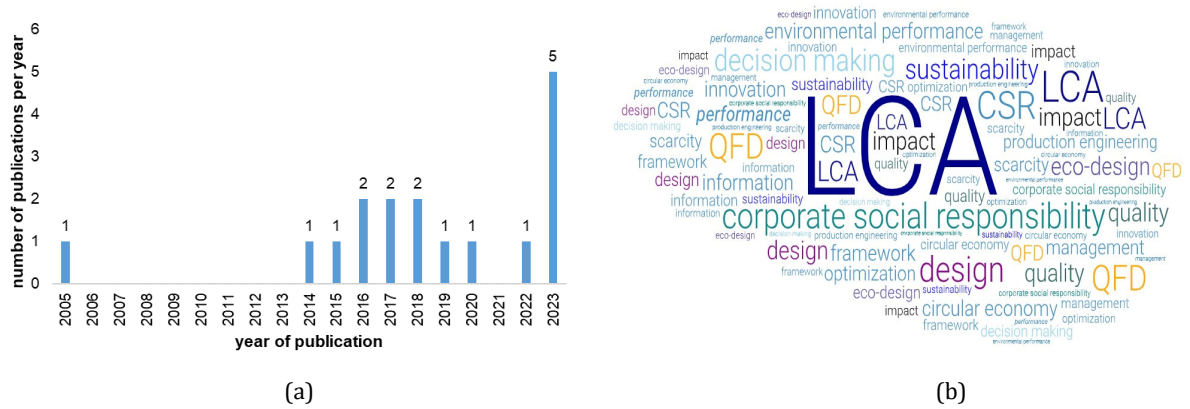

(a) (b)

Fig. 1 Analysis of: (a) publication trends and future developments in the research area of QESR decision-making for sustainable product design and improvement; (b) word cloud for Web of Science database metasearch keywords

The first publication dates from year 2005, but no publications were revealed be-tween 2006 and 2013. Search keywords emerged from 2014 onwards, with only up to two publications per year until 2023, where a slightly higher number (5 publications) was noted. These findings suggest that the selected research area is in a developmental phase, characterized by numerous research gaps, making it an area worthy of further investigation.

Keyword analysis revealed that across the 17 reviewed studies, there were a total of 162 unique keywords (including those provided by authors and indexed in WoS). The most frequently occurring keyword (12 times) was "LCA" (including variations like “life cycle assessment”). Following closely were: "corporate social responsibility" (6), "design" (6), "QFD" (6), "decision making" (5), and "sustainability" (4). Keywords related to "eco-design" (3), "impact" (3), and "quality" (3) appeared slightly less frequently. The remaining keywords appeared twice (11 words) or once (92 words). The high-frequency keywords related to the analysed thematic area and resulted from the search scope used in the selection of works in WoS.

Subsequently, mutual citation analysis was conducted to identify the most frequently cited studies critical to the development of the analysed research area. This analysis was supported by the Gephi 0.10.1 software. Initially, a network of connections was established among the 17 reviewed publications. Subsequently, the focus was narrowed down to the primary citations occurring among these works (Fig. 2).

Fig. 2 Mutual connections among the key publications in content analysis in the Gephi 0.10.1 software, based on the metasearch of the Web of Science database

The 17 analysed studies collectively contained 585 citations (bibliographic entries). When examining their mutual citations, inconsistency was observed both among the studies and within the cited works. This inconsistency may stem from the limited number of studies addressing the chosen thematic area, as well as the previously identified low level of development in this research domain. Among all references, only four most frequently cited works were identified, namely [11-14]. These studies encompassed LCA, decision support, and customer expectation processing using the Quality Function Deployment (QFD) method, acknowledging these issues as integral to sustainable product design.

All selected works underwent synthetic content analysis. It was observed that the most frequently proposed solutions for assessing product quality and environmental impact in the life cycle involved combining QFD for processing customer expectations and LCA for environmental impact assessment [15-18]. Besides combining results from QFD and LCA methods, other approaches were also employed, such as: integrating Failure Mode and Effects Analysis (FMEA), Theory of Inventive Problem Solving (TRIZ), and Fuzzy Technique for Order of Preference by Similarity to Ideal Solution (FTOPSIS) to develop product criteria rankings indicating the most favourable prototypes for existing products [14]; conducting surveys to gather customer expectations regarding product quality and subsequently processing them considering LCA results for different product materials [19]; developing decision support processes during the design phase by modelling LCA outcomes based on customer demand for alternative design solutions [9]; analysing customer sensitivity towards recyclable products [20].

Initial attempts at comprehensive integration of product quality assessment during development phase with environmental impact assessment of product solutions were presented, for example, in [21, 22].

Existing studies on socially responsible design focus on ensuring environmentally friendly products by analysing:

- Customer reactions to eco-labels in the context of their awareness and perceptions of corporate social responsibility [23];
- Social effects following technological support in the product life cycle, demonstrating that sustainable social development impacts sustainable environmental and economic development [24];
- Business social responsibility in the light of customer demand factors determining the expected level of eco-friendliness of new products [25];
- Changing roles and responsibilities of designers in environmentally conscious product design [26];
- Opportunities for implementing the Cradle to Cradle (C2C) approach in conceptual product design focusing on environmental and social benefits [27];
- Motivations of designers in making socially responsible decisions, indicating that the interaction of designer beliefs depends on business feasibility levels, and proper management should focus not only on social but also environmental aspects in product development [28];
- Characteristic product criteria and customer perceptions to align them with CSR [29].

Table 1 summarizes the results of the literature analysis. Following conclusions were drawn from the literature review:

- A limited number of studies (17) focus on product design considering quality (customer satisfaction), environmental impact in LCA, and social responsibility;
- The selected research area is not widely studied and is still in a developmental phase since 2005, with slow predicted growth in subsequent years, indicating significant research gaps;
- The most frequently discussed topics among the analysed works were LCA, corporate social responsibility, product design, QFD, and decision-making;
- Common proposed solutions for assessing product quality and environmental im-pact in the life cycle typically involve combining QFD for processing customer expectations and LCA for environmental impact assessment;

- Existing studies on socially responsible design aim to ensure environmentally friendly products, often overlooking the aspect of achieving customer-desired product quality.

Critically discussed conceptual design processes providing analysis of current products and alternative product solutions (prototypes) in a multidimensional evaluation process considering sustainable development criteria (quality, environmental, and social responsibility) are notably absent, and therefore were identified as our research gap.

Table 1 Summary of literature analysis results

Research Area	Description	Methods	Examples of studies
Product quality assessment and environmental life cycle assessment (LCA)	Acquiring and processing customer requirements for product quality and environmental impact assessment in product life cycle	QFD and LCA	[15, 16, 18, 30]
		Customer survey and LCA	[19]
		Customer demand data, LCA	[9]
		Analysis of customer sensitivity to recyclable products in their life cycle	[20]
	Acquiring and processing customer requirements for product quality and environmental impact assessment in product life cycle; analysis of product nonconformities and identification of product innovations	QFD, LCA, FMEA, TRIZ, FTOPSIS	[31]
	Combining product quality assessment with environmental impact assessment in product design	Customer surveys, TOPIS, LCA	[21 22]
Ensuring socially responsible design and environmentally friendly products	Customer reactions to product eco-labels in the context of their awareness and motives for perceiving corporate social responsibility	CSR, customer expectations for product eco-labels	[23]
	Assessment of social impacts in the case of technological support in the product life cycle	LCA, sustainable development criteria, CSR	[24]
	Modelling customer demand for the level of environmental friendliness of new products	Game theory, ethical operations, CSR	[25]
	Identification of customer expectations for product criteria for their compatibility with the CSR	CSR, analysis of customer expectations	[29]
	Analysis of changes in product roles and responsibilities in the field of conscious ecological product design	Focus groups with product designers	[26]
	Examining designers' motivations in socially responsible product design decisions	Socially responsible design (SRD), CSR	[28]
	Assessment of implementation potential of the C2C approach in conceptual product design for environmental and social benefits	C2C, analysis of qualitative and quantitative experiments	[27]

3. Model design

The research framework, including the developed model, is illustrated in Fig. 3. It involves determining the development direction of the current product by considering design alternatives (prototypes) in the context of sustainable development. The model primarily operates during the conceptual phase, translating and transforming the functional requirements of the product, its environmental impacts, and social acceptability into design parameters.

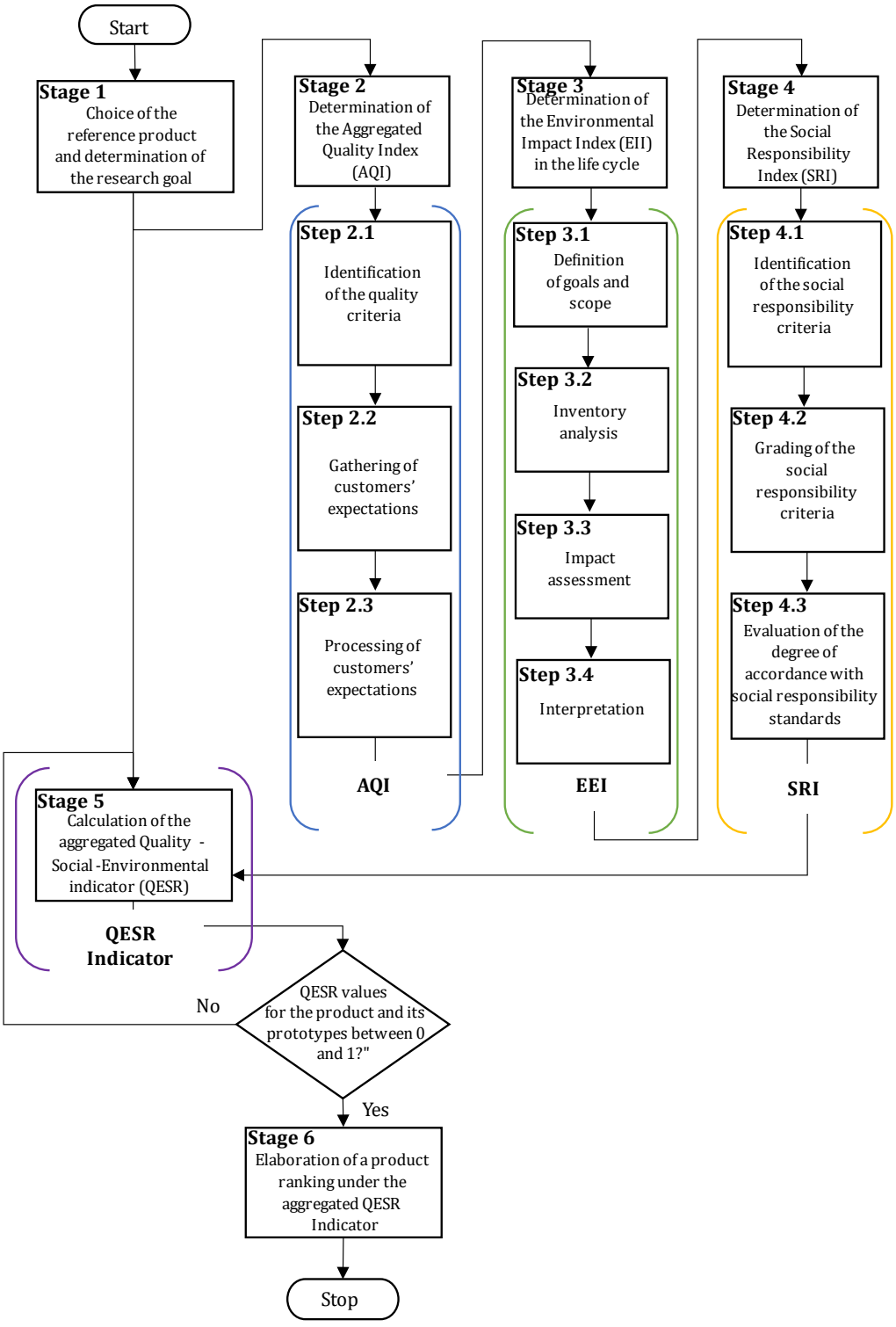

Fig. 3 Research design: model development for products enhancement with use of design prototypes within the context of sustainable development

The design parameters are both quantitative and qualitative, encompassing multidimensional aspects of the product and its prototypes in terms of meeting customer quality expectations, environmental impact throughout their life cycle, and fulfilling social responsibility criteria. This process involves a comprehensive and detailed analysis and prioritization of various sustainable development parameters. It integrates customer expectations and insights from interdisciplinary expert teams. Within the developed model, each key aspect (quality, environment, and society) can be considered independently or simultaneously using designated decision-making indicators. This ensures the model's versatility and flexibility in adapting to changing market demands. Based on the aggregated decision-making indicator, the model predicts the most favourable development direction for the product, aiming to simultaneously enhance customer satisfaction with product quality, reduce the product's negative environmental impacts throughout its entire life cycle, and achieve acceptable levels of social responsibility fulfilment.
Consecutive stages of model's application are presented below.

3.1 Stage 1: Choice of the reference product and determination of the research goal

The selection of the product falls within the purview of the entity utilizing the model. This choice can be justified based on numerous factors, including the product's development stage (favouring the maturity phase), customer expectations, or the entity's individual preferences. The chosen product should be widely recognized and used, thereby increasing the efficiency of its analysis in subsequent stages of the model. This product serves as a reference product, representing a generalization of products of a particular type [32].

In accordance with the selected product, the entity defines the research objective using the SMARTER method (Specific, Measurable, Achievable, Relevant, Time-bound, Evaluate, and R - Reevaluate or Risks) [33]. It is assumed that the objective will involve determining the most favourable direction for enhancing the product using proposed alternative production solutions (prototypes), while simultaneously considering their: i) quality, ii) environmental impact throughout the life cycle, and iii) fulfilment of social responsibility criteria.

3.2 Stage 2: Determination of the Aggregated Quality Index (AQI)

The Aggregated Quality Index (*AQI*) is estimated for the current product and its prototypes. This index can be considered an aggregated measure due to its analysis of compliance and non-compliance (coverage) for all analysed quality criteria. It is considered based on two approaches: i) user-centred, where quality is the degree to which the product meets or exceeds customer requirements, and ii) production-driven, where quality is conformity to standards and design specifications [34, 35]. Following the works of [35-37], it is assumed that the assessment of product quality (and its alternatives) should be conducted using a multidimensional measure of product quality. This multidimensionality refers to the inclusion of various numbers and types of component dimensions (criteria or quality indicators) related to the product, such as performance, durability, or functionality [38]. Insights from an extensive literature review presented in [39] indicate that previous studies have focused on one-dimensional measures of product quality or provided quality assessments based on selected quality metrics. Therefore, aiming to fill this gap, original methodological frameworks for multidimensional assessment of product quality (and its alternatives/prototypes) have been developed.

The proposed method includes assessing the importance of product criteria (as determined by customers) and assessing the fulfilment of customer expectations regarding the quality of these criteria (while simultaneously considering customer expectations and expert team requirements). The product and its prototypes quality index are determined sequentially, as outlined in steps 2.1-2.3.

- Step 2.1. Identification of the quality criteria

Quality criteria relate to customer satisfaction with product usage. These criteria can be perceived as external (e.g., brand, price, country of origin) or internal [39]. In the proposed approach, product quality criteria refer to an internal conceptualization of quality perception [40]. This implies that modifying product criteria changes the nature of the product, thus affecting the perception of

quality both objectively and subjectively. As stated in [41], objective quality determines whether a product fulfils its functions as expected by customers. Objective quality also encompasses engineering design, where product criteria are measured to shape perceived quality as objectively recognized by experts. On the other hand, subjective quality concerns customers' perception of product quality and serves to conceptualize it [39, 42].

Product quality criteria can be selected according to the ISO/IEC 25010 standard, which includes criteria such as functional suitability, performance, compatibility, usability, reliability, security, maintainability, and portability [43]. Additionally, the selection of criteria can be based on foundational research in this area, such as [34, 37] and aligned with other works from a literature review [35, 39, 44]. Based on these sources, the proposed model focuses on internal quality criteria. Criteria should be chosen that relate to the target product (the subject of the study). However, reducing the analysis to criteria that meet all quality indicators is impractical and inefficient for assessing overall product quality. As mentioned in [45], identifying numerous product criteria, most of which are insignificant in the holistic perception of product quality, is unnecessary. Therefore, following [45], it is advisable to limit the criteria to key factors that have the greatest impact on customer satisfaction with product usage [46].

The selection of criteria is carried out by an expert team, chosen based on their knowledge and qualifications relevant to the study and analysis. Methodical selection of expert teams is outlined in [47, 48]. According to literature reviews, a sufficient number of experts can range from six to eight [49], four to fifteen [50], or, as proposed in [51], an optimal team size could be ten experts. Following [52], experts may include employees of companies manufacturing the selected product, assuming that this product is interpreted as a reference product (products of varied brands differing in specifics but serving the same purpose and belonging to the same type). Delegating decision-making to an expert team, including employees of manufacturing companies, reflects current practices of well-functioning organizations where employees participate in participatory practices and teamwork, and interdisciplinary or multifunctional teams are key assets in the improvement process [53].

This expert team can effectively select criteria, basing their choices on the specificity, usefulness, and often ambiguity of the criteria. The selection of criteria is carried out according to the product catalogue (specification), which includes key product criteria in terms of customer usage. To efficiently select the main criteria, it is recommended to utilize teamwork and decision-making methods [52], such as Preliminary Criteria Reduction (PCR) [54]. The total number of quality criteria should be below 10, adhering to the principle of a minimum number of 7±2 [46].

Since quality criteria have different parameters (measures, specifications), it is necessary to characterize them for further evaluation. This characterization involves defining the parameters of the criteria, such as those used to measure their quality, e.g., parameters in the product catalogue (specification). The magnitude of these parameter measures should be expressed in international metric units, such as value, value range, or a verbal description of the criterion's state. It is assumed that the current (marketed) product is characterized according to its specification, meaning that the criteria are expressed in their current state, as in the product catalogue.

The model concept assumes that the direction of product improvement will be determined based on a multidimensional assessment of various modifications of this product, referred to as design solution alternatives (product prototypes). These prototypes are developed as modifications of the current product's quality criteria. The number of prototypes should adhere to the principles of effective comparison, so the total number of prototypes along with the reference product should not exceed 15 [55], where the minimum number should meet the 7±2 principle [46]. Prototypes are developed as modifications of the current state of the reference product's criteria. Modifying current criteria to hypothetical ones is done according to the Pareto principle [21 ,56, 57], meaning that various modifications of quality criteria, changing their characteristic values (parameters), are proposed by increasing or decreasing them by 20 % in a sequential manner. Decisions regarding these modifications are made by the previously selected expert team.

- Step 2.2. Gathering of customers' expectations

To assess the quality of the product and its prototypes, obtaining customer expectations is essential. Customers express their expectations regarding the importance (weights) of product criteria and their satisfaction with the quality fulfilment of these criteria. At this stage, the expert team plays a crucial role in supporting the assessment process of quality criteria fulfilment. Incorporating the Voice of Customer (VoC) [58] and expert opinion is important because customers tend to express their satisfaction through overall ratings or perceptions of product quality, rather than objective measures of criteria compliance with technical standards [35, 59]. Meanwhile, the expert team can verify these assessments by analysing their alignment with customer requirements, for example, through focus groups [51].

Customer expectations are gathered through exploratory research, with survey research being the most popular method used in customer satisfaction studies [60]. If the survey responses are imprecise, in-depth interviews may be necessary. The recruitment strategy for survey participants should be well-planned to ensure high-quality results and sample representativeness. It is expected that the database will be built on real customer experiences with the product, with customers participating in the survey having used the studied product for at least a month [61]. The representative sample size of customers can be estimated using the method from [57].

During the survey, customers rate the importance (weights) of the product's quality criteria, including its prototypes. The importance rating reflects the significance of these criteria in terms of their utility in the product. The ratings are given on a 5-point Likert scale [62], where 1 represents a criterion that is insignificant, and 5 represents a criterion that is significantly important.

Additionally, customer satisfaction with the fulfilment of these criteria is assessed during the survey. This assessment indicates the extent to which each criterion meets customer expectations regarding the product's utility. Satisfaction ratings are also provided on a Likert scale [62], where 1 represents a criterion that does not meet the expected quality, and 5 represents a criterion that significantly meets the expected quality.

An advantage of the proposed model is its ability to compare the *i-th* product criterion against the *j-th* product alternative, ensuring increased precision in the assigned ratings. This approach involves a pairwise comparison of the same criteria across different solution variants, which is effective in multi-criteria decision-making [12].

- Step 2.3. Processing customers' expectations

After obtaining customer expectations regarding the importance of criteria, the next step is to rank the criteria's importance to form them into groups distinguished by the significance of these criteria to customers. Due to the assumption regarding the total number of quality criteria (7±2) [46] and the adopted five-point scale for rating the im-portance of these criteria, the criteria weights are calculated as the arithmetic mean of the criteria importance ratings [55, 57].

Subsequently, the assessment of product and its prototypes quality is conducted. To maintain the multidimensionality of this assessment corresponding to a varying number of criteria across different component dimensions (criteria or quality indicators) of the product [38], an expert assessment of quality is proposed, which applies to calculating the level of multi-aspect quality for any products or processes that may be in the design, production, or operational phase. For this purpose, Eq. 1 is utilized to calculate the *AQI*:

$$AQI_i = \frac{\sum w_{ij} q_{ij}}{\sum w_{ij}} \tag{1}$$

where: *i* – product or prototype; *j* – criterion, *j, i* = 1, 2,..., *n*; w_{ij} – weight of the *j-th* criterion for the *i-th* product or prototype; q_{ij} – quality of the *j-th* criterion for the *i-th* product or prototype.

AQI pertains to customer satisfaction with the utility of the product (and its pro-posed alternatives). It enables the development of a product ranking based on customer satisfaction with their quality. The maximum value of the *AQI* corresponds to the most favourable product.

3.3 Stage 3: Determination of the Environmental Impact Index (EII) in the life cycle

The model assumption is, that the direction of product improvement will be considered regarding the environmental impact of its prototypes throughout their life cycle. To achieve this, an Environmental Impact *Index (EEI)* for the product (and its prototypes) over the entire life cycle has been developed. This indicator is determined using results obtained from the LCA method. It is a structured, comprehensive, and internationally standardized method that quantitatively assesses important emissions and resources, including environmental and societal impacts, resource depletion, and other issues arising throughout the life cycle of any product (as well as processes or services). LCA is recognized as an effective decision-support method that, when supplemented with other tools, contributes effectively to more environmentally sustainable consumption and production practices.

LCA is often applied in the area of product design (including improvement) as a specialized method dedicated to strategic assessments of new concepts [63]. It is most often conducted in accordance with ISO 14040 [64], which includes phases such as defining goals and scope, inventory analysis, impact assessment, and interpretation [61] (Fig. 4).

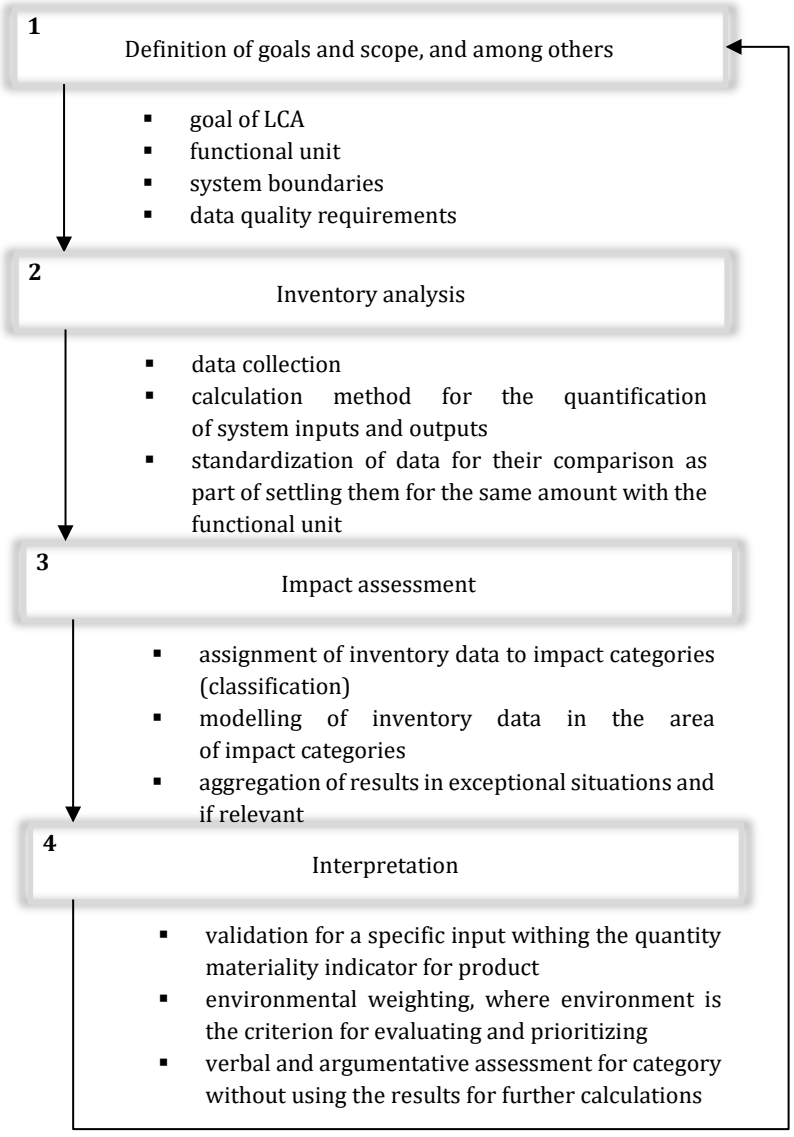

Fig. 4 LCA in ISO 14040 norm [63]

In our model, the existing product is compared with existing products (prototypes, modified products within the framework of the current/real product). The challenge of using LCA in this approach is conditioned by the lack of complete definitions and data for estimation during the design process, where the concept and architecture of prototypes are developed. Consequently, the use of LCA is focused on answering environmental protection questions, such as "Which of the proposed design solutions is more environ-mentally favourable?" The ability to answer this question accurately lies with specific experts, ideally environmental experts [63].

The full and detailed scope of an LCA system begins with the extraction and pro-cessing of materials, continues through production, usage, and ends with the product's end-of-life stage, adhering to the fundamental cradle-to-grave approach for life cycle assessment [65]. LCA involves analysing each stage of material transformation, including intermediate states, culminating in the synthesis of the final product [66, 67]. LCA application can be supported by software, e.g.: OpenLCA, SimaPro, Gabi [68, 69].

For less rigorous LCA applications, it is preferable to use Level 1 LCA or Level 2 LCA [70]. These levels were deemed adequate for the proposed model. LCA should be conducted for the reference product (current and commercially available), resulting in a single $EII > 0$ value, such as for carbon footprint, which has a measurable, numerical nature.

After evaluating the reference product, a prospective life cycle assessment (LCA) of its prototypes – alternative products modified according to quality criteria parameters and specifications – is conducted. LCAs for prototypes still in the design phase face inherent limitations due to incomplete data, which can result in compilation challenges and an increased risk of errors [63]. Traditionally, scenario analysis has been employed to conduct LCAs for products during the design phase [71, 72].

Our research, however, seeks to advance this process by more comprehensively integrating results from various model stages, addressing qualitative, environmental, and social aspects. To this end, we propose a novel approach that predicts environmental impact changes in prototypes relative to the quality levels of the reference product. This method utilizes simplified modelling of LCA value changes, aligning with quality parameter modifications, and adheres to the Pareto principle [73]. For instance, if the current quality level of a product results in a particular LCA outcome, a 20 % increase in quality level is expected to produce a corresponding 20 % increase in the LCA result, as previously tested in [21, 56].

The prospective and simplified LCA for product prototypes is conducted following Eq. 2 [21]:

$$EII_i = EII\ (1 + p) \tag{2}$$

where: EII – reference product in its life cycle, p – percentage change of EII represented in decimal form; i – prototype, $i = 1, 2, \ldots, n$.

Obtained EII enables the ranking of products, and their prototypes based on their environmental impact in LCA. The top position in the ranking corresponds to the minimum EII value, where a lower EII value indicates a smaller negative environmental impact.

3.4 Stage 4: Determination of the Social Responsibility Index (SRI)

Research design assumes that product improvement will also consider the fulfilment of social responsibility standards. This derives from the concept of sustainable enterprise development, where it is essential for companies to take actions based on a shared understanding of social responsibility. Social responsibility according to ISO 26000 [74] is defined as the impact of a company's decisions and actions on society through transparent and ethical behaviours across seven core areas: organizational governance, human rights, labour practices, environment, fair operating practices, consumer issues, and community involvement and development.

Various approaches exist in our fields of research (management, production engineering), e.g.: social innovation design [75], which emphasizes the role of designers, or transformation design [76], focusing on designing within social transformation in a local context. These approaches confirm that designers can directly and indirectly encompass social responsibility in their products, processes, and services. Social responsibility within products is derived from individual ethical

values of designers [77], as well as customer needs, including engagement of other enterprise stakeholders, e.g., through Corporate Social Responsibility (CSR) [78]. In our model, social responsibility specifically pertains to Socially Responsible Design (SRD) [79].

SRD focuses on alleviating societal problems to improve the quality of life through intentional design. During socially responsible design, it is necessary to address macro-social issues (e.g., health, governance, education, crime, fair trade, social inclusion, and economic policy) and macro-environmental requirements (poverty, energy, climate change, rapid population growth, etc.) [78]. For manufacturing enterprises, decisions involving social responsibility should be made as early as possible in the product engineering process, ideally during product design – to increase the likelihood of cost reduction and efficiency. This is achieved by understanding the societal impacts of offered products and how changes in these products can contribute to sustainable production [77 ,80].

In this regard, we propose the Social Responsibility Index (*SRI*) for products and their prototypes, calculated through steps 4.1-4.3 described below and conducted by team of experts. They are selected independently [47, 48]. The number of experts vary from 6-8 [49], 4-15 [50], or 10 [51] experts. According to [81], fewer experts in the team are beneficial because a collective opinion leads to fewer socially responsible decisions resulting from an increase in the moral leeway of their opinions. Experts should also come from various disciplines (interdisciplinary collaboration) [77] and include: i) de-signers from the model applicating enterprise; ii-a) CSR experts from the company, or, in a more ambitious approach, ii-b) experts in Sustainable Development Goals (SDGs) from relevant NGOs. Such a team composition assures a socially responsible approach to business, including defining a sustainable development perspective and supporting sustainable production and consumption analyses [75-77, 79].

- Step 4.1. Identification of the social responsibility criteria

The model design focuses on evaluating products and their prototypes by assessing the importance and feasibility of social responsibility criteria. These criteria are selected by a team of experts and are based on six areas specified in ISO 26000, excluding the environmental area as it is addressed in the third stage of the model [74]: i) Organizational governance; ii) Human rights (due diligence; human rights situations at risk; avoidance of complicity; resolving grievances; discrimination and vulnerable groups; civil and political rights; economic, social, and cultural rights); iii) Labour practices (employment and working relationships; working conditions and social protection; social dialogue; occupational health and safety; employee training and development); iv) Fair operating practices (anti-corruption measures; responsible political engagement; fair competition; promoting social responsibility in value chains; respect for property rights); v) Consumer issues (fair marketing, factual and impartial information, and fair contractual practices; consumer health and safety protection; sustainable consumption; customer service, support, complaint resolution, and dispute settlement; consumer data protection and privacy; access to basic services; education and awareness); vi) Community involvement and development (community engagement; education and culture; job creation and skills development; development and access to technology; wealth and income creation; health; social investments).

Analysing all social responsibility criteria is inefficient, as many may be irrelevant to the overall assessment of a product's or prototype's social responsibility [45]. Therefore, the selected social criteria should specifically relate to the target product (research subject) and establish a strong connection to fulfilling social responsibility objectives [46].

The selection process for these criteria is carried out by an expert team using methods such as focus groups or alternative approaches like PCR [54]. To ensure consistency in the criteria analysis throughout the model, the total number of social responsibility criteria should ideally fall within the range of 7±2 [46], aligning with the number of qualitative criteria used in Stage 2.

- Step 4.2. Grading of the social responsibility criteria

The social responsibility criteria selected in Step 4.1 are subjected to significance grading. Experts evaluate these criteria based on their relevance to overall customer satisfaction with the product.

The importance of each criterion is rated using a five-point Likert scale [62], where: 1 – criterion irrelevant, 5 – most important criterion.

The weight (g_i) of each social responsibility criterion is then calculated as the arithmetic mean of the importance ratings assigned to that criterion.

- Step 4.3. Evaluation of the degree of accordance with social responsibility standards

The analysed product and its prototypes are assessed for their compliance with social responsibility standards. Ratings are assigned by an expert team using a scale from 0 to 1 [82], where: 0 indicates the criterion does not meet social expectations; 1 indicates full satisfaction of social expectations; and 0.7 denotes acceptable fulfilment of social expectations [55, 57].

Focus groups [51] are often employed for assigning these ratings. The evaluation is conducted based on the social responsibility criteria identified in Step 4.1. Simultaneously, analysing the qualitative criteria parameters (from Stage 2 of the model) that may influence the social responsibility fulfilment of the product and its prototypes is beneficial.

Assessing socially responsible products is inherently linked to uncertainty, including epistemic uncertainty regarding actual consequences and ethical uncertainty concerning the purpose of the evaluation [77, 80]. This ambiguity arises from questions about whether the outcomes of socially responsible products will be desirable, particularly if they introduce potential disadvantages for stakeholders, such as increased prices or reduced usability compared to alternative solutions.

To reduce this uncertainty, the proposed model incorporates an analysis of the potential negative effects of social responsibility initiatives [77, 80]. Expert assessments of social expectation fulfilment can be supported by supplementary questions, such as those proposed in [83, 84]. Achieving a comprehensive assessment of social responsibility fulfilment in verified products and prototypes requires ethical conduct by the expert team. Additionally, the process encourages the integration of sustainable design practices—an ongoing global challenge [82].

After assessing the social responsibility fulfilment, the *SRI* is determined for the product and its prototypes, considering the importance of social responsibility criteria (identified in Step 4.2.). The *SRI* index is based on the concept proposed in [43], adopting the Coverage of Fulfilment method. This method distinguishes between fulfilment coverage for different social criteria and total coverage for these criteria across the analysed products and prototypes. Initially, the Total Coverage for each social criterion (*OP*) is calculated for the product and its prototypes, considering the importance of these criteria (Eq. 3):

$$OP_i = \sum g_i \frac{ps_i}{rs_i} \tag{3}$$

where: ps_i – the number of positive grades (value = 1) of fulfilment of social responsibility standards for per criterion; rs_i – the total number of all grades per criteria within the fulfilment of social responsibility standards; g_i – criterion weight; i – product or prototype, i = 1, 2,..., n.

Subsequently, the *SRI* is determined for a given product and prototype (Eq. 4):

$$SRI_i = \sum OP_i \tag{4}$$

where: OP_i – total coverage for social criteria of the i-th product or its prototype; i – product or prototype, i = 1, 2,..., n.

The *SRI* allows to create a ranking of products or their prototypes in terms of accordance with social responsibility standards. Higher *SRI* values indicate a more favourable level of this index.

3.5 Stage 5: Calculation of the aggregated Quality-Environment-Social-Responsibility Indicator (QESR)

The model aims to determine the most favourable direction for product development, considering its quality, environmental impact throughout the life cycle, and fulfilment of social responsibility standards. Therefore, at this stage of the model, the *AQI*, *EII,* and *SRI* are aggregated into a single composite Quality-Environment-Social-Responsibility Indicator (*QESR*).

It is assumed that each index determined within the model, *AQI*, *EII*, and *SRI*, is a normalized index. This is necessary to standardize these index values into a unified and comparable measure [85], given the inability to standardize the values of an LCA index, where the value does not have an upper boundary limit. Therefore, this relativization (normalization) is necessary and consequently requires appropriate actions on the quality and social indices. The proposed relativization is applicable if the total number of analysed products meets the principle of a minimum of 7±2 products [46].

Initially, the normalized *AQI* for the *i*-th product or prototype is calculated (Eq. 5):

$$w_{ji} = \frac{AQI_{max} - AQI_i}{AQI_{max} - AQI_{min}} \tag{5}$$

where: w_{ji} – normalized *AQI* for the i-th product or prototype; AQI_{max} – highest quality; AQI_{min} – lowest quality (both max and min can be calculated with any method, but consequently the same throughout the whole *QESR* application); *i* – product or prototype, *i* = 1, 2,..., *n*.

Then, the normalized *EII* is calculated (Eq. 6):

$$W_{si} = \frac{EII_{max} - EII_i}{EII_{max} - EII_{min}} \tag{6}$$

where: ws_i – normalized *EII* for the i-th product or prototype; EII_{max} – highest LCA value; EII_{min} – lowest LCA value; *i* – product or prototype, *i* = 1, 2,..., *n*.

Then, the normalized *SRI* is calculated (Eq. 7):

$$w_{pi} = \frac{SRI_{max} - SRI_i}{SRI_{max} - SRI_{min}} \tag{7}$$

where: wp_i – normalized *SRI* for the i-th product or proto-type; SRI_{max} – highest *SRI* value, SRI_{min} – lowest *SRI* value; *i* – product or prototype, *i* = 1, 2,..., *n*.

Then, the aggregated *QESR* indicator is calculated as in Eq. 8:

$$QESR_i = \frac{\alpha w_{ji} + \beta w_{si} + \gamma w_{pi}}{\alpha + \beta + \gamma} \tag{8}$$

where: α – relevance of the quality component; β – relevance of the environment component; γ – relevance of the social responsibility component; w_{ji} – normalized *AQI*; w_{si} – normalized *EII*; w_{pi} – normalized *SRI*; *i* – product or prototype, *i* = 1, 2,..., *n*.

Then, considering the normalized indexes, their weights can be adjusted in the process of calculating the aggregated index. The weights of each aspect are assigned collectively by experts from teams selected in stages 2, 3, and 4 of the model. It is possible to establish such weights [55, 86, 87], e.g. α = 7, β = 3, γ = 2. In such a case the Eq. 9:

$$\alpha{:}\beta{:}\gamma{:}\delta = 7{:}3{:}2 \tag{9}$$

It should be noted that the change of adopted ratios between the indexes would result in changes in the final hierarchy of decision alternatives. Hence, the model is sensitive to the weights of normalized indexes.

The total weight sum does not have to equal 1, allowing for considerable flexibility in determining the weight proportions. The aggregated *QESR* indicator is calculated with use of Eq. 10:

$$QESR_i = 1 - \left(0.083\left(7w_{ji} + 3w_{si} + 2w_{pi}\right)\right) \tag{10}$$

where: w_{ji} – normalized *AQI*; w_{si} – normalized *EII*; w_{pi} – normalized *SRI*; *i* – product or prototype, *i* = 1, 2,..., *n*.

The *QESR* indicator is interpreted as follows: i) from a qualitative perspective, it represents the level of customer satisfaction with using the product; ii) from an environmental perspective, it indicates the potential for achieving a product that is environmentally friendly throughout its lifecycle, depending on the analysed environmental impacts; iii) from a social perspective, it signifies the fulfilment of societal expectations within the product. A higher *QESR* indicator value reflects a closer-to-perfect level of the three analysed aspects simultaneously.

3.6 Stage 6: Elaboration of a product ranking under the aggregated QESR Indicator

Based on the Quality-Environment-Social-Responsibility (*QESR*) indicator, a ranking of products (or their alternatives) is created. Products should be ordered from highest to lowest *QESR* value. A higher *QESR* value indicates a more favourable index and higher customer satisfaction level. Therefore, the top position in the ranking corresponds to the maximum *QESR* value and represents the product that is most desired in terms of quality, environmental impact, and social responsibility. The verbal interpretation of the *QESR* indicator is conducted on a relative scale (Fig. 5).

The *QESR* indicator can help improving products, i.e. a prototype with the maximum *QESR* value will best meet customer expectations in terms of quality, while also having a minimal negative environmental impact in its entire life cycle, at the same time keeping the social responsibility standards.

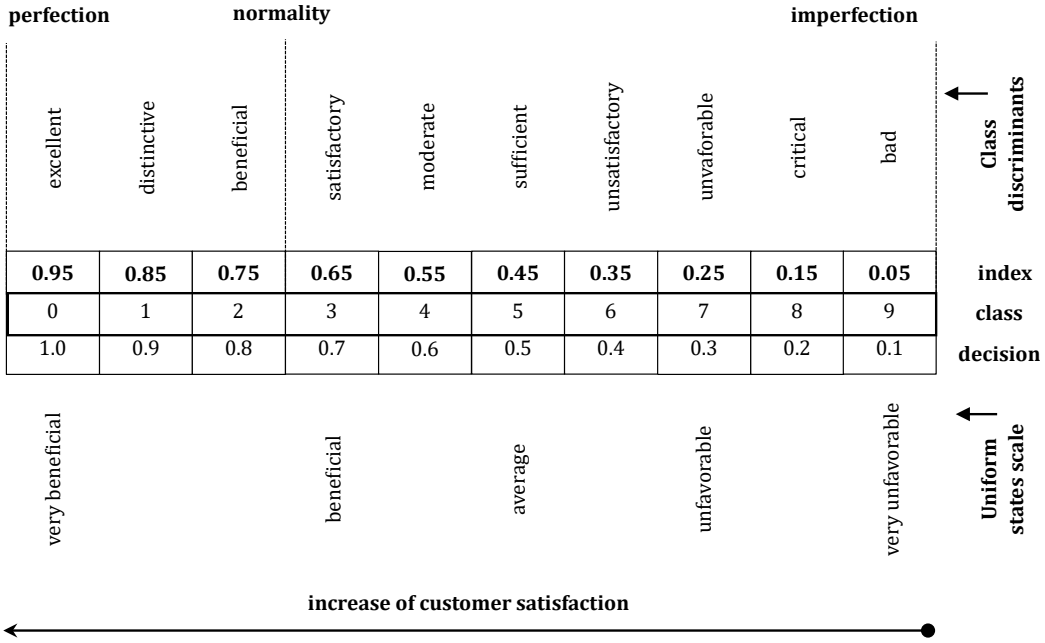

Fig. 5 Interpretation scale of the QESR indicator: customer satisfaction with the products in terms of quality, environmental impact, and social responsibility [51, 60].

4. Results

Light Passenger Vehicles (LPVs) of a global manufacturer were employed as study subject. They are pivotal in mitigating climate change due to their energy efficiency and reduced environmental impact during use [88]. The analysis focused on a Hybrid Electric Vehicle (HEV) [89], which proves to be a promising solution for fuel savings, moderating fuel costs for consumers, and aiding in pollution reduction while meeting environmental regulations. The key advantage of HEVs lies in their drivetrain, which re-duces fuel consumption through an electric motor (EM) to achieve the required vehicle power. The electric motor utilizes energy from a battery or regenerative braking to power auxiliary systems and minimize engine idling [90]. A detailed characterization of HEVs is presented, for instance, in [91]. Moreover, hybrid vehicles are widely recognized and utilized globally, thus meeting model assumptions. Due to the research's specificity, the analysed HEV is seen as a reference vehicle, or a generalization of vehicles of this type [32].

For Stage 1 of the model, the research goal was established for the selected subject of study: determining the most favourable direction for improving HEVs through proposed manufacturing alternatives (prototypes), considering their: i) quality, ii) environmental impact throughout their lifecycle, and iii) meeting the social responsibility standards.

In Stage 2 a team of five experts undertook the task of defining a quality index for HEV and its prototypes. Initially, quality criteria were established to internally conceptualize quality perception. The selection process was guided by broad categories of quality criteria outlined in ISO/IEC

25010 [43], the HEV catalogue (specification), and quality criteria proposed by other authors (e.g., [90-93]. The primary quality criteria chosen for verification included: total mass (kg), maximum engine power (kW), maxi-mum speed (km/h), battery range (km), battery charging time (hours), vehicle colour, vehicle dimensions (mm), equipment, fuel consumption (average), and drivetrain. The assumptions regarding the number of quality criteria, with a maximum of 10 and a minimum of 5 [46], were met.

Subsequently, all criteria were characterized based on their descriptive measures. For the reference HEV, the catalogue (specification) and current parameters of these criteria were utilized. Six design solution prototypes for the reference HEV were pro-posed. These prototypes were developed as modifications of the current states of the analysed HEV criteria. According to the proposed model concept, the Pareto-Lorenz principle (20/80) was applied in this process. Seven design solutions were obtained (the current solution and its six modifications/alternative design solutions), as shown in Table 2.

Table 2 Characteristic of reference HEV criteria and its prototypes

Alternative	C1	C2	C3	C4	C5
Ref. product	1815	140	200	1195	≈30 min
Prototype 1	2178	84	220	1434	> 30 min to 3 h
Prototype 2	2541	112	240	1673	> 3 h to 6 h
Prototype 3	2904	168	260	1912	> 6 h to 9 h
Prototype 4	3267	196	180	2151	> 9 h to 12 h
Prototype 5	1452	224	160	956	> 12 h to 15 h
Prototype 6	1089	252	140	717	> 15 h
Alternative	C6	C7	C8	C9	C10
Ref. Product	white pearl	4630 × 1780 × 1435	basic	4.40	front axis
Prototype 1	clean white	5556 × 2136 × 1722	advanced	5.28	rear axis
Prototype 2	light grey	6482 × 2492 × 2009	full	6.16	AWD
Prototype 3	dark grey	7408 × 2848 × 2296	advanced	7.04	4 × 4
Prototype 4	black	3704 × 1424 × 1148	basic	7.92	front axis
Prototype 5	red	2778 × 1068 × 861	full	3.52	rear axis
Prototype 6	white pearl	1852 × 712 × 574	basic	2.64	4 × 4

C1: total mass (kg); C2: maximum engine power (kW); C3: maximum speed (km/h); C4: battery range (km); C5: battery charging time (hours); C6: vehicle colour; C7: vehicle dimensions (mm); C8: equipment; C9: fuel consumption (average) (l); C10: drivetrain.

To assess the quality of HEV and its prototypes, customer expectations were gathered through a survey conducted as a pilot study to verify the proposed model concept. The survey was conducted in March and April 2024 among 116 randomly selected customers who use LPVs. Pilot studies [94, 95] proved this sample size to be sufficient. The survey was administered electronically through Microsoft Forms. The response rate for the survey was 100 %, and the collected data complete. This resulted from the form of pilot studies, which were conducted in a targeted (non-random) manner to specific customers who had previously expressed a willingness to participate in the survey. Additionally, the studies were carried out in-depth by utilizing direct communication techniques with customers. This involved obtaining surveys during direct interviews, which aimed to identify potential difficulties in completing the survey (understanding the survey questions). Simultaneously, the use of a computer tool aided in avoiding mistakes regarding skipping a question or a required response. In the survey, customers rated the importance of selected vehicle criteria on a Likert scale and evaluated the quality fulfilment of these criteria based on the proposed design alternatives.

Based on the acquired ratings of criterion weights for the reference HEV, the im-portance and quality of criteria were determined by calculating the arithmetic mean of these ratings. Following the developed model, Eq. 1 was utilized to calculate the *AQI* for reference vehicle and its prototypes (Table 3).

Table 3 Relevance of the quality criteria for the HEV and ranking of HEV

No.	Quality criteria	Criterion weight	Quality of criteria for HEV and its prototypes						
			Ref.	P1	P2	P3	P4	P5	P6
C2	maximum engine power (KM)	4.09	3.66	2.07	2.76	3.75	4.06	4.33	4.33
C4	battery range (km)	4.18	3.37	3.71	4.00	4.33	4.47	2.46	2.04
C5	battery charging time (h)	4.09	4.57	3.83	2.76	2.24	1.81	1.46	1.30
C9	fuel consumption (average) (l)	4.21	4.47	4.11	3.61	3.19	2.98	4.63	4.68
C3	maximum speed (km/h)	3.86	3.97	4.17	4.27	4.28	3.33	2.70	2.33
C7	vehicle dimensions (mm)	3.43	3.51	3.23	2.92	2.75	3.60	3.34	2.86
C8	equipment	3.84	3.31	4.44	4.70	4.44	3.31	4.44	3.31
C10	drivetrain	3.85	3.99	3.82	3.84	4.64	3.99	3.82	4.64
C1	total mass (kg)	2.95	3.66	3.36	3.09	2.74	2.36	3.34	2.90
C6	vehicle colour	2.74	3.82	3.56	3.75	3.97	4.42	3.39	2.49
	AQI		3.81	3.64	3.58	3.65	3.43	3.39	3.12
	Ranking		1	3	4	2	5	6	7

AQI ranks the utility of the reference HEV and its prototypes. It was observed that the reference vehicle performed best. However, the ranking may be reversed in further stages of model application, when considering environmental impact and social responsibility.

In Stage 3, the *EEI* of the HEV throughout its life cycle was determined. A second level LCA was conducted under ISO 14040 rigor [64], utilizing GREET v1.3.0.13991 software data [96], covering material extraction and processing, production, usage, and recycling.

The functional unit was defined as the vehicle traveling 150,000 km [89, 97, 98]. This unit allowed for data normalization to facilitate comparison with vehicle prototypes. However, the functional unit could vary, e.g. [99] proposes 200,000 km. The system boundaries were set within the timeframe of 2021-2024 and data from the GREET model.

The first phase of LCA included carbon dioxide (CO_2) from material extraction and processing in vehicle component construction, involving extraction, smelting, beneficiation, and refining [100]. Following [101], CO_2 emissions in this initial phase are calculated with Eq. 11:

$$\begin{cases} C_M = \sum_x \left(C_{x,f} + C_{x,e}\right) \\ C_{x,f} = m_x \sum_n \left[E_{x,n} \sum_k \omega_{x,n,k} \alpha_k\right] \\ C_{x,e,} = m_x \sum_n \left(\frac{E_{x,n} \omega_{x,n,e}}{3600}\right) \end{cases} \tag{11}$$

where: $C_{x,f}$ – CO_2 emission from fuel consumption at material production; $C_{x,e}$ – CO_2 emission from electricity consumption at material production; x – material; m – weight (kg); n – production process; $E_{x,n}$ – energy consumption per material unit in its production process (kJ/kg); k – fuel; $\omega_{x,n,k}$ – share of fuel consumption in $E_{x,n}$; $\omega_{x,n,e}$ – share of electricity consumption in $E_{x,n}$; α_k – CO_2 emission factor from fuel consumption (CO_2kg/kJ).

Main materials in HEV production were identified, excluding low mass materials. Emissions during the processing of these materials were specified according to the literature [102] (Table 4). Data from the GREET model and [100, 101] results allowed us to adopt the energy consumption coefficient for material production and the CO_2 emission factor for energy consumption in the

entire life cycle. In this way, CO_2 emissions from the material extraction and processing phase for the analysed reference vehicle were calculated (Table 4). The total CO_2 emissions during the material extraction and processing phase for the HEV amounted to 623.19 kJ = 0.623 MJ. It was inferred that fuel consumption emissions contributed significantly more to the total CO_2 emissions during the first LCA phase.

Table 4 Main materials in HEV production and CO_2 emissions

Material	Material (kg)	Emission factor of material production (CO_2/kg)	CO_2 emission from fuel consumption	CO_2 emission from electricity consumption	Total CO_2 emission
Steel	899.80	2.00	403.28	0.10	403.38
Iron	77.20	0.55	0.10	0.00	0.11
Cast aluminium	67.50	2.62	86.95	0.08	87.02
Wrought aluminium	27.60	5.92	76.15	0.07	76.22
Copper	57.90	2.35	25.20	0.02	25.22
Glass	35.80	1.62	1.95	0.00	1.95
Plastic	148.80	3.05	16.19	0.02	16.21
Rubber	23.40	3.62	403.28	0.10	403.38

Next, emissions resulting from vehicle and component production were analysed. This analysis focused on emissions during the processing and assembly of key com-ponents, with the possibility of additionally considering emissions during their distribution [100]. Following the methodology presented in [101], CO_2 emissions were calculated using Eq. 12:

$$\begin{cases} C_{VA} = \sum_{x} \left(C_{y,f} + C_{y,e}\right) + \dfrac{E_{VA}}{3600} \\ C_{y,f} = \sum_{q} \left[E_{y,q} \sum_{k} \omega_{y,q,k} \alpha_k \right] \\ C_{y,e,} = \sum_{q} \left(\dfrac{E_{y,q} \omega_{y,q,e}}{3600} \right) \end{cases} \tag{12}$$

where: C_{va} – CO_2 emission from vehicle components production; $C_{y,f}$ – CO_2 emission from fuel consumption at component production; $C_{y,e}$ – CO_2 emission from electricity consumption at component production; y – vehicle component (part); E_{va} – electricity consumption at vehicle assembly; q – production process; $E_{y,q}$ – energy consumption per component in its production process (kJ); $\omega_{y,q,k}$ – share of fuel consumption in $E_{y,q}$; $\omega_{y,q,e}$ – share of electricity consumption in $E_{y,q}$; α_k – CO_2 emission factor from fuel consumption (CO_2kg/kJ).

GREET data and detailed characteristics of the vehicle production process allowed us to estimate the energy consumption and CO_2 emission levels when producing components for the reference HEV (Table 5). The assembly of the main components is assumed to consume approximately 862 MJ of energy.

A crucial component of an HEV is the battery. In this analysis, a lithium-ion (Li-Ion) battery was examined, consisting of elements such as the cathode, anode, separator, electrolyte, packaging, and battery management system. Based on the GREET model and [98, 103, 104], a material list for this type of battery was assumed.

Table 5 Energy consumption and CO_2 emissions in the production process of an LPV

Production process	Energy (MJ)	CO_2 (kg)
material transformation	22912.60	1261.73
machining	1163.40	66.34
vehicle painting	4936.75	317.51
HVAC & lighting	3951.06	266.56
heating	3684.50	231.02
material handling	817.46	54.50
welding	1089.95	73.45
compressed air	1634.92	110.18

Additionally, based on studies presented in [98, 103, 104] and data from the GREET model, the energy consumption during the production of the Li-Ion battery was determined. The assembly of a Li-Ion battery consumes approximately 2.67 MJ/kg, resulting in about 1002 MJ for the entire battery. With Eq. 12, CO_2 emissions during the production and assembly of HEV components (including the battery) are estimated to be around 43,572.18 MJ.

Subsequently, an analysis of energy consumption and carbon emissions during the vehicle's usage phase, which constitutes the third phase of the life cycle, was conducted. This phase includes fuel consumption and vehicle maintenance [100]. Eq. 13 was applied [101]:

$$C_{VU} = \frac{dF_k}{100}(\rho_k \alpha_k LHV_k + C_k) \tag{13}$$

where: C_{vu} – CO_2 emission from vehicle exploitation; d – total distance driven (km); F_k – combustive fuel consumption (l/100 km); ρ_k – fuel viscosity; k – fuel; LHV_k – lower calorific value of fuel (kJ/kg); C_k – CO_2 emissions per k unit of fuel production.

The lifespan of an HEV is around 150,000 km [97], we assumed the use of PB 98 gasoline within standard specifications. Based on the manufacturer's characteristics, the average fuel consumption of the HEV is assumed 4.4 L/100 km, and the total driving range with a full tank and hybrid drive is up to 1000 km. Using Eq. 13, CO_2 emissions during the reference phase of HEV over its lifespan are estimated to be ap-proximately 470,969 MJ.

Next, an analysis of emissions during the recycling of selected HEV components was conducted. This pertains to the fourth phase of LCA — recycling, disposal, and reuse [99]. This phase includes disassembly, separation, and purification of metals and other non-metallic materials. Metals are recycled, while other materials like plastics and glass are typically landfilled or incinerated. For Li-Ion batteries, the recycling process includes cooling the battery, cutting, and shredding, separating, and sorting shredded material, converting lithium to lithium carbonate (or lithium oxide), neutralizing electrolytes to stable compounds, and, if applicable, recovering cobalt from lithium cobalt oxide [105]. CO_2 emissions in the fourth phase of LCA are estimated using Eq. 14 [101]:

$$\begin{aligned} C_{RE} &= C_{re,f} + C_{re,e} \\ C_{re,f} &= \sum_x \left[m_x E_{re,x} \sum_k (\omega_{re,x,k} \alpha_k) \right] \\ C_{re,e} &= \left[\frac{E_{vd}}{3600} + \sum_x \left(m_x \frac{E_{re,x} \omega_{re,x,e}}{3600} \right) \right] \end{aligned} \tag{14}$$

where: C_{RE} – CO_2 emissions from vehicle recycling; $C_{re,f}$ – CO_2 emissions from fuel consumption during vehicle recycling; $C_{re,e}$ – CO_2 emissions from electricity consumption during vehicle recycling; $E_{re,x}$ – energy consumption per unit of material x in the recycling phase (kJ/kg); x – recycled material; $\omega_{re,x,k}$ – share of fuel consumption in $E_{re,x}$; $\omega_{re,x,k}$ – share of electricity consumption in $E_{re,x}$; m – weight (kg); E_{vd} – energy consumption during vehicle disassembly.

GREET data implies an assumption, that CO_2 emissions during the recycling of an HEV include approximately 630 kWh of electricity for disassembly, and for recycling the remaining components: 1114 kWh of electricity, 8.4 kWh of natural gas, and 10 kg of coal. Based on these assumptions and using Eq. 15, CO_2 emissions in the final phase of the LCA for the reference HEV are estimated to be 6608 MJ.

The total environmental impact in the LCA for the reference HEV was calculated with Eq. 15:

$$EII = C_M + C_{VA} + C_{VU} + C_{RE} \tag{15}$$

where: *EII* – *EEI* of the reference HEV in its entire life cycle; C_M – CO_2 emission from material extraction and processing; C_{va} – CO_2 emission from vehicle components production; C_{vu} – CO_2 emission from vehicle exploitation; C_{RE} – CO_2 emission from vehicle recycling.

The estimated CO_2 emissions over the life cycle of the analysed reference HEV are approximately 520,150 MJ. It was observed that the largest emissions occur during the vehicle's usage

phase, followed by component production, recycling, and the smallest amount during material extraction and processing.

After assessing the reference HEV, an LCA of its prototypes was conducted under the assumptions of the model, i.e. using simplified modelling to reflect changes in LCA values based on changes in the parameters of HEV quality criteria, following the Pareto principle [73]. The prospective and simplified LCA of HEV prototypes was carried out using Eq. 5. The results are presented in Table 6.

Table 6 Prospective LCA of HEV prototypes

Alternative	EII [MJ]	Ranking
Ref. product	520150	3
Prototype 1	624180	4
Prototype 2	728210	5
Prototype 3	832240	6
Prototype 4	936270	7
Prototype 5	416120	2
Prototype 6	312090	1

Aggregated *EII* was obtained for the reference HEV and its prototypes over their life cycle. Vehicles were ranked, with Prototype 6 securing the top position, which anticipates its least negative total environmental impact.

Next, the *SRI* for the reference HEV and its prototypes was obtained, with participation of a multidisciplinary team of four experts, including CSR specialists and the authors of the article. Initially, HEV – relevant social responsibility criteria were selected from those presented in Step 4.3 of our model. Ultimately, nine main criteria belonging to six areas indicated in ISO 26000 were chosen: (CC1) fair competition – assessment of the possibility of applying fair (including unfair) competition by using very distant or remarkably similar product solutions as another manufacturer; (CC2) promoting social responsibility in the value chain – assessment of the ap-plication of a solution that can shape social attitudes; (CC3) access to essential services – assessment of the product or prototype functionality in terms of selected usability criteria; (CC4) technology development and access – assessment of the advancement and accessibility for customers of selected technological features; (CC5) social investment – assessment of the degree of implementation of pro-social investments in terms of usability criteria of the product or its prototype; (CC6) community involvement – assessment of differences between the product and prototypes in terms of initiating pro-social behaviours for the common good; (CC7) wealth and income creation – assessment of differences in basic technological features of the product and prototypes that affect the increase in customer satisfaction level from owning a given product/prototype compared to others; (CC8) sustainable consumption – assessment of the environmental-consumption balance in the form of achieving satisfaction from the most sustainable product solution or its prototypes; (CC9) education and awareness – assessment of the possibility of providing ap-propriate product or prototype solutions as a result of customer education and awareness.

Subsequently, the relevance of these criteria was assessed in terms of accordance to social responsibility standards. The highly relevant criteria (g1) were: fair competition (CC1), promoting social responsibility in the value chain (CC2), access to essential ser-vices (CC3), technology development and access (CC4), and sustainable consumption (CC8). The moderately relevant criteria (g2) were: community involvement (CC6), wealth and income creation (CC7), and social investments (CC5). The less important criterion (g3) was: education and awareness (CC9). Fixed weights were assigned to these criteria in the ratio 50:10:1 [55, 57].

Then, the reference HEV and its prototypes were evaluated for social responsibility compliance. The evaluations were conducted by a team of experts using a 0-1 scale, where scores equal to or above 0.7 indicated an acceptable level of compliance. The social responsibility compliance scores were then processed into binary values (0 - does not comply, 1 - complies). The results are presented in Table 7.

Table 7 Social responsibility compliance of reference HEV and its prototypes

Alternative	Level of social responsibility compliance by the decision criteria (0-1)								
	CC1	CC2	CC3	CC4	CC5	CC6	CC7	CC8	CC9
Ref. product	0.5	0.8	0.9	0.6	0.6	0.6	0.8	0.6	1.0
Prototype 1	0.6	0.7	0.8	0.8	0.6	0.7	0.5	0.5	0.9
Prototype 2	0.5	0.6	0.9	0.9	0.9	0.9	0.7	0.5	0.8
Prototype 3	0.7	0.5	0.9	0.8	0.9	0.7	0.5	0.5	0.7
Prototype 4	0.8	0.4	0.7	0.7	0.7	0.6	0.6	0.4	0.6
Prototype 5	0.5	0.9	0.6	0.7	0.6	0.8	0.9	0.8	0.5
Prototype 6	0.6	1.0	0.5	0.6	0.7	0.5	0.9	0.9	0.5
Alternative	Fulfilment of social responsibility standards by the decision criteria (0 or 1)								
	CC1	CC2	CC3	CC4	CC5	CC6	CC7	CC8	CC9
Ref. product	0	1	1	0	0	0	1	0	1
Prototype 1	0	1	1	1	0	1	0	0	1
Prototype 2	0	0	1	1	1	1	1	0	1
Prototype 3	1	0	1	1	1	1	0	0	1
Prototype 4	1	0	1	1	1	0	0	0	0
Prototype 5	0	1	0	1	0	1	1	1	0
Prototype 6	0	1	0	0	1	0	1	1	0

(CC1) fair competition; (CC2) promoting social responsibility in the value chain; (CC3) access to essential services; (CC4) technology development and access; (CC5) social investment; (CC6) community involvement; (CC7) wealth and income creation; (CC8) sustainable consumption; (CC9) education and awareness.

After assessing social responsibility compliance, an aggregated *SRI* was deter-mined for the reference HEV and its prototypes with use of Eq. 6 and Eq. 7 (Table 8).

The calculated *SRI* allowed to establish a ranking of the reference HEV and its prototypes in terms of social responsibility compliance. Prototype 3 secured the top position, with Prototype 5 closely following. The reference product performed the worst among the assessed models, though these results may vary depending on expert opinions.

Finally, an aggregated *QESR* indicator was determined (model – stage 5). This in-volved combining the quality (*AQI*), environmental (*EII*), and social responsibility (*SRI*) indexes into a single *QESR* indicator. The three abovementioned indexes indices were normalized with respect to the reference HEV and its prototypes, using Eq. 8, Eq. 9, Eq. 10. Eq. 11, Eq. 12, Eq. 13 served for the estimation of the aggregated *QESR* indicator, which resulted in a ranking of the reference HEV and its prototypes. The ranking proves Prototype 3 being the most favourable and Prototype 6 the least favourable. For a verbal interpretation of the results, a further analysis was conducted (Stage 6). A verbal relative scale was used for this purpose, with the final model results and in-depth analysis presented in Table 9.

Table 8 SRI for the reference HEV and its prototypes

Alternative	SRI	Ranking
Ref. product	12.33	7
Prototype 1	17.89	3
Prototype 2	14.56	5
Prototype 3	19.00	1
Prototype 4	17.78	4
Prototype 5	18.89	2
Prototype 6	13.33	6

Table 9 Aggregated QESR indicator for the reference HEV and its prototypes

Alternative	Normalized weighted AQI	Normalized weighted EII	Normalized weighted SRI	QESR	Interpretation	Ranking
Ref. product	0.00	2.00	2.00	0.67	satisfactory	3
Prototype 1	1.72	1.50	0.33	0.70	beneficial	2
Prototype 2	2.33	1.00	1.33	0.61	satisfactory	5
Prototype 3	1.62	0.50	0.00	0.82	distinctive	1
Prototype 4	3.86	0.00	0.37	0.65	satisfactory	4
Prototype 5	4.26	2.50	0.03	0.44	sufficient	6
Prototype 6	7.00	3.00	1.70	0.03	bad	7

Prototype 3 was identified as the most suitable in terms of quality, environmental, and social responsibility aspects. It is then rational to guide accordingly the design of the reference HEV. Should Prototype 3 not be financially viable for the company, the ranking points at the next highest-ranked product, i.e. Prototype 1. A comprehensive comparison of the results obtained at each stage of model application is summarized in Table 10.

It was observed that Prototype 3, identified as the most advantageous, ranked second in the quality index (*AQI*), first in social responsibility (*SRI*), and sixth in environmental impact (*EII*). The final development decisions were influenced by the as-signed weights to each aspect (quality, environment, social responsibility) in the ratios of 7:3:2 [55]). It was noted that quality and environmental impact had a greater influence on the final ranking, with a smaller contribution of social responsibility. This phenomenon is evident in the case of the reference product, which ranked third according to the *QESR* indicator. The in-depth analysis of the impact of model indexes on the final product ranking was verified through a sensitivity analysis presented in the Discussion section of the article.

Table 10 Comparison of model indexes and resulting prototype rankings

Alternative	AQI and prototype ranking		EII and prototype ranking		SRI and prototype ranking		Final QESR indicator and prototype ranking	
Ref. product	3.81	1	520150	3	2.00	7	0.67	3
Prototype 1	3.64	3	624180	4	0.33	3	0.70	2
Prototype 2	3.58	4	728210	5	1.33	5	0.61	5
Prototype 3	3.65	2	832240	6	0.00	1	0.82	1
Prototype 4	3.43	5	936270	7	0.37	4	0.65	4
Prototype 5	3.39	6	416120	2	0.03	2	0.44	6
Prototype 6	3.12	7	312090	1	1.70	6	0.03	7

5. Discussion

The research aimed to develop a multicriteria decision-making model for predicting the improvement direction of current products based on methodically verified prototypes (alternative production solutions) through a multidimensional framework encompassing key sustainable development aspects: product quality (customer satisfaction), environmental impact throughout the product's life cycle, and compliance to social responsibility standards. These aspects, whether considered separately or in combination, have already been subjects of previous research [11, 12, 14, 15, 17].

The proposed approach integrates three respective indicators (*AQI, EII, SRI*) into a single Quality-Environmental-Social-Responsibility (*QESR*) indicator, providing a comprehensive assessment method. This integration represents the model's primary originality and its contribution to the field of management, sustainable development and production engineering, as corroborated by [4, 5, 9, 118], which responds to the ongoing challenges in sustainable product design. The developed *QESR* indicator aims to guide product development through personalized rankings of product prototypes, which remains a valuable approach for exploring new product opportunities or enhancing existing ones [106-109; 119-120].

The model's effectiveness was tested using HEV as a case study. The resulting prototype rankings aligned with the outcomes of each stage of the model, confirming the appropriateness of the chosen methodology. Consequently, a sensitivity analysis of the model was deemed necessary. This analysis aimed to verify the significance of the quality (*AQI*), environmental impact (*EII*), and social responsibility (*SRI*) indexes on the aggregated *QESR* indicator.

The sensitivity analysis was conducted using machine learning in Statistica 13.3 software. The input variables (independent) were the *AQI*, *EII*, and *SRI* values obtained from the model test for the reference HEV and its prototypes. The sensitivity analysis was performed twice: a) for unweighted relativized values, and b) for weighted relativized values, to additionally verify the impact of aspect weights on the final *QESR* ranking.

The sensitivity analysis was conducted using machine learning tools, specifically regression analysis, suitable for quantitative data. Random sampling was applied, with the following sample

sizes: 70 % for training, 15 % for testing, and 15 % for validation [110, 111]. The initial value of the random generator was set to 1000. The search focused on identifying a Multilayer Perceptron (MLP) network with a minimum of 3 and a maximum of 10 hidden layers. Twenty networks were trained, retaining the five with the most favourable learning parameters each time.

For processing the relativized (unweighted) model indexes in the neural network, the most optimal set of networks was generated, from which the MLP 3-10-1 network was selected. This network had three input neurons, ten hidden layer neurons, and one output neuron. In contrast, for processing the relativized weighted model indexes, the MLP 3-6-1 network was chosen, featuring three input neurons, six hidden layer neurons, and one output neuron.

Based on the developed neural network models and the specified input and output data, a global sensitivity analysis was conducted. Global sensitivity analysis for the analysed model indicators for unweighted normalized indexes were: *AQI*=7.609, *EII*=24.641, *SRI*=8.999, and for weighted normalized indexes were: *AQI*=1.997, *EII*=8.7675, *SRI*=4.857. The interpretation of global sensitivity analysis results boils down to identifying input variables with values above 1, indicating significant influence on the output variable (including model quality) [112]. It was observed that in both cases, all analysed indicators *AQI*, *EII*, and *SRI* significantly impacted the aggregated *QESR* indicator. In the global sensitivity analysis for unweighted relative indicators, the pre-dominant influence on the final *QESR* indicator (including the final product ranking) was the *EII* indicator (24.641). Subsequently, the *SRI* indicator (8.999) had a significant but notably smaller impact, followed by the *AQI* indicator (7.609). Sensitivity analysis for weighted relative indicators revealed the impact of weights assigned to these indicators on the final ranking (including *QESR*), leading to approximate alignment of model indicator values. The conducted sensitivity analysis demonstrated that all ana-lysed indicators significantly influenced the final model outcome, confirming the validity and effectiveness of the developed model and research methodology. It was shown that weighting qualitative, environmental, and social aspects significantly affects the final model indicator (*QESR*), and consequently, the final ranking of products and their prototypes. Therefore, these weights should be thoughtfully assigned based on the needs of the model user, business development strategies, legal regulations, or market dynamics.

The main limitation of the model is the lack of direct consideration of customer preferences in the decision-making process at the environmental impact assessment stage in the product lifecycle, as well as in the assessment of social responsibility compliance. Nevertheless, it is justified to conduct these assessments by a competent and qualified expert team [49, 52, 53]. Another significant limitation is the limited access to data or the lack of assurance of comparability of results obtained from LCA – which is a widely known and discussed issue of LCA methodology [113,114]. Despite this limitation we still decided to employ LCA in our model, as it is currently considered to be the most popular and most efficient method for estimating the environmental impact of products throughout their life cycle [115-117]. Another limitation is the potential for divergent interpretations of social responsibility (not always synonymous with CSR), which also concern the diversity of socially responsible business practices, leading to varying model outcomes depending on the country or region of application. Consequently, this limits the comparability of model results when applied in culturally diverse markets.

Future research aims to consider incorporating customer feedback at the environmental impact analysis stage. Additionally, the model structure allows for further development with other indicators and sustainable development criteria. Addressing the model limitations, efforts will be made to establish assumptions enhancing the accuracy and reliability of environmental impact assessment. Further studies will also involve other products to ensure the universality of the developed model.

6. Conclusion

In the era of dynamic customer expectations, including concerns about global warming, adapting products to market and societal needs is crucial. However, achieving sustainable product development remains challenging. Therefore, the aim of this re-search was to develop an MCDM model for predicting the direction of improving cur-rent products towards prototypes (alternative

production solutions) methodically verified in a multidimensional approach covering key aspects of sustainable development: quality, environmental impact throughout the life cycle, and social responsibility. The model was tested for a specific type of LPVs the HEVs.

Initially, the *AQI* was determined, requiring the identification of the vehicle's main quality criteria: total mass, maximum engine power, maximum speed, battery range, battery charging time, vehicle colour, vehicle dimensions, equipment, fuel consumption, and drivetrain. These criteria were modified by proposing six alternative design solutions (prototypes). Through survey research, expectations from 116 customers were obtained and processed, resulting in the *AQI*. According to this index, the reference product and its prototypes were ranked, with Prototype 1 deemed the most favourable in terms of quality. Next, the *EII* throughout the life cycle was determined. This involved conducting an LCA "from cradle to grave" according to ISO 14040 and using data from the GREET v1.3.0.13991 software. LCA results were employed for the prospective environmental impact assessment of the reference HEV and its prototypes, resulting in the *EII* index, which formed the basis for ranking these products. Prototype 6 showed the least negative environmental impact.

Subsequently, the *SRI* was determined. Selected social criteria from the ISO 26000 set were: fair competition, promoting social responsibility in the value chain, access to essential services, technology development and access, social investment, community involvement, wealth and income creation, sustainable consumption, education, and awareness. These criteria were assessed on a Likert scale for the reference HEV and its prototypes for relevance and social responsibility compliance. *SRI* resulted in a ranking, with Prototype 3 on top.

Finally, *AQI*, *EII* and *SRI* were aggregated into a single *QESR* indicator, considering their relativization and weighting. The indices were interpreted qualitatively and quantitatively on a relative scale. Ultimately, Prototype 2 was selected as possibly the most favourable in terms of quality, environment, and social responsibility aspects. In line with the model concept, it provides a good basis for determining the development direction of the reference HEV. Thus, the model test confirmed its effectiveness in prospectively deter-mining product development directions in accordance with the principles of sustainable development.

The model is dedicated to managerial decision-making in product design and production management. Therefore, it can support individuals, companies, and public entities in sustainable product development decisions, aiming to achieve socially re-sponsible production engineering that also ensures high product quality and environ-mental friendliness.

Acknowledgement

The publication presents the result of research financed from the subsidy granted to the Krakow University of Economics within the Support for Publishing Activities 2024 (Wsparcie Aktywności Publikacyjnej 2024) programme.

References

[1] Wang, S., Su, D. (2022). Sustainable product innovation and consumer communication, *Sustainability*, Vol. 14, No. 14, Article No. 8395, doi: 10.3390/su14148395.

[2] Xie, X., Wang, L., Zhang, T. (2023). Involving online community customers in product innovation: The double-edged sword effect, *Technovation*, Vol. 123, Article No. 102687, doi: 10.1016/j.technovation.2022.102687.

[3] Luglietti, R., Rosa, P., Terzi, S., Taisch, M. (2016). Life cycle assessment tool in product development: Environmental requirements in decision making process, *Procedia CIRP*, Vol. 40, 202-208, doi: 10.1016/j.procir.2016.01.103.

[4] Chang, D., Lee, C.K.M., Chen, C.-H. (2014). Review of life cycle assessment towards sustainable product development, *Journal of Cleaner Production*, Vol. 83, 48-60, doi: 10.1016/j.jclepro.2014.07.050.

[5] Medini, K., Boucher, X. (2015). Decision making support to steer offering variety during production planning, *Procedia CIRP*, Vol. 30, 486-491, doi: 10.1016/j.procir.2015.02.157.

[6] Lager, T., Simms, C.D. (2023). From customer understanding to design for processability: Reconceptualizing the formal product innovation work process for non-assembled products, *Technovation*, Vol. 125, Article No. 102750, doi: 10.1016/j.technovation.2023.102750.

[7] Barreto, L.V., Anderson, H.C., Anglin, A., Tomovic, C.L. (2010). Product lifecycle management in support of green manufacturing: Addressing the challenges of global climate change, *International Journal of Manufacturing Technology and Management*, Vol. 19, No. 3-4, 294-305, doi: 10.1504/IJMTM.2010.031374.

[8] Suhariyanto, T.T., Wahab, D.A., Rahman, M.N.A. (2018). Product design evaluation using life cycle assessment and design for assembly: A case study of a water leakage alarm, *Sustainability*, Vol. 10, No. 8, Article No. 2821, doi: 10.3390/su10082821.
[9] Keoleian, G.A. (1993). The application of life cycle assessment to design, *Journal of Cleaner Production*, Vol. 1, No. 3-4, 143-149, doi: 10.1016/0959-6526(93)90004-U.
[10] Xing, Y., Liu, Y. (2023). Integrating product-service innovation into green supply chain management from a life cycle perspective: A systematic review and future research directions, *Technovation*, Vol. 126, Article No. 102825, doi: 10.1016/j.technovation.2023.102825.
[11] Rebitzer, G., Ekvall, T., Frischknecht, R., Hunkeler, D., Norris, G., Rydberg, T., Schmidt, W.-P., Suh, S., Wiedema, B.P., Pennington, D.W. (2004). Life cycle assessment: Part 1: Framework, goal and scope definition, inventory analysis, and applications, *Environmental International*, Vol. 30, No. 5, 701-720, doi: 10.1016/j.envint.2003.11.005.
[12] Saaty, T.L. (2003). Decision-making with the AHP: Why is the principal eigenvector necessary?, *European Journal of Operational Research*, Vol. 145, No. 1, 85-91, doi: 10.1016/S0377-2217(02)00227-8.
[13] Zhang, Y. (1999). Green QFD-II: A life cycle approach for environmentally conscious manufacturing by integrating LCA and LCC into QFD matrices, *International Journal of Production Research*, Vol. 37, No. 5, 1075-1091, doi. 10.1080/002075499191418.
[14] Hameed, A.Z., Kandasamy, J., Aravind Raj, S., Baghdadi, M.A., Shahzad, M.A. (2022). Sustainable product development using FMEA ECQFD TRIZ and fuzzy TOPSIS, *Sustainability*, Vol. 14, No. 21, Article No. 14345, doi: 10.3390/su142114345.
[15] Popoff, A., Millet, D. (2017). Sustainable life cycle design using constraint satisfaction problems and quality function deployment, *Procedia CIRP*, Vol. 61, 75-80, doi. 10.1016/j.procir.2016.11.147.
[16] Kobayashi, Y., Kobayashi, H., Hongu, A., Sanehira, K. (2008). A practical method for quantifying eco-efficiency using eco-design support tools, *Journal of Industrial Ecology*, Vol. 9, No. 4, 131-144, doi: 10.1162/108819805775247990.
[17] Romli, A., Prickett, P., Setchi, R., Soe, S. (2015). Integrated eco-design decision-making for sustainable product development, *International Journal of Production Research*, Vol. 53, No. 2, 549-571, doi: 10.1080/00207543.2014.958593.
[18] Neramballi, A., Sakao, T., Willskytt, S., Tillman, A.-M. (2020). A design navigator to guide the transition towards environmentally benign product/service systems based on LCA results, *Journal of Cleaner Production*, Vol. 277, Article No. 124074, doi: 10.1016/j.jclepro.2020.124074.
[19] Adriyanti, A.L., Sahroni, T.R. (2023). Design sustainability for battery packaging to increase customer satisfaction, *Journal of Engineering*, Vol. 2023, No. 1, Article No. 9916084, doi: 10.1155/2023/9916084.
[20] Cimatti, B., Campana, G., Carluccio, L. (2017). Eco design and sustainable manufacturing in fashion: A case study in the luxury personal accessories industry, *Procedia Manufacturing*, Vol. 8, 393-400, doi: 10.1016/j.promfg.2017.02.050.
[21] Ulewicz, R., Siwiec, D., Pacana, A. (2023). Sustainable vehicle design considering quality level and life cycle environmental assessment (LCA), *Energies*, Vol. 16, No. 24, Article No. 8122, doi: 10.3390/en16248122.
[22] Pacana, A., Siwiec, D., Bednárová, L., Petrovský, J. (2023). Improving the process of product design in a phase of life cycle assessment (LCA), *Processes*, Vol. 11, No. 9, Article No. 2579, doi: 10.3390/pr11092579.
[23] Gosselt, J.F., van Rompay, T., Haske, L. (2019). Won't get fooled again: The effects of internal and external CSR eco-labeling, *Journal of Business Ethics*, Vol. 155, 413-424, doi: 10.1007/s10551-017-3512-8.
[24] Owodunni, O. (2018). Social sustainability in technologically-supported product realization process, *Procedia Manufacturing*, Vol. 21, 313-320, doi: 10.1016/j.promfg.2018.02.126.
[25] Choi, T.-M., Feng, L., Li, Y. (2023). Ethical fashion supply chain operations: Product development and moral hazards, *International Journal of Production Research*, Vol. 61, No. 4, 1058-1075, doi: 10.1080/00207543.2022.2025943.
[26] Deniz, D. (2016). Sustainable thinking and environmental awareness through design education, *Procedia Environmental Sciences*, Vol. 34, 70-79, doi: 10.1016/j.proenv.2016.04.008.
[27] Zhang, X., Liu, X., Zhang, Y., Xu, X., Xiao, J., Luh, D.-B. (2023). Assessing the feasibility of practical cradle to cradle in sustainable conceptual product design, *Sustainability*, Vol. 15, No. 8, Article No. 6755, doi: 10.3390/su15086755.
[28] Koo, Y., Cooper, R. (2016). What drives socially responsible design in organizations?: Empirical evidence from South Korea, *The Design Journal*, Vol. 19, No. 6, 879-901, doi: 10.1080/14606925.2016.1216211.
[29] Janssen, C., Vanhamme, J., Lindgreen, A., Lefebvre, C. (2014). The catch-22 of responsible luxury: Effects of luxury product characteristics on consumers' perception of fit with corporate social responsibility, *Journal of Business Ethics*, Vol. 119, 45-57, doi: 10.1007/s10551-013-1621-6.
[30] Romli, A., Prickett, P., Setchi, R., Soe, S. (2015). Integrated eco-design decision-making for sustainable product development, *International Journal of Production Research*, Vol. 53, No. 2, 549-571, doi: 10.1080/00207543.2014.958593.
[31] Hameed, A.Z., Kandasamy, J., Aravind Raj, S., Baghdadi, M.A., Shahzad, M.A. (2022). Sustainable product development using FMEA ECQFD TRIZ and fuzzy TOPSIS, *Sustainability*, Vol. 14, No. 21, Article No. 14345, doi: 10.3390/su142114345.
[32] Gao, L., Wang, Z., Wang, Y., Peng, T., Liu, W., Tang, R. (2023). LCA-based multi-scenario study on steel or aluminum wheel hub for passenger vehicles, *Procedia CIRP*, Vol. 116, 191-196, doi: 10.1016/j.procir.2023.02.033.

[33] Edwards, W., Barron, F.H. (1994). SMARTS and SMARTER: Improved simple methods for multiattribute utility measurement, *Organizational Behavior and Human Decision Processes*, Vol. 60, No. 3, 306-325, doi: 10.1006/obhd.1994.1087.
[34] Garvin, D.A. (1984). Product quality: An important strategic weapon, *Business Horizons*, Vol. 27, No. 3, 40-43, doi: 10.1016/0007-6813(84)90024-7.
[35] Das Guru, R.R., Paulssen, M. (2020). Customers' experienced product quality: Scale development and validation, *European Journal of Marketing*, Vol. 54, No. 4, 645-670, doi: 10.1108/EJM-03-2018-0156.
[36] Brucks, M., Zeithaml, V.A., Naylor, G. (2000). Price and brand name as indicators of quality dimensions for consumer durables, *Journal of the Academy of Marketing Science*, Vol. 28, 359-374, doi: 10.1177/0092070300283005.
[37] Garvin, D.A. (1984). What does "product quality" really mean?, *Sloan Management Review*, Vol. 25, 25-43.
[38] Wolniak, R. (2018). The use of QFD method: Advantages and limitations, *Production Engineering Archives*, Vol. 18, No. 18, 14-17, doi: 10.30657/pea.2018.18.02.
[39] Molina-Castillo, F.-J., Calantone, R.J., Stanko, M.A., Munuera-Aleman, J.-L. (2013). Product quality as a formative index: Evaluating an alternative measurement approach, *Journal of Product Innovation Management*, Vol. 30, No. 2, 380-398, doi: 10.1111/j.1540-5885.2012.01005.x.
[40] Curkovic, S., Vickery, S.K., Droge, C. (2000). An empirical analysis of the competitive dimensions of quality performance in the automotive supply industry, *International Journal of Operations & Production Management*, Vol. 20, No. 3, 386-403, doi: 10.1108/01443570010308121.
[41] Veryzer, R.W. (2005). The roles of marketing and industrial design in discontinuous new product development, *Journal of Product Innovation Management*, Vol. 22, No. 1, 22-41, doi: 10.1111/j.0737-6782.2005.00101.x.
[42] Hertenstein, J.H., Platt, M.B., Veryzer, R.W. (2005). The impact of industrial design effectiveness on corporate financial performance, *Journal of Product Innovation Management*, Vol. 22, No. 1, 3-21, doi: 10.1111/j.0737-6782.2005.00100.x.
[43] Falco, M., Robiolo, G. (2021). Product quality evaluation method (PQEM): To understand the evolution of quality through the iterations of a software product, *International Journal of Software Engineering & Applications*, Vol. 12, No. 5, 1-20, doi: 10.5121/ijsea.2021.12501.
[44] Calantone, R., Knight, G. (2000). The critical role of product quality in the international performance of industrial firms, *Industrial Marketing Management*, Vol. 29, No. 6, 493-506, doi: 10.1016/S0019-8501(00)00124-3.
[45] Rossiter, J.R. (2002). The C-OAR-SE procedure for scale development in marketing, *International Journal of Research in Marketing*, Vol. 19, No. 4, 305-335, doi: 10.1016/S0167-8116(02)00097-6.
[46] Mu, E., Pereyra-Rojas, M. (2017). *Practical decision making*, Springer Cham, Switzerland, doi: 10.1007/978-3-319-33861-3.
[47] Pacana, A., Siwiec, D. (2021). Universal model to support the quality improvement of industrial products, *Materials*, Vol. 14, No. 24, Article No. 7872, doi: 10.3390/ma14247872.
[48] Kupraszewicz, W., Zółtowski, B. (2002). Dobór zespołu ekspertów do diagnozowania stanu maszyn [The selection of the experts team to diagnose the condition of the machines], *Diagnostyka*, Vol. 26, 94-100.
[49] Krueger, R.A., Casey, M.A. (2014). *Focus groups: A practical guide for applied research*, Sage Publications, Thousand Oaks, California, USA.
[50] Fern, E.F. (1982). The use of focus groups for idea generation: The effects of group size, acquaintanceship, and moderator on response quantity and quality, *Journal of Marketing Research*, Vol. 19, No. 1, 1-13, doi: 10.1177/002224378201900101.
[51] Nyumba, T.O., Wilson, K., Derrick, C.J., Mukherjee, N. (2018). The use of focus group discussion methodology: Insights from two decades of application in conservation, *Methods in Ecology and Evolution*, Vol. 9, No. 1, 20-32, doi: 10.1111/2041-210X.12860.
[52] Halvorsen, K. (2013). Team decision making in the workplace, *Journal of Applied Linguistics and Professional Practice*, Vol. 7, No. 3, 273-296, doi: 10.1558/japl.v7i3.273.
[53] Sarangi, S. (2004). Editorial: Towards a communicative mentality in medical and healthcare practice, *Communication and Medicine,* Vol. 1, No. 1, 1-11, doi: 10.1515/come.2004.002.
[54] Gawlik, R. (2008). Preliminary criteria reduction for the application of analytic hierarchy process method*,* In: Fuxman, L., Delener, N., Lu, V., Rivera-Solis, L.-E. (eds.), *Evolution and revolution in the global economy: Enhancing innovation and competitiveness worldwide,* Global Business and Technology Association, New York, USA, 366-374.
[55] Kolman, R. (1992). *Inżynieria jakości* [Quality engineering], PWE, Warszawa, Poland.
[56] Siwiec, D., Pacana, A. (2024). Predicting design solutions with scenarios considering the quality of materials and products based on a life cycle assessment (LCA), *Materials*, Vol. 17, No. 4, Article No. 951, doi: 10.3390/ma17040951.
[57] Siwiec, D., Pacana, A. (2021). A pro-environmental method of sample size determination to predict the quality level of products considering current customers' expectations, *Sustainability*, Vol. 13, No. 10, Article No. 5542, doi: 10.3390/su13105542.
[58] Shen, Y., Zhou, J., Pantelous, A.A., Liu, Y., Zhang, Z. (2022). A voice of the customer real-time strategy: An integrated quality function deployment approach, *Computers & Industrial Engineering*, Vol. 169, Article No. 108233, doi: 10.1016/j.cie.2022.108233.
[59] Wang, F., Li, H., Liu, A., Zhang, X. (2015). Hybrid customer requirements rating method for customer-oriented product design using QFD, *Journal of Systems Engineering and Electronics*, Vol. 26, No. 3, 533-543, doi: 10.1109/JSEE.2015.00061.

[60] Kelley, K., Clark, B., Brown, V., Sitzia, J. (2003). Good practice in the conduct and reporting of survey research, *International Journal for Quality in Health Care*, Vol. 15, No. 3, 261-266, doi: 10.1093/intqhc/mzg031.
[61] Ponto, J. (2015). Understanding and evaluating survey research, *Journal of Advanced Practice Oncology,* Vol. 6, No. 2, 168-171, doi: 10.6004/jadpro.2015.6.2.9.
[62] Sullivan, G.M., Artino, A.R. (2013). Analysing and interpreting data from Likert-type scales, *Journal of Graduate Medical Education,* Vol. 5, No. 4, 541-542, doi: 10.4300/JGME-5-4-18.
[63] Millet, D., Bistagnino, L., Lanzavecchia, C., Camous, R., Poldma, T. (2007). Does the potential of the use of LCA match the design team needs?, *Journal of Cleaner Production,* Vol. 15, No. 4, 335-346, doi: 10.1016/j.jclepro.2005.07.016.
[64] Finkbeiner, M., Inaba, A., Tan, R., Christiansen, K., Klüppel, H.-J. (2006). The new international standards for life cycle assessment: ISO 14040 and ISO 14044, *The International Journal of Life Cycle Assessment,* Vol. 11, 80-85, doi: 10.1065/lca2006.02.002.
[65] Lagerstedt, J., Luttropp, C., Lindfors, L.-G. (2003). Functional priorities in LCA and design for environment, *The International Journal of Life Cycle Assessment,* Vol. 8, 160-166, doi: 10.1007/BF02978463.
[66] Kralisch, D., Ott, D., Gericke, D. (2015). Rules and benefits of life cycle assessment in green chemical process and synthesis design: A tutorial review, *Green Chemistry,* Vol. 17, 123-145, doi: 10.1039/C4GC01153H.
[67] Frischknecht, R., Wyss, F., Büsser Knöpfel, S., Lützkendorf, T., Balouktsi, M. (2015). Cumulative energy demand in LCA: The energy harvested approach, *The International Journal of Life Cycle Assessment,* Vol. 20, 957-969, doi: 10.1007/s11367-015-0897-4.
[68] Ciroth, A. (2007). ICT for environment in life cycle applications: OpenLCA – A new open-source software for life cycle assessment, *The International Journal of Life Cycle Assessment,* Vol. 12, 209-210, doi: 10.1065/lca2007.06.337.
[69] SimaPro Database Manual, Methods Library, from *https://simapro.com/wp-content/uploads/2020/06/DatabaseManualMethods.pdf*, accessed June 20, 2024.
[70] Khoo, H.H., Isoni, V., Sharratt, P.N. (2018). LCI data selection criteria for a multidisciplinary research team: LCA applied to solvents and chemicals, *Sustainable Production and Consumption,* Vol. 16, 68-87, doi: 10.1016/j.spc.2018.06.002.
[71] Bisinella, V., Christensen, T.H., Astrup, T.F. (2021). Future scenarios and life cycle assessment: Systematic review and recommendations, *The International Journal of Life Cycle Assessment,* Vol. 26, 2143-2170, doi: 10.1007/s11367-021-01954-6.
[72] Ostermann, M., Grenz, J., Triebus, M., Cerdas, F., Marten, T., Tröster, T., Herrmann, C. (2023). Integrating prospective scenarios in life cycle engineering: Case study of lightweight structures, *Energies,* Vol. 16, No. 8, Article No. 3371, doi: 10.3390/en16083371.
[73] Lestyánszka Škůrková, K., Fidlerová, H., Niciejewska, M., Idzikowski, A. (2023). Quality improvement of the forging process using Pareto analysis and 8D methodology in automotive manufacturing: A case study, *Standards*, Vol. 3, No. 1, 84-94, doi: 10.3390/standards3010008.
[74] Polish Committee for Standardization (Polski Komitet Normalizacyjny) (2012). *Guidelines for social responsibility* (*Wytyczne dotyczące społecznej odpowiedzialnosci*), PN-ISO 26000, PKN.
[75] Peng, F., Altieri, B., Hutchinson, T., Harris, A.J., McLean, D. (2022). Design for social innovation: A systemic design approach in creative higher education toward sustainability, *Sustainability,* Vol. 14, No. 13, Article No. 8075, doi: 10.3390/su14138075.
[76] Bryson, J.M., Barberg, B., Crosby, B.C., Patton, M.Q. (2021). Leading social transformations: Creating public value and advancing the common good, *Journal of Change Management,* Vol. 21, No. 2, 180-202, doi: 10.1080/14697017.2021.1917492.
[77] Koo, Y. (2016). The role of designers in integrating societal value in the product and service development processes, *International Journal of Design,* Vol. 10, No.2, 49-65.
[78] Rosati, F., Faria, L.G.D. (2019). Business contribution to the sustainable development agenda: Organizational factors related to early adoption of SDG reporting, *Corporate Social Responsibility and Environmental Management,* Vol. 26, No. 3, 588-597, doi: 10.1002/csr.1705.
[79] Monson, M. (2023). Socially responsible design science in information systems for sustainable development: A critical research methodology, *European Journal of Information Systems,* Vol. 32, No. 2, 207-237, doi: 10.1080/0960085X.2021.1946442.
[80] Haug, A., Busch, J. (2017). Dealing with uncertainties in socially responsible design, In Stuedahl, D., Morrison, A. (eds.), *Nordes 2017: Design + Power,* Oslo School of Architecture and Design, Oslo, Norway, doi: 10.21606/nordes.2017.034.
[81] Vecchi, M. (2022). Groups and socially responsible production: An experiment with farmers, *Journal of Economic Behavior & Organization,* Vol. 196, 372-392, doi: 10.1016/j.jebo.2022.01.020.
[82] Dobson, A. (2007). Environmental citizenship: Towards sustainable development, *Sustainable Development,* Vol. 15, No. 5, 276-285, doi: 10.1002/sd.344.
[83] Hernandez, R.J., Goñi, J. (2020). Responsible design for sustainable innovation: Towards an extended design process, *Processes,* Vol. 8, No. 12, Article No. 1574, doi: 10.3390/pr8121574.
[84] Melles, G., de Vere, I., Misic, V. (2011). Socially responsible design: Thinking beyond the triple bottom line to socially responsive and sustainable product design, *CoDesign,* Vol. 7, No. 3-4, 143-154, doi: 10.1080/15710882.2011.630473.
[85] Vafaei, N., Ribeiro, R.A., Camarinha-Matos, L.M. (2022). Assessing normalization techniques for simple additive weighting method, *Procedia Computer Science,* Vol. 199, 1229-1236, doi: 10.1016/j.procs.2022.01.156.

[86] Pacana, A., Siwiec, D., Bednárová, L. (2020). Method of choice: A fluorescent penetrant taking into account sustainability criteria, *Sustainability,* Vol. 12, No. 14, Article No. 5854, doi: 10.3390/su12145854.
[87] Ostasz, G., Siwiec, D., Pacana, A. (2022). Model to determine the best modifications of products with consideration of customers' expectations, *Energies,* Vol. 15, No. 21, Article No. 8102, doi: 10.3390/en15218102.
[88] Accardo, A., Dotelli, G., Miretti, F., Spessa, E. (2023). End-of-life impact on the cradle-to-grave LCA of light-duty commercial vehicles in Europe, *Applied Sciences,* Vol. 13, No. 3, Article No. 1494, doi: 10.3390/app13031494.
[89] Nordelöf, A., Messagie, M., Tillman, A.-M., Ljunggren Söderman, M., Van Mierlo, J. (2014). Environmental impacts of hybrid, plug-in hybrid, and battery electric vehicles—What can we learn from life cycle assessment*?, The International Journal of Life Cycle Assessment,* Vol. 19, 1866-1890, doi: 10.1007/s11367-014-0788-0.
[90] Fernandes, P., Macedo, E., Tomás, R., Coelho, M.C. (2024). Hybrid electric vehicle data-driven insights on hot-stabilized exhaust emissions and driving volatility, *International Journal of Sustainable Transportation,* Vol. 18, No. 1, 84-102, doi: 10.1080/15568318.2023.2219629.
[91] Singh, K.V., Bansal, H.O., Singh, D. (2019). A comprehensive review on hybrid electric vehicles: Architectures and components, *Journal of Modern Transportation,* Vol. 27, 77-107, doi: 10.1007/s40534-019-0184-3.
[92] Baskar, S., Vijayan, V., Premkumar, I.J.I., Arunkumar, D., Thamaran, D. (2021). Design and material characteristics of hybrid electric vehicle, *Materials Today: Proceedings,* Vol. 37, Part 2, 351-353, doi: 10.1016/j.matpr.2020.05.352.
[93] Silaen, R.V., Windasari, N.A. (2022). Customer preference analysis on attributes of hybrid electric vehicle: A choice-based conjoint approach, *International Journal of Current Science Research and Review,* Vol. 5, No. 12, 4703-4713, doi: 10.47191/ijcsrr/V5-i12-30.
[94] Memon, M.A., Ting, H., Cheah, J.-H., Thurasamy, R., Chuah, F., Cham, T.H. (2020). Sample size for survey research: Review and recommendations, *Journal of Applied Structural Equation Modeling,* Vol. 4, No. 2, 1-20, doi: 10.47263/JASEM.4(2)01.
[95] Hyman, M.R., Sierra, J.J. (2016). Selecting a sample size for your customer survey, *Business Outlook,* Vol. 14, No. 5, 1-5.
[96] Wong, E.Y.C., Ho, D.C.K., So, S., Tsang, C.-W., Chan, E.M.H. (2021). Life cycle assessment of electric vehicles and hydrogen fuel cell vehicles using the GREET model – A comparative study, *Sustainability,* Vol. 13, No. 9, Article No. 4872, doi: 10.3390/su13094872.
[97] Shafique, M., Azam, A., Rafiq, M., Luo, X. (2022). Life cycle assessment of electric vehicles and internal combustion engine vehicles: A case study of Hong Kong, *Research in Transportation Economics,* Vol. 91, Article No. 101112, doi: 10.1016/j.retrec.2021.101112.
[98] Koroma, M.S., Costa, D., Philippot, M., Cardellini, G., Hosen, M.S., Coosemans, T., Messagie, M. (2022). Life cycle assessment of battery electric vehicles: Implications of future electricity mix and different battery end-of-life management, *Science of The Total Environment,* Vol. 831, Article No. 154859, doi: 10.1016/j.scitotenv.2022.154859.
[99] Guzmán, J.I., Faúndez, P., Jara, J.J., Retamal, C. (2022). On the source of metals and the environmental sustainability of battery electric vehicles versus internal combustion engine vehicles: The lithium production case study, *Journal of Cleaner Production,* Vol. 376, Article No. 133588, doi: 10.1016/j.jclepro.2022.133588.
[100] Yang, L., Yu, B., Yang, B., Chen, H., Malima, G., Wei, Y.-M. (2021). Life cycle environmental assessment of electric and internal combustion engine vehicles in China, *Journal of Cleaner Production,* Vol. 285, Article No. 124899, doi: 10.1016/j.jclepro.2020.124899.
[101] Tang, B., Xu, Y., Wang, M. (2022). Life cycle assessment of battery electric and internal combustion engine vehicles considering the impact of electricity generation mix: A case study in China, *Atmosphere,* Vol. 13, No. 2, Article No. 252, doi: 10.3390/atmos13020252.
[102] Bauer, C., Hofer, J., Althaus, H.-J., Del Duce, A., Simons, A. (2015). The environmental performance of current and future passenger vehicles: Life cycle assessment based on a novel scenario analysis framework, *Applied Energy,* Vol. 157, 871-883, doi: 10.1016/j.apenergy.2015.01.019.
[103] Qiao, Q., Zhao, F., Liu, Z., Jiang, S., Hao, H. (2017). Cradle-to-gate greenhouse gas emissions of battery electric and internal combustion engine vehicles in China, *Applied Energy,* Vol. 204, 1399-1411, doi: 10.1016/j.apenergy.2017.05.041.
[104] Sulaeman, I., Chandra Mouli, G.R., Shekhar, A., Bauer, P. (2021). Comparison of AC and DC nanogrid for office buildings with EV charging, PV, and battery storage, *Energies,* Vol. 14, No. 18, Article No. 5800, doi: 10.3390/en14185800.
[105] Guzek, M., Jackowski, J., Jurecki, R.S., Szumska, E.M., Zdanowicz, P., Żmuda, M. (2024). Electric vehicles – An overview of current issues – Part 1 – Environmental impact, source of energy, recycling, and second life of battery, *Energies,* Vol. 17, No. 1, Article No. 249, doi: 10.3390/en17010249.
[106] Wang, J., Ranscombe, C., Eisenbart, B. (2023). Prototyping in smart product design: Investigating prototyping tools to support communication in the early stage smart product development, *International Journal of Design Creativity and Innovation,* Vol. 11, No. 3, 159-184, doi: 10.1080/21650349.2023.2222115.
[107] Elverum, C.W., Welo, T., Tronvoll, S. (2016). Prototyping in new product development: Strategy considerations, *Procedia CIRP,* Vol. 50, 117-122, doi: 10.1016/j.procir.2016.05.010.
[108] Lu, K., Zou, T., Du, J. (2024). Two forms of customer involvement and new product development performance in the digital context: The moderating role of new product development stage, *Technovation,* Vol. 134, Article No. 103023, doi: 10.1016/j.technovation.2024.103023.
[109] Gkeka-Serpetsidaki, P., Skiniti, G., Tournaki, S., Tsoutsos, T. (2024). A review of the sustainable siting of offshore wind farms, *Sustainability,* Vol. 16, No. 14, Article No. 6036, doi: 10.3390/su16146036.

[110] Isabona, J., Imoize, A.L., Ojo, S., Karunwi, O., Kim, Y., Lee, C.-C., Li, C.-T. (2022). Development of a multilayer perceptron neural network for optimal predictive modeling in urban microcellular radio environments, *Applied Sciences,* Vol. 12, No. 11, Article No. 5713, doi: 10.3390/app12115713.
[111] Naskath, J., Sivakamasundari, G., Begum, A.A.S. (2023). A study on different deep learning algorithms used in deep neural nets: MLP, SOM, and DBN, *Wireless Personal Communications,* Vol. 128, 2913-2936, doi: 10.1007/s11277-022-10079-4.
[112] Siderska, J. (2013). Analysis of the possibilities of using artificial neural networks to model social capital values in IT companies (Analiza możliwości zastosowania sieci neuronowych do modelowania wartości kapitału społecznego w firmach IT), *Ekonomia i Zarządzanie,* Vol. 5, No. 1, 84-97.
[113] Karuppiah, K., Sankaranarayanan, B., Ali, S.M. (2023). Evaluating the challenges to life cycle assessment using best–worst method and decision–making trial and evaluation laboratory, *Environmental Progress & Sustainable Energy,* Vol. 42, No. 1, Article No. e13991, doi: 10.1002/ep.13991.
[114] Karaman Öztaş, S. (2018). The limitations of LCA methodology towards sustainable construction materials, In: Fırat, S., Kinuthia, J., Abu-Tair, A. (eds.), *Proceedings of the 3rd International Sustainable Buildings Symposium (ISBS 2017)*, ISBS 2017, Lecture Notes in Civil Engineering, Vol. 6, Springer, Cham, 102-113, doi: 10.1007/978-3-319-63709-9_8.
[115] Bulle, C., Margni, M., Patouillard, L., Boulay, A.-M., Bourgault, G., De Bruille, V., Cao, V., Hauschild, M., Henderson, A., Humbert, S., Kashef-Haghighi, S., Kounina, A., Laurent, A., Levasseur, A., Liard, G., Rosenbaum, R.K., Roy, P.-O., Shaked, S., Fantke, P., Jolliet, O. (2019). IMPACT World+: A globally regionalized life cycle impact assessment method, *The International Journal of Life Cycle Assessment,* Vol. 24, 1653-1674, doi: 10.1007/s11367-019-01583-0.
[116] Toniolo, S., Borsoi, L., Camana, D. (2021). Chapter 7 - Life cycle assessment: methods, limitations, and illustrations, In: Ren, J. (ed.), *Methods in sustainability science*, Elsevier, Amsterdam, Netherlands, 105-118, doi: 10.1016/B978-0-12-823987-2.00007-6.
[117] Dorr, E., Goldstein, B., Aubry, C., Gabrielle, B., Horvath, A. (2023). Best practices for consistent and reliable life cycle assessments of urban agriculture, *Journal of Cleaner Production,* Vol. 419, Article No. 138010, doi: 10.1016/j.jclepro.2023.138010.
[118] Jankovič, D., Šimic, M., Herakovič, N. (2024). A comparative study of machine learning regression models for production systems condition monitoring, *Advances in Production Engineering & Management,* Vol. 19, No. 1, 78-92, doi: 10.14743/apem2024.1.494.
[119] Shi, J.L., Lu, Z.C., Xu, H.H., Ren, M.M., Shu, F.L. (2023). Comparing fault tree analysis methods combined with generalized grey relation analysis: A new approach and case study in the automotive industry, *Advances in Production Engineering & Management*, Vol. 18, No. 4, 462-474, doi: 10.14743/apem2023.4.485.
[120] Wang, D.L., Ding, A., Chen, G.L., Zhang, L. (2023). A combined genetic algorithm and A* search algorithm for the electric vehicle routing problem with time windows, *Advances in Production Engineering & Management,* Vol. 18, No. 4, 403-416, doi: 10.14743/apem2023.4.481.

APEM journal
Advances in Production Engineering & Management
Volume 19 | Number 4 | December 2024 | pp 489–511
https://doi.org/10.14743/apem2024.4.520
ISSN 1854-6250
Journal home: apem-journal.org
Original scientific paper

An algorithmic review of the technological progress and milestones in resource-constrained project planning

Pourhejazy, P.[a,*], **Ying, K.-C.**[b,*], **Cheng, C.-Y.**[c]

[a]Department of Industrial Engineering, UiT – The Arctic University of Norway, Narvik, Norway
[b]Department of Industrial Engineering and Management, National Taipei University of Technology, Taipei, Taiwan
[c]Taiwan Semiconductor Manufacturing Company (TSMC) Limited, Hsinchu City, Taiwan

ABSTRACT

Engineering, procurement, and construction projects are time-intensive and subject to resource constraints. Modern project planning software requires optimization algorithms to schedule tasks while considering resource availability. A comprehensive review of the optimization algorithms used in project planning has not yet been conducted. This study seeks to bridge the gap through an algorithmic review of the Resource-constrained Project Scheduling Problems (RCPSPs) literature and investigates the following research questions: What are the milestones on the main development trajectory of optimization algorithms for solving RCPSPs? How might this influence future advancements in the field? To answer these questions, the Main Path Analysis (MPA) method is employed to review the development trajectory and milestones from over 1100 project scheduling articles published between 1980 and 2024. Cluster Analysis (CA) complements the investigations by identifying the prevalent research themes, mathematical features, and solution algorithms. Recommendations for future research directions, supported by the systematic review, conclude the study. This review provides a reference for project management researchers focused on industrial applications of project scheduling problems.

ARTICLE INFO

Keywords:
Project management;
Task scheduling;
Resource constraint;
Multi-objective optimization;
Evolutionary computation;
Swarm intelligence;
Metaheuristics;
Main path analysis;
Cluster analysis

**Corresponding authors:*
pourya.pourhejazy@uit.no
(Pourhejazy, P.)
kcying@ntut.edu.tw
(Ying, K.-C.)

Article history:
Received 27 October 2024
Revised 6 December 2024
Accepted 17 December 2024

1. Introduction

Modern project planning must account for the rapid changes in the resources [1]. Traditionally, project managers use planning tools based on the Critical Path Method (CPM) and the Program Evaluation and Review Technique (PERT) to schedule tasks and predict project progress, milestones, and completion times. These methods are predominantly based on operative and predictive models [2]; they overlook resource availability, requiring schedules to be adjusted each time a task is delayed due to the lack of resources. As the scope and complexity of projects increase, such tools, although powerful, cannot provide dependable solutions that are both optimal and robust. Mathematical models and solution algorithms are required for optimal project planning, taking into account various practical constraints. The Resource-Constrained Project Scheduling

Problem (RCPSP) is an advanced planning alternative that optimizes resource allocation while sequencing project tasks.

The primary investigation shows that research on project scheduling has grown steadily since 1995, reaching a peak of 107 published articles in 2021. The early works focused on developing priority rules for resource-constrained project scheduling [3]. More recent studies evolved towards developing advanced heuristics and metaheuristics. Among the seminal works, Debels *et al.* [4] developed a hybrid Scatter Search/Electromagnetism algorithm for project scheduling. Kolisch and Hartmann [5] contributed an experimental analysis of heuristic algorithms for resource-constrained project scheduling. Van Peteghem and Vanhoucke [6] developed a Genetic Algorithm for solving preemptive and non-preemptive multi-mode RCPSPs. Most recently, several constructive heuristic algorithms were developed by Nekoueian *et al.* [7] for selecting and scheduling alternative subgraphs in resource-constrained projects. Melchiors *et al.* [8] conducted an experimental analysis comparing the performance of priority rules for dynamic stochastic RCPSPs. Servranckx *et al.* [9] proposed a Genetic Algorithm integrated with a Boolean satisfiability solver to solve RCPSP with alternative subgraphs.

Identifying the main development trajectory of RCPSP sheds light on scientific progress and milestones in project planning. There are several reviews of the literature on project scheduling, three of which are recent and relevant. Gomez *et al.* [10] reviewed multi-project scheduling problems as one of the several variants of RCPSP. Aghileh *et al.* [11] contributed a more focused literature review focusing on multi-project scheduling problems under uncertainty and resource flexibility. These articles investigated specific variants of RCPSP. The most relevant study, Hartmann *et al.* [12] surveyed the prominent extensions of RCPSP. They considered a theoretical lens, focusing solely on mathematical features; *solution methods* for solving RCPSP were not investigated. Moreover, their review *scope* covered only articles published between 2010 and 2020. Most importantly, the existing surveys are based on a traditional literature reviews, i.e. *manual reading* of articles, which is *subjective* and cannot trigger big-picture thinking.

To the authors' best knowledge, the present study is the first algorithmic review (see [13]) of the project planning literature using mathematical methods. Main Path Analysis (MPA) and Cluster Analysis (CA) are used to analyze the literature published between 1980 and 2024. The objective is to explore the following research questions: What are the milestones on the development trajectory of RCPSP solution algorithms? How might this influence future advances in the field?

This article continues in three more sections. The research methods are first described in Section 2. MPA results are presented in Section 3, followed by discussions on the outcomes of CA and keyword analysis. This research concludes in Section 4, where directions for future studies are suggested.

2. Research framework

The Web of Science (WoS) database serves as the data collection source in this study. WoS comprises six index databases, namely Emerging Sources Citation Index (ESCI), Science Citation Index Expanded (SCIE), Social Sciences Citation Index (SSCI), Arts & Humanities Citation Index (A&HCI), Book Citation Index (BCI), and Conference Proceedings Citation Index (CPCI). Compared to other databases such as Google Scholar and Scopus, WoS strictly controls the quality of its collections, and only includes peer-reviewed documents of high quality.

Step 1. *Data collection*

The keyword TS = (Resource-Constrained Project Scheduling) was considered the primary term for the search. "AND" and "*" operators were used for keyword searches to reduce the chances of missing relevant documents: TS = (Resource-Constrained) AND TS = (project*) AND TS = (scheduling*). The search was conducted on April 25, 2024, covering the period FPY = (1980-2023). Initial investigations showed that 1,264 documents fall within the defined research scope considering the articles' titles, abstracts, and keywords. The manual screening was then conducted to remove irrelevant records from the analysis; 1,189 documents remained in the database. Next, 32 retrospective articles were excluded to ensure their high citation count would not

influence the path analysis procedure. Finally, the main path analysis software, MainPath 480, identified 42 isolated documents that neither cited other articles nor were cited by others; these were also removed from the database. A total of 1,130 documents were considered for further investigations.

The accuracy index Precision in Eq. 1, and the Digital Object Identifier percentage DOI in Eq. 2 were used to check whether the database is representative of the entire literature; values greater than 0.7 are considered a green flag for MPA and CA analysis [14, 15]. The former index compares the number of articles before and after the removal of isolated points. In this study, the numbers of articles before and after excluding isolated points were 1,174 and 1,130, respectively. The search accuracy was 0.96, which is pretty high. Additionally, a high DOI percentage confirms the representativeness of the database. The total citation count of the topic is 43,550 while the DOI Total is 32,301 times, accounting for 0.74, which is acceptable and indicates that the database can be used for further analysis.

$$\text{Precision} = \frac{\text{Network Size}}{\text{Number of Articles in the Original Database}} \times 100\ \% \tag{1}$$

$$\text{DOI ratio} = \frac{\text{DOI Total}}{\text{Citation Record}} \times 100\ \% \tag{2}$$

Step 2. *Data processing using MPA, CA, and keyword analysis*

The database must be converted into a citation network to establish the basis for data processing. This network categorizes documents into *source* (where knowledge dissemination begins), *intermediate* (where knowledge is transferred from one node to another), or *sink* (where knowledge dissemination ends). The citation relationships within the network are represented by directed arrows, indicating knowledge diffusion.

The analysis continues by calculating the weights of the arrows, taking into account all possible citation chains from source to sink. MPA uses these weights to identify the backbone of the citation network. Search Path Count (SPC; from all source nodes to all sink nodes of the network), Search Path Link Count (SPLC; all the ancestors of a tail node for a specific link), or Search Path Node Pair (SPNP; all the ancestors and descendants of a specific link) methods can be used to calculate and assign weights to the network links. SPLC best represents the knowledge dissemination process in academic literature [16] and is therefore used in the analysis. The weighted network forms the basis for identifying the main path and the key development branches.

Using the weighted network as input, the MPA function of MainPath480 considers all possible citation chains and selects the one with the largest overall SPLC as the main path. The Global Main Path setting is used to identify the major citation chain over the entire literature period, i.e. from sink to source nodes. The Key-route Main Path is further used to identify the main path while including top-cited references; this study uses Key-route 10, which ensures that the top ten contributions are included in the analysis.

The same database is also used for the data-driven categorization of articles using the CA [17] function of MainPath480. A three-step procedure organizes articles based on their similarities (the shortest path between all the node pairs, calculating edge credit using Eq. 3, and removing the edge(s) with the highest score to isolate groups of articles). Additionally, similar terms are merged to identify the cluster containing the most frequently used words.

$$\text{Edge\_Credit} = (1 + \sum \text{Incoming Edge Credit}) \times \frac{\text{Score of Destination}}{\text{Score of Start}} \tag{3}$$

Step 3. *Literature content analysis*

The literature content analysis will explore the advances in solution algorithms for solving RCPSPs. A three-field notation, $\alpha|\beta|\gamma$ is used to characterize the reviewed RCPSPs; the problem characteristics are treated as an influencing factor in the advances in project scheduling algorithms. In the notation system, α specifies the process type; β identifies the practical features

and characteristics considered in the studied RCPSP; and γ represents the objective function. Tables 1-3 define the notations used in the three sections, respectively.

Table 1 Process type-related notations, α

Notation	Definition
PS	General project scheduling.
MPS	Multi-mode project scheduling.
$PS_{m,\sigma,\rho}$	General project scheduling considering m resources, σ units of available resources, each activity requiring at most ρ units of the resources.
$MPS_{m,\sigma,\rho;\mu,\tau,\omega}$	Multi-mode project scheduling with m renewable and μ non-renewable resources; σ and τ units of renewable and non-renewable resources with each activity requiring at most ρ and ω units of the renewable and non-renewable resources, respectively.
$\alpha_1 = 0$	No resource types are considered.
$\alpha_1 = 1$	One resource type is considered.
α_1=m	The number of resource types is equal to *m.*
$\alpha_2 = 0$	Absence of any resource type specification.
$\alpha_2 = 1$	Renewable resources; availability is specified for a time unit.
$\alpha_2 = T$	Non-renewable resources, the availability of which is specified for the entire project horizon *T.*
$\alpha_2 = 1T$	Both renewable and non-renewable resources are considered.
$\alpha_2 = \upsilon$	Partially (non-)renewable resources the availability of which is renewed in specific periods.
$\alpha_3 = 0$	(Partially) Renewable resources available in constant amounts.
$\alpha_3 = \upsilon a$	(Partially) Renewable resources available in variable amounts.
$\alpha_3 = \tilde{a}$	Stochastic resource availability with constant value over time.
$\alpha_3 = \upsilon\tilde{a}$	Stochastic resource availability with variable values over time.
$MPS_{m,\sigma,\rho;\mu,\tau,\omega} - MR$	RCPSP with Multiple Routes.
$PS_{m,\sigma,\rho} - MOP - DC$	Integrated RCPSP and material ordering with discounted cash flows.
$PS_{m,\sigma,\rho} - PS$	RCPSP with a model-endogenous decision on the project structure.
$MS - PS_{m,\sigma,\rho}$	Multi-Skill Resource-Constrained Project Scheduling Problem.
$MPS_{m,\sigma,\rho;\mu,\tau,\omega} - CS$	Multi-mode Integrated RCPSP with Contractor Selection.
$M - MPS_{m,\sigma,\rho;\mu,\tau,\omega}$	Multi-objective Multi-mode RCPSP.
$MMPS_{m,\sigma,\rho;\mu,\tau,\omega}$	Multi-mode, Multi-project RCPSP.
$MS - MPS_{m,\sigma,\rho;\mu,\tau,\omega}$	Multi-skill Multi-modal RCPSP.
$MPPS_{m,\sigma,\rho}$	Resource-constrained multi-project scheduling problem.
$CCPS_{m,\sigma,\rho}$	Resource-constrained project scheduling with critical chain.

Table 2 Process characteristics-related notations, β

Notation	Definition
$p_j = 1$	All processing times are equal to one.
$p_j = sto$	Stochastic processing times.
d	Deadline for project duration.
$prec$	Precedence constraints between activities.
$chain, intree, outtree, tree$	Precedence relations between activities are specified.
$temp$	General temporal constraints, given the minimum and maximum start-start time lag between activities.
$\beta_1 = 0$	No preemption is allowed.
$\beta_1 = pmtn$	Preemptions of the preempt-resume type are allowed.
$\beta_1 = pmtn - rep$	Preemptions of the preempt-repeat type are allowed.
$\beta_2 = 0$	No precedence constraints.
$\beta_2 = cpm$	Strict finish-start precedence constraints with zero time lag, as used in the basic PERT/CPM model.
$\beta_2 = min$	Precedence diagramming constraints of the types start-start,finish-start, start-finish, and finish-finish with minimal time lags.
$\beta_2 = gpr$	Generalized precedence relations of the types start-start, finish-start, start-finish, and finish-finish with both minimal and maximal time lags.
$\beta_2 = prob$	The activity network is of probabilistic type where the evolution of the correspond-ing project is not determined in advance.

Table 2 (Continuation)

$\beta_3 = 0$	All ready times are zero.
$\beta_3 = \rho_j$	Ready times differ per activity.
$\beta_4 = 0$	Activities have arbitrary integer durations.
$\beta_4 = cont$	Activities have arbitrary continuous durations.
$\beta_4 = (d_j = d)$	All activities have a duration equal to *d* units.
$\beta_4 = \tilde{d}_j$	The activity durations are stochastic.
$\beta_5 = 0$	No deadlines are assumed in the system.
$\beta_5 = \delta_j$	Deadlines are imposed on activities.
$\beta_5 = \delta_n$	A project deadline is imposed.
$\beta_6 = 0$	Constant discrete resource requirements.
$\beta_6 = vr$	Variable discrete resource requirements.
$\beta_6 = \tilde{r}$	Stochastic constant discrete resource requirements.
$\beta_6 = v\tilde{r}$	Stochastic discrete variable resource requirements.
$\beta_6 = disc$	The requirements are a discrete function of the activity duration.
$\beta_6 = cont$	The requirements are a continuous function of the activity duration.
$\beta_6 = int$	The requirements are expressed as an intensity or rate function.
$\beta_7 = 0$	Activities must be performed in a single execution mode.
$\beta_7 = mu$	Activities have multiple prespecified execution modes.
$\beta_7 = id$	Activities are subject to mode identity constraints.
$\beta_8 = 0$	No cash flows are specified in the project scheduling problem.
$\beta_8 = c_j$	Activities have an arbitrary cash flow.
$\beta_8 = \tilde{c}_j$	Cash flows are stochastic.
$\beta_8 = c_j^+$	Activities have an associated positive cash flow.
$\beta_8 = per$	Periodic cash flows are specified for the project.
$\beta_8 = sched$	Both the amount and the timing of the cash flows are determined.
$\beta_9 = 0$	No change-over (transportation) times.
$\beta_9 = s_{jk}$	Sequence-dependent change-over times.

Table 3 Objective function-related notations, γ

Notation	Definition
$\sum c_j^F \beta^{c_j}$	Net present value.
$\sum c_k f(r_k(S,t))$	Resource leveling.
$\sum c_k \max r_k(S,t)$	Resource investment.
$\gamma = reg$	The performance measure is any early completion (regular) measure.
$\gamma = nonreg$	The performance measure is any free completion (non-regular) measure.
$\gamma = C_{max}$	Minimize the project makespan.
$\gamma = \bar{F}$	Minimize the average flow time across all sub-projects or activities.
$\gamma = L_{max}$	Minimize the project lateness.
$\gamma = T_{max}$	Minimize the project tardiness.
$\gamma = earlv/tardv$	Minimize the weighted earliness-tardiness of the project.
$\gamma = n_T$	Minimize the number of tardy activities.
$\gamma = \sum sq.dev.$	The sum of squared deviations of the resource requirements from the average.
$\gamma = av$	Minimize the resource availabilities to meet the project deadline.
$\gamma = rac$	Minimize the resource availability costs.
$\gamma = curve$	Determine the complete time/cost trade-off curve.
$\gamma = npv$	Maximize the net present value of the project.
$\gamma = E[\cdot]$	Optimize the expected value of a performance measure.
$\gamma = cdf$	Determines the cumulative density function of the project realization date.
$\gamma = ci$	Determines the criticality index of an activity or a path.
$\gamma = mci$	Determines the most critical path(s) or activities based on the criticality index.
$\gamma = multi$	Different objectives are weighted or combined.
$\gamma = multicrit$	Multi-criteria functions.
$\gamma = EPD$	Minimizes the expected project duration.
$\gamma = EC_{max}$	Expected makespan.
$\gamma = CF$	Minimize the carbon footprints.
$\gamma = TC$	Minimize the Total cost.
$\gamma = TD$	Minimize the Total Duration.

Step 4. *Dissemination*

The outputs of MainPath480 consist solely of character results. The results were further processed using Pajek 5.18 (*http://mrvar.fdv.uni-lj.si/pajek/*) and VOSviewer 1.6.18 [18] for dissemination. A satellite-like view, which illustrated the major knowledge diffusion paths is used to visualize the findings.

3. Results and discussions

3.1 Main development trajectory of solution algorithms

A total of 27 articles formed the main development trajectory of RCPSPs. The contributions predominantly fall under at least one of the following categories: new solution algorithms or optimization models, new datasets, and benchmarking or organizing the available methods. The trajectory is shown in Fig. 1, which is followed by an elaboration on the scientific progress and milestones.

Fig. 1 The main development trajectory of RCPSPs

As the starting point of the main development trajectory, Bell and Park [19] studied $PS_{m,\sigma,\rho}|prec|C_{max}$ and developed the A-STAR search method to solve it, which operates by identifying active nodes that violate resource restrictions and prioritizing them to reduce resource conflicts. Bell and Han [20] proposed a new heuristic to solve $PS_{m,\sigma,\rho}||C_{max}$. The algorithm first generates an initial solution and uses a procedure inspired by the Hill Climbing method to improve the solution. They used Patterson's dataset to compare their algorithm with six traditional heuristic rules. Sampson and Weiss [21] developed several local search techniques to solve $PS_{m,\sigma,\rho}||C_{max}$ and used Patterson's 110 datasets to test their performance, comparing it with the as-is situation in a hypothetical problem.

Kolisch *et al*. [22] developed a new dataset for the problems of $PS_{m,\sigma,\rho}\|C_{max}$, $PS_{m,\sigma,\rho}\|tardv$, and a multi-objective variant of the two. Experimental analysis showed that some of the small-scale instances from their test bank can be solved in polynomial time under certain circumstances. Kolisch and Drexl [23] developed an Adaptive Search Procedure with new sorting rules and random search techniques for $MPS_{m,\sigma,\rho;\mu,\tau,\omega}\|C_{max}$. They used the 308 instances of Gen-instances to show that the algorithm can effectively limit the solution space and compared it with four other heuristics coded using different programming languages. Kolisch and Sprecher [24] referred to the ProGen system to develop the new database, Project Scheduling Problem Library (PSPLIB) for RCPSPs. Their platform generated instances of different sizes for minimizing the overall project completion time and considers the number of activities, single-mode and multi-mode activity execution modes, activity duration, and resource constraints. Brucker *et al.* [25] developed a new Branch and Bound algorithm for solving $PS_{m,\sigma,\rho}|\beta_6 = {}^{o}, prec|C_{max}$. Kolisch's PSPLIB test bank was used to test the algorithm comparing it with the best solutions found by Demeulemeester and Herroelen [26].

Hartmann [27] developed a Competitive Genetic Algorithm for $PS_{m,\sigma,\rho}\|C_{max}$ and used the PSPLIB database to compare its performance with other variants of the Genetic Algorithm. Hartmann and Kolisch [28] compared the Genetic Algorithm, Tabu Search, and Simulated Annealing for $PS_{m,\sigma,\rho}\|C_{max}$ and the PSPLIB dataset. They analyzed the impact of different sorting rules, computational mechanisms, problem size, and resource limitations on algorithm performance. Hartmann [29] introduced the self-adapting Genetic Algorithm to solve $PS_{m,\sigma,\rho}\|C_{max}$ and used the PSPLIB database to compare its performance with Simulated Annealing, Tabu Search, and several variants of the Genetic Algorithm.

Valls *et al.* [30] proposed a Four-Phase-Based procedure that uses the Convex Search Algorithm to generate the initial solution and the Homogeneous Interval Algorithm to improve the initial solution. The algorithm was compared with state-of-the-art heuristics using randomly generated instances for solving $PS_{m,\sigma,\rho}\|C_{max}$. *Valls et al.* [31] proposed a heuristic with several justification techniques for solving $PS_{m,\sigma,\rho}|prec|C_{max}$. They used the ProGen test bank to compare their algorithm with 22 different heuristics. Kolisch and Hartmann [5] used the PSPLIB test bank to evaluate many of the algorithms commonly used to solve RCPSPs and analyzed their characteristics to speculate on the reasons for their performance.

Vanhoucke and Debels [32] explored the impact of practical characteristics, such as activity duration, task splitting, and fast-tracking on the total lead time and improved the Branch and Bound method to solve RCPSPs. Van Peteghem and Vanhoucke [6] proposed the bi-population Genetic Algorithm to address $MPS_{m,\sigma,\rho;\mu,\tau,\omega}|\beta_1 = pmtn - rep|C_{max}$. They used the PSPLIB database to evaluate the solution algorithm's performance with and without preemption. Coelho and Vanhoucke [33] introduced the AND-OR network for the project structure of $MPS_{m,\sigma,\rho;\mu,\tau,\omega}, \alpha_2 = 1T\|C_{max}$ and compared hybrid algorithms based on Tabu Search and Non-dominated Sorting Genetic Algorithms (NSGA) -I and -II using the PSPLIB database. Zamani [34] proposed a Magnet-Based Genetic Algorithm to solve $MPS_{m,\sigma,\rho;\mu,\tau,\omega}, \alpha_2 = 1T\|C_{max}$ and used the PSPLIB database to compare their algorithm with baseline Genetic Algorithms.

Cheng *et al.* [35] proposed the Fuzzy Clustering Chaotic-based Differential Evolution to minimize the project duration in $MPS_{m,\sigma,\rho;\mu,\tau,\omega}|prec|C_{max}$ and used a case study from the construction sector to demonstrate the practical implications of implementing their optimization method. Tran *et al.* [36] developed a new hybrid solution method based on the Artificial Bee Colony and Differential Evolution algorithms to solve $PS_{m,\sigma,\rho}|prec|C_{max}$. They used PSPLIB as a benchmark set to compare their algorithm with improved versions of the Genetic Algorithm, Particle Swarm Optimization, Artificial Bee Colony and Differential Evolution algorithms. Sonmez and Gürel [37] developed the Harmony Search Algorithm to solve $MPS_{m,\sigma,\rho;\mu,\tau,\omega}|prec|C_{max}$ and used PSPLIB to evaluate its performance against two improved Genetic Algorithms, as well as Particle Swarm and Ant Colony Optimization algorithms. Tao and Dong [38] studied the problem of $MPS_{m,\sigma,\rho;\mu,\tau,\omega}|prec|curve$ and developed an improved hybrid method based on the Tabu Search

and NSGA-II to solve it. They used the PSPLIB to compare the solution algorithm's performance with two basic versions of NSGA-II.

Birjandi and Mousavi [39] proposed a Cluster-based Tabu Search integrated with the Particle Swarm Optimization algorithm to solve $MPS-MR_{m,\sigma,\rho;\mu,\tau,\omega}|prec|curve$. The new algorithm was evaluated using random test instances and compared with basic versions of Particle Swarm Optimization and Genetic Algorithms. Chakrabortty *et al.* [40] developed Variable Neighborhood Search-based Local Search Heuristic algorithms to solve $PS_{m,\sigma,\rho}|prec,\beta_4=\tilde{d}_j,\beta_6=^o|C_{max}$ and $PS_{m,\sigma,\rho}|prec,\beta_4=\tilde{d}_j,\beta_6=vr|C_{max}$. They considered six different priority rules and analyzed the algorithms' performance using random test instances in dynamic environments.

Asadujjaman *et al.* [41] developed the Immune Genetic Algorithm for the problem of $PS_{m,\sigma,\rho}|prec,\beta_5=\delta_n|npv$ and benchmarked its performance against the Lagrangian relaxation-based forward-backward improvement heuristic and the Scatter Search using the database from [42]. Asadujjaman *et al.* [43] proposed $PS_{m,\sigma,\rho}-MOP-DC|prec,\beta_5=\delta_n|npv,pf$, which integrated an RCPSP with a material ordering problem. The author used the Immune Genetic Algorithm to solve the problem considering random test instances and comparing the results with those of the basic Genetic and Immune algorithms. Asadujjaman *et al.* [44] proposed a multi-operator version of the Immune Genetic Algorithm to solve $PS_{m,\sigma,\rho}|prec,\beta_4=cont|npv$. They used 17,280 different instances from the database of Vanhoucke [42] to evaluate and compare the algorithm's performance against the Branch & Cut algorithm as the baseline.

The last study on the main development trajectory, Rahman *et al.* [45], proposed the Genetic Algorithm-based Memetic Algorithm to solve $PS_{m,\sigma,\rho}|prec|TC,CF$, considering Carbon Footprints as one of the optimization objectives. They developed a new test set to compare the performance of their algorithm with the basic Genetic and Memetic algorithms, as well as the basic and enhanced versions of NSGA-II.

Overall, early studies developed exhaustive solution methods and decision trees suitable for solving small-scale problems with low computational complexity. Studies evolved after 2006, incorporating practical constraints to bridge the gap between scheduling theory and practice. The precedence condition is a prime example. The optimization models and algorithms shifted from single-objective to multi-objective optimization after 2016. Initial works focused on minimizing project completion time, but later studies considered optimization objectives such as Resource Utilization Rate, total project cost, net present value, and environmental factors.

3.2 Key branches in the development of solution methods

Different values for the key-route parameter, i.e. 5, 10, 15, 20, 25, 30, 35, 40, and 45, are considered to find the most reasonable setting for the literature analysis. The key-route value of 30 is deemed suitable, resulting in a total of 51 articles: 2 sources, 2 sinks, and 47 intermediate nodes, including the articles on the main path. The key branches are shown in Fig. 2, followed by a review of the articles that emerged from the main path.

The first source node, Patterson *et al.* [46], proposed a Backtracking Algorithm to solve $PS_{m,\sigma,\rho}|prec,\alpha_2=1,\alpha_2=T|C_{max}$ and confirmed its efficiency through numerical experiments while considering different problem characteristics. The second source, Bell and Park [19], is present on the main development path; this study was later cited by Bell and Han [20], and was followed by Sampson and Weiss [21], both of which are main path articles. Sprecher *et al.* [47] explored the active, semi-active, and non-delay schedules in the context of RCPSPs. They used small illustrative examples to explain the applicability and implications of their method. This article was later cited by Kolisch and Drexl [23], which is considered a main path article. Kolisch and Drexl [48] explored $MPS_{m,\sigma,\rho;\mu,\tau,\omega}|prec,\alpha_2=1,\alpha_2=T|C_{max}$ and proposed a new local search technique to find feasible solutions as well as a neighborhood search method to improve it. The authors used the test bank generated by ProGen to compare results with two general non-preemptive algorithms developed by Drexl and Gruenewald [49].

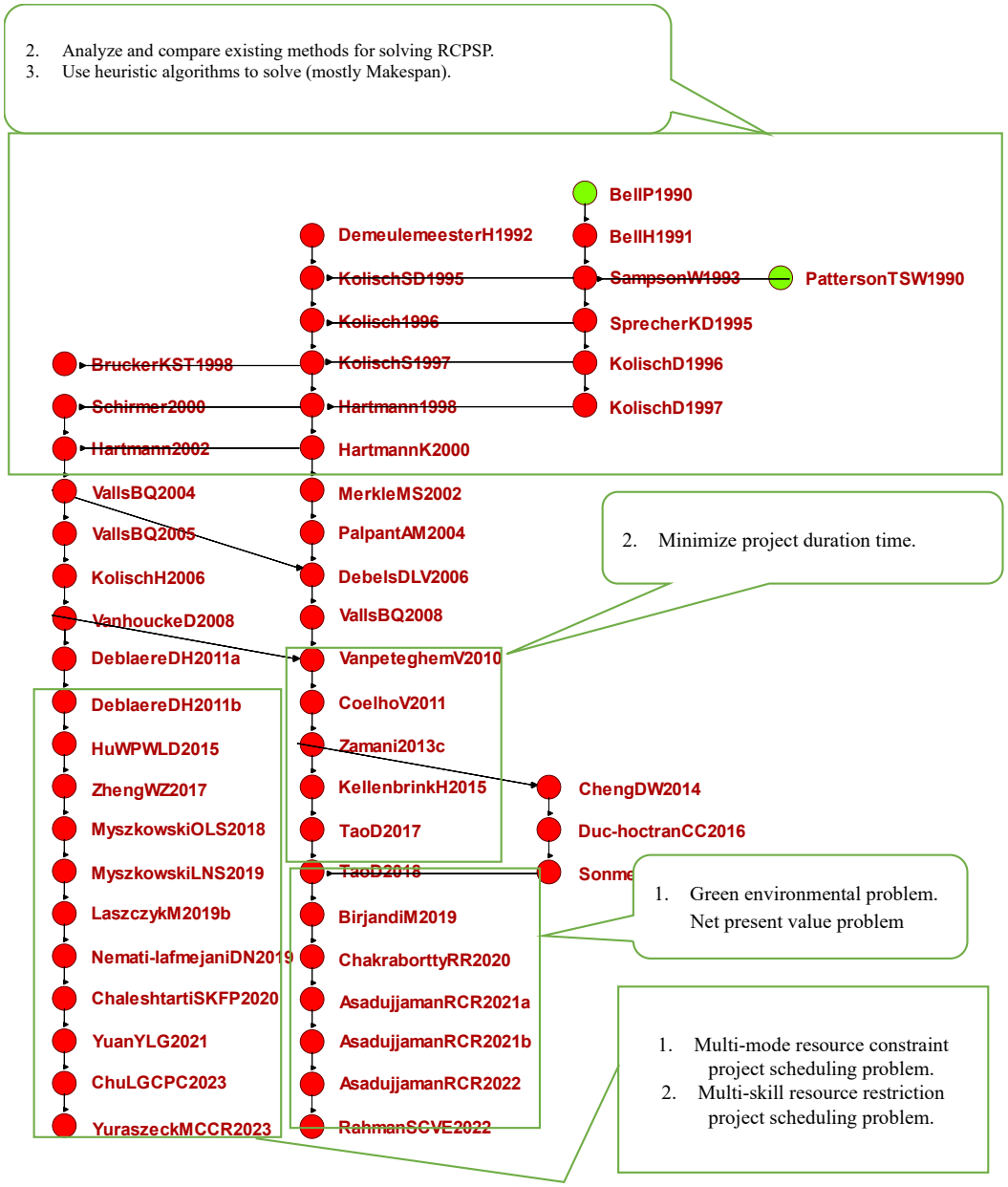

Fig. 2 The key development branches from the main path

The middle path constitutes many references from the main path, i.e. Kolisch *et al.* [22], Kolisch and Sprecher [24], Hartmann [27], and Hartmann and Kolisch [28]. Demeulemeester and Herroelen [50] developed a new Branch-and-Bound method suitable for addressing PERT/CPM problems with preconditions and solving $MPS_{m,\sigma,\rho;\mu,\tau,\omega}|prec,\beta_1 =^o|C_{max}$; they used Patterson's test bank to evaluate its performance, comparing it with the Branch-and-Bound method developed by Stinson *et al.* [51]. Kolisch [52] investigated the limitations of the serial and parallel scheduling methods; they put forward new strategies that were tested using the PSPLIB databases in comparison to well-known priority rules, including the most total successors, latest start time, latest finish time, minimum slack, and the greatest rank position weight.

Merkle *et al.* [53] developed an Ant Colony Optimization algorithm to solve $PS_{m,\sigma,\rho}|prec|C_{max}$. This algorithm was tested on the PSPLIB instances and compared with the lower bounds using a critical path heuristic. Palpant *et al.* [54] developed the neighborhood search algorithm with exact resolution of sub-problems to solve $PS_{m,\sigma,\rho}|prec|C_{max}$ and considered Patterson's 110 *easy* instances, along with some other datasets, to evaluate its performance by comparing the results with the best-known solutions at that time. Debels *et al.* [4] introduced the hybrid Scatter

Search Electromagnetism algorithm to solve $PS_{m,\sigma,\rho}|prec|C_{max}$ and used PSPLIB to showcase its superiority over self-adaptive and robust Genetic Algorithms, Tabu Search, and Simulated Annealing. Valls *et al.* [55] proposed a hybrid Genetic Algorithm to solve $PS_{m,\sigma,\rho}|prec|C_{max}$. They used ProGen's instances and performed extensive comparisons with several versions of the Genetic Algorithm, Tabu Search, and solution methods based on network decomposition.

After the studies of Van Peteghem and Vanhoucke [6], Coelho and Vanhoucke [33], and Zamani [34], which are considered on the main path, Kellenbrink and Helber [56] explored the problem of model-endogenous decisions on the project structure in RCPSPs, and developed a novel Genetic Algorithm with a module that adjusts the activity structure of inter-project activities to improve the solutions; the authors extended the ProGen generator and compared the results with those of CPLEX. Tao and Dong [57] introduced a new AND-OR network, proposed a new mathematical formulation for $PS_{m,\sigma,\rho}|prec|C_{max}$, and adjusted the Simulated Annealing algorithm to solve the problem. They designed a new instance set to evaluate the algorithm's performance, comparing it with an exact solver and several variants of the same algorithm. These studies also considered stochastic activity restrictions. The study of Zamani [34] was continued along the main path by Cheng *et al.* [35], Tran *et al.* [36], and Sonmez and Gürel [37]. The next seven articles were reviewed in the main path section, namely: Tao and Dong [38], Birjandi and Mousavi [39], Chakrabortty *et al.* [40], Asadujjaman *et al.* [41], Asadujjaman *et al.* [43], Asadujjaman *et al.* [44], and Rahman *et al.* [45]. These articles focused on green operational factors and multi-skill RCPSPs.

The left path in Fig. 2 includes Brucker *et al.* [25], Hartmann [29], Valls *et al.* [30], Valls *et al.* [31], Kolisch and Hartmann [5], and Vanhoucke and Debels [32], all of which are part of the main path. Schirmer [58] incorporated the Case-Based Reasoning, which is a learning method, into adaptive search algorithms to solve $PS_{m,\sigma,\rho}|prec, \alpha_2 = 1, \alpha_2 = T|C_{max}$. The authors focused on developing a mechanism for selecting algorithms based on the problem characteristics and used PSPLIB to confirm the practicability of the method.

Deblaere *et al.* [59] proposed a new execution strategy for the stochastic RCPSPs, $PS_{m,\sigma,\rho}|prec, \alpha_3 = v\tilde{a}|\gamma = E[\cdot]$. They used PSPLIB to compare their Simulation-based Descent Algorithm with the general heuristic developed by Van de Vonder et al. [60]. Deblaere *et al.* [61] explored $MPS_{m,\sigma,\rho;\mu,\tau,\omega}|prec|C_{max}$ and extended the Iterative Deepening A-STAR algorithm that is equipped with a module to repair the disrupted schedules. They considered the PSPLIB project scheduling library to compare the algorithm with different dominance rules as well as different search strategies, including the regular Branch-and-Bound and one integrated with Tabu Search.

Hu *et al.* [62] proposed an Outer-Inner Fuzzy Cellular Automaton for the Dynamic Uncertainty Multi-Project Scheduling Problem, $PS_{m,\sigma,\rho}|prec, \beta_4 = \tilde{d}_j|\gamma = curve, \gamma = RUR$. They considered the PSPLIB database for performance comparison with a Bee Swarm Optimization that utilizes forward-backward interchange and a hybrid Genetic Algorithm. Zheng *et al.* [63] developed the Teaching–Learning-Based Optimization algorithm to solve $MS - PS_{m,\sigma,\rho}|prec|C_{max}$. They used the iMOPSE database to compare the results obtained by their method with those from the Hybrid Ant Colony Optimization algorithm. Myszkowski *et al.* [64] developed a Hybrid Differential Evolution and Greedy Algorithm for $MS - PS_{m,\sigma,\rho}|prec|C_{max}$ and considered the iMOPSE database to compare its performance with Hybrid Ant Colony Optimization algorithm that utilizes Greedy Randomized Adaptive Search Procedure (GRASP). Myszkowski *et al.* [65] introduced the iMOPSE platform for the $S - PS_{m,\sigma,\rho}$ variant of RCPSPs. The software includes test instances, visualization tools, and other material. Laszczyk and Myszkowski [66] developed the Non-dominated Tournament Genetic Algorithm to solve $MS - PS_{m,\sigma,\rho}|prec|\gamma = curve$. The authors considered the iMOPSE dataset to evaluate the effectiveness of the algorithms, comparing the results with those of NSGA-II and Differential Evolution hybridized with Greedy Algorithm.

Nemati-Lafmejani *et al.* [67] developed dual-objective optimization methods, NSGA-II, and Multi-Objective Particle Swarm Optimization to solve $MPS_{m,\sigma,\rho;\mu,\tau,\omega} - CS|prec|\gamma = curve, \gamma = TD$, and compared them using the PSPLIB test set. Chaleshtarti *et al.* [68] developed a Hybrid

Genetic and Lagrangian Relaxation Algorithm to solve $PS_{m,\sigma,\rho},\alpha_2 = T|prec|C_{max}$. Yuan *et al.* [69] developed a Hybrid Cooperative Co-evolution Algorithm to solve $M - MPS_{m,\sigma,\rho;\mu,\tau,\omega}|prec|\gamma = curve$. The algorithm performed exceptionally well in terms of robustness when compared to the Genetic Algorithm, Particle Swarm Optimization, and hybrid multi-objective version of the Estimation of Distribution Algorithm. Chu *et al.* [70] introduced a metaheuristic recommendation model to address $MPS_{m,\sigma,\rho;\mu,\tau,\omega}|prec|C_{max}$, which can select the most suitable solution algorithm based on the problem characteristics. The authors used PSPLIB as the testbed to evaluate the performance of the developed solution method, considering various practical scenarios. Yuraszeck *et al.* [71] proposed a new constraint programming model to address the problem of $M - MPS_{m,\sigma,\rho;\mu,\tau,\omega}|prec|C_{max}$. The authors considered a total of 321 test instances from five earlier studies and compared the results with the best-found lower bounds reported by Dauzère-Pérès *et al.* [72].

Overall, the key branch articles focused primarily on developing case-specific project scheduling variants. Multi-mode RCPSPs and the differentiation between renewable and non-renewable resources became prevalent in the key branches. The most recent studies explored multi-skill RCPSPs and project scheduling that considers green factors. Hybridization played a significant role in key development branches of RCPSP algorithms.

3.3 Major thematics

Fig. 3 provides an overlay view of the most frequently occurring keywords over time. Larger nodes represent words with higher frequencies of occurrence. The closer the connection between the two nodes is, the stronger their correlation. Nodes with more recent occurrences appear in brighter colors, with yellow indicating the most recent ones. This visualizes the shift in focus within the literature over time.

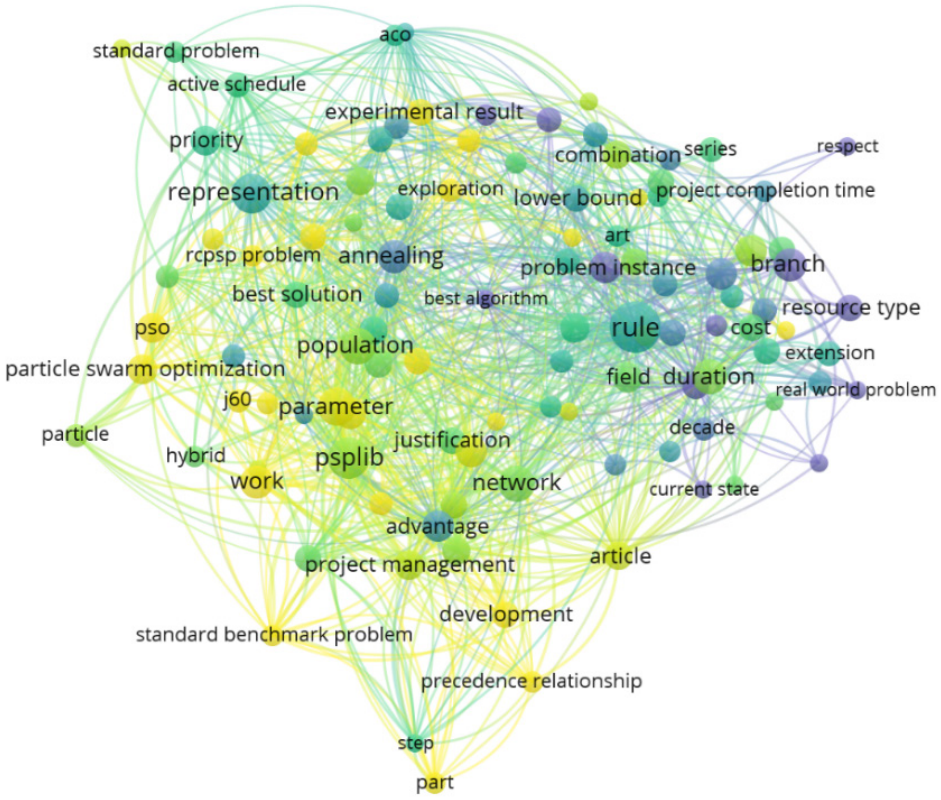

Fig. 3 Overlay visualization of the keywords network

CA indicates that the literature on RCPSPs can be divided into 23 themes. The top three themes will be considered for further analysis. Each theme is identified based on the proportion of keyword occurrences in the associated cluster. The first theme is *priority rules and heuristic*

algorithms, which include 191 articles. This research theme experienced significant growth between 1995 and 2015. Methods for modeling and solving *multi-mode RCPSPs*, with 99 articles, constitute the second major research theme. The cluster began in 1993 and continued to grow until 2017. The first two clusters are currently in the saturation stage. Algorithms for *RCPSPs with random activity durations* constitute the third major theme, highlighting its practical relevance with 93 articles. This research theme received recognition only after 2010 and is now in the final years of the growth stage. The growth forecast trends and keyword proportions of these clusters are presented in Table 4. This is followed by a brief analysis of the seminal literature within each cluster.

Table 4 Major research themes

Cluster / Count	Keyword – Occurrence Ratio	Growth trend
Cluster A: *priority rules and heuristic algorithms* /191	Rule – 0.178 PSPLIB – 0.115 Representation – 0.109 Parameter – 0.104 Network – 0.094 Duration – 0.083	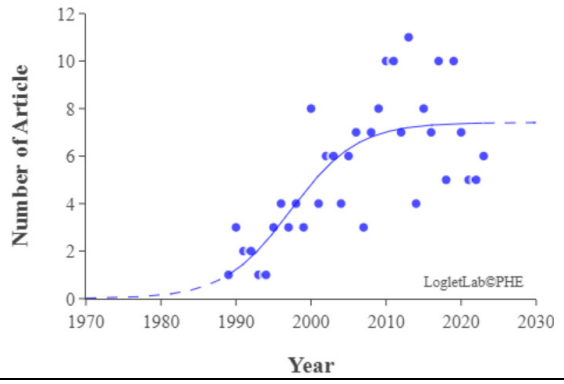
Cluster B: *multi-mode RCPSPs* /99	Experiment – 0.263 Computational result – 0.172 Parameter – 0.162 Multiple execution mode – 0.152 Type – 0.152 Efficiency – 0.132	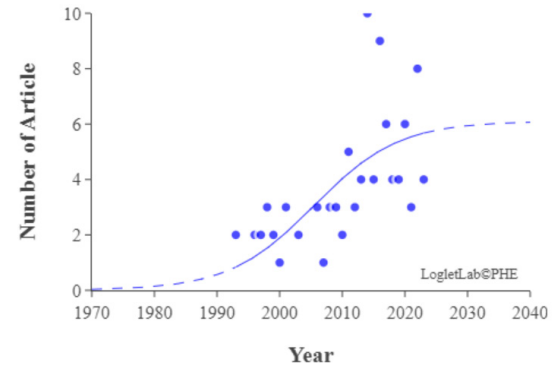
Cluster C: *RCPSPs with random activity durations* /93	Baseline schedule – 0.28 Stochastic resource – 0.24 Robustness – 0.2 Cost – 0.19 Computational experiment – 0.17 Heuristic – 0.17	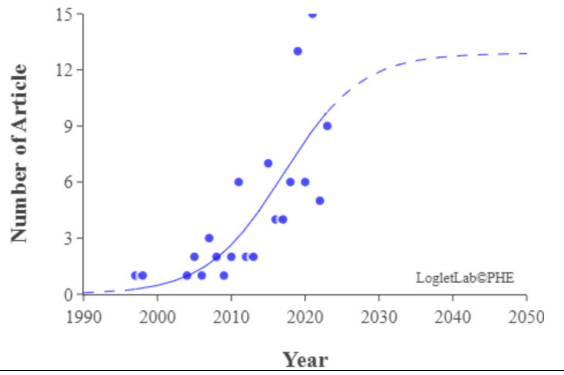

3.3.1 Priority rules and heuristics for RCPSPs

Fig. 4 illustrates the primary development trajectory within the first cluster. Among the 23 articles recognized as significant development progress in developing priority rules and heuristic algorithms, only four articles are absent from the main path and the key development branches.

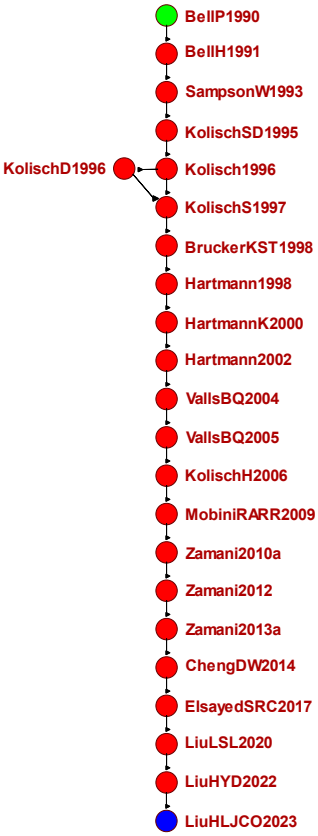

Fig. 4 Progress in the development of priority rules and heuristics for RCPSPs

From the remaining articles, Mobini *et al.* [73] improved the Scatter Search algorithm to solve $PS_{m,\sigma,\rho}|prec|C_{max}$. Using the PSPLIB database, the algorithm was compared with the basic Scatter Search, the hybrid of Genetic Algorithm and Tabu Search with path relinking, and several other versions of Genetic Algorithms. Zamani [74] developed an Accelerating Two-Layer Anchor Search algorithm to solve $PS_{m,\sigma,\rho}|prec|C_{max}$, and used the PSPLIB database to compare its performance with the Local Search algorithm integrated with subproblem exact resolution. Zamani [75] introduced the Polarized Adaptive Scheduling Scheme for $PS_{m,\sigma,\rho}|prec|C_{max}$, which dynamically adjusts the priority of activities in the project. He used the PSPLIB database and Local Search with subproblem exact resolution to evaluate the performance of the new scheme. Elsayed *et al.* [76] proposed a consolidated optimization algorithm, which combines GA and the Multi-operator Differential Evolution to solve $PS_{m,\sigma,\rho}|prec|C_{max}$. Using the PSPLIB databases, they showed that their algorithm outperforms 11 algorithms, including the decomposition-based Genetic Algorithm, the hybrid of Ant Colony Optimization and Scatter Search, Particle Swarm Optimization, Bee Colony Algorithm, and an improved version of the Shuffled Frog-leaping Algorithm.

This research theme dominated scientific progress in the early development stages of RCPSPs. These studies are mainly focused on testing the developed rules and heuristics on simple RCPSPs and establishing the foundations for solution modeling and representation.

3.3.2 Multi-mode resource-constrained project scheduling algorithms

Fig. 5 shows the main development trajectory of solution algorithms to solve multi-mode RCPSPs. In contrast to the first theme, this group of studies did not contribute much to the main development trajectory. The progress in this specific category shows the wide real-world applications of multi-mode RCPSPs. Considering the increase in the scale and complexity of problems, the articles under this theme are focused on improving the efficiency of solution algorithms and calibrating the parameters.

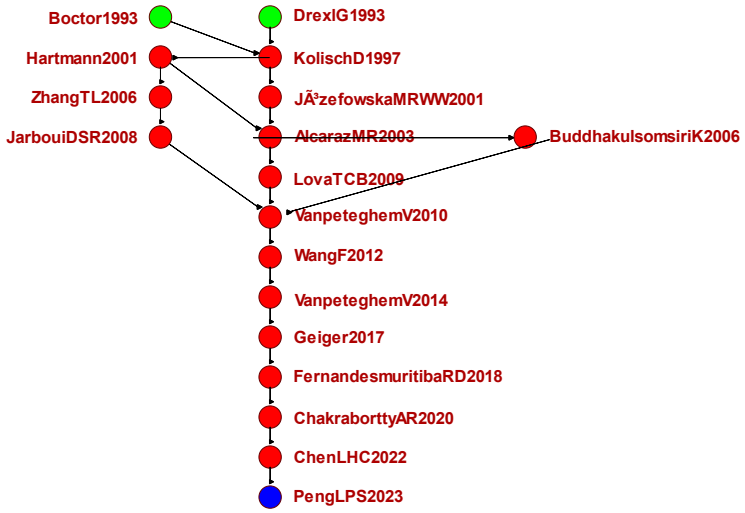

Fig. 5 Progress in multi-mode resource-constrained project scheduling algorithms

Boctor [77] proposed several effective heuristic rules for $MPS_{m,\sigma,\rho;\mu,\tau,\omega}|prec,\alpha_2 = 1T|C_{max}$. He randomly generated 240 test problems to compare them with 18 other heuristics. Drexl and Gruenewald [49] proposed a novel stochastic scheduling method for the general class of non-preemptive RCPSPs. They used randomly generated test problems to compare their method with the min LF method, which was the state-of-the-art deterministic search method at the time. Kolisch and Drexl [48] cited both source nodes and is recognized as one of the key branch articles. Hartmann [78] extended the Genetic Algorithm to optimize $MPS_{m,\sigma,\rho;\mu,\tau,\omega}|prec|C_{max}$. Their experiments confirmed that the improved algorithm outperforms both Simulated Annealing and Branch and Bound algorithms. Józefowska *et al.* [79] introduced a new Simulated Annealing algorithm to optimize $MPS_{m,\sigma,\rho;\mu,\tau,\omega}|prec|C_{max}$, and used PSPLIB to confirm its effectiveness with and without a penalty function. The results were compared with the Genetic Algorithm developed by Hartmann. Alcaraz *et al.* [80] proposed the Multi-Mode Two-Point Forward-Backward Crossover Genetic Algorithm for $MPS_{m,\sigma,\rho;\mu,\tau,\omega}|prec|C_{max}$. The algorithm performed better than those developed by Hartmann [78], Kolisch and Drexl [48], and the Genetic Algorithm developed by Ozdamar [81].

Buddhakulsomsiri and Kim [82] improved Hartmann's Branch and Bound algorithm and adjusted it so that the activities can be split in $MPS_{m,\sigma,\rho;\mu,\tau,\omega}|prec|C_{max}$. The algorithm was used to compare the project performance in various practical scenarios. Zhang *et al.* [83] proposed the Multimode Particle Swarm Optimization to solve $MPS_{m,\sigma,\rho;\mu,\tau,\omega}|prec|C_{max}$, and compared the algorithm with the current best algorithms such as SA, BB, and so on. The results confirm its superior performance. Jarboui *et al.* [84] extended the Particle Swarm Optimization algorithm with a new local search method for $MPS_{m,\sigma,\rho;\mu,\tau,\omega}|prec|C_{max}$. They used PSPLIB to test it and showed that the algorithm outperforms the Simulated Annealing Algorithm, and the algorithm proposed by ZhangTL2006. Lova *et al.* [85] proposed a multi-mode Hybrid Genetic Algorithm for $MPS_{m,\sigma,\rho;\mu,\tau,\omega}|prec|C_{max}$. They considered the instances generated by the project generator ProGen to compare their algorithm with the Simple Genetic Algorithm as a baseline, as well as those developed by Hartmann [78], Kolisch and Drexl [48], Ozdamar [81], and Bouleimen and Lecocq [86]. Van Peteghem an Vanhoucke [6] proposed the Bi-Population Genetic Algorithm for solving $MPS_{m,\sigma,\rho;\mu,\tau,\omega}|prec,\beta_1 = pmtn,\beta_1 = pmtn - rep|C_{max}$. The algorithm outperformed the Hybrid Genetic Algorithms developed by Lova *et al.* [85] and Alcaraz *et al.* [80], the extended Particle Swarm Optimization of Jarboui *et al.* [84], and the Hybrid Scatter Search of Ranjbar *et al.* [87].

Wang and Fang [88] adapted the Estimation of Distribution Algorithm to optimize $MPS_{m,\sigma,\rho;\mu,\tau,\omega}|prec|\gamma = \sum sq.dev$. Experimental results based on PSPLIB instances showed that the average percentage deviation of this algorithm is smaller than that of the Simulated Anneal-

ing of Józefowska *et al.* [79], the Genetic Algorithms of Alcaraz *et al.* [80], Van Peteghem and Vanhoucke [6], the Hybrid Scatter Search of Ranjbar *et al.* [87], the Artificial Immune System of [89], and the Hybrid Genetic Algorithm of Lova *et al.* [85]. Vanpeteghem and Vanhoucke [90] introduced the Multi-Mode Library, which is a new database for Multi-mode RCPSPs. They compared MMLIB and PSPLIB using different metaheuristics to verify the new instances. Geiger [91] studied $MMPS_{m,\sigma,\rho;\mu,\tau,\omega},\alpha_2 = 1T|prec|Cmax_{max}$. He combined Variable Neighborhood Search with the Iterated Local Search algorithm for a Multi-Threaded Local Search Algorithm to solve it. Using the MMLIB database, it was shown that the new algorithm outperforms several state-of-the-art metaheuristics, including those developed by Hartmann [78], Lova *et al.* [85], VanpeteghemV2010, and the Differential Evolution algorithm by Damak *et al.* [92].

Fernandes Muritiba *et al.* [93] proposed a Path-Relinking algorithm to explore the solution spaces of $MPS_{m,\sigma,\rho;\mu,\tau,\omega}|prec,\alpha_2 = 1T|C_{max}$. Experimental results confirmed that its performance is better than the competing methods proposed earlier, such as the Genetic Algorithms of Lova et al. [85], Vanpeteghem and Vanhoucke [6], the Differential Evolution algorithm by Damak *et al.* [92], and the Estimation of Distribution Algorithms of Wang and Fang [88], among others. Chakrabortty *et al.* [94] proposed a modified Variable Neighborhood Search Heuristic algorithm for $MMPS_{m,\sigma,\rho;\mu,\tau,\omega},\alpha_2 = 1T|prec,\beta_1 =^{o}|C_{max}$. They used PSPLIB to confirm its effectiveness against adopted versions of the Simulated Annealing, Genetic Algorithm, Particle Swarm Optimization and its discrete variant, Differential Evolutionary Algorithm, Estimation of Distribution Algorithm, and Ant Colony Optimization algorithm. Chen *et al.* [95] developed a Hybrid Genetic Algorithm that combines different priority rules, as well as the series and parallel scheduling methods to solve $MMPS_{m,\sigma,\rho;\mu,\tau,\omega},\alpha_2 = 1T|prec|C_{max}$. The experimental results show that this algorithm is particularly effective in reducing the construction period while evaluating the integration with various priority rules. Finally, Peng *et al.* [96] introduced the Hybrid Quantum Particle Swarm Optimization to solve $MS-MPS_{m,\sigma,\rho;\mu,\tau,\omega},,\alpha_2 = 1T|prec|C_{max}$. The authors used PSPLIB to test, and the experimental results show that the algorithm provides more accuracy and better convergence than the baseline Particle Swarm Optimization algorithm.

Genetic Algorithms have been the cornerstone of the developments in multi-mode resource-constrained project scheduling. Nearly all seminal studies under this research theme included different versions of the Genetic Algorithms in their numerical experiments.

3.3.3 Integrating stochasticity into RCPSPs

The last major theme constitutes the integration of stochasticity into RCPSPs. Fig. 6 shows the backbone of scientific progress in this research theme, where the studies are predominantly concerned with uncertain time parameters and resource availability. Developing robust solution methods to minimize the expected project completion time and makespan has been at the center of attention in the development of this theme.

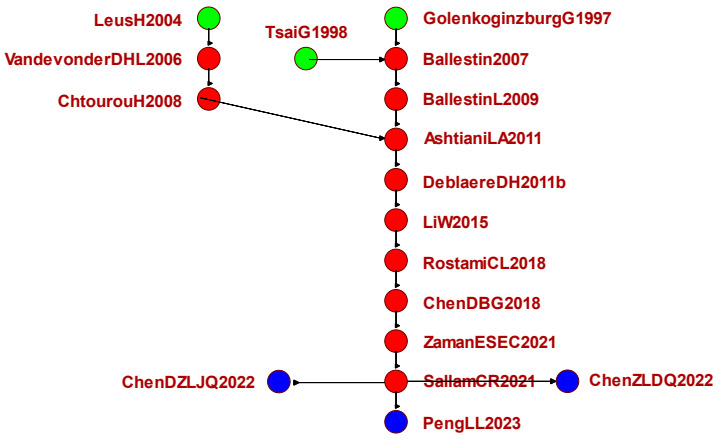

Fig. 6 Scientific progress in the integration of stochasticity into RCPSPs

Golenko-Ginzburg and Gonik [97], Tsai and Gemmill [98], and Leus and Herroelen [99] are the source articles in the development trajectory of this research theme. Golenko-Ginzburg and Gonik [97] proposed a heuristic method for $PS_{m,\sigma,\rho}|\beta_4 = \tilde{d}_j|\gamma = EPD$ and tested it by considering various possibility terms. Tsai and Gemmill [98] developed a Tabu Search algorithm to enhance the computational performance when solving $PS_{m,\sigma,\rho}|prec, \beta_4 = \tilde{d}_j|C_{max}$. They tested the method by considering various combinations of heuristics. Leus and Herroelen [99] proposed a resource allocation model for $PS_{m,\sigma,\rho}|prec, \beta_4 = \tilde{d}_j|C_{max}$. They used the RanGen platform to generate test instances and improved the Branch and Bound algorithm developed by Demeulemeester and Herroelen [50] to test their method, comparing it with insertion techniques for both online and offline RCPSPs.

Vandevonder *et al.* [100] developed a new heuristic method to solve $PS_{m,\sigma,\rho}|prec, \beta_4 = \tilde{d}_j|C_{max}$. The instances used in their numerical experiment were generated using RanGen software to analyze the impact of the weighting parameter, the number of activities, the order strength, buffer sizes, and the resource constraints. Ballestín [101] developed an adaptive Genetic Algorithm to study $PS_{m,\sigma,\rho}|prec, \beta_4 = \tilde{d}_j|C_{max}$. The performance of the developed algorithm was compared with Simulated Annealing and Tabu Search algorithms using the ProGen-generated question bank. Chtourou and Haouari [102] developed the Two-Stage Priority Rule-Based Algorithm for investigating $PS_{m,\sigma,\rho}|prec, \beta_4 = \tilde{d}_j|\gamma = av$, mentioning the stability of the project schedule as the main motivation. They conducted a simulation analysis based on the instances of Kolisch *et al.* [103]. Ballestín and Leus [104] developed the GRASP algorithm to solve $PS_{m,\sigma,\rho}|prec, \beta_4 = \tilde{d}_j|\gamma = EPD$. Using instances from PSPLIB, they compared this algorithm with the Genetic Algorithm developed in an earlier study, Ballestín [101]. Ashtiani *et al.* [105] introduced a novel scheduling policy, namely the Preprocessor Polic for $PS_{m,\sigma,\rho}|prec, \beta_4 = \tilde{d}_j|\gamma = C_{max}$. Using instances generated by the ProGen data generator and RanGen, they compared this policy with an activity-based (priority) policy using Genetic Algorithms.

Li and Womer [106] developed an Approximate Dynamic Programming algorithm with Hybrid Backward and Forward Approximation for $PS_{m,\sigma,\rho}|prec, \beta_4 = \tilde{d}_j|\gamma = C_{max}$. This type of solution algorithm is particularly useful for scheduling highly uncertain and variable projects. The authors tested their method using Patterson's benchmark and PSPLIB instances and compared the algorithm with the GRASP algorithm developed by Ballestín and Leus [104]. Rostami *et al.* [107] proposed a new strategy and a new two-stage heuristic algorithm for $PS_{m,\sigma,\rho}|prec, \beta_4 = \tilde{d}_j|\gamma = C_{max}$. Instances from the PSPLIB library were used to compare the two-phase metaheuristic procedure with the Estimation of Distribution algorithm by Wang and Fang [88], the Genetic Algorithm of Ashtiani *et al.* [105], as well as the GRASP method of Ballestín and Leus [104]. Chen *et al.* [108] developed five new priority rules and compared them with twelve from the literature while solving $PS_{m,\sigma,\rho}|prec, \beta_4 = \tilde{d}_j|\gamma = C_{max}$. They considered instances from PSPLIB with three different probability distribution functions for activity durations. Zaman *et al.* [109] developed the Scenario-based Combined Optimization Algorithm by integrating the Multi-operator Genetic Algorithm with the Multi-operator Differential Evolution to solve $PS_{m,\sigma,\rho}|prec, \beta_4 = \tilde{d}_j|\gamma = C_{max}$. The algorithm was compared with Genetic Algorithm of Ballestín [101], GRASP of Ballestín and Leus [104], the Two-phase Genetic Algorithm of Ashtiani *et al.* [105], and the Estimation of Distribution Algorithm of Fang *et al.* [110], while using PSPLIB instances. Sallam *et al.* [111] developed a Reinforcement Learning-Based Multi-Method Approach, which is a hybrid of the Multi-Objective Genetic Algorithm and Differential Evolution, to solve $PS_{m,\sigma,\rho}|prec, \beta_4 = \tilde{d}_j|\gamma = C_{max}$. They considered three different industrial cases along with instances from the PSPLIB to showcase its effectiveness compared with the enhanced local search heuristic of Chakrabortty *et al.* [94], the Genetic Algorithm of Ballestín [101], the GRASP of Ballestín and Leus [104], the Two-phase Genetic Algorithm of Ashtiani *et al.* [105], and the Approximate dynamic programming of Li and Womer [106], and the optimization algorithm developed by Zaman *et al.* [109]. This is a seminal work on applications of machine learning in project scheduling.

Chen *et al.* [112] proposed a Hierarchical Hybrid Filtering Genetic Programming method that regulates the scope and attributes of priority rules to solve $MPPS_{m,\sigma,\rho}|prec, \beta_4 = \tilde{d}_j|C_{max}$. They used the test instances from PSPLIB and considered a set of traditional priority rules to showcase the superiority of their algorithm. Chen *et al.* [113] developed a Hyper-heuristic-based Two-Stage Genetic Programming Framework to solve $MPPS_{m,\sigma,\rho}|prec, \beta_4 = \tilde{d}_j|C_{max}$. They considered a benchmark of 1,000 instances based on PSPLIB to compare their method, using SPEA2 and NSGA-II as the evaluation methods, as well as the traditional priority rules as the baseline. Peng *et al.* [114] introduced the Proactive-Reactive Scheduling Algorithm, which combines a novel scheduling strategy with CPM to study $CCPS_{m,\sigma,\rho}|prec, \beta_4 = \tilde{d}_j|C_{max}$. They used the datasets J30, J60, and J120 from the PSPLIB to evaluate their algorithm against the Approximate Dynamic Programming algorithm of Li and Womer [106] under various settings.

Overall, studies under this cluster paid special attention to establishing a balance between computational stability, efficiency, and solution quality, especially when dealing with the randomness of activity durations, interruptions, and other uncertainty issues. Robust solution algorithms were at the center of scientific progress under this research theme.

4. Concluding remarks and future research

This study comprehensively reviewed the resource-constrained project scheduling articles published between 1980 and 2024. The development paths and milestones in knowledge dissemination in project planning research were analyzed systematically. It was found that the impactful research directions gradually shifted from basic scheduling models and priority rules to multi-modal, multi-objective problems considering practical research constraints. The most recent focus shift of RCPSPs is towards dynamic scheduling. Practical aspects of resource uncertainty and multi-project coordination have also gained attention in recent years.

Research on RCPSPs has risen steadily, reaching a record high in published articles in 2021 (see Fig. 7a). Investigating the past development trajectory, including the maximum records, the starting point of the growth curve, and the turning point from growth to saturation indicates continuing growth until the late 2030s (see Fig. 7b).

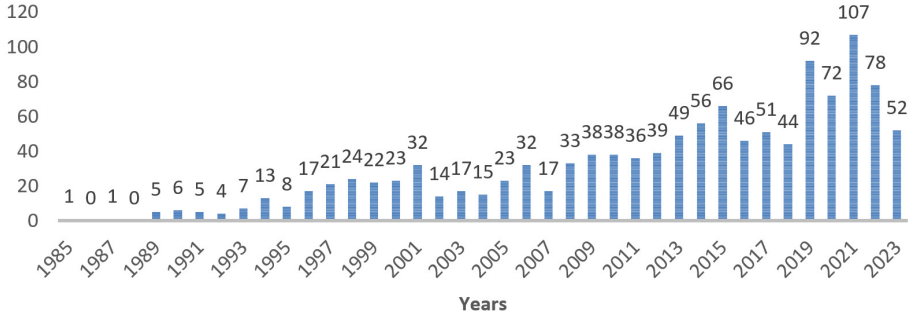

a) The historical trend on the scientific progress of RCPSPs

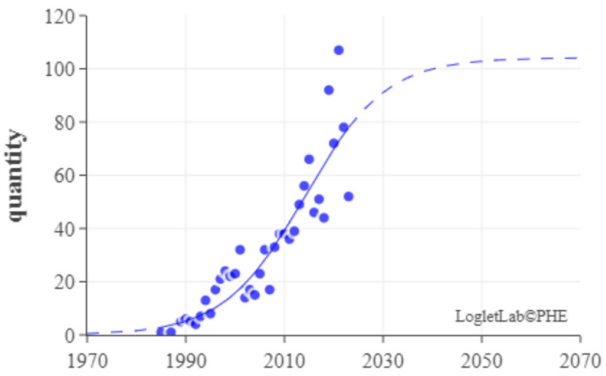

b) An estimation of the future growth

Fig. 7 Historical trends and an estimation of the future development trend using a Logistic model

The less tangible patterns of development in the literature on RCPSPs were also explored. It was found that solution methods based on network structure analysis and dynamic programming approaches have received limited attention and therefore require further development. Overall, project planning requires a fresh multidisciplinary perspective to enrich task scheduling and extend mathematical applications by incorporating real-life needs and features into RCPSPs. More specific suggestions follow for future research directions.

- Process mining and dynamic scheduling. This allows for real-time adjustment of tasks, considering changes in both tangible parameters and intangible operational patterns.
- Changes in resource availability driven by machine failures, maintenance, and employee shiftwork require more attention. Additionally, resource conflicts and multi-agent systems in multi-project management require new coordination strategies.
- Standard datasets considering multiple heterogeneous projects and projects with dynamic resource allocation are needed to provide a more diverse test platform for advances in solution algorithms.
- Learning from large datasets to improve the search in solution spaces. Machine learning-based solution algorithms are required to balanced computational efficiency and solution quality.
- Interactive multi-objective optimization schemes to balance conflicting objectives in real-time. Minimizing carbon footprints in large-scale projects is a prime example of an objective that conflicts with financial considerations.
- Finally, we think that some of RCPSPs features reviewed in this article can inspire new directions for future research in the production scheduling literature. Taking the dual-resource-constrained flexible job-shop scheduling problem [115] as an example, differentiating between renewable and non-renewable resources may be of interest to be able to account for additional practical features in the optimization process.

References

[1] Ciric, D., Delic, M., Lalic, B., Gracanin, D., Lolic, T. (2021). Exploring the link between project management approach and project success dimensions: A structural model approach, *Advances in Production Engineering & Management*, Vol. 16, No. 1, 99-111, doi: 10.14743/apem2021.1.387.

[2] Munoz-Ibanez, C., Chairez, I., Jimenez-Martinez, M., Molina, A., Alfaro-Ponce, M. (2023). Hybrid forecasting modelling of cost and time entities for planning and optimizing projects in the die-cast aluminium industry, *Advances in Production Engineering & Management*, Vol. 18, No. 2, 163-174, doi: 10.14743/apem2023.2.464.

[3] Kolisch, R. (1996). Efficient priority rules for the resource-constrained project scheduling problem, *Journal of Operations Management*, Vol. 14, No. 3, 179-192, doi: 10.1016/0272-6963(95)00032-1.

[4] Debels, D., De Reyck, B., Leus, R., Vanhoucke, M. (2006). A hybrid scatter search/electromagnetism meta-heuristic for project scheduling, *European Journal of Operational Research*, Vol. 169, No. 2, 638-653, doi: 10.1016/j.ejor.2004.08.020.

[5] Kolisch, R., Hartmann, S. (2006). Experimental investigation of heuristics for resource-constrained project scheduling: An update, *European Journal of Operational Research*, Vol. 174, No. 1, 23-37, doi: 10.1016/j.ejor.2005.01.065.

[6] Van Peteghem, V., Vanhoucke, M. (2010). A genetic algorithm for the preemptive and non-preemptive multi-mode resource-constrained project scheduling problem, *European Journal of Operational Research*, Vol. 201, No. 2, 409-418, doi: 10.1016/j.ejor.2009.03.034.

[7] Nekoueian, R., Servranckx, T., Vanhoucke, M. (2023). Constructive heuristics for selecting and scheduling alternative subgraphs in resource-constrained projects, *Computers & Industrial Engineering*, Vol. 182, Article No. 109399, doi: 10.1016/j.cie.2023.109399.

[8] Melchiors, P., Kolisch, R., Kanet, J.J. (2024). The performance of priority rules for the dynamic stochastic resource-constrained multi-project scheduling problem: An experimental investigation, *Annals of Operations Research*, Vol. 338, 569-595, doi: 10.1007/s10479-024-05841-9.

[9] Servranckx, T., Coelho, J., Vanhoucke, M. (2024). A genetic algorithm for the Resource-Constrained Project Scheduling Problem with alternative subgraphs using a boolean satisfiability solver, *European Journal of Operational Research*, Vol. 316, No. 3, 815-827, doi: 10.1016/j.ejor.2024.02.041.

[10] Gómez Sánchez, M., Lalla-Ruiz, E., Fernández Gil, A., Castro, C., Voß, S. (2023). Resource-constrained multi-project scheduling problem: A survey, *European Journal of Operational Research*, Vol. 309, No. 3, 958-976, doi: 10.1016/j.ejor.2022.09.033.

[11] Aghileh, M., Tereso, A., Alvelos, F., Monteiro Lopes, M.O. (2024). Multi-project scheduling under uncertainty and resource flexibility: A systematic literature review, *Production & Manufacturing Research*, Vol. 12, No. 1, doi: 10.1080/21693277.2024.2319574.
[12] Hartmann, S., Briskorn, D. (2021). An updated survey of variants and extensions of the resource-constrained project scheduling problem, *European Journal of Operational Research*, Vol. 297, No. 1, 1-14, doi: 10.1016/j.ejor.2021.05.004.
[13] Schryen, G., Sperling, M. (2023). Literature reviews in operations research: A new taxonomy and a meta review, *Computers & Operations Research*, Vol. 157, Article No. 106269, doi: 10.1016/j.cor.2023.106269.
[14] Ying, K.-C., Pourhejazy, P., Huang, X.-Y. (2024). Revisiting the development trajectory of parallel machine scheduling, *Computers & Operations Research*, Vol. 168, Article No. 106709, doi: 10.1016/j.cor.2024.106709.
[15] Ying, K.-C., Pourhejazy, P., Huang, T. (2024). Exploring the development trajectory of single-machine production scheduling, *Annals of Operations Research*, doi: 10.1007/s10479-024-06395-6.
[16] Liu, J.S., Lu, L.Y.Y., Ho, M.H.-C. (2019). A few notes on main path analysis, *Scientometrics*, Vol. 119, 379-391, doi: 10.1007/s11192-019-03034-x.
[17] Girvan, M., Newman, M.E.J. (2002). Community structure in social and biological networks, *Proceedings of the National Academy of Sciences*, Vol. 99, No. 12, 7821-7826, doi: 10.1073/pnas.122653799.
[18] van Eck, N.J., Waltman, L. (2010). Software survey: VOSviewer, a computer program for bibliometric mapping, *Scientometrics*, Vol. 84, 523-538, doi: 10.1007/s11192-009-0146-3.
[19] Bell, C.E., Park, K. (1990). Solving resource-constrained project scheduling problems by a* search, *Naval Research Logistics*, Vol. 37, No. 1, 61-84, doi: 10.1002/1520-6750(199002)37:1<61::AID-NAV3220370104>3.0.CO;2-S.
[20] Bell, C.E., Han, J. (1991). A new heuristic solution method in resource-constrained project scheduling, *Naval Research Logistics*, Vol. 38, No. 3, 315-331, doi: 10.1002/1520-6750(199106)38:3<315::AID-NAV3220380304>3.0.CO;2-7.
[21] Sampson, S.E., Weiss, E.N. (1993). Local search techniques for the generalized resource constrained project scheduling problem, *Naval Research Logistics,* Vol. 40, No. 5, 665-675, doi: 10.1002/1520-6750(199308)40:5<665::AID-NAV3220400509>3.0.CO;2-J.
[22] Kolisch, R., Sprecher, A., Drexl, A. (1995). Characterization and generation of a general class of resource-constrained project scheduling problems, *Management Science,* Vol. 41, No. 10, 1693-1703, doi: 10.1287/mnsc.41.10.1693.
[23] Kolisch, R., Drexl, A. (1996). Adaptive search for solving hard project scheduling problems, *Naval Research Logistics,* Vol. 43, No. 1, 23-40, doi: 10.1002/(SICI)1520-6750(199602)43:1<23::AID-NAV2>3.0.CO;2-P.
[24] Kolisch, R., Sprecher, A. (1997). PSPLIB – A project scheduling problem library, *European Journal of Operational Research,* Vol. 96, No. 1, 205-216, doi: 10.1016/S0377-2217(96)00170-1.
[25] Brucker, P., Knust, S., Schoo, A., Thiele, O. (1998). A branch and bound algorithm for the resource-constrained project scheduling problem, *European Journal of Operational Research,* Vol. 107, No. 2, 272-288, doi: 10.1016/S0377-2217(97)00335-4.
[26] Demeulemeester, E.L., Herroelen, W.S. (1997). New benchmark results for the resource-constrained project scheduling problem, *Management Science,* Vol. 43, No. 11, 1485-1492, doi: 10.1287/mnsc.43.11.1485.
[27] Hartmann, S. (1998). A competitive genetic algorithm for resource-constrained project scheduling, *Naval Research Logistics,* Vol. 45, No. 7, 733-750, doi: 10.1002/(SICI)1520-6750(199810)45:7<733::AID-NAV5>3.0.CO;2-C.
[28] Hartmann, S., Kolisch, R. (2000). Experimental evaluation of state-of-the-art heuristics for the resource-constrained project scheduling problem, *European Journal of Operational Research,* Vol. 127, No. 2, 394-407, doi: 10.1016/S0377-2217(99)00485-3.
[29] Hartmann, S. (2002). A self-adapting genetic algorithm for project scheduling under resource constraints, *Naval Research Logistics,* Vol. 49, No. 5, 433-448, doi: 10.1002/nav.10029.
[30] Valls, V., Ballestín, F., Quintanilla, S. (2004). A population-based approach to the resource-constrained project scheduling problem, *Annals of Operations Research,* Vol. 131, 305-324, doi: 10.1023/B:ANOR.0000039524.09792.c9.
[31] Valls, V., Ballestín, F., Quintanilla, S. (2005). Justification and RCPSP: A technique that pays, *European Journal of Operational Research,* Vol. 165, No. 2, 375-386, doi: 10.1016/j.ejor.2004.04.008.
[32] Vanhoucke, M., Debels, D. (2008). The impact of various activity assumptions on the lead time and resource utilization of resource-constrained projects, *Computers & Industrial Engineering,* Vol. 54, No. 1, 140-154, doi: 10.1016/j.cie.2007.07.001.
[33] Coelho, J., Vanhoucke, M. (2011). Multi-mode resource-constrained project scheduling using RCPSP and SAT solvers, *European Journal of Operational Research,* Vol. 213, No. 1, 73-82, doi: 10.1016/j.ejor.2011.03.019.
[34] Zamani, R. (2013). A competitive magnet-based genetic algorithm for solving the resource-constrained project scheduling problem, *European Journal of Operational Research,* Vol. 229, No. 2, 552-559, doi: 10.1016/j.ejor.2013.03.005.
[35] Cheng, M.-Y., Tran, D.-H., Wu, Y.-W. (2014). Using a fuzzy clustering chaotic-based differential evolution with serial method to solve resource-constrained project scheduling problems, *Automation in Construction,* Vol. 37, 88-97, doi: 10.1016/j.autcon.2013.10.002.
[36] Tran, D.-H., Cheng, M.-Y., Cao, M.-T. (2016). Solving resource-constrained project scheduling problems using hybrid artificial bee colony with differential evolution, *Journal of Computing in Civil Engineering,* Vol. 30, No. 4, doi: 10.1061/(ASCE)CP.1943-5487.0000544.

[37] Sonmez, R., Gürel, M. (2016). Hybrid optimization method for large-scale multimode resource-constrained project scheduling problem, *Journal of Management in Engineering,* Vol. 32, No. 6, doi: 10.1061/(ASCE)ME.1943-5479.0000468.
[38] Tao, S., Dong, Z. S. (2018). Multi-mode resource-constrained project scheduling problem with alternative project structures, *Computers & Industrial Engineering,* Vol. 125, 333-347, doi: 10.1016/j.cie.2018.08.027.
[39] Birjandi, A., Mousavi, S.M. (2019). Fuzzy resource-constrained project scheduling with multiple routes: A heuristic solution, *Automation in Construction,* Vol. 100, 84-102, doi: 10.1016/j.autcon.2018.11.029.
[40] Chakrabortty, R.K., Rahman, H.F., Ryan, M.J. (2020). Efficient priority rules for project scheduling under dynamic environments: A heuristic approach, *Computers & Industrial Engineering,* Vol. 140, 106287, doi: 10.1016/j.cie.2020.106287.
[41] Asadujjaman, M., Rahman, H.F., Chakrabortty, R.K., Ryan, M.J. (2021). An immune genetic algorithm for solving NPV-based resource-constrained project scheduling problem, *IEEE Access,* Vol. 9, 26177-26195, doi: 10.1109/ACCESS.2021.3057366.
[42] Vanhoucke, M. (2010). A scatter search heuristic for maximising the net present value of a resource-constrained project with fixed activity cash flows, *International Journal of Production Research,* Vol. 48, No. 7, 1983-2001, doi: 10.1080/00207540802010781.
[43] Asadujjaman, M., Rahman, H.F., Chakrabortty, R.K., Ryan, M.J. (2021). Resource constrained project scheduling and material ordering problem with discounted cash flows, *Computers & Industrial Engineering,* Vol. 158, Article No. 107427, doi: 10.1016/j.cie.2021.107427.
[44] Asadujjaman, M., Rahman, H.F., Chakrabortty, R.K., Ryan, M.J. (2022). Multi-operator immune genetic algorithm for project scheduling with discounted cash flows, *Expert Systems with Applications,* Vol. 195, Article No. 116589, doi: 10.1016/j.eswa.2022.116589.
[45] Rahman, H.F., Servranckx, T., Chakrabortty, R.K., Vanhoucke, M., El Sawah, S. (2022). Manufacturing project scheduling considering human factors to minimize total cost and carbon footprints, *Applied Soft Computing,* Vol. 131, Article No. 109764, doi: 10.1016/j.asoc.2022.109764.
[46] Patterson, J.H., Talbot, F.B., Slowinski, R., Węglarz, J. (1990). Computational experience with a backtracking algorithm for solving a general class of precedence and resource-constrained scheduling problems, *European Journal of Operational Research,* Vol. 49, No. 1, 68-79, doi: 10.1016/0377-2217(90)90121-Q.
[47] Sprecher, A., Kolisch, R., Drexl, A. (1995). Semi-active, active, and non-delay schedules for the resource-constrained project scheduling problem, *European Journal of Operational Research,* Vol. 80, No. 1, 94-102, doi: 10.1016/0377-2217(93)E0294-8.
[48] Kolisch, R., Drexl, A. (1997). Local search for nonpreemptive multi-mode resource-constrained project scheduling, *IIE Transactions,* Vol. 29, No. 11, 987-999, doi: 10.1080/07408179708966417.
[49] Drexl, A., Gruenewald, J. (1993). Nonpreemptive multi-mode resource-constrained project scheduling, *IIE Transactions,* Vol. 25, No. 5, 74-81, doi: 10.1080/07408179308964317.
[50] Demeulemeester, E., Herroelen, W. (1992). A branch-and-bound procedure for the multiple resource-constrained project scheduling problem, *Management Science,* Vol. 38, No. 12, 1803-1818. doi: 10.1287/mnsc.38.12.1803.
[51] Stinson, J.P., Davis, E.W., Khumawala, B.M. (1978). Multiple resource–constrained scheduling using branch and bound, *AIIE Transactions,* Vol. 10, No. 3, 252-259, doi: 10.1080/05695557808975212.
[52] Kolisch, R. (1996). Serial and parallel resource-constrained project scheduling methods revisited: Theory and computation, *European Journal of Operational Research,* Vol. 90, No. 2, 320-333, doi: 10.1016/0377-2217(95)00357-6.
[53] Merkle, D., Middendorf, M., Schmeck, H. (2002). Ant colony optimization for resource-constrained project scheduling, *IEEE Transactions on Evolutionary Computation,* Vol. 6, No. 4, 333-346, doi: 10.1109/TEVC.2002.802450.
[54] Palpant, M., Artigues, C., Michelon, P. (2004). LSSPER: Solving the resource-constrained project scheduling problem with large neighbourhood search, *Annals of Operations Research,* Vol. 131, 237-257, doi: 10.1023/B:ANOR.0000039521.26237.62.
[55] Valls, V., Ballestín, F., Quintanilla, S. (2008). A hybrid genetic algorithm for the resource-constrained project scheduling problem, *European Journal of Operational Research,* Vol. 185, No. 2, 495-508, doi: 10.1016/j.ejor.2006.12.033.
[56] Kellenbrink, C., Helber, S. (2015). Scheduling resource-constrained projects with a flexible project structure, *European Journal of Operational Research,* Vol. 246, No. 2, 379-391, doi: 10.1016/j.ejor.2015.05.003.
[57] Tao, S., Dong, Z.S. (2017). Scheduling resource-constrained project problem with alternative activity chains, *Computers & Industrial Engineering,* Vol. 114, 288-296, doi: 10.1016/j.cie.2017.10.027.
[58] Schirmer, A. (2000). Case-based reasoning and improved adaptive search for project scheduling, *Naval Research Logistics,* Vol. 47, No. 3, 201-222, doi: 10.1002/(SICI)1520-6750(200004)47:3<201::AID-NAV2>3.0.CO;2-L.
[59] Deblaere, F., Demeulemeester, E., Herroelen, W. (2011). Proactive policies for the stochastic resource-constrained project scheduling problem, *European Journal of Operational Research,* Vol. 214, No. 2, 308-316, 10.1016/j.ejor.2011.04.019.
[60] Van de Vonder, S., Demeulemeester, E., Herroelen, W. (2008). Proactive heuristic procedures for robust project scheduling: An experimental analysis, *European Journal of Operational Research,* Vol. 189, No. 3, 723-733, 10.1016/j.ejor.2006.10.061.

[61] Deblaere, F., Demeulemeester, E., Herroelen, W. (2011). Reactive scheduling in the multi-mode RCPSP, *Computers & Operations Research*, Vol. 38, No. 1, 63-74, doi: 10.1016/j.cor.2010.01.001.
[62] Hu, W., Wang, H., Peng, C., Wang, H., Liang, H., Du, B. (2015). An outer–inner fuzzy cellular automata algorithm for dynamic uncertainty multi-project scheduling problem, *Soft Computing*, Vol. 19, 2111-2132, doi: 10.1007/s00500-014-1395-5.
[63] Zheng, H., Wang, L., Zheng, X. (2017). Teaching–learning-based optimization algorithm for multi-skill resource constrained project scheduling problem, *Soft Computing*, Vol. 21, 1537-1548, doi: 10.1007/s00500-015-1866-3.
[64] Myszkowski, P.B., Olech, Ł.P., Laszczyk, M., Skowroński, M.E. (2018). Hybrid Differential Evolution and Greedy Algorithm (DEGR) for solving Multi-Skill Resource-Constrained Project Scheduling Problem, *Applied Soft Computing*, Vol. 62, 1-14, doi: 10.1016/j.asoc.2017.10.014.
[65] Myszkowski, P.B., Laszczyk, M., Nikulin, I., Skowroński, M. (2019). iMOPSE: A library for bicriteria optimization in Multi-Skill Resource-Constrained Project Scheduling Problem, *Soft Computing*, Vol. 23, 3397-3410, doi: 10.1007/s00500-017-2997-5.
[66] Laszczyk, M., Myszkowski, P.B. (2019). Improved selection in evolutionary multi–objective optimization of multi–skill resource–constrained project scheduling problem, *Information Sciences*, Vol. 481, 412-431, doi: 10.1016/j.ins.2019.01.002.
[67] Nemati-Lafmejani, R., Davari-Ardakani, H., Najafzad, H. (2019). Multi-mode resource constrained project scheduling and contractor selection: Mathematical formulation and metaheuristic algorithms, *Applied Soft Computing*, Vol. 81, Article No. 105533, doi: 10.1016/j.asoc.2019.105533.
[68] Shirzadeh Chaleshtarti, A., Shadrokh, S., Khakifirooz, M., Fathi, M., Pardalos, P.M. (2020). A hybrid genetic and Lagrangian relaxation algorithm for resource-constrained project scheduling under nonrenewable resources, *Applied Soft Computing*, Vol. 94, Article No. 106482, doi: 10.1016/j.asoc.2020.106482.
[69] Yuan, Y., Ye, S., Lin, L., Gen, M. (2021). Multi-objective multi-mode resource-constrained project scheduling with fuzzy activity durations in prefabricated building construction, *Computers & Industrial Engineering*, Vol. 158, Article No. 107316, doi: 10.1016/j.cie.2021.107316.
[70] Chu, X., Li, S., Gao, F., Cui, C., Pfeiffer, F., Cui, J. (2023). A data-driven meta-learning recommendation model for multi-mode resource constrained project scheduling problem, *Computers & Operations Research*, Vol. 157, Article No. 106290, doi: 10.1016/j.cor.2023.106290.
[71] Yuraszeck, F., Montero, E., Canut-De-Bon, D., Cuneo, N., Rojel, M. (2023). A constraint programming formulation of the multi-mode resource-constrained project scheduling problem for the flexible job shop scheduling problem, *IEEE Access*, Vol. 11, 144928-144938, doi: 10.1109/ACCESS.2023.3345793.
[72] Dauzère-Pérès, S., Ding, J., Shen, L., Tamssaouet, K. (2024). The flexible job shop scheduling problem: A review, *European Journal of Operational Research*, Vol. 314, No. 2, 409-432, doi: 10.1016/j.ejor.2023.05.017.
[73] Mahdi Mobini, M.D., Rabbani, M., Amalnik, M.S., Razmi, J., Rahimi-Vahed, A.R. (2009). Using an enhanced scatter search algorithm for a resource-constrained project scheduling problem, *Soft Computing*, Vol. 13, 597-610, doi: 10.1007/s00500-008-0337-5.
[74] Zamani, R. (2010). An Accelerating Two-layer anchor search with application to the resource-constrained project scheduling problem, *IEEE Transactions on Evolutionary Computation*, Vol. 14, No. 6, 975-984, doi: 10.1109/TEVC.2010.2047861.
[75] Zamani, R. (2012). A polarized adaptive schedule generation scheme for the resource-constrained project scheduling problem, *RAIRO - Operations Research*, Vol. 46, 23-39, doi: 10.1051/ro/2012006.
[76] Elsayed, S., Sarker, R., Ray, T., Coello, C.C. (2017). Consolidated optimization algorithm for resource-constrained project scheduling problems, *Information Sciences*, Vol. 418-419, 346-362, doi: 10.1016/j.ins.2017.08.023.
[77] Boctor, F.F. (1993). Heuristics for scheduling projects with resource restrictions and several resource-duration modes, *International Journal of Production Research*, Vol. 31, No. 11, 2547-2558, doi: 10.1080/00207549308956882.
[78] Hartmann, S. (2001). Project scheduling with multiple modes: A genetic algorithm, *Annals of Operations Research*, Vol. 102, 111-135, doi: 10.1023/A:1010902015091.
[79] Józefowska, J., Mika, M., Różycki, R., Waligóra, G., Węglarz, J. (2001). Simulated annealing for multi-mode resource-constrained project scheduling, *Annals of Operations Research*, Vol. 102, 137-155, doi: 10.1023/A:1010954031930.
[80] Alcaraz, J., Maroto, C., Ruiz, R. (2003). Solving the Multi-Mode Resource-Constrained Project Scheduling Problem with genetic algorithms, *Journal of the Operational Research Society*, Vol. 54, No. 6, 614-626, doi: 10.1057/palgrave.jors.2601563.
[81] Ozdamar, L. (1999). A genetic algorithm approach to a general category project scheduling problem, *IEEE Transactions on Systems, Man, and Cybernetics, Part C (Applications and Reviews)*, Vol. 29, No. 1, 44-59, doi: 10.1109/5326.740669.
[82] Buddhakulsomsiri, J., Kim, D.S. (2006). Properties of multi-mode resource-constrained project scheduling problems with resource vacations and activity splitting, *European Journal of Operational Research*, Vol. 175, No. 1, 279-295, doi: 10.1016/j.ejor.2005.04.030.
[83] Zhang, H., Tam, C.M., Li, H. (2006). Multimode project scheduling based on particle swarm optimization, *Computer-Aided Civil and Infrastructure Engineering*, Vol. 21, No. 2, 93-103, doi: 10.1111/j.1467-8667.2005.00420.x.

[84] Jarboui, B., Damak, N., Siarry, P., Rebai, A. (2008). A combinatorial particle swarm optimization for solving multi-mode resource-constrained project scheduling problems, *Applied Mathematics and Computation*, Vol. 195, No. 1, 299-308, doi: 10.1016/j.amc.2007.04.096.
[85] Lova, A., Tormos, P., Cervantes, M., Barber, F. (2009). An efficient hybrid genetic algorithm for scheduling projects with resource constraints and multiple execution modes, *International Journal of Production Economics*, Vol. 117, No. 2, 302-316, doi: 10.1016/j.ijpe.2008.11.002.
[86] Bouleimen K., Lecocq, H. (2003). A new efficient simulated annealing algorithm for the resource-constrained project scheduling problem and its multiple mode version, *European Journal of Operational Research*, Vol. 149, No. 2, 268-281, doi: 10.1016/S0377-2217(02)00761-0.
[87] Ranjbar, M., De Reyck, B., Kianfar, F. (2009). A hybrid scatter search for the discrete time/resource trade-off problem in project scheduling, *European Journal of Operational Research*, Vol. 193, No. 1, 35-48, doi: 10.1016/j.ejor.2007.10.042.
[88] Wang, L., Fang, C. (2012). An effective estimation of distribution algorithm for the multi-mode resource-constrained project scheduling problem, *Computers & Operations Research*, Vol. 39, No. 2, 449-460, doi: 10.1016/j.cor.2011.05.008.
[89] Van Peteghem, V., Vanhoucke, M. (2009). An artificial immune system for the multi-mode resource-constrained project scheduling problem, In: *Proceedings of the International Conference on Computational Intelligence for Modeling, Control and Automation*, 85-96, doi: 10.1007/978-3-642-01009-5_8.
[90] Van Peteghem, V., Vanhoucke, M. (2014). An experimental investigation of metaheuristics for the multi-mode resource-constrained project scheduling problem on new dataset instances, *European Journal of Operational Research*, Vol. 235, No. 1, 62-72, doi: 10.1016/j.ejor.2013.10.012.
[91] Geiger, M.J. (2017). A multi-threaded local search algorithm and computer implementation for the multi-mode, resource-constrained multi-project scheduling problem, *European Journal of Operational Research*, Vol. 256, 729-741, No. 3, doi: 10.1016/j.ejor.2016.07.024.
[92] Damak, N., Jarboui, B., Siarry, P., Loukil, T. (2009). Differential evolution for solving multi-mode resource-constrained project scheduling problems, *Computers & Operations Research*, Vol. 36, No. 9, 2653-2659, doi: 10.1016/j.cor.2008.11.010.
[93] Fernandes Muritiba, A.E., Rodrigues, C.D., Araùjo da Costa, F. (2018). A path-relinking algorithm for the multi-mode resource-constrained project scheduling problem, *Computers & Operations Research*, Vol. 92, 145-154, doi: 10.1016/j.cor.2018.01.001.
[94] Chakrabortty, R.K., Abbasi, A., Ryan, M.J. (2020). Multi-mode resource-constrained project scheduling using modified variable neighborhood search heuristic, *International Transactions in Operational Research*, Vol. 27, No. 1, 138-167, doi: 10.1111/itor.12644.
[95] Chen, J.C., Lee, H.-Y., Hsieh, W.-H., Chen, T.-L. (2022). Applying hybrid genetic algorithm to multi-mode resource constrained multi-project scheduling problems, *Journal of the Chinese Institute of Engineers*, Vol. 45, No. 1, 42-53, doi: 10.1080/02533839.2021.1983461.
[96] Peng, J.L., Liu, X., Peng, C., Shao, Y. (2023). Multi-skill resource-constrained multi-modal project scheduling problem based on hybrid quantum algorithm, *Scientific Reports*, Vol. 13, Article No. 18502, doi: 10.1038/s41598-023-45970-y.
[97] Golenko-Ginzburg, D., Gonik, A. (1997). Stochastic network project scheduling with non-consumable limited resources, *International Journal of Production Economics*, Vol. 48, No. 1, 29-37, doi: 10.1016/S0925-5273(96)00019-9.
[98] Tsai, Y.-W., Gemmill, D.D. (1998). Using tabu search to schedule activities of stochastic resource-constrained projects, *European Journal of Operational Research*, Vol. 111, No. 1, 129-141, doi: 10.1016/S0377-2217(97)00311-1.
[99] Leus, R., Herroelen, W. (2004). Stability and resource allocation in project planning, *IIE Transactions*, Vol. 36, No. 7, 667-682, doi: 10.1080/07408170490447348.
[100] Van De Vonder, S., Demeulemeester, E., Herroelen, W., Leus, R. (2006). The trade-off between stability and makespan in resource-constrained project scheduling, *International Journal of Production Research*, Vol. 44, No. 2, 215-236, doi: 10.1080/00207540500140914.
[101] Ballestín, F. (2007). When it is worthwhile to work with the stochastic RCPSP?, *Journal of Scheduling*, Vol. 10, 153-166, doi: 10.1007/s10951-007-0012-1.
[102] Chtourou, H., Haouari, M. (2008). A two-stage-priority-rule-based algorithm for robust resource-constrained project scheduling, *Computers & Industrial Engineering*, Vol. 55, No. 1, 183-194, doi: 10.1016/j.cie.2007.11.017.
[103] Kolisch, R., Schwindt, C., Sprecher, A. (1999). Benchmark instances for project scheduling problems, In: *Proceedings of the International Conference on Project Scheduling,* 197-212, doi: 10.1007/978-1-4615-5533-9_9.
[104] Ballestín, F., Leus, R. (2009). Resource-constrained project scheduling for timely project completion with stochastic activity durations, *Production and Operations Management*, Vol. 18, No. 4, 459-474, doi: 10.1111/j.1937-5956.2009.01023.x.
[105] Ashtiani, B., Leus, R., Aryanezhad, M.-B. (2011). New competitive results for the stochastic resource-constrained project scheduling problem: Exploring the benefits of pre-processing, *Journal of Scheduling*, Vol. 14, 157-171, doi: 10.1007/s10951-009-0143-7.
[106] Li, H., Womer, N.K. (2015). Solving stochastic resource-constrained project scheduling problems by closed-loop approximate dynamic programming, *European Journal of Operational Research*, Vol. 246, No. 1, 20-33, doi: 10.1016/j.ejor.2015.04.015.

[107] Rostami, S., Creemers, S., Leus, R. (2018). New strategies for stochastic resource-constrained project scheduling, *Journal of Scheduling*, Vol. 21, 349-365, doi: 10.1007/s10951-016-0505-x.
[108] Chen, Z., Demeulemeester, E., Bai, S., Guo, Y. (2018). Efficient priority rules for the stochastic resource-constrained project scheduling problem, *European Journal of Operational Research*, Vol. 270, No. 3, 957-967, doi: 10.1016/j.ejor.2018.04.025.
[109] Zaman, F., Elsayed, S., Sarker, R., Essam, D., Coello Coello, C.A. (2021). An evolutionary approach for resource-constrained project scheduling with uncertain changes, *Computers & Operations Research*, Vol. 125, Article No. 105104, doi: 10.1016/j.cor.2020.105104.
[110] Fang, C., Kolisch, R., Wang, L., Mu, C. (2015). An estimation of distribution algorithm and new computational results for the stochastic resource-constrained project scheduling problem, *Flexible Services and Manufacturing Journal*, Vol. 27, 585-605, doi: 10.1007/s10696-015-9210-x.
[111] Sallam, K.M., Chakrabortty, R.K., Ryan, M.J. (2021). A reinforcement learning based multi-method approach for stochastic resource constrained project scheduling problems, *Expert Systems with Applications*, Vol. 169, Article No. 114479, doi: 10.1016/j.eswa.2020.114479.
[112] Chen, H., Ding, G., Zhang, J., Li, R., Jiang, L., Qin, S. (2022). A filtering genetic programming framework for stochastic resource-constrained multi-project scheduling problem under new project insertions, *Expert Systems with Applications*, Vol. 198, Article No. 116911, doi: 10.1016/j.eswa.2022.116911.
[113] Chen, H., Zhang, J., Li, R., Ding, G., Qin, S. (2022). A two-stage genetic programming framework for stochastic resource constrained multi-project scheduling problem under new project insertions, *Applied Soft Computing*, Vol. 124, Article No. 109087, doi: 10.1016/j.asoc.2022.109087.
[114] Peng, W., Lin, X., Li, H. (2023). Critical chain based Proactive-Reactive scheduling for resource-constrained project scheduling under uncertainty, *Expert Systems with Applications*, Vol. 214, Article No. 119188, doi: 10.1016/j.eswa.2022.119188.
[115] Peng, F., Zheng, L. (2023). An improved multi-objective Wild Horse optimization for the dual-resource-constrained flexible job shop scheduling problem: A comparative analysis with NSGA-II and a real case study, *Advances in Production Engineering & Management*, Vol. 18, No. 3, 271-287, doi: 10.14743/apem2023.3.472.

APEM journal

Advances in Production Engineering & Management
Volume 19 | Number 4 | December 2024 | pp 512–526
https://doi.org/10.14743/apem2024.4.521

ISSN 1854-6250
Journal home: apem-journal.org
Original scientific paper

Integrated production and maintenance policy for manufacturing systems prone to products' quality degradation

BouAbid, H.[a], **Dhouib, K.**[b], **Gharbi, A.**[c,*]

[a]LMPE Laboratory, Mechanical Engineering & Production Department, École Nationale Supérieure d'Ingénieurs de Tunis (ENSIT), University of Tunis, Tunis, Tunisia
[b]RIFTSI Laboratory, Mechanical Engineering & Production Department, École Nationale Supérieure d'Ingénieurs de Tunis (ENSIT), University of Tunis, Tunis, Tunisia
[c]C2SP Laboratory, Systems Engineering Department, École de Technologies Supérieure (ÉTS), Montréal, Canada

ABSTRACT

This paper proposes an integrated production planning and preventive maintenance strategy for manufacturing systems prone to quality degradation. The production planning focus on the regulation of production rates and the sizing of finished product's safety stock to meet costumer's demand. The safety stock is built to palliate shortages when the manufacturing operation begins generating non-conforming products and is shutdown to perform restoration action. In the other hand, preventive maintenance activities are also planned to minimise the quantity of non-conforming products. Mathematical models are proposed and consider all sub-policies and scenarios contingent on the production control policy as well as the entire range of possible values for the safety stock level. A numerical procedure has been established to ascertain the optimal integrated policy, aiming to minimize the total accrued cost per time unit along an infinite horizon. A simulation model has also been created to check and validate the analytical results. Finally, a comparative analysis is presented to prove that the proposed joint policy outperforms other strategies considered in the literature and practice and can result in substantial economic gains.

ARTICLE INFO

Keywords:
Production planning;
Stock control;
Preventive maintenance;
Quality degradation;
Hedging point policy;
Analytical modelling;
Simulation analysis

**Corresponding author:*
Ali.Gharbi@etsmtl.ca
(Gharbi, A.)

Article history:
Received 12 December 2023
Revised 1 December 2024
Accepted 15 December 2024

1. Introduction

Production, quality, and maintenance management play an essential role to improve efficiency, profitability, competitiveness as well as sustainability of today's industrial companies affected by the technical developments of Industry 4.0 [1, 2]. Manufacturing businesses are becoming more and more concerned with producing high-quality goods in a sustainable way which establishes the basis for Quality 4.0 [3, 4]. As equipment maintenance, at a level which can produce an appropriate quality product is essential for keeping them operating, sustainable quality products cannot be produced unless they are subject to efficient maintenance [5].

The Growing adherence to Industry 4.0 proposes a novel framework that links the different facets of industrial systems supervision: production, inventory, maintenance, and quality. In general, the main objective is to reduce operating costs and to increase business opportunities which

can only be achieved when production, maintenance and quality strategies are jointly addressed. The integration of these aspects leads to important improvement of the system's performance, especially the significant growing of the industrial profit which can be increased up to 40 % [6]. In a recent study, this joint consideration allows a reduction in overall production cost of up to 44 % [7].

However, more efforts must be made to propose mutual production, maintenance, and quality policies according to the multiple industrial environments and to their own specificities [8, 9]. In this situation, production control is closely associated with inventory management and particularly the safety stock. The majority of researchers do not consider all potential value ranges of security stock capacity. and focus only on high levels ignoring possible optimal solutions related to middle security stock level (i.e. low value of repair time) or to zero-stock strategy (i.e. expensive stock cost). This reflection often leads to the identification of suboptimal policies and implies excessive costs.

This paper studies the combined optimization of production, stock, and maintenance strategy for industrial systems prone to quality degradation. We propose a multi-model framework and a broad holistic strategy that considers all potential security stock value ranges. Mathematical models are developed studying all sub-policies and scenarios that my raise based on the production control policy, level of security stock, and the moment when the system moves into the 'out-of-control state'. A simulation model is also designed to validate mathematical models.

In next Section, a literature review covering integrated production and preventive maintenance policies for industrial systems prone to quality degradation is provided. The system synopsis, dynamic behaviour, and notations are stated in Section 3. Section 4 proposes analytical models for the generated sub-policies and associated scenarios according to all potential security stock value ranges. Section 5 presents a numerical procedure to determine the optimal combined policy. A simulation model is designed to validate analytical models. The beneficial effect of the suggested combined policy is then demonstrated through numerical examples and a comparison analysis involving various control policies drawn from the literature and implemented in practice. Conclusions are finally reported in Section 6.

2. Literature revue

During the last decades, several contributions have been proposed integrating production, inventory, maintenance and quality in production planning and control. These contributions can be classified according to several criteria; mainly, the production control policy, the degree of integration, and the industrial context.

Production control focus on the regulation of the production rate to respond to a continuous demand. Several control policies have been considered in the literature [10, 11]. In their pioneer paper, Akella and Kumar [10] introduce the Hedging Point Policy for systems prone to failures and subject to corrective maintenance and prove its optimality. The HPP policy entails to build a security stock to reduce the impact of breakdowns on demand satisfaction.

The basic HPP policy has been extended by several authors to palliate against the negative impact of random failures using reserve resources [12], outsourcing [13] and preventive maintenance [14]. Other researchers have extended these models to consider the quality degradation of produced items. Some authors studied the specific case of perishable products [15]. Several works consider inspection policies to evaluate the quality of produced items [16]. These works have been extended by integrating static and dynamic sampling plans [7, 9] where the manufacturing system is prone to operation-dependent degradations [17].

The majority of preceding research assumes that industrial systems are prone to failures and that the produced quantity of non-conforming items depends on the equipment age; thus, the quality degradation is correlated with the degradation of the equipment reliability. But several researchers consider that the degradation of product quality is not correlated with the aging of the manufacturing equipment. Therefore, the production system can transit to the 'out-of-control' state and starts generating a proportion of non-conforming parts, according to a probability distribution, [18-30].

Pandey *et al*. [18] propose an analytical model to jointly optimize the production scheduling, quality and maintenance in a one-machine industrial system that produces identical batches. Other researchers dealt mainly with the joint consideration of the economic production quantity, product quality degradation, and preventive maintenance policies [19-25].

A combined production-maintenance policy is suggested by Chelbi *et al*. for single-machine systems that generates items that comply as well as those that don't [26]. The presented model aims to determine the optimum lot size and preventive maintenance plan. Colledani and Tolio developed an analytical approach for mutually optimizing control charts and production parameters for unreliable multi-stage transfer lines. The control policy is based on a kanban system [27]. Dhouib *et al*. considered a joint production/maintenance strategy for systems subject to quality degradation [28]. Bahria *et al*. investigate the problem of the assimilation of production planning and the design of control charts [29]. This work has been extended to involve a preventive maintenance policy [30].

These studies, dealing with the one-product single-machine production systems, focus only on high levels of the safety stock, ignoring low levels which can result in non-optimal policies involving excessive incurred costs. In the other hand, these works do not proceed to the validation of analytical results and limit this important step in the modelling methodology to a sensitivity analysis based on the variation of some parameters.

This study addresses the problem of building stochastic analytical models for the combined optimization of production rate control and PM schedule for manufacturing systems prone to quality degradation. The proposed approach allows addressing all possible security stock value ranges.

The primary contributions include: i) Combined control of production, inventory, and maintenance for systems prone to quality degradation; ii) Multi-model approach according to potential security stock value ranges; iii) Resolution of complex stochastic mathematical models via numerical procedure; iv) Dynamic-stochastic simulation model to validate the analytical results; v) Proposed approach outperforms strategies examined in the literature and put into practice.

3. Manufacturing cell description, dynamic behaviour, and notations

3.1 System description and dynamics

The system subject to this study is an automatic one-machine cell devoted to make and inspect one product type to respond to a constant and ongoing demand (d) (Fig. 1). The equipment, representing an aggregation of several machines, is prone to random quality degradation during the production phase.

Initially, it starts in an 'in-control' situation, generating good products. The duration of this 'in-control' situation is a stochastic variable (τ) characterized by a general probability distribution having a density (cumulative) function f (τ) ($F(\tau)$) with a mean time within 'in-control' state ($MTIC$). After that, the cell may move to an 'out-of-control' situation, manufacturing non-conforming products with a proportion (α).

Preventive maintenance interventions are scheduled during the in-control period to decrease the shift frequency to the 'out-of-control' situation. They obey to an age maintenance policy (AMP), planned at age (T), and allow to recover the system to an 'as-good as-new' condition. After a situation becomes out of control, a *L*ogistic *D*elay *P*eriod (LDP) is required ensuing the switch to an out-of-control condition to organize total essential resources (both human and material) for the restoration procedure. To guarantee that the demand is met during the LDP, the machine keeps manufacturing. Then, the production process is aborted to undergo restoration which brings the system to the 'as-good as-new' condition, and then starts again generating good products. The delay of the restoration is a r.v. (t_r) defined by a general probability distribution having a density (cumulative) function $h(t_r)$ ($H(t_r)$) with a mean time to restore ($MTTR$).

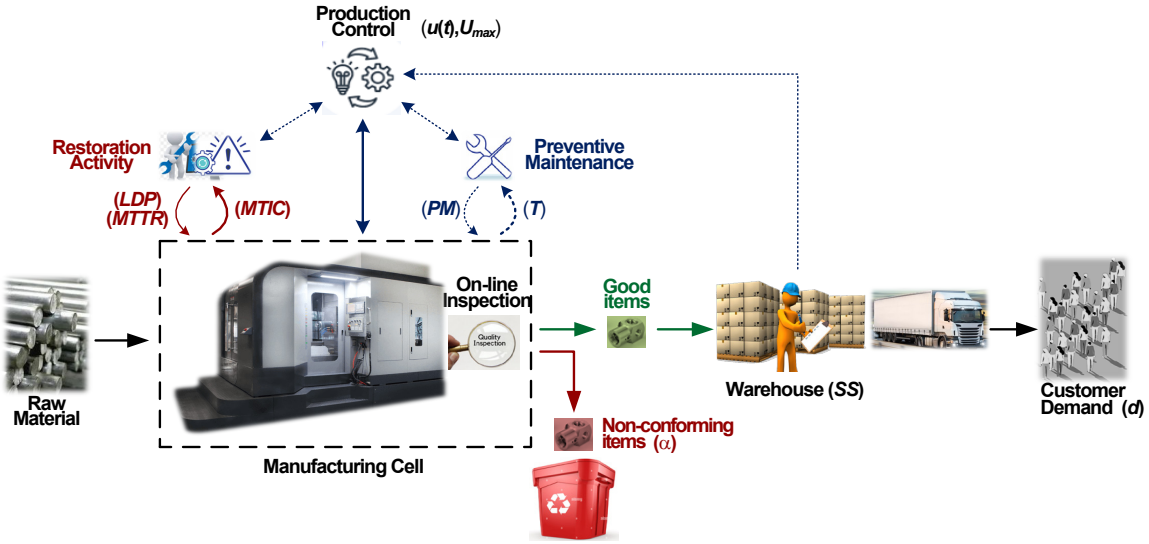

Fig. 1 Manufacturing system dynamics

Throughout the production phase, a reserve of good products is established to address demand and avoid shortages throughout the restoration period. Only after the available inventory runs out can production resume, at which point a setup action is initiated. If a shortage is observed after the restoration, the necessary quantities are not supplied during a period of scarcity; these are seen as penalty costs for missed demand.

The manufacturing process is managed across time through a unified policy governing production, inventory, and maintenance, according to HPP policy. The main aim is to determine the optimal production rates, the level of safety stock, and the preventive maintenance schedule. It aims to minimize the overall incurred cost per time unit over the long range, encompassing costs related to setup, quality, preventive maintenance, restoration, inventory holding, and shortages.

According to the HPP plan, the production cell runs at maximum rate (U_{max}) until the safety stock is built (SS). After then, it lowers its production rate ($u(t)$) to match the demand. A deep analysis of the manufacturing system dynamics has shown different behaviours depending on the value of the safety stock level. In fact, this control strategy, which permits the production of non-conforming goods during LDP while the safety stock is built, leads to three joint control sub-policies, each having a distinct scenario, depending on the many conceivable value ranges of SS:

- Sub-Policy I: HPP and zero-inventory policy (SS = 0) (Fig. 2).

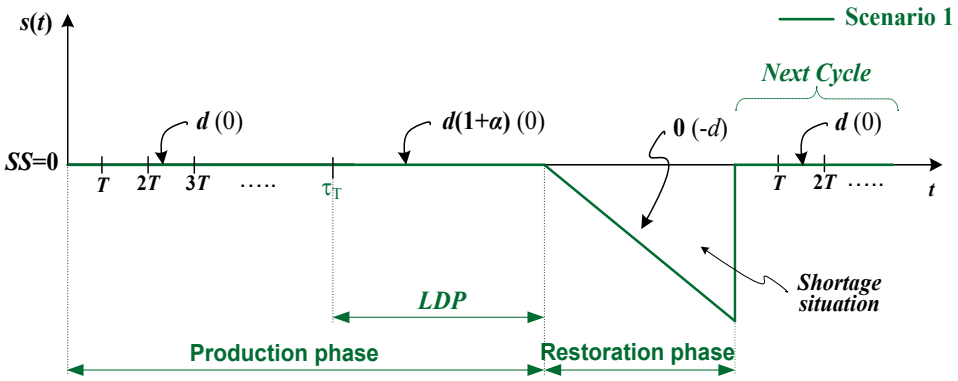

Fig. 2 Inventory level evolution under joint Sub-Policy I

- Sub-Policy II: HPP and stock policy $SS < S_{LDP}$ (middle level of security stock) (Fig. 3). This policy is characterized by the safety stock threshold S_{LDP} (Eq. 1); S_{LDP} is the number of compliant items places in the security stock during LDP.

$$S_{LDP} = LDP(U_{max}(1-\alpha) - d) \quad (1)$$

This crucial threshold signifies that the preparations for restoration conclude upon the completion of constructing the safety stock *SS*. So, and like sub-policy I, non-conforming item manufacture is carried out also during *LDP*.

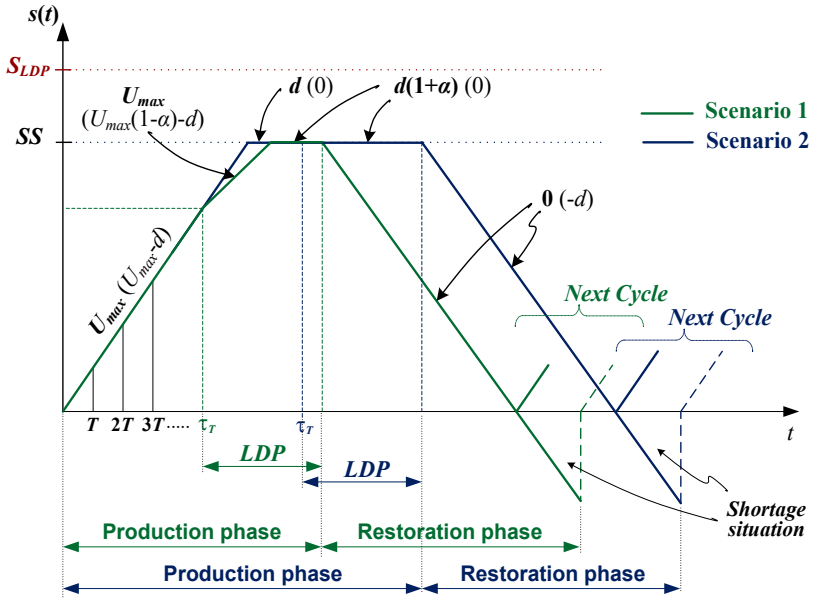

Fig. 3 Inventory level evolution under joint Sub-Policy II

- Sub-Policy III: HPP and stock policy $SS \geq S_{LDP}$ (high-security stock) (Fig. 4). Unlike Sub-Policies I and II, the accomplishment of the preparation action's planning may be achieved prior to the construction of the safety stock *SS* (Scenario 1). In agreement with Sub-policy III, the production of non-compliant goods can extend for a period greater than *LDP*.

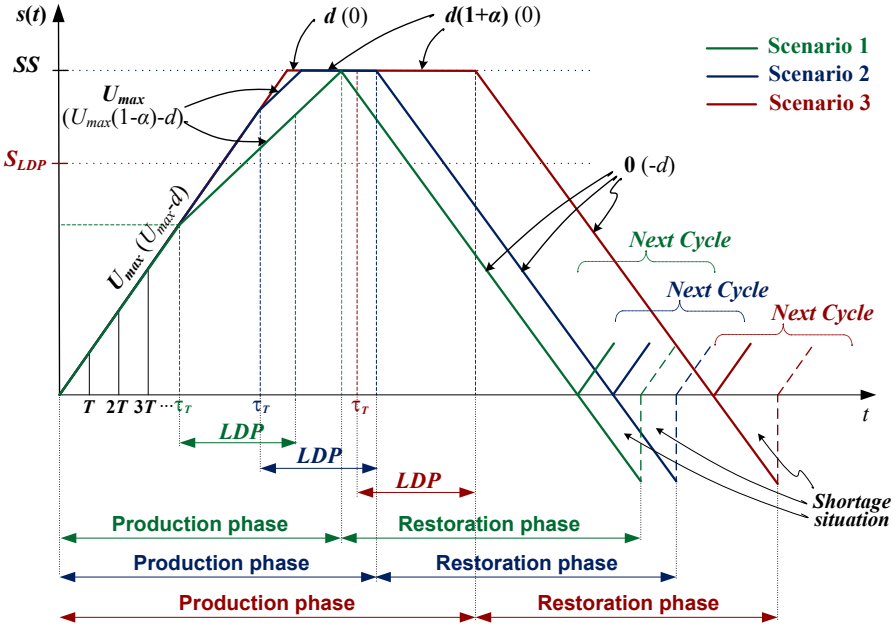

Fig. 4 Inventory level evolution under joint Sun-Policy III

3.2 Notations

In this paper, we consider the following notations, where indices *j* and *i* denote a specific scenario (*j* = 1, 2, 3) in the sub-policy (*i* = I, II, III). Additional notations are defined in the text.

n_i	Number of scenarios associated with the sub-policy *i* (*i* = I, II, III).
$s(t)$	Inventory level at instant *t*.
τ_T	Random instant to transit to the 'out-of-control' situation according to the AMP.
$E_{ij}(\tau_T)$	Mean duration of residence in control situation associated to sub-policy *i*-scenario *j*.
E_{ij} (t_r)	Anticipated restoration delay while scarcity case associated to sub-policy *i*-scenario *j*.
$\Pr_{ij}$	For sub-policy *i*, Probability of falling into scenario *j*.
$\Pr_{Hij}$ ($\Pr_{Sij}$)	Probability of experiencing an excess inventory (scarcity) condition for sub-policy *i*, following the occurrence of scenario *j*.
CL_{Hij} (CL_{Sij})	Expected length of the production/restoration cycle in an excess inventory (scarcity) condition for sub-policy *i*, following the occurrence of scenario *j*.
$\overline{IH_{ij}}$	Average stock level held during the production phase for sub-policy *i*, in scenario *j*.
$PPIC_{ij}$	Expected Inventory holding cost incurred during Production Phase associated to sub-policy *i*, following the occurrence of scenario *j*.
NCC_{ij}	Cost of Non-Compliant parts for sub-policy *i*, scenario *j* .
$NbPM_{ij}$	Mean number of Preventive Maintenance interventions for sub-policy *i*, in scenario *j*.
PMC_{ij}	Cost of Preventive Maintenance for sub-policy *i*, in scenario *j*.
PPC_{ij}	Anticipated cost accrued through the Production Phase associated to sub-policy *i*-scenario *j*.
$\overline{IH_{Rij}}$	Average inventory kept during restoration phase for sub-policy *i*, in scenario *j*.
$RPIC_{ij}$	Expected Inventory holding cost incurred during Restoration Phase associated to sub-policy *i*, following the occurrence of scenario *j*.
$NbLD_{ij}$	Expected amount of Missing Demand for sub-policy *i*, in scenario *j*.
SC_{ij}	Expected Shortage cost for sub-policy *i*, in scenario *j*.
RPC_{Hij} (RPC_{Sij})	Anticipated cost accrued through the Restoration Phase in an excess (lack) circumstance for sub-policy *i*-scenario *j*.
TC_i	Overall Expected cost associated with the joint sub-policy *i*.

4. Modelling joint control policies

To model the behaviour of the proposed joint control policies, the cycle of the studied system is divided into two phases: the production phase, during which the cell is producing, and the phase of restoration following the shutdown of the manufacturing cell. The machine transits, cyclically, from 'operating' to 'shutdown' and from 'shutdown' to 'operating' state. Figs. 2, 3, and 4 show that each cycle starts and ends with an empty stock. Based on these observations, we are certain that the system dynamics is a renewal process since cycles are independent of one another. Therefore, 'the elementary renewal theorem' [31] can be employed to calculate the mean value of any KPI per time unit beyond an infinite time span (TC, WIP, preventive actions number, Amount of non-conforming items, etc.).

The global cost for sub-policy *i* (*i* = I, II, III) is assessed by Eq. 2. It consists of the expenses paid both during manufacturing and restoration stages whether there is excess or lack of inventory, weighted by corresponding probability of scenario.

$$TC_i = \frac{\sum_{j=1}^{n_i}\left(\left(PPC_{ij} + RPC_{Hij}\right)\Pr_{Hij} + \left(PPC_{ij} + RPC_{Sij}\right)\Pr_{Sij}\right)\Pr_{ij}}{\sum_{j=1}^{n_i}\left(CL_{Hij}\Pr_{Hij} + CL_{Sij}\Pr_{Sij}\right)\Pr_{ij}} \tag{2}$$

The production phase cost comprises the expenses due to setup (C_{SU}), non-compliant items, inventory holding, and preventive maintenance activities (Eq. 3).

$$PPC_{ij} = C_{SU} + PPIC_{ij} + NCC_{ij} + PMC_{ij} \tag{3}$$

The inventory keeping cost is computed by multiplying the cost of an item held in stock per time unit (C_H) with the average quantity seized in the safety stock (Eq. 4).

$$PPIC_{ij} = C_H \, \overline{IH_{\iota J}} \tag{4}$$

The non-conforming items expense includes the costs of raw material (C_{RM}) and operating of the manufacturing cell per time unit (C_{MCO}).

The preventive maintenance charge is determined by multiplying the expense of a preventive activity (C_{PM}) with the anticipated number of performed preventive interventions (Eq. 5).

$$PMC_{ij} = C_{PM} \, NbPM_{ij} \tag{5}$$

The restoration phase cost comprises, in case of surplus, the inventory holding and the restoration cost (C_R) (Eq. 6). In scarcity situation, it also includes the unit shortage expense (C_S) multiplied by the non-delivered parts (Eqs. 7 and 9).

$$RPC_{Hij} = C_R + RPIC_{ij} \tag{6}$$

$$RPC_{Sij} = C_R + RPIC_{ij} + SC_{ij} \tag{7}$$

where

$$RPIC_{ij} = C_H \, \overline{IH_{R\iota J}} \tag{8}$$

and

$$SC_{ij} = C_S \, NbLD_{ij} \tag{9}$$

The cycle length equals the mean time to transit to 'out-of-control' condition under an AMP policy, the *LDP* while reaching *SS*, and the *MTTR* in a situation of a shortage or the delay to consume all the safety inventory in instance of excess inventory.

4.1 Sub-policy I: HPP and zero-inventory policy

If a zero-stock policy is required based on production parameters ($SS = 0$), the production control sub-policy can be expressed by Eq. 10.

$$u(t) = \begin{cases} d & \text{If the cell is producing in the 'in control' state} \\ d(1+\alpha) & \text{If the cell is producing during } LDP \\ 0 & \text{alternatively} \end{cases} \tag{10}$$

The progression of the stock level is presented in Fig. 2, where shortage situation is inevitable; in fact, only one scenario can occur according to Sub-Policy I ($n_I = 1$). Fig. 2 also indicates the production and the inventory construction/depletion rates during production and restorations phases. The global accrued cost TC_I is assessed by Eq. 2, where:

- $Pr_{I1} = 1$, $Pr_{HI1} = 0$, and $Pr_{SI1} = 1$.
- The cycle length is calculated using Eq. 11.

$$CL_{SI1} = E_{I1}(\tau_T) + LDP + MTTR \tag{11}$$

$E_{I1}(\tau_T)$ is the expected time to move to 'out-of-control' condition beneath a *T*-age AMP policy (Eq. 12), and *MTTR* is calculated by Eq. 13.

$$E_{I1}(\tau_T) = \sum_{k=0}^{\infty} R(T)^k \int_{kT}^{(k+1)T} \tau \, f(\tau - kT) d\tau \tag{12}$$

$$MTTR = \int_0^{\infty} t_r \, h(t_r) dt_r \tag{13}$$

- PPC_{I1} can be assessed with Eq. 3, with $PPIC_{I1}$ is 0 as no stock building is allowed (Fig. 2). NCC_{I1} and PMC_{I1} costs can be assessed by Eqs. 14 and 5, respectively, where $NbPM_{I1}$ is given by Eq. 15.

$$NCC_{I1} = \alpha \, LDP \left(d \, C_{RM} + \frac{1}{1+\alpha} \, C_{MCO} \right) \tag{14}$$

$$NbPM_{I1} = \sum_{k=0}^{\infty} k\, R(T)^k F(T) \tag{15}$$

- $RPC_{S\,I1}$ is given by Eq. 7; $RPIC_{I1}$ is 0 and SC_{I1} is expressed with Eq. 9, where:

$$NbLD_{I1} = d \int_0^{\infty} t_r\, h(t_r) dt_r \tag{16}$$

4.2 Sub-policy II: HPP and the stock policy $SS < S_{LDP}$

When mandatory security stock quantity is fewer than S_{LDP} based on production parameters (middle level), the production control sub-policy will be described by Eq. 17.

$$u(t) = \begin{cases} U_{max} & \text{If } s(t) < SS \\ d & \text{If } s(t) = SS \text{ where the cell is 'in control' state} \\ d(1+\alpha) & \text{If } s(t) = SS \text{ where the cell is 'out of control' state} \\ 0 & \text{alternatively} \end{cases} \tag{17}$$

In the production phase, the system may exist in one of two scenarios ($n_{II} = 2$) contingent on the shift instant (τ_T) to the 'out-of-control' condition (Fig. 3).

Scenario 1: Takes place if the cell go into the 'out-of-control' condition before attaining *SS*. Constraint $\tau_T < SS/(U_{max} - d)$ imposes the occurrence of scenario 1.

Scenario 2: Conditioned by the constraint $\tau_T \geq SS/(U_{max} - d)$, it takes place if the security inventory is at present filled.

The probability to be into Scenario 1 (Scenario 2) can be expressed by Eq. 18 (Eq. 19).

$$\Pr_{II1} = \sum_{k=0}^{NM_S - 1} R(T)^k\, F(T) + R(T)^{NM_S}\, F\left(\frac{SS}{U_{max} - d} \bmod T\right) \tag{18}$$

$$\Pr_{II2} = 1 - \Pr_{II1} \tag{19}$$

NM_S denotes the highest preventive maintenance interventions performed prior to the attainment of the inventory level *SS* ($NM_S = \frac{SS}{U_{max} - d} \operatorname{div} T$).

According to sub-policy II, the occurrence probability of an inventory excess (scarcity) circumstance does not depend on manifestation of Scenario 1 (Scenario 2). Thus, these probabilities are provided by Eqs. 20 and 21, for i = II and j = 1, 2.

$$\Pr_{Hij} = H(SS/d) \tag{20}$$

$$\Pr_{Sij} = 1 - H(SS/d) \tag{21}$$

The total expense CT_{II} is given by Eq. 2, with cycle lengths and production/restoration phase costs are assessed in the following paragraphs.

The average renewal cycle length in a surplus (shortage) situation is given by Eq. 22 (Eq. 23), for i = II and j = 1, 2.

$$CL_{Hij} = E_{ij}(\tau_T) + LDP + SS/d \tag{22}$$

$$CL_{Sij} = E_{ij}(\tau_T) + LDP + E_{ij}(t_r) \tag{23}$$

$E_{ij}(\tau_T)$ and $E_{ij}(t_r)$ are given by Eqs. 24, 25, and 26, respectively (i = II, j = 1, 2).

$$E_{II1}(\tau_T) = \left(\sum_{k=0}^{NM_S - 1} R(T)^k \int_{k\,T}^{(k+1)T} \tau\, f(\tau - k\,T) d\tau + R(T)^{NM_S} \int_{NM_S\,T}^{\frac{SS}{U_{max} - d}} \tau\, f(\tau - NM_S\,T) d\tau \right) \Big/ \Pr_{II1} \tag{24}$$

$$E_{II2}(\tau_T) = \left(\sum_{k=NM_S}^{\infty} R(T)^k \int_{k\,T}^{(k+1)T} \tau\, f(\tau - kT) d\tau - R(T)^{NM_S} \int_{NM_S\,T}^{\frac{SS}{U_{max} - d}} \tau\, f(\tau - NM_S\,T) d\tau \right) \Big/ \Pr_{II2} \tag{25}$$

$$E_{ij}(t_r) = \int_{SS/d}^{\infty} t_r\, h(t_r) dt_r \Big/ \Pr_{Sij} \tag{26}$$

Eq. 3 assesses the encountered charge throughout the production stage where the inventory expense is evaluated by Eq. 4 and the average amount seized into security stock for Scenario 1 (Scenario 2) is calculated by Eq. 27 (Eq. 28).

$$\begin{aligned}\overline{IH_{\mathrm{II1}}} = (U_{max}-d)\left(LDP\ E_{\mathrm{II1}}(\tau_T) + \int_0^{\frac{SS}{U_{max}-d}} \tau^2\, f(\tau)d\tau/2\ \mathrm{Pr}_{\mathrm{II1}}\right)\\ +\left(SS^2 - 2SS\ E_{\mathrm{II1}}(\tau_T)(U_{max}-d) + (U_{max}-d)^2 \int_0^{\frac{SS}{U_{max}-d}} \tau^2\, f(\tau)d\tau \Big/ \mathrm{Pr}_{\mathrm{II1}}\right)\Big/ 2(U_{max}(1-\alpha)-d)\\ +\big(SS - E_{\mathrm{II1}}(\tau_T)\ (U_{max}-d)\big)\big(LDP - \big(SS - E_{\mathrm{II1}}(\tau_T)\ (U_{max}-d)\big)/(U_{max}(1-\alpha)-d)\big)\end{aligned} \tag{27}$$

$$\overline{IH_{\mathrm{II2}}} = SS\ (E_{\mathrm{II2}}(\tau_T) + LDP) - SS^2/2(U_{max}-d) \tag{28}$$

The NCC_{ij} are given by Eqs. 29 and 30 and the PMC_{ij} by Eq. 5, where $NbPM_{ij}$ are given by Eqs. 31 and 32, for i = II and j = 1, 2.

$$\begin{aligned}NCC_{\mathrm{II1}} = (C_{RM}U_{max} + C_{MCO})\alpha\big(SS - E_{\mathrm{II1}}(\tau_T)(U_{max}-d)\big)/(U_{max}(1-\alpha)-d) +\\ (C_{RM}d + C_{MCO}/(1+\alpha))\alpha\big(LDP - \big(SS - E_{\mathrm{II1}}(\tau_T)(U_{max}-d)\big)/(U_{max}(1-\alpha)-d)\big)\end{aligned} \tag{29}$$

$$NCC_{\mathrm{II2}} = \alpha\ (C_{RM}d + C_{MCO}/(1+\alpha))\ LDP \tag{30}$$

$$NbPM_{\mathrm{II1}} = \left(\sum_{k=0}^{NM_S-1} k\ R(T)^k\ F(T) + NM_S\ R(T)^{NM_S}\ F\left(\frac{SS}{U_{max}-d} \bmod T\right)\right)\Big/ \mathrm{Pr}_{\mathrm{II1}} \tag{31}$$

$$NbPM_{\mathrm{II2}} = \left(NM_S\ R(T)^{NM_S}\ \left(F(T) - F\left(\frac{SS}{U_{max}-d} \bmod T\right)\right) + \sum_{k=NM_S+1}^{\infty} k\ R(T)^k\ F(T)\right)\Big/ \mathrm{Pr}_{\mathrm{II2}} \tag{32}$$

The incurred expense throughout the restoration stage can be expressed by Eq. 6 (Eq. 7) in a surplus (shortage) situation, and Eq. 8, with the mean amount detained in inventory and the sum of lost demands can be appraised by Eqs. 33 and 34, respectively, for i = II and j = 1, 2.

$$\overline{IH_{RiJ}} = SS^2/2d \tag{33}$$

$$NbLD_{ij} = d\ \big(E_{ij}(t_r) - SS/d\big) \tag{34}$$

4.3 Sub-policy III: HPP and the stock policy $SS \geq S_{LDP}$

When mandatory security stock quantity is superior to S_{LDP} based on production parameters (high level), the production rate will also be governed by Eq. 17.

Throughout the stage of production, the system may occur in either of three following scenarios ($n_{\mathrm{III}} = 3$) dependent on the change instant to the 'out-of-control' condition (Fig. 4).

Scenario 1: Takes place if the producing cell enters 'out-of-control' condition before attaining S_{LDP}. This is the only scenario in which non-conforming items are manufactured for a period exceeding the *LDP*. The proposed sub-policy explicitly recommends continuing manufacturing until reaching the *SS* to mitigate the possibility of deficiencies. Constraint $\tau_T < \frac{SS-S_{LDP}}{U_{max}-d}$ imposes the occurrence of Scenario 1.

Scenario 2: Trained by the constraint $\frac{SS-S_{LDP}}{U_{max}-d} \leq \tau_T < \frac{SS}{U_{max}-d}$, it happens when the cell enters out-of-control state as its inventory is split between S_{LDP} and *SS*.

Scenario 3: Conditioned by the constraint $\tau_T \geq SS/(U_{max}-d)$, it occurs once the security stock *SS* level is by now reached.

The probability of being in Scenarios 1, 2, and 3 are given by Eqs. 35, 36, and 37.

$$\mathrm{Pr}_{\mathrm{III1}} = \sum_{k=0}^{NM_L-1} R(T)^k\ F(T) + R(T)^{NM_L}\ F\left(\frac{S_{LDP}}{U_{max}-d} \bmod T\right) \tag{35}$$

$$\mathrm{Pr}_{\mathrm{III2}} = \sum_{k=NM_L}^{NM_S-1} R(T)^k\ F(T) - R(T)^{NM_L}\ F\left(\frac{S_{LDP}}{U_{max}-d} \bmod T\right) + R(T)^{NM_S}\ F\left(\frac{SS}{U_{max}-d} \bmod T\right) \tag{36}$$

$$\mathrm{Pr}_{\mathrm{III3}} = 1 - (\mathrm{Pr}_{\mathrm{III1}} + \mathrm{Pr}_{\mathrm{III2}}) \tag{37}$$

NM_L expresses the highest preventive maintenance interventions executed prior to the completion of the inventory level S_{LDP} ($NM_L = \frac{S_{LDP}}{U_{max}-d}\,\mathrm{div}\,T$).

The probability of being in excess (lack) circumstances is given by Eq. 20 (Eq. 21).

The total charge CT_{III} is given by Eq. 2, with cycle lengths and production/restoration phase costs are assessed as follows.

The average renewal cycle length for Scenario 1 in a holding (shortage) case is given by Eq. 38 (Eq. 39), and by Eq. 22 (Eq. 23) for Scenarios 2 and 3, where i = III and j = 2, 3.

$$CL_{H\mathrm{III1}} = (SS - \alpha\, E_{\mathrm{III1}}(\tau_T)\, U_{max})/(U_{max}(1-\alpha) - d) + SS/d \tag{38}$$

$$CL_{S\mathrm{III1}} = (SS - \alpha\, E_{\mathrm{III1}}(\tau_T)\, U_{max})/(U_{max}(1-\alpha) - d) + E_{\mathrm{III1}}(t_r) \tag{39}$$

$E_{ij}(\tau_T)$ is given by Eqs. 40, 41, and 42, and $E_{ij}(t_r)$ is given by Eq. 26, for i = III and j = 1, 2, 3.

$$E_{\mathrm{III1}}(\tau_T) = \left(\sum_{k=0}^{NM_L-1} R(T)^k \int_{kT}^{(k+1)T} \tau\, f(\tau - kT)d\tau + R(T)^{NM_L} \int_{NM_L\,T}^{\frac{S_{LDP}}{U_{max}-d}} \tau\, f(\tau - NM_L\,T)d\tau\right) \Big/ \mathrm{Pr}_{\mathrm{III1}} \tag{40}$$

$$E_{\mathrm{III2}}(\tau_T) = \left(\begin{array}{c} R(T)^{NM_S} \int_{NM_S\,T}^{\frac{SS}{U_{max}-d}} \tau\, f(\tau - NM_S\,T)d\tau + \sum_{k=NM_L}^{NM_L-1} R(T)^k \int_{kT}^{(k+1)T} \tau\, f(\tau - kT)d\tau \\ -R(T)^{NM_L} \int_{NM_L\,T}^{\frac{S_{LDP}}{U_{max}-d}} \tau\, f(\tau - NM_L\,T)d\tau \end{array}\right) \Big/ \mathrm{Pr}_{\mathrm{III2}} \tag{41}$$

$$E_{\mathrm{III3}}(\tau_T) = \left(\sum_{k=NM_S}^{\infty} R(T)^k \int_{k\,T}^{(k+1)T} \tau\, f(\tau - kT)d\tau - R(T)^{NM_S} \int_{NM_S\,T}^{\frac{SS}{U_{max}-d}} \tau\, f(\tau - NM_S\,T)d\tau\right) \Big/ \mathrm{Pr}_{\mathrm{III3}} \tag{42}$$

The recorded cost during the fabrication stage is evaluated by Eq. 3. The cost of inventory held can be assessed by Eq. 4 with the expected amount seized at occurrence of Scenarios 1, 2, and 3 can be evaluated by Eqs. 43, 44, and 45, respectively.

$$\begin{array}{c} \overline{IH_{\mathrm{III1}}} = (U_{max} - d) \int_0^{S_{LDP}/U_{max}-d} \tau^2\, f(\tau)d\tau/2\ \mathrm{Pr}_{\mathrm{III1}} + \\ \left(SS^2 - (U_{max} - d)^2 \int_0^{S_{LDP}/U_{max}-d} \tau^2\, f(\tau)d\tau/\mathrm{Pr}_{\mathrm{III1}}\right)/2(U_{max}(1-\alpha) - d) \end{array} \tag{43}$$

$$\begin{array}{c} \overline{IH_{\mathrm{III2}}} = (U_{max} - d) \int_{S_{LDP}/U_{max}-d}^{SS/U_{max}-d} \tau^2\, f(\tau)d\tau/2\ \mathrm{Pr}_{\mathrm{III2}} + SS\ LDP - \\ \left(SS - E_{\mathrm{III2}}(\tau_T)(U_{max} - d)\right)^2/2(U_{max}(1-\alpha) - d) \end{array} \tag{44}$$

$$\overline{IH_{\mathrm{III3}}} = SS\ (E_{\mathrm{III3}}(\tau_T) + LDP - SS/(U_{max} - d)) + SS^2/2(U_{max} - d) \tag{45}$$

The NCC_{ij} are given by Eqs. 46, 47, and 48 and the PMC_{ij} by Eq. 5, where $NbPM_{ij}$ are given by Eqs. 49, 50, and 51, for i = III and j = 1, 2, 3.

$$NCC_{\mathrm{III1}} = (C_{RM}U_{max} + C_{MCO})\alpha\big(SS - E_{\mathrm{III1}}(\tau_T)(U_{max} - d)\big)/(U_{max}(1-\alpha) - d) \tag{46}$$

$$\begin{array}{c} NCC_{\mathrm{III2}} = (C_{RM}U_{max} + C_{MCO})\alpha\big(SS - E_{\mathrm{III2}}(\tau_T)(U_{max} - d)\big)/(U_{max}(1-\alpha) - d) + \\ (C_{RM}d + C_{MCO}/(1+\alpha))\alpha\big(LDP - \big(SS - E_{\mathrm{III2}}(\tau_T)(U_{max} - d)\big)/(U_{max}(1-\alpha) - d)\big) \end{array} \tag{47}$$

$$NCC_{\mathrm{III3}} = \alpha\ (C_{RM}d + C_{MCO}/(1+\alpha))\ LDP \tag{48}$$

$$NbPM_{\mathrm{III1}} = \left(\sum_{k=0}^{NM_L-1} k\, R(T)^k\, F(T) + NM_L\, R(T)^{NM_L}\, F\left(\frac{S_{LDP}}{U_{max} - d} \bmod T\right)\right) \Big/ \mathrm{Pr}_{\mathrm{III1}} \tag{49}$$

$$NbPM_{\mathrm{III2}} = \left(\begin{array}{c} NM_L\, R(T)^{NM_L} \left(F(T) - F\left(\frac{S_{LDP}}{U_{max} - d} \bmod T\right)\right) + \\ \sum_{k=NM_L+1}^{NM_S-1} k\, R(T)^k\, F(T) + NM_S\, R(T)^{NM_S}\, F\left(\frac{SS}{U_{max} - d} \bmod T\right) \end{array}\right) \Big/ \mathrm{Pr}_{\mathrm{III2}} \tag{50}$$

$$NbPM_{\mathrm{III3}} = \left(NM_S\, R(T)^{NM_S} \left(F(T) - F\left(\frac{SS}{U_{max} - d} \bmod T \right) \right) + \sum_{k=NM_S+1}^{\infty} k\, R(T)^k\, F(T) \right) \Big/ \Pr_{\mathrm{III3}} \quad (51)$$

In an excess (deficiency) condition, the accrued restoration phase charge is given by Eq. 6 (Eq. 7) and Eq. 8 with the expected amount detained in inventory and the amount of lost demands can be given by Eqs. 33 and 34, respectively, for i = III and j = 1, 2, 3.

5. Numerical resolution methodology, results and comparative analysis

5.1 Optimization numerical procedure

Two decision variables specify the optimal solution: the security stock capacity *SS*, and the preventive maintenance age *T*. A numerical resolution procedure has been designed and coded based on the programming language 'Fortran', to determine the optimal solution (SS^*, T^*) minimizing the overall expected cost (CT^*). This algorithm, which is illustrated in Fig. 5, combines a number of subroutines to calculate the probability of each scenario, predicted cycle durations, several *KPI*s, and expenses suffered during the production and restoration cycles for the three sub-policies.

5.2 Numerical results and analytical model validation

Consider first a base case describing the production cell. All costs and operating, demand, quality, and maintenance parameters are provided in Table 1. The time in-control state (to restore) has a Weibull (Gamma) distribution. After executing the numerical program, we established that the minimum total cost (CT^*), as determined by the optimal decision variables SS^* = 1,314 items & T^* = 0.14 months, is equal to 96,621.37 $/month. Fig. 6 presents the evolution of *CT* depending on decision variables *SS* and *T*. One can note the convex character of the surface confirming the presence of the optimum value.

Table 1 Sample of 6 manufacturing cell configurations with randomly generated parameters

Case	Cost Parameters							Operating Parameters					
	C_H	C_S	C_{RM}	C_{MCO}	C_{SU}	C_R	C_{PM}	d	U_{max}	*MTIC*	α (%)	*LDP*	*MTTR*
Base	40	400	500	150,000	5,000	10,000	2,000	20,160	32,400	0.9027	1	0.10	0.05
1	80	385	150	200,500	2,800	9,000	3,800	22,350	40,000	1.2638	19	0.11	0.022
2	50	200	250	250,000	3,000	15,000	2,800	18,000	35,000	1.8054	5	0.08	0.10
3	90	500	300	220,000	5,500	20,000	4,000	13,000	20,000	0.9027	20	0.10	0.02
4	25	430	240	160,000	6,200	7,000	4,200	21,540	38,500	1.1735	11	0.03	0.1
5	120	420	290	350,000	6,000	14,000	2,500	20,000	35,100	1.0832	12	0.12	0.067
6	15	630	140	90,000	3,000	4,000	2,700	28,000	44,000	0.6319	8	0.09	0.033

To validate the proposed approach, the analytical stochastic models and the numerical resolution procedure, a simulation model is constructed with ARENA simulation package. It imitates the production cell dynamic and stochastic behaviour. Table 2 presents first the validation of the base case. Hundreds of cell configurations were randomly generated, evaluated for optimal solutions, and then analytical results were validated through simulation. Each simulation is executed during 1,000,000 cycles (Production-Restoration) with warmup delay of 100,000 cycles to assure the steadiness of performance measures. Ten replications were carried out for every cell configuration.

Table 2 also presents a sample of 6 cell configurations (cases 1 to 6) with randomly generated parameters validated through simulation model (Tab. 1); the results show that all analytically computed *KPI*s fell inside the simulation's 95 % confidence interval. The key performance indicators analysed in this paper are the expected values of the following: cycle length (*CL*), work in process (*WIP*), number of lost demand (*NbLD*), number of non-conforming items (*NbNC*), number of preventive maintenance interventions (*NbPM*), and total incurred cost (TC^*).

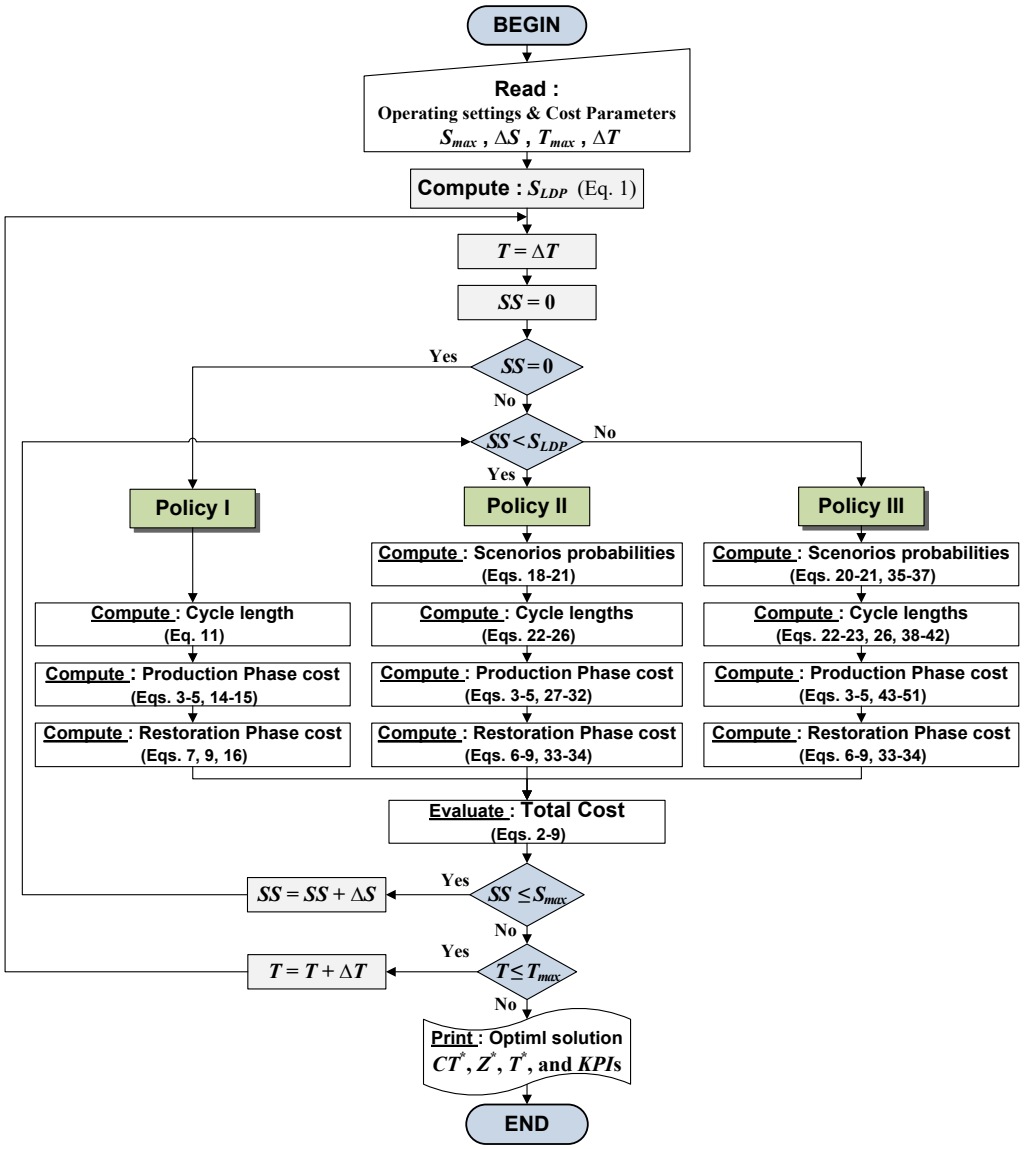

Fig. 5 Optimal policy resolution algorithm

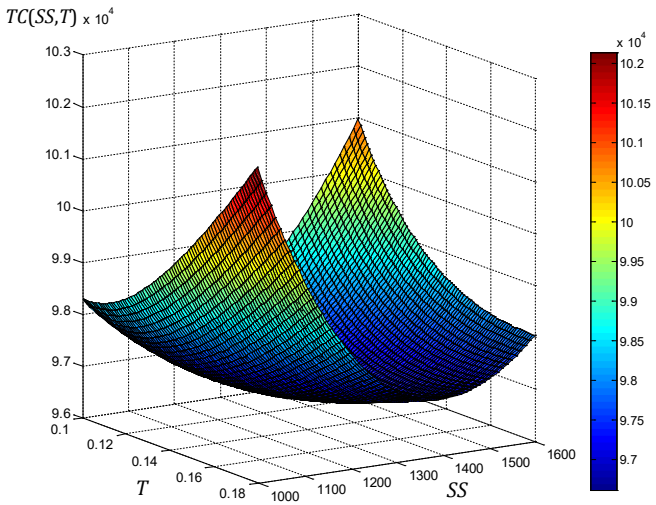

Fig. 6 Evolution of the total incurred cost $CT(SS,T)$

Table 2 Analytical results validation by simulation for manufacturing cell configurations defined in Table 1

Case	Key Performance Indicators					Optimal Solution		
	CL	*WIP*	*NbLD*	*NbNC*	*NbPM*	TC^*	T^*	SS^*
Base	**2.860**	**1,270.52**	**171.24**	**20.35**	**18.59**	**96,621.4**	**0.14**	**1,314**
	[2.853 - 2.863]	[1,270.37 - 1,270.59]	[170.61 - 172.27]	[20.34 - 20.36]	[18.55 - 18.62]	[96,540.1 - 96,761.8]		
1	**4.420**	**120.36**	**379.44**	**476.12**	**28.01**	**86008.1**	**0.15**	**121**
	[4.416 - 4.427]	[120.367 - 120.369]	[379.06 - 379.86]	[467.12 - 467.12]	[27.97 - 28.03]	[85,959.4 - 86,107.7]		
2	**8.719**	**0**	**1,800**	**72**	**77.02**	**70,263.73**	**0.11**	**0**
	[8.707 - 8.728]	[0 - 0]	[1,798.8 - 1,801.5]	[72 - 72]	[76.92 - 77.11]	[70,210.7 - 70,361.9]		
3	**2.720**	**225.351**	**84.47**	**260.25**	**16.71**	**99,821.7**	**0.15**	**228**
	[2.718 - 2.721]	[225.350 - 225.353]	[84.26 - 84.62]	[260.24 - 260.26]	[16.69 - 16.72]	[99,797.8 - 99,871.7]		
4	**3.914**	**2,998.14**	**286.38**	**89.55**	**22.66**	**139,729.7**	**0.16**	**3,142**
	[3.903 - 3.918]	[2,997.75 - 2,998.26]	[285.13 - 288.53]	[89.49 - 89.70]	[22.59 - 22.68]	[139,655.4 - 140,004.7]		
5	**6.070**	**0**	**1,333.33**	**288**	**117.07**	**158,260.3**	**0.05**	**0**
	[6.061 - 6.079]	[0 - 0]	[1332.35 - 1334.46]	[288 - 288]	[116.88 - 117.24]	[158,110.6 - 158,507.9]		
6	**1.480**	**2,275.11**	**16.77**	**215.93**	**5.60**	**77,041.9**	**0.21**	**2,481**
	[1.478 - 1.483]	[2,274.56 – 2,275.36]	[16.54 - 17.01]	[215.83 - 216.07]	[5.59 - 5.62]	[76,937.9 - 77,160.1]		

5.3 Comparative analysis

To highlight the contribution of the suggested approach, a comparative investigation was carried out with strategies considered in the literature and practice:

Strat. 1: The Proposed policy, described by 3 sub-policies and 6 scenarios.

Strat. 2: proposal of Chelbi *et al*. [29], described by 2 scenarios (no sub-policies), and can only handle the case $SS > S_{LDP}$.

Strat. 3: proposal of Dhouib *et al*. [31], described by 3 scenarios (no sub-policies), and can only handle the case $SS > S_{LDP}$.

Strat. 4: The proposed policy (*Strat.* 1) but limited to a range of safety stock level $SS > S_{LDP}$ as considered in *Strat.* 2 and *Strat.* 3.

Strat. 5: The proposed policy (*Strat.* 1) without preventive maintenance.

The comparative study is based on the sample of 7 manufacturing cell configurations with randomly generated parameters presented in Table 1 (Base case and cases 1 to 6).

Table 3 displays first the optimal control solution for the proposed *Strat*. 1 (SS^*,T^*,TC^*) and according to which optimal sub-policy (P^*) it belongs (P^* = I, II or III). It also presents optimal solutions for the other compared strategies. First, we must recall that all the results generated by the proposed approach (*Strat.* 1) are validated by comparing them with those made by simulation, confirming the exactness of the proposed analytic models. The results demonstrate that the recommended approach (*Strat.* 1) outperforms other ones and allowing cost savings of up to 96 % (60 %) compared to the proposal of Chelbi *et al*. (2008) (*Strat.* 2 – case 1) (Dhouib *et al*. (2012) (*Strat.* 3 – case 5)); The primary reason for this discrepancy is because these models do not account for any potential security stock value ranges.

Table 3 Comparison of the proposed policy to ones from literature and practice

Case	*Strat.* 1 - Proposed -				*Strat.* 2				*Strat.* 3				*Strat.* 4				*Strat.* 5			
	SS^*	T^*	TC^*	P^*	SS^*	T^*	TC^*	*Cost Red.* (%)	SS^*	T^*	TC^*	*Cost Red.* (%)	SS^*	T^*	TC^*	*Cost Red.* (%)	SS^*	T^*	TC^*	*Cost Red.* (%)
Base	1,314	0.14	96,621	III	1,202	0.09	116,924	21.1	1,493	0.17	105,955	9.7	1,314	0.14	96,621	0	2,087	-	113,809	17.8
1	121	0.15	86,008	II	1,106	0.14	168,782	96.3	1,106	0.3	131,641	53.1	1,106	0.29	127,107	47.8	638	-	134,278	56.1
2	0	0.11	70,129	I	1,220	0.16	112,269	60.1	1,220	0.20	107,329	53.1	1,220	0.20	102,766	46.5	1,666	-	150,759	114.9
3	228	0.15	99,821	II	521	0.11	154,108	54.4	300	0.16	111,862	12.1	300	0.17	100,646	8.3	426	-	152,680	52.9
4	3,142	0.16	139,729	III	4,218	0.19	172,126	23.2	3,691	0.31	155,617	11.4	3,142	0.16	139,729	0	4,712	-	153,390	9.8
5	0	0.05	158,260	I	1,307	0.06	281,517	77.8	1,307	0.07	253,460	60.2	1,307	0.09	237,428	50.1	1,592	-	346,397	125.2
6	2,481	0.21	77,041	III	3,246	0.16	100,747	30.8	2,532	0.24	89,867	16.7	2,481	0.21	77,041	0	2,869	-	88,905	15.4

Strat. 4, which is a limited version of *Strat.* 1, surpasses *Strat*. 2 and *Strat*. 3 on all studied configurations, but it generates errors of up to 50 % compared to *Strat*. 1 (case 5). Finally, comparing *Strat*. 5 to the proposed *Strat*. 1 show that preventive maintenance allowed reducing the total incurred cost of up to 125 % (case 5). We note that the high-cost reductions are obtained when the zero-stock is the best sub-policy; in fact, this joint policy is based on high inventory holding

cost, and since no preventive maintenance is planned with *Strat*. 5, it reacts by increasing the security stock capacity (SS^*), from 0 (*Strat*. 1 – case 5) to 1,592 (*Strat*. 5 – case 5) implying high and costly *WIP*.

6. Conclusion

In this manuscript, we introduce a comprehensive strategy for production planning and preventive maintenance concerning manufacturing systems prone to quality degradation considering every potential range of values for the security stock. An age-based AMP plan is implemented to diminish the amount of non-compliant items. Three joint control sub-policies are developed based on a specific value of the security stock capacity determined by the production system characteristics and the amount added to the security stock during the logistic delay period (S_{LDP}): Sub-policy I – HPP and the zero-inventory policy, Sub-policy II – HPP and the stock policy $SS < S_{LDP}$, and Sub-policy III – HPP and the stock policy $SS \geq S_{LDP}$.

The three inferred sub-policies and related scenarios are addressed using a broad stochastic multi-model method for industrial systems with general distributions of the restoration delay and the alteration period to the 'out-of-control' condition. We develop a numerical approach to address intricate stochastic models and assess the optimal integrated control policy by computing the expected overall cost. A simulation model has also been built and hundreds of system configurations with randomly generated parameters were tested to validate the recommended analytical models showing the quality and the effectiveness of the provided approach. Finally, we examined various control policies derived as of existing literature and applied in practical situations to underline the efficacy of the recommended integrated policy. The findings indicate that, for all randomly generated configurations, the proposed policy outperforms other ones and can achieve substantial economic gains.

This work is intended to inspire additional research on integrated production control and preventive maintenance policies. Indeed, the suggested strategy can be extended to circumstances involving maintenance and restoration efforts which are imperfect. Control charts and sampling inspection programs are two more quality inspection procedures that may be taken into consideration in a future work. In the other hand, further research is needed to analyse more complex production cells with several product kinds and multiple manufacturing workstations.

References

[1] Rosin, F., Forget, P., Lamouri, S., Pellerin, R. (2021). Impact of Industry 4.0 on decision-making in an operational context, *Advances in Production Engineering & Management*, Vol. 16, No. 4, 500-514, doi: 10.14743/apem2021.4.416.

[2] Patalas-Maliszewska, J., Łosyk, H (2022). An approach to maintenance sustainability level assessment integrated with Industry 4.0 technologies using Fuzzy-TOPSIS: A real case study, *Advances in Production Engineering & Management*, Vol. 17, No. 4, 455-468, doi: 10.14743/apem2022.4.448.

[3] Fonseca, L., Amaral, A., Oliveira, J. (2021). Quality 4.0: The EFQM 2020 model and Industry 4.0 relationships and implications, *Sustainability*, Vol. 13, No. 6, Article No. 3107, doi: 10.3390/su13063107.

[4] Psarommatis, F., Sousa, J., Mendonça, J.P., Kiritsis, D. (2022). Zero-defect manufacturing the approach for higher manufacturing sustainability in the era of Industry 4.0: A position paper, *International Journal of Production Research,* Vol. 60, No. 1, 73-91, doi: 10.1080/00207543.2021.1987551.

[5] Psarommatis, F., May, G., Azamfirei, V. (2023). Envisioning maintenance 5.0: Insights from a systematic literature review of Industry 4.0 and a proposed framework, *Journal of Manufacturing Systems*, Vol. 68, 376-399, doi: 10.1016/j.jmsy.2023.04.009.

[6] Colledani, M., Tolio, T. (2012). Integrated quality, production logistics and maintenance analysis of multi-stage asynchronous manufacturing systems with degrading machines. *CIRP Annals,* Vol. 61, No. 1, 455-458, doi: 10.1016/j.cirp.2012.03.072.

[7] Ait-El-Cadi, A., Gharbi, A., Dhouib, K., Artiba, A. (2021). Integrated production, maintenance, and quality control policy for unreliable manufacturing systems under dynamic inspection, *International Journal of Production Economics*, Vol. 236, Article No. 108140, doi: 10.1016/j.ijpe.2021.108140.

[8] Wang, L., Lu, Z., Han, X. (2019). Joint optimization of production, maintenance, and quality for batch production system subject to varying operational conditions, *International Journal of Production Research*, Vol. 57, No. 24, 7552-7566, doi: 10.1080/00207543.2019.1581956.

[9] Ait-El-Cadi, A., Gharbi, A., Dhouib, K., Artiba, A. (2024). Joint production, maintenance, and quality control in manufacturing systems with imperfect inspection, *Journal of Manufacturing Systems*, Vol. 77, 848-858, doi: 10.1016/j.jmsy.2024.10.020.
[10] Akella, R., Kumar, P. (1986). Optimal control of production rate in a failure prone manufacturing system, *IEEE Transactions on Automatic Control,* Vol. 31, No. 2, 116-126, doi: 10.1109/TAC.1986.1104206.
[11] Xanthopoulos, A.S., Koulouriotis, D.E. (2021). A comparative study of different pull control strategies in multi-product manufacturing systems using discrete event simulation, *Advances in Production Engineering & Management*, Vol. 16, No. 4, 473-484, doi: 10.14743/apem2021.4.414.
[12] Gharbi, A., Hajji, A., Dhouib, K. (2011). Production rate control of an unreliable manufacturing cell with adjustable capacity, *International Journal of Production Research*, Vol. 49, No. 21, 6539-6557, doi: 10.1080/00207543.2010.519734.
[13] Dhahri, A., Gharbi, A., Ouhimmou, M. (2022). Integrated production-transshipment control policy for a two location unreliable manufacturing system, *International Journal of Production Economics*, Vol. 247, Article No. 108440, doi: 10.1016/j.ijpe.2022.108440.
[14] Berthaut, F., Gharbi, A., Dhouib, K. (2011). Joint modified block replacement and production/inventory control policy for a failure-prone manufacturing cell, *Omega*, Vol. 39, No. 6, 642-654, doi: 10.1016/j.omega.2011.01.006.
[15] Kaddachi, R., Gharbi, A., Kenné, J.P. (2022). Integrated production and maintenance control policies for failure-prone manufacturing systems producing perishable products, *The International Journal of Advanced Manufacturing Technology*, Vol. 119, 4635-4657, doi: 10.1007/s00170-021-08273-y.
[16] Farahani, A., Tohidi, H., Shoja, A. (2019). An integrated optimization of quality control chart parameters and preventive maintenance using Markov chain, *Advances in Production Engineering & Management*, Vol. 14, No. 1, 5-14, doi: 10.14743/apem2019.1.307.
[17] Dhouib, K., Gharbi, A., Landolsi, N. (2010). Availability modelling and analysis of multi-product flexible transfer lines subject to random failures, *The International Journal of Advanced Manufacturing Technology,* Vol. 50, 329-341, doi: 10.1007/s00170-009-2487-8.
[18] Pandey, D., Kulkarni, M.S., Vrat, P. (2011). A methodology for joint optimization for maintenance planning, process quality and production scheduling, *Computers & Industrial Engineering*, Vol. 61, No. 4, 1098-1106, doi: 10.1016/j.cie.2011.06.023.
[19] Ben-Daya, M. (2002). The economic production lot-sizing problem with imperfect production processes and imperfect maintenance, *International Journal of Production Economics*, Vol. 76, No. 3, 257-264, doi: 10.1016/S0925-5273(01)00168-2.
[20] Nourelfath, M., Nahas, N., Ben-Daya, M. (2016). Integrated preventive maintenance and production decisions for imperfect processes, *Reliability Engineering & System Safety,* Vol. 148, No. 1, 21-31, doi: 10.1016/j.ress.2015.11.015.
[21] Salmasnia, A., Abdzadeh, B., Namdar, M. (2017). A joint design of production run length, maintenance policy and control chart with multiple assignable causes, *Journal of Manufacturing Systems*, Vol. 42, 44-56, doi: 10.1016/j.jmsy.2016.11.003.
[22] Khatab, A., Diallo, C., Aghezzaf, E.-H., Venkatadri, U. (2019). Integrated production quality and condition-based maintenance optimisation for a stochastically deteriorating manufacturing system, *International Journal of Production Research*, Vol. 57, No. 8, 2480-2497, doi: 10.1080/00207543.2018.1521021.
[23] Zhang, C., Zhu, H., Wu, J., Ma, L., Cheng, J., Wang, H. (2020). An economical optimization model for deteriorating system integrated with statistical process control and condition-based maintenance, *Quality Engineering*, Vol. 32, No. 3, 465-477, doi: 10.1080/08982112.2020.1757702.
[24] Zhang, N., Tian, S., Liu, B., Zhang, J. (2022). Joint optimization of production lot-sizing and condition-based maintenance in an imperfect production process with dependent indicators, *Quality Technology & Quantitative Management*, Vol. 20, No. 4, 511-527, doi: 10.1080/16843703.2022.2126263.
[25] Zhang, N., Tian, S., Xu, J., Deng, Y., Cai, K. (2023). Optimal production lot-sizing and condition-based maintenance policy considering imperfect manufacturing process and inspection errors, *Computers & Industrial Engineering*, Vol. 177, Article No. 108929, doi: 10.1016/j.cie.2022.108929.
[26] Chelbi, A., Rezg, N., Radhoui, M. (2008). Simultaneous determination of production lot size and preventive maintenance schedule for unreliable production system, *Journal of Quality in Maintenance Engineering*, Vol. 14, No. 2, 161-176, doi: 10.1108/13552510810877665.
[27] Colledani, M., Tolio, T. (2011). Joint design of quality and production control in manufacturing systems, *CIRP Journal of Manufacturing Science and Technology*, Vol. 4, No. 3, 281-289, doi: 10.1016/j.cirpj.2011.06.008.
[28] Dhouib, K., Gharbi, A., Ben Aziza, M.N. (2012). Joint optimal production control/preventive maintenance policy for imperfect process manufacturing cell, *International Journal of Production Economics*, Vol. 137, No. 1, 126-136, doi: 10.1016/j.ijpe.2012.01.023.
[29] Bahria, N., Chelbi, A., Bouchriha, H., Dridi, I.H. (2018). Integrated production, statistical process control, and maintenance policy for unreliable manufacturing systems, *International Journal of Production Research*, Vol. 57, No. 8, 2548-2570, doi: 10.1080/00207543.2018.1530472.
[30] Bahria, N., Harbaoui Dridi, I., Chelbi, A., Bouchriha, H. (2021). Joint design of control chart, production and maintenance policy for unreliable manufacturing systems, *Journal of Quality in Maintenance Engineering*, Vol. 27, No. 4, 586-610, doi: 10.1108/JQME-01-2020-0006.
[31] Çinlar, E. (2013). *Introduction to stochastic processes*, Dover Publications, New-York, USA.

APEM journal
Advances in Production Engineering & Management
Volume 19 | Number 4 | December 2024 | pp 527–538
https://doi.org/10.14743/apem2024.4.522
ISSN 1854-6250
Journal home: apem-journal.org
Original scientific paper

Integrating simulation modelling for sustainable, human-centred Industry 5.0: ESG-based evaluation in collaborative workplaces

Ojstersek, R.[a,*], **Javernik, A.**[a], **Buchmeister, B.**[a]

[a]University of Maribor, Faculty of Mechanical Engineering, Maribor, Slovenia

ABSTRACT

This research explores the role of simulation modelling in the development of human-centred, sustainable manufacturing processes in the context of Industry 5.0. We analyse collaborative workplaces where humans and collaborative robots (CR) work together, emphasizing the environmental, social, and governance (ESG) criteria. The research work focuses on how personalized CR parameters and optimized work environments contribute to improved productivity, well-being, and sustainability. Through simulations, the paper evaluates the operational efficiency of both manual assembly and human-robot collaborative (HRC) setups, providing insight into the economic, environmental, and social impacts of Industry 5.0 manufacturing systems. The results show significant improvements in sustainability, productivity, and worker well-being achieved through adaptive CR integration and ESG-driven engineering practices.

ARTICLE INFO

Keywords:
Human-Centred manufacturing;
Simulation modelling;
Sustainability – ESG;
Industry 5.0;
Collaborative workplace;
Human-robot interaction;
Assembly process

**Corresponding author:*
robert.ojstersek@um.si
(Ojstersek, R.)

Article history:
Received 23 August 2024
Revised 28 November 2024
Accepted 5 December 2024

1. Introduction

In the rapidly evolving landscape of industrial manufacturing, the transition from Industry 4.0 to Industry 5.0 [1] marks a paradigm shift toward human-centred and sustainable production systems [2]. While Industry 4.0 focused on automation, digitization, and connectivity [3], Industry 5.0 emphasizes the integration of advanced technologies with human well-being as a main optimization goal [4]. This transformation addresses the multiple objectives of enhancing productivity and fostering a sustainable, ethical, and socially responsible global competitive manufacturing environments [5, 6].

A significant challenge in manufacturing today lies in achieving optimal synergy between humans and collaborative robots (CRs), while maintaining a balance among economic performance, worker well-being, and environmental sustainability [7, 8]. Current manufacturing systems are often either overly automated (lacking manufacturing flexibility) or heavily reliant on manual labour (with a lack of suitable labour force), leading to inefficiencies in resource utilization, high

operational costs, worker fatigue (physical and physical), and inconsistent quality [9]. Furthermore, while Environmental, Social, and Governance (ESG) criteria are increasingly emphasized in industrial settings, existing systems frequently fail to integrate these metrics effectively into the design and evaluation of collaborative workplaces [10, 11]. A lot of research works are trying to answer the question: Can growing field of Human-Robot Collaboration (HRC) offers a promising solution to obtain efficient competitive manufacturing systems [12]? HRC systems combine the precision, speed, and reliability of robots with the creativity, flexibility, and problem-solving capabilities of humans [13]. Various implementations of HRC have demonstrated improvements in production efficiency, reduced worker fatigue, and enhanced products quality [14]. Simulation modelling has also emerged as a powerful tool for analysing and optimizing these systems, enabling the evaluation of production processes under different scenarios without disrupting real-world operations [15]. Among existing solutions, simulation-based evaluations of HRC systems stand out as the most effective approach. These models provide a holistic view of production processes, incorporating economic, environmental, and social factors into performance assessments. By simulating dynamic interactions between humans and robots, these tools help identify bottlenecks, optimize task allocation, and evaluate ESG impacts [16]. Despite its potential, the current simulation-based methods face significant limitations [17]. Most models focus heavily on economic performance while neglecting the social aspects of manufacturing, such as worker well-being, safety, and engagement. Additionally, few studies effectively integrate environmental and governance criteria, such as energy efficiency and ethical labour practices, into the simulation frameworks [18]. This lack of comprehensive models hinders the ability of manufacturers to design truly sustainable and human-centred systems, particularly in the context of Industry 5.0 [19, 20].

This research aims to address these limitations by developing a simulation-based approach that evaluates collaborative workplaces through the lens of ESG criteria [21]. By incorporating real-world data, the paper seeks to:

- Enhance economic performance by reducing operational costs, idle times, and energy consumption.
- Improve worker well-being by redistributing repetitive and physically demanding tasks to robots, thereby reducing fatigue and enhancing safety.
- Promote environmental sustainability by minimizing energy usage and waste generation.
- Strengthen governance practices by aligning production processes with ethical and regulatory standards.

Paper research goal is to provide a framework for designing human-centred and sustainable manufacturing systems, enabling the realization of Industry 5.0 principles in diverse industrial settings [22, 23]. This study contributes to the existing body of knowledge by demonstrating how simulation modelling can bridge the gap between productivity and sustainability, offering actionable insights for optimizing human-robot collaboration while meeting ESG goals.

2. Problem description

In the context of Industry 5.0, where the integration of human-centred and sustainable practices is crucial, the need for effective simulation modelling to evaluate manufacturing systems from an ESG (Environmental, Social, Governance) perspective has become critical. While Industry 4.0 emphasized the integration of automation and data-driven systems, Industry 5.0 highlights the necessity of aligning technological advancements with human well-being and environmental sustainability. The ESG framework, presented in Fig. 1, provides comprehensive criteria's for assessing the impact of manufacturing processes, but there remains a significant gap in evaluating collaborative workplaces especially those involving human-robot collaboration (HRC). The ESG framework shown in the Fig. 1 emphasizes the integration of sustainable, ethical, and socially responsible practices into production systems. By adopting this framework, production facilities can monitor and improve their impact on the environment, enhance worker conditions, and considering governance regulations. Simulation models, when integrated with these ESG criteria, can help optimize production systems while balancing productivity with sustainability, aligning closely with Industry 5.0 principles.

ESG Framework for Production Systems

Environment	Social	Governance
1. Energy management	1. Employee engagement	1. Business ethics
2. CO2 footprint	2. Health and safety	2. Cyber security
3. Waste management	3. Innovation	3. Privacy
4. Use of natural resources	4. Customer and product responsibility	4. Risk management
5. Supply chain management	5. Knowledge management	5. Transparency

Fig. 1 Proposed ESG framework for production systems

Existing models are often limited with the social aspects of worker well-being, which are essential for long-term operational efficiency. This gap is particularly notable in production processes supported by the concepts of the Industry 5.0, where technology must not only optimize productivity but also support sustainable and socially responsible practices. To address this issue, this research work proposes a simulation-based approach to evaluate HRC based on ESG metrics, specifically focusing on the integration of environmental sustainability, social impacts, and governance in decision-making processes. Our research emphasizes the role of human-centred design in optimizing production systems, ensuring that both economic efficiency and worker well-being are balanced through simulation.

Fig. 2 illustrates the evaluated production process in a typical dynamic job shop manufacturing environment, where machines and human workers share tasks. The figure provides a layout of the production line, showing how each machine (from M1 to M7 and manual assembly workplace WP1) interacts within the production process. The machines M1 to M7 include the following: M1 and M7 are KUKA KR 40 industrial robots. Machines M2 and M3 are Haas UMC 500 5-axis CNC centres, while machines M4 and M6 are Okuma MA 550-VB 3-axis CNC machine centres. Machine M5 is a Mazak QTS 200 model CNC machine. WP1 presents manual assembly operation, which will be replaced by HRC for the purpose of ESG simulation model evaluation. We will present how this change influence entire manufacturing system in corelation to Industry 5.0 aspects.

Table 1 presents the real-world data collected from the evaluated production process, including costs associated with machines, worker involvement, and energy consumption across multiple machines from M1 to M7 and manual assembly workplace WP1. These parameters are critical in calculating the ESG Index, as they reflect the economic, environmental, and social impacts of the manufacturing process. The table highlights key metrics which was used for calculating Total machines and WP1 costs presented by the processing and idle costs. These parameters are then incorporated into data drive simulation model to assess the production system's sustainability performance, focusing on reducing energy and scrap rate, electrical energy consumption and optimizing worker conditions while maintaining production efficiency.

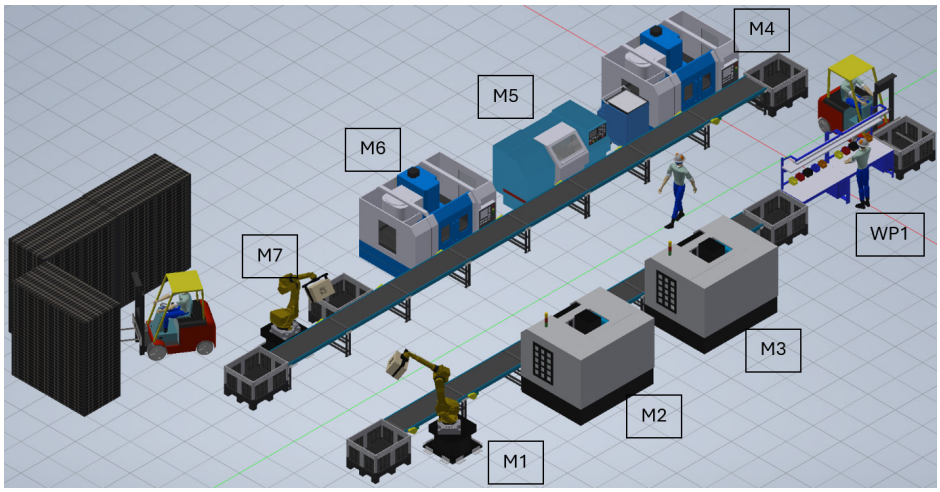

Fig. 2 Evaluated production process

Table 1 Production process real-world data

Cost calculation parameter	M1	M2	M3	WP1 (MA/HRC)		M4	M5	M6	M7
Purchase value of the machine (1000 of €)	40	140	140	31.25	6.25	150	50	150	40
Machine power (kW)	3.75	20	20	0.05	0.15	20	7.5	20	3.75
Workplace area (m^2)	8.5	8.8	8.8	1.7	1.7	17.5	4.2	17.5	8.5
Depreciation period (year)	5	5	5	5	5	5	5	5	5
Useful capacity (h/year)	4649	4649	4649	4649	4649	4649	4649	4649	4649
Machine write-off value (€/h)	1.72	6.02	6.02	1.34	0.27	6.45	2.15	6.45	1.72
Interests (€/h)	0.26	0.90	0.90	0.20	0.04	0.97	0.32	0.97	0.26
Maintenance costs (€/h)	0.26	0.90	0.90	0.20	0.04	0.97	0.32	0.97	0.26
Workplace area costs (€/h)	1.828	1.893	1.893	0.366	0.366	3.764	0.903	3.764	1.828
Energy consumption costs (€/h)	0.3	1.6	1.6	0.004	0.004	1.6	0.6	1.6	0.3
Workplace tool costs (€/h)	0.17	0.60	0.60	0.13	0.03	0.65	0.22	0.65	0.17
Total machine costs (€/h)	4.54	11.92	11.92	2.25	0.75	14.40	4.51	14.40	4.54
Worker costs (€/h)	6	6	6	15	15	6	6	6	6
Additional costs (€/h)	0.07	0.18	0.18	0.03	0.01	0.22	0.07	0.22	0.07
Workplace total processing costs (€/h)	10.61	18.10	18.10	17.29	15.76	20.61	10.58	20.61	10.61
Workplace total idle costs (€/h)	5.30	12.13	12.13	17.29	15.76	13.81	5.29	13.81	3.5

To evaluate the sustainability of collaborative workplaces, the simulation model integrates the following ESG-related metrics:

- Energy consumption was modelled based on machine power (as shown in Table 1). Energy-efficient processes are simulated to compare their impacts on overall production costs.
- Worker costs and utilization rates from Table 1 are used to simulate worker efficiency.
- Governance aspects such as worker effective capacity planning with regulations and ethical labour practices are integrated as constraints in the simulation, ensuring that the production process reflects high standards of corporate responsibility.

By combining these factors, the simulation model provides a comprehensive ESG-based evaluation of the production system, identifying areas for improvement in production efficiency, sustainability and worker well-being, from a human-centred perspective.

3. Methodology

This research work uses simulation modelling to evaluate the sustainable performance of collaborative and manual workstations, incorporating real-world data and simulation environment Simio to analyse both the economic, environmental, and social (ESG) metrics. The simulation scenarios are developed to assess how collaborative workplace and manual assembly workstation perform in terms of production efficiency, worker well-being, and environmental impact in an Industry 5.0 context. The production system, consists of machines from M1 to M7, operates under two distinct setups:

- Manual assembly WP1, human worker performs assembly tasks, with no collaborative robot assistance.
- HRC WP1, human worker is assisted by collaborative robot in assembly tasks, reducing human workload.

Each machine and WP1 operate based on actual production data from the factory floor. The following assumptions and parameters were included in the simulation model:

- Effective production system capacity is 4649 hours/year, where 252 working days/year is considered, with 3 shifts/day, 7.5 effective working hours/shift with the 82 % production process efficiency are assumed.
- The hourly salary rate for workers operating machines M1 to M7 is 18 EUR/h, with three workers required to supervising all seven machines. For manual assembly workstation WP1, one additional worker is needed with salary of 15 EUR/h.

- The electrical energy cost is 0.16 EUR/kWh, with machine-specific power consumption included in the analysis. In addition, electrical energy consumption for each machine is based on its power rating, where used value is presented by 50 % of individual machine maximum power consumption.
- Operational and idle costs are included as calculated in Table 1, where maintenance costs are 3 %, tool costs are 2 % and additional machine costs are 1.5 % of the machine purchase value.
- The conveyor belt in the system operates at a speed of 0.75 m/s, while the forklift moves at 2 m/s, with loading and unloading times of 10 s each.
- Simulation time was 92 h with the warm-up period of 8 h.

Table 2 outlines the parameters used for modelling the manual assembly workstation WP1 and the associated machines. Processing time of the machines ranges from 15 s (M1) to 85 s (WP1) at the manual assembly workplace. Processing time of the WP1 is modelled by random normal distribution, where 85 s present mean value and 12 s its standard deviation (85; 12). Electrical energy power is given such as M2, M3, M4, and M6 consume 20 kW, while others like M1 and M7 consume 3.75 kW. WP1, a manual workstation, uses only 0.05 kW. Calculated workplace total costs for each machine's ranges from 10.61 EUR/h (M1, M7) to 20.61 EUR/h (M4, M6). For the manual assembly workplace scrap rate of 8 % is modelled. Data in Table 2 serves as a baseline for modelling manual assembly WP1 production process.

Table 2 Manual assembly WP1 modelling parameters

	Machine/workplace							
Simulation model parameter	M1	M2	M3	WP1	M4	M5	M6	M7
Processing time (s)	15	35	40	85; 12	40	60	35	25
Machine power (kW)	3.75	20	20	0.05	20	7.5	20	3.75
Workplace total processing costs (€/h)	10.61	18.10	18.10	15.76	20.61	10.58	20.61	10.61
Workplace total idle costs (€/h)	5.30	12.13	12.13	15.76	20.61	10.58	20.61	10.61
Scrap rate (%)	-	-	-	8	-	-	-	-

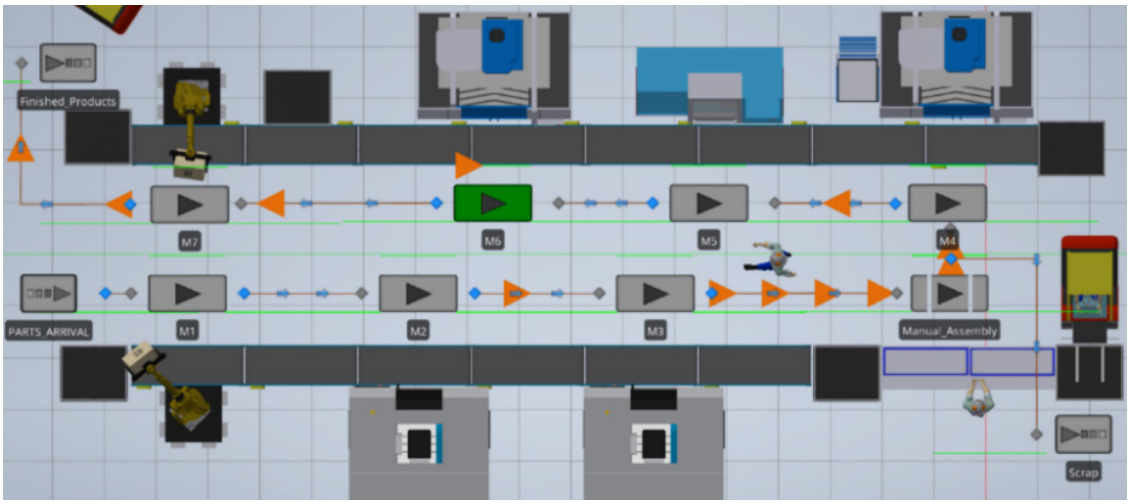

Fig. 3 Manual assembly production system model

Fig. 3 presents the configuration of the production system with the manual assembly workplace WP1, showing how machines (M1-M7) and the manual assembly workstation (WP1) are laid out in the production process. It visualizes the interactions between machines and workers, providing a clear representation of how simulation model inside Simio software is modelled in correlation to the real-world data.

Table 3 presents simulation modelling parameters for WP1 where manual assembly operation is replaced with the HRC workplace. In relation to the manual assembly operation, processing times for the machines from M1 to M7 remain the same, but for WP1 with HRC, the processing

time is significantly reduced to 55 seconds with a standard deviation of 6 seconds, compared to 85 seconds in the manual assembly operation. From an environmental perspective, the scrap rate of the HRC WP1 shows an improvement in production quality, with a reduced scrap rate of 4.5 %, compared to 8 % modelled at the manual assembly WP1.

Fig. 4 visualizes the layout of the production system with the HRC WP1, where collaborative robot performs assembly tasks with human worker. The model presents how human-robot collaboration can reduce task processing times and improve overall system efficiency by optimizing the task allocation for CR and workers.

The simulation model compares two scenarios (manual assembly operation vs. collaborative workstations), using the ESG framework described in Fig 1. Key performance indicators of energy consumption, scrap rate, worker utilization, processing and idle costs rates are evaluated to identify areas for improvement the economic, environmental and social sustainability. By incorporating ESG metrics and scenario-based analysis, the study demonstrates the potential for HRC to optimize production systems while improving worker well-being.

Table 3 HRC assembly WP1 modelling parameters

	Machine/workplace							
Simulation model parameter	M1	M2	M3	WP1	M4	M5	M6	M7
Processing time (s)	15	35	40	42; 6	40	60	35	25
Machine power (kW)	3.75	20	20	0.05	20	7.5	20	3.75
Workplace total processing costs (€/h)	10.61	18.10	18.10	17.29	20.61	10.58	20.61	10.61
Workplace total idle costs (€/h)	5.30	12.13	12.13	17.29	13.81	5.29	13.81	3.5
Scrap rate (%)	-	-	-	4.5	-	-	-	-

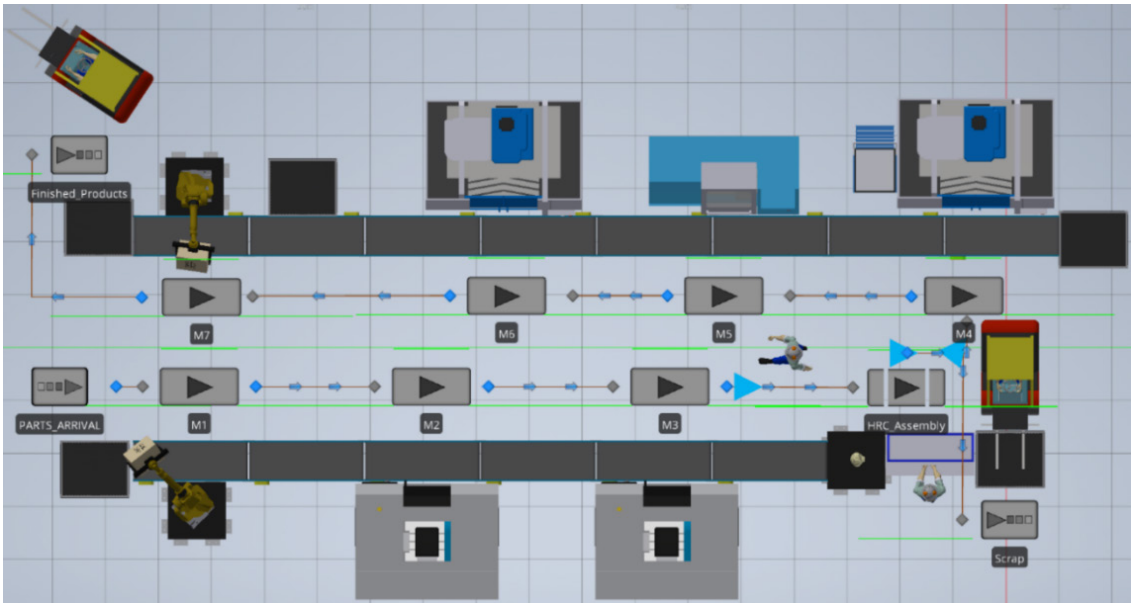

Fig. 4 HRC assembly production system model

4. Results

The simulation model was run to compare the performance of manual assembly operations with HRC at the WP1 in terms of utilization, power consumption, processing and idle costs, output quantity and scrap rate. The results highlight the differences in production efficiency, energy use, and operational costs between the two setups, emphasizing the benefits of HRC in achieving Industry 5.0 objectives. In Table 4, the utilization of the manual workstation WP1 reached a high value of 98.9 %, reflecting the bottleneck of the production process. However, several machines such as M1 (35.7 %), M4 (43.7 %), and M7 (27.3 %), exhibited significantly lower utilization, indicating unequal machine balancing. Total power consumption in the manual assembly setup was

relatively high for the major machines. M2 and M3 consumed 1532.7 kW and 1751.7 kW, respectively, while WP1, being largely manual, consumed just 4.5 kW. The processing costs for the manual setup remained high, particularly for machines like M3 (€1585.3) and WP1 (€1434.0). The manual operation incurred significant idle costs for machines such as M7 (€709.6), demonstrating inefficiency in resource utilization. The manual assembly system produced 3613 finished products, with 289 scrap products, representing an 8 % scrap rate, supported by the real-world modelled parameter.

Table 4 Simulation model results of the manual assembly WP1

	Machine/workplace							
Simulation model parameter	M1	M2	M3	WP1	M4	M5	M6	M7
Utilization (%)	35.7	83.3	95.2	98.9	43.7	65.5	38.2	27.3
Machine power consumption (kW)	123.2	1532.7	1751.7	4.5	804.1	452.0	702.9	94.2
Processing costs (EUR)	348.5	1387.1	1585.3	1434.0	828.6	637.6	724.3	266.5
Idle costs (EUR)	313.5	186.4	53.6	15.9	1067.5	335.8	1171.8	709.6
Number of finished products (pcs)	3613							
Scrap products (pcs)	289							

In contrast, the HRC workstation WP1, presented in Table 5, utilization slightly decreased to 95.9 %, but this reduction was compensated by a significant increase in the utilization of other machines. For example, M4 utilization improved to 90.9 %, and M7 to 41.6 %, showing that HRC distributes the workload more evenly across the manufacturing system. In the HRC scenario, the power consumption for WP1 increased to 13.2 kW due to the CR integration. However, more efficient operation across the system led to better overall energy usage, with M4 consuming 1672.6 kW, much higher than the manual setup but justified by improved product workflow. Processing costs increased for WP1 (€1525.5) due to the CR integration investments costs but resulted in an overall improvement in resource use. The idle costs for machines like M7 decreased to €570.1, indicating better synchronization between human and CR activities. The HRC system produced 5515 finished products, a significant improvement while scrap products increased to 344 products, reducing the scrap rate to 4.5 %. This shows that HRC improves overall product quality and reduces waste.

Table 5 Simulation model results of the HRC WP1

	Machine/workplace							
Simulation model parameter	M1	M2	M3	WP1	M4	M5	M6	M7
Utilization (%)	36.8	82.9	94.9	95.9	90.9	99.1	58.3	41.6
Machine power consumption (kW)	127.0	1525.4	1746.2	13.2	1672.6	683.8	1072.7	143.5
Processing costs (EUR)	359.2	1380.5	1580.3	1525.5	1723.6	964.6	1105.4	406.1
Idle costs (EUR]	308.2	190.8	56.9	65.2	172.5	8.8	790.7	570.1
Number of finished products (pcs)	5515							
Scrap products (pcs)	344							

Fig. 5 presents that HRC WP1 significantly improves machine utilization, reducing idle time and improving overall productivity. The higher utilization in HRC indicates that CR help manage tasks, reducing worker strain and improving throughput. The average utilization of the manual assembly WP1 was 69.7 %, reflecting a high workload on human workers but suboptimal distribution of tasks across other machines. In the HRC system, the average utilization increased to 85.8 %, showing a more balanced distribution of work between humans and robots, leading to better resource efficiency.

Fig. 6 demonstrates that while the HRC system consumes more energy, this increase is accompanied by improved production efficiency. The trade-off between higher energy use and greater output efficiency is clear in the comparison, where total power consumption for the manual assembly WP1 was 5465.2 kW, with machines like M2 and M3 consuming a significant portion of energy. The HRC setup showed a higher total power consumption of 6984.2 kW, mainly due to the added power required for HRC WP1 (13.2 kW vs. 4.5 kW in the manual assembly WP1).

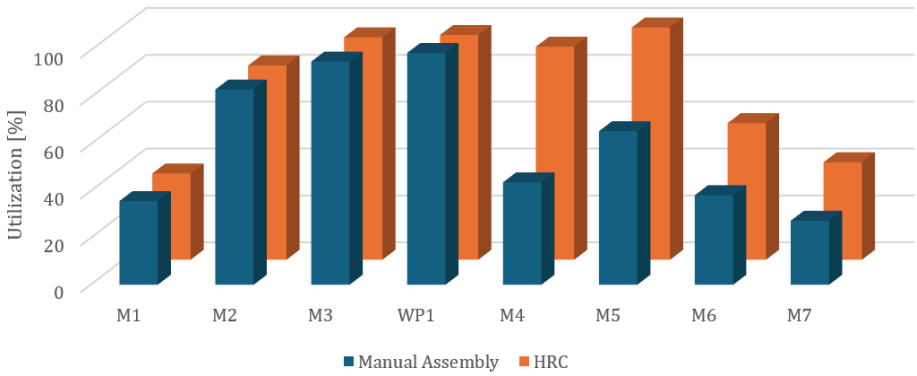

Fig. 5 Workplaces utilization results comparison

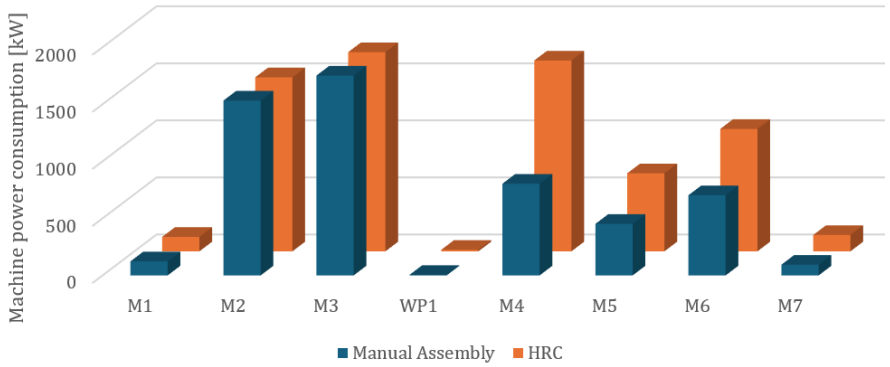

Fig. 6 Workplaces power consumption comparison

The total processing costs at the manual assembly WP1 amounted to 7211.8 EUR, largely driven by the intensive human labour required. Processing costs in the HRC system were 9045.1 EUR, reflecting the higher costs associated with integrating CR, but also the benefits of increased productivity. As shown in Fig. 7, the higher costs of HRC are offset by the increase in finished products, making it a more cost-effective option in the long term due to the reduction in errors and improved utilization.

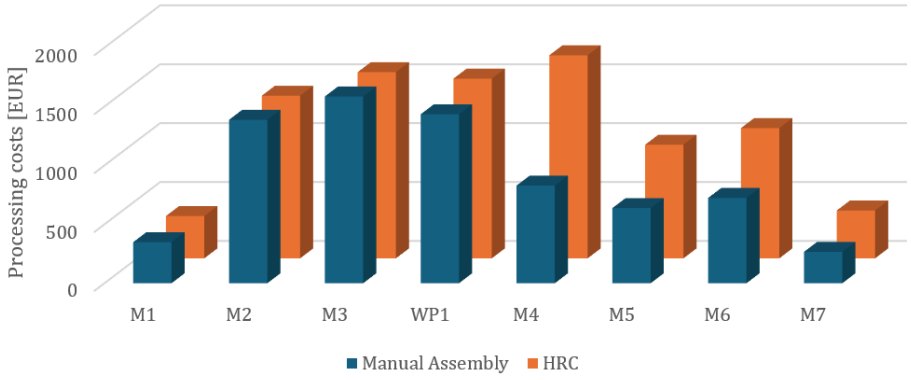

Fig. 7 Processing costs results comparison

In Fig. 8, idle costs for the manual assembly WP1 were high, totalling 3540.6 EUR, with machines such as M7 incurring significant idle time due to underutilization. The HRC WP1 dramatically reduced idle costs to 2163.2 EUR, as the CR helped minimize downtime by keeping machines and workers engaged in tasks.

As shown in Fig. 9, the integration of HRC not only increased total production but also improved product quality by reducing the scrap rate, which is essential for sustainable production systems.

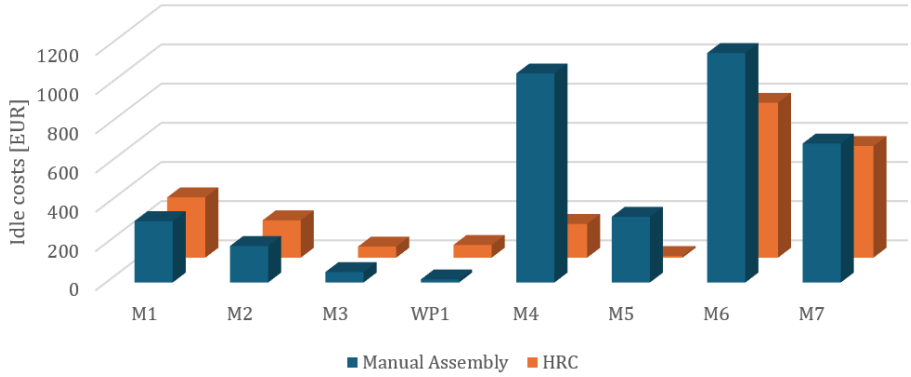

Fig. 8 Idle costs results comparison

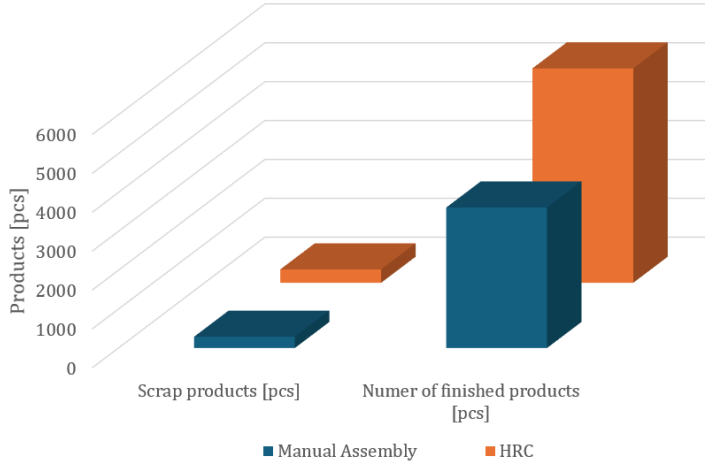

Fig. 9 Number of finished and scrap products comparison

5. Discussion

The results demonstrate the advantages of HRC workplaces in the context of Industry 5.0 manufacturing, particularly from the human-centred manufacturing perspective. By integrating HRC at the WP1, we observed improvements in both production efficiency and sustainability, aligned with proposed ESG criteria in Fig. 1. Regarding energy consumption per product, at the manual assembly WP1, the average energy consumption was 1.51 W per product, where at the HRC WP1 energy consumption decreased to 1.27 W per product, representing a 15.9 % electrical energy consumption reduction. This reduction in energy consumption is attributed to the optimized task distribution between worker and CR. The HRC help reduce idle times and ensure smoother production flows, thus lowering the energy footprint per product. In the context of ESG, this improvement supports environmental sustainability, as reduced energy use leads to lower carbon emissions and a more energy-efficient production. On the other hand, processing costs per product at the manual assembly WP1 were 2 EUR per product, where at the HRC WP1 processing costs dropped to 1.64 EUR per product, resulting in an 18 % processing cost reduction. The integration of CR in the HRC significantly lowers labour costs, as robots take over repetitive and high-strain physical tasks, enabling workers to focus on higher-value tasks. This reduction in processing costs underscores the economic benefits of HRC, making it a more cost-effective solution over the long term, particularly when considering reduced errors and improved output quality. More detailed costs evaluation was taking into concern with the idle costs per product parameter where idle cost for manual assembly WP1 were 0.98 EUR per product. At the HRC WP1 idle costs were reduced to 0.39 EUR per product, indicating a significant 60.2 % decrease. The reduction in idle costs demonstrates the enhanced efficiency of HRC, as CR can maintain consistent operations and reduce downtime between tasks. From a governance perspective, this improvement in resource utilization reflects better production capacity, which is critical in highly dynamic production

environments. If summarizing total cost per product at the manual assembly WP1 were 2.98 EUR and at the HRC WP1 were reduced to 2.03 EUR, representing a 31.9 % total cost reduction. This significant reduction in total costs per product reinforces the economic advantages of HRC. Not only does HRC improve resource utilization, but it also reduces operational costs, leading to a more sustainable manufacturing process that aligns with ESG goals. Form the environmental view the production output and scrap rate were evaluated, where at the manual assembly WP1 3613 finished products with a scrap rate of 8 % were made. At the HRC WP1 output quantity increased to 5515 finished products with a reduced scrap rate of 4.5 %. HRC's higher production output and lower scrap rate reflect the improved product quality and efficiency of HRC. This improvement supports the social sustainability aspect of ESG, as it reduces waste, improves product reliability, and enhances the overall working environment. The HRC offers substantial benefits in terms of human-centred manufacturing, which is a core principle of Industry 5.0. By redistributing tasks between humans and CR, HRC ensures that workers are less exposed to physically demanding or monotonous tasks, which contributes to better worker well-being and reduces stress levels. This improvement in working conditions supports the social pillar of ESG, emphasizing safety, engagement, and health in the workplace. The increased production efficiency and reduced waste contribute to the environmental and governance aspects of ESG by minimizing resource use, enhancing productivity, and promoting more sustainable and responsible manufacturing practices.

6. Conclusion

The implementation of the HRC workstations in manufacturing has been shown that can lead to significant improvements in both economic and production processes performance, while simultaneously supporting sustainability goals as defined by ESG criterion. By reducing energy consumption, processing costs, idle times, and scrap rates, HRC systems offer a way to optimize production efficiency while enhancing the working environment. The integration of HRC is not only beneficial from an economic standpoint, but it also directly impacts worker well-being, a central theme in Industry 5.0. By redistributing strenuous and repetitive tasks to CR, workers experience lower physical and cognitive stress, leading to improved job satisfaction. This reinforces the social sustainability aspect of the ESG framework, ensuring safer and healthier workplaces. Presented results emphasize the potential for HRC to drive the future of manufacturing, enabling a harmonious balance between productivity, worker well-being, and environmental responsibility. As industries continue to move toward sustainable manufacturing, HRC systems present a solution for maintaining competitiveness while addressing the increasing demand for ethical and sustainable production practices.

The presented research has broad applicability across various industries. The findings from this research could be applied in the manufacturing processes optimization, where the distribution of labour and production capacities between manual and automated systems can enhance overall production system performance. Insights can support the integration of ESG criteria into operational decision-making, ensuring that manufacturing systems are not only economically viable but also socially and environmentally responsible.

In the future research we will focus on evaluation the physical and mental stress experienced by workers in HRC environments. Wearable technologies such as heart rate monitors or stress sensors will be employed to measure the impact of HRC on worker health. With those we will be able to provide additional insights into the human-centred design of workstations. While HRC systems improve operational performance, the next step is to optimize these systems for worker well-being. This could involve adjusting CR parameters to reduce cognitive load and physical strain on workers, potentially using adaptive algorithms that adjust CR speeds and tasks in real-time based on worker feedback. In addition, our future research work involves integrating worker knowledge management into HRC systems. By leveraging worker experience and expertise, manufacturing systems could be dynamically adapted to improve both efficiency and quality. For example, artificial intelligence driven knowledge management systems could capture worker inputs and suggestions, enhancing manufacturing system performance and further reducing errors or downtime. Incorporating these research directions would help evolve the Industry 5.0 paradigm,

where human creativity and knowledge are enhanced by CR and artificial intelligence, leading to a more sustainable, efficient, and worker-friendly production environment.

Acknowledgement

The authors gratefully acknowledge the support of the Slovenian Research and Innovation Agency (ARIS), Research Core Funding No. P2-0190. The authors acknowledge the use of research equipment system for development and testing cognitive production approaches in Industry 4.0: Collaborative robots with equipment and Sensors, hardware and software for ergonomic analysis of a collaborative workplace, procured within the project "Upgrading national research infrastructures – RIUM", which was cofinanced by the Republic of Slovenia, the Ministry of Education, Science and Sport and the European Union from the European Regional Development Fund.

References

[1] Adel, A. (2022). Future of industry 5.0 in society: Human-centric solutions, challenges and prospective research areas, *Journal of Cloud Computing*, Vol. 11, Article No. 40, doi: 10.1186/S13677-022-00314-5.
[2] Ojstersek, R., Javernik, A., Buchmeister, B. (2022). Importance of sustainable collaborative workplaces-simulation modelling approach, *International Journal of Simulation Modelling*, Vol. 21, No. 4, 627-638, doi: 10.2507/IJSIMM21-4-623.
[3] Mourtzis, D., Angelopoulos, J., Panopoulos, N. (2022). A literature review of the challenges and opportunities of the transition from Industry 4.0 to Society 5.0, *Energies*, Vol. 15, No. 17, Article No. 6276, doi: 10.3390/EN15176276.
[4] Montini, E., Cutrona, V., Dell'Oca, S., Bettoni, A., Landolfi, G., Rocco, P., Carpanzano, E. (2024). An industrial human-robot collaboration case study for workers' well-being, *Procedia CIRP*, Vol. 130, 924-929, doi: 10.1016/J.PROCIR.2024.10.186.
[5] Calzavara, M., Faccio, M., Granata, I., Trevisani, A. (2024). Achieving productivity and operator well-being: A dynamic task allocation strategy for collaborative assembly systems in Industry 5.0, *The International Journal of Advanced Manufacturing Technology*, Vol. 134, 3201-3216, doi: 10.1007/S00170-024-14302-3/FIGURES/17.
[6] Tripathi, M.A., Sawant, P.D., Kaur, H., Almahairah, M.S., Chandel, P.S., Balakumar, A. (2024). Human-robot collaboration in the workplace: Assessing the impact on employee well-being and productivity, In: *Proceedings of 2024 Third International Conference on Intelligent Techniques in Control, Optimization and Signal Processing*, Krishnankoil, India, 1-7, doi: 10.1109/INCOS59338.2024.10527509.
[7] Bouaziz, N., Bettayeb, B., Sahnoun, M., Yassine, A. (2024). Incorporating uncertain human behavior in production scheduling for enhanced productivity in Industry 5.0 context, *International Journal of Production Economics*, Vol. 274, Article No. 109311, doi: 10.1016/J.IJPE.2024.109311.
[8] Azemi, F., Šimunović, G., Lujić, R., Tokody, D., Mulaku, L. (2023). Green manufacturing and environmental sustainability manufacturing in Kosovo's small and middle enterprises, barriers to implementation, *Tehnički Vjesnik – Technical Gazette,* Vol. 30, No. 3, 988-992, doi: 10.17559/TV-20220528121801.
[9] Javernik, A., Buchmeister, B., Ojstersek, R. (2023). The NASA-TLX approach to understand workers workload in human-robot collaboration, *International Journal of Simulation Modelling*, Vol. 22, No. 4, 574-585, doi: 10.2507/IJSIMM22-4-658.
[10] Asif, M., Searcy, C., Castka, P. (2023). ESG and Industry 5.0: The role of technologies in enhancing ESG disclosure, *Technological Forecasting and Social Change*, Vol. 195, Article No. 122806, doi: 10.1016/J.TECHFORE.2023.122806.
[11] Wang, H., Jiao, S., Bu, K., Wang, Y., Wang, Y. (2023). Digital transformation and manufacturing companies' ESG responsibility performance, *Finance Research Letters*, Vol. 58, Part B, Article No. 104370, doi: 10.1016/J.FRL.2023.104370.
[12] Liu, L., Schoen, A.J., Henrichs, C., Li, J., Mutlu, B., Zhang, Y., Radwin, R.G. (2024). Human robot collaboration for enhancing work activities, *Human Factors: The Journal of the Human Factors and Ergonomics Society*, Vol. 66, No. 1, 158-179, doi: 10.1177/00187208221077722.
[13] Gültekin, A., Diri, S., Becerikli, Y. (2023). Simplified and smoothed rapidly-exploring random tree algorithm for robot path planning, *Tehnički Vjesnik – Technical Gazette,* Vol. 30, No. 3, 891-898, doi: 10.17559/TV-20221015080721.
[14] Javernik, A., Buchmeister, B., Ojstersek, R. (2022). Impact of Cobot parameters on the worker productivity: Optimization challenge, *Advances in Production Engineering & Management*, Vol. 17, No. 4, 494-504, doi: 10.14743/apem2022.4.451.
[15] Matheson, E., Minto, R., Zampieri, E.G.G., Faccio, M., Rosati, G. (2019). Human–robot collaboration in manufacturing applications: A review, *Robotics*, Vol. 8, No. 4, Article No. 100, doi: 10.3390/ROBOTICS8040100.
[16] Petzoldt, C., Harms, M., Freitag, M. (2023). Review of task allocation for human-robot collaboration in assembly, *International Journal of Computer Integrated Manufacturing*, Vol. 36, No. 11, 1675-1715, doi: 10.1080/0951192X.2023.2204467.
[17] Othman, U., Yang, E. (2023). Human–robot collaborations in smart manufacturing environments: Review and outlook, *Sensors*, Vol. 23, No. 12, Article No. 5663, doi: 10.3390/S23125663.

[18] Murali, P.K., Darvish, K., Mastrogiovanni, F. (2020). Deployment and evaluation of a flexible human–robot collaboration model based on AND/OR graphs in a manufacturing environment, *Intelligent Service Robotics*, Vol. 13, No. 4, 439-457, doi: 10.1007/S11370-020-00332-9.
[19] Lorenzini, M., Lagomarsino, M., Fortini, L., Gholami, S., Ajoudani, A. (2023). Ergonomic human-robot collaboration in industry: A review, *Frontiers,* Vol. 9, Article No. 813907, doi: 10.3389/FROBT.2022.813907.
[20] Panagou, S., Neumann, W.P., Fruggiero, F. (2024). A scoping review of human robot interaction research towards Industry 5.0 human-centric workplaces, *International Journal of Production Research*, Vol. 62, No. 3, 974-990, doi: 10.1080/00207543.2023.2172473.
[21] Xiao, J., Huang, K. (2024). A comprehensive review on human–robot collaboration remanufacturing towards uncertain and dynamic disassembly, *Manufacturing Review*, Vol. 11, Article No. 17, doi: 10.1051/MFREVIEW/2024015.
[22] Šegota, S.B., Anđelić, N., Car, Z., Šercer, M. (2022). Prediction of robot grasp robustness using artificial intelligence algorithms, *Tehnički Vjesnik – Technical Gazette,* Vol. 29, No. 1, 101-107, doi: 10.17559/TV-20210204092154.
[23] Hopko, S., Wang, J., Mehta, R. (2022). Human factors considerations and metrics in shared space human-robot collaboration: A systematic review, *Frontiers,* Vol. 9, Article No. 799522, doi: 10.3389/FROBT.2022.799522.

Calendar of events

- 16th EAI International Conference on Simulation Tools and Techniques, December 9-10, 2024, Bratislava, Slovakia.
- International Conference on Smart Materials & Structures, March 27-28, 2025, Berlin, Germany.
- 14th Spring World Congress on Engineering and Technology (SCET 2025), April 19-21, 2025, Guilin, China.
- International Connect & Expo on Material Science and Engineering, April 28-20, 2025, Rome, Italy.
- 2025 Annual Modeling and Simulation Conference (ANNSIM'25), May 26-29, 2025, Madrid, Spain.
- Fifth International Conference on Simulation for Additive Manufacturing (Sim-AM 2025), September 9-11, 2025, Pavia, Italy.

This page intentionally left blank.

Notes for contributors

General

Articles submitted to the *APEM journal* should be original and unpublished contributions and should not be under consideration for any other publication at the same time. Manuscript should be written in English. Responsibility for the contents of the paper rests upon the authors and not upon the editors or the publisher. The content from published paper in the *APEM journal* may be used under the terms of the Creative Commons Attribution 4.0 International Licence (CC BY 4.0). For most up-to-date information please see the APEM journal homepage *apem-journal.org*.

Submission of papers

A submission must include the corresponding author's complete name, affiliation, address, phone and fax numbers, and e-mail address. All papers for consideration by *Advances in Production Engineering & Management* should be submitted by e-mail to the journal Editor-in-Chief:

Miran Brezocnik, Editor-in-Chief
UNIVERSITY OF MARIBOR
Faculty of Mechanical Engineering
Chair of Production Engineering
Smetanova ulica 17, SI – 2000 Maribor
Slovenia, European Union
E-mail: apem@apem-journal.org

Manuscript preparation

Manuscript should be prepared in *Microsoft Word 2010* (or higher version) word processor. *Word .docx* format is required. Papers on A4 format, single-spaced, typed in one column, using body text font size of 11 pt, should not exceed 12 pages, including abstract, keywords, body text, figures, tables, acknowledgements (if any), references, and appendices (if any). The title of the paper, authors' names, affiliations and headings of the body text should be in *Calibri* font. Body text, figures and tables captions have to be written in *Cambria* font. Mathematical equations and expressions must be set in *Microsoft Word Equation Editor* and written in *Cambria Math* font. For detail instructions on manuscript preparation please see instruction for authors in the *APEM journal* homepage *apem-journal.org*.

The review process

Every manuscript submitted for possible publication in the *APEM journal* is first briefly reviewed by the editor for general suitability for the journal. Notification of successful submission is sent. After initial screening, and checking by a special plagiarism detection tool, the manuscript is passed on to at least two referees. A double-blind peer review process ensures the content's validity and relevance. Optionally, authors are invited to suggest up to three well-respected experts in the field discussed in the article who might act as reviewers. The review process can take up to eight weeks on average. Based on the comments of the referees, the editor will take a decision about the paper. The following decisions can be made: accepting the paper, reconsidering the paper after changes, or rejecting the paper. Accepted papers may not be offered elsewhere for publication. The editor may, in some circumstances, vary this process at his discretion.

Proofs

Proofs will be sent to the corresponding author and should be returned within 3 days of receipt. Corrections should be restricted to typesetting errors and minor changes.

Offprints

An e-offprint, i.e., a PDF version of the published article, will be sent by e-mail to the corresponding author. Additionally, one complete copy of the journal will be sent free of charge to the corresponding author of the published article.

APEM journal

Advances in Production Engineering & Management

Chair of Production Engineering (CPE)
University of Maribor
APEM homepage: apem-journal.org

Volume 19 | Number 4 | December 2024 | pp 411-542

Contents

Published by CPE, University of Maribor

ISSN 1854-6250

apem-journal.org